2014-09

Optimal estimation of glider's underwater trajectory with depth-dependent correction using the Navy Coastal Ocean Model with application to antisubmarine warfare

NAVAL POSTGRADUATE SCHOOL

MONTEREY, CALIFORNIA

THESIS

OPTIMAL ESTIMATION OF GLIDER'S UNDERWATER TRAJECTORY WITH DEPTH-DEPENDENT CORRECTION USING THE NAVY COASTAL OCEAN MODEL WITH APPLICATION TO ANTISUBMARINE WARFARE

by

JooEon Shim

September 2014

Thesis Advisor:	Peter C. Chu
Second Reader:	Chenwu Fan
Second Reader:	Ronald E. Betsch

Approved for public release; distribution is unlimited

THIS PAGE INTENTIONALLY LEFT BLANK

REPORT DOCUMENTATION PAGE

Form Approved OMB No. 0704–0188

1. AGENCY USE ONLY *(Leave blank)*	**2. REPORT DATE** September 2014	**3. REPORT TYPE AND DATES COVERED** Master's Thesis

4. TITLE AND SUBTITLE
OPTIMAL ESTIMATION OF GLIDER'S UNDERWATER TRAJECTORY WITH DEPTH-DEPENDENT CORRECTION USING THE NAVY COASTAL OCEAN MODEL WITH APPLICATION TO ANTISUBMARINE WARFARE

5. FUNDING NUMBERS

6. AUTHOR(S) JooEon Shim

7. PERFORMING ORGANIZATION NAME(S) AND ADDRESS(ES)
Naval Postgraduate School
Monterey, CA 93943-5000

8. PERFORMING ORGANIZATION REPORT NUMBER

9. SPONSORING /MONITORING AGENCY NAME(S) AND ADDRESS(ES)
N/A

10. SPONSORING/MONITORING AGENCY REPORT NUMBER

11. SUPPLEMENTARY NOTES The views expressed in this thesis are those of the author and do not reflect the official policy or position of the Department of Defense or the U.S. Government. IRB Protocol number ____N/A____.

12a. DISTRIBUTION / AVAILABILITY STATEMENT
Approved for public release; distribution is unlimited

12b. DISTRIBUTION CODE
A

13. ABSTRACT (maximum 200 words)

An underwater glider is a cost-effective underwater unmanned vehicle with high-endurance for oceanographic research or naval applications. Its navigation and localization accuracy are important because these accuracies provide spatiotemporally high resolution ocean data with saving energy and time. The glider, however, is affected by the ocean currents because of its minimal velocity, which is due to its buoyancy-driven propulsion system. It also lacks of inexpensive and efficient localization sensors during its subsurface mission. Therefore, knowing its precise underwater position is a challenging task.

This study attempts to develop a novel correction method for estimating a glider's optimal underwater trajectory. In four steps, it compares the corrected trajectories, which are developed using depth-averaged and depth-dependent correction methods using the Regional Navy Coastal Ocean Model (NCOM). The results suggest that the depth-dependent correction method is more accurate. This study for estimating a glider's underwater trajectory accurately would be beneficial to oceanographic research and naval applications, especially antisubmarine warfare (ASW) such as operating Intelligence, Surveillance, and Reconnaissance (ISR); operating littoral ASW; providing communication networks; and supporting tactical oceanography.

14. SUBJECT TERMS Underwater Glider, Optimal Estimation, Underwater Trajectory, Dead Reckoning, Depth-dependent Correction, Depth-averaged Correction, the Regional NCOM, Antisubmarine Warfare	**15. NUMBER OF PAGES** 165
	16. PRICE CODE

17. SECURITY CLASSIFICATION OF REPORT	**18. SECURITY CLASSIFICATION OF THIS PAGE**	**19. SECURITY CLASSIFICATION OF ABSTRACT**	**20. LIMITATION OF ABSTRACT**
Unclassified	Unclassified	Unclassified	UU

NSN 7540–01-280-5500 Standard Form 298 (Rev. 2–89)
Prescribed by ANSI Std. 239–18

THIS PAGE INTENTIONALLY LEFT BLANK

Approved for public release; distribution is unlimited

OPTIMAL ESTIMATION OF GLIDER'S UNDERWATER TRAJECTORY WITH DEPTH-DEPENDENT CORRECTION USING THE NAVY COASTAL OCEAN MODEL WITH APPLICATION TO ANTISUBMARINE WARFARE

JooEon Shim
Lieutenant Commander, Republic of Korea Navy
B.A., Republic of Korea Naval Academy, 2003

Submitted in partial fulfillment of the
requirements for the degree of

MASTER OF SCIENCE IN PHYSICAL OCEANOGRAPHY

from the

NAVAL POSTGRADUATE SCHOOL
September 2014

Author: JooEon Shim

Approved by: Peter C. Chu
Thesis Advisor

Chenwu Fan
Second Reader

Ronald E. Betsch
Second Reader

Peter C. Chu
Chair, Department of Oceanography

THIS PAGE INTENTIONALLY LEFT BLANK

ABSTRACT

An underwater glider is a cost-effective underwater unmanned vehicle with high-endurance for oceanographic research or naval applications. Its navigation and localization accuracy are important because these accuracies provide spatiotemporally high resolution ocean data with saving energy and time. The glider, however, is affected by the ocean currents because of its minimal velocity, which is due to its buoyancy-driven propulsion system. It also lacks of inexpensive and efficient localization sensors during its subsurface mission. Therefore, knowing its precise underwater position is a challenging task.

This study attempts to develop a novel correction method for estimating a glider's optimal underwater trajectory. In four steps, it compares the corrected trajectories, which are developed using depth-averaged and depth-dependent correction methods using the Regional Navy Coastal Ocean Model (NCOM). The results suggest that the depth-dependent correction method is more accurate. This study for estimating a glider's underwater trajectory accurately would be beneficial to oceanographic research and naval applications, especially antisubmarine warfare (ASW) such as operating Intelligence, Surveillance, and Reconnaissance (ISR); operating littoral ASW; providing communication networks; and supporting tactical oceanography.

THIS PAGE INTENTIONALLY LEFT BLANK

TABLE OF CONTENTS

LIST OF FIGURES

LIST OF TABLES

THIS PAGE INTENTIONALLY LEFT BLANK

LIST OF ACRONYMS AND ABBREVIATIONS

2-D	two-dimensional
4-D	four-dimensional
6 DOF	6 degrees of freedom
ADCP	acoustic Doppler currents profiler
AO	area of operations
ARGOS	Advanced Research and Global Observation Satellite
ASW	antisubmarine warfare
AUVs	autonomous underwater vehicles
C4ISR	Command, Control, Communications, Computers, and ISR
CN3	communication/navigation network nodes
CONOPs	concept of operations
CSG	carrier strike group
CTD	Conductivity, Temperature, and Depth
DOD	Department of Defense
DON	Department of Navy
DR	dead reckoning
DVL	Doppler velocity log
EKF	extended Kalman Filter
EOD	explosive ordnance disposal
ESG	expeditionary strike group
GNCOM	Global NCOM
GPS	Global Positioning System
HYCOM	HYbrid Coordinate Ocean Model
INS	inertial navigation system
IPOE	intelligence preparation of the operational environment
ISR	intelligence, surveillance and reconnaissance
KF	Kalman Filter
LCM	linear correction method
MCM	mine countermeasures
MDA	maritime domain awareness

MND	Ministry of National Defense
NAVOCEANO	Naval Oceanographic Office
NCM	non-linear correction method
NCODA	Navy Coupled Ocean Data Assimilation
NCOM	Navy Coastal Ocean Model
NCW	network centric warfare
NOAA	National Oceanic and Atmospheric Administration
NRL	Naval Research Laboratory
OPC	Ocean Prediction Center
POM	Princeton Ocean Model
RF	radio frequency
RMS	root mean square
ROK	Republic of Korea
ROKN	Republic of Korea Navy
ROMS	Regional Ocean Modeling System
SIO	Scripps Institution of Oceanography
SSH	sea surface height
SSS	side scan sonar
SST	sea surface temperature
SZM	Sigma/Z-level Model
TDAs	tactical decision aids
UKF	unscented Kalman Filter
USW	undersea warfare
UUVMP	The Navy Unmanned Undersea Vehicle Master Plan
UUV	unmanned underwater vehicle
WHOI	Woods Hole Oceanographic Institution

ACKNOWLEDGMENTS

First of all, I would like to acknowledge the invaluable assistance of my advisor, Distinguished Professor Peter C. Chu. His scientific knowledge and guidance, dedication, and patience have expanded and enhanced my knowledge, and this thesis would not have been able to be completed without his continuous support. Furthermore, I would like to thank to my second reader, Mr. Chenwu Fan, for his time, patience and professional knowledge in MATLAB programing. Without his help, I would not have been able to accomplish my thesis in a timely manner. Additionally, I would like to thank Mr. Ronald E. Betsch from Naval Oceanographic Office (NAVOCEANO) for being a second reader on this thesis.

Moreover, I would like to express my appreciation to Dr. Kwang sub Song of the Naval Postgraduate School Oceanography Department and Dr. Kyeongju Park of the Republic of Korea Naval Academy. Their recommendations and guidance on my thesis opened my eyes toward a physical oceanography academic world.

I also would like to recognize and express my appreciation to my lovely country, the Republic of Korea, and my navy for all the support that they provided to me with this invaluable academic experience at Naval Postgraduate School.

Finally, I would like to thank my wife, Shinyoung; son, Seunghyun; daughter, Chaeyun; and numerous other family members and friends in the Republic of Korea and United States for providing me with their love, patience, and the understanding necessary for me to achieve my academic goals. I thank you all.

Dedicated to the sacrifice of the 46 heroic warriors of the ROKS *Cheonan* and Warrant Officer Ju-ho Han.

THIS PAGE INTENTIONALLY LEFT BLANK

I. INTRODUCTION

This chapter deals with the background of the thesis topic, the problem statement, hypothesis and explanations, research questions, and the benefits of this study. It also describes the scope and methodology and concludes with an outline of the thesis.

A. BACKGROUND

An underwater glider is a small, cost-effective, and multifunctional unmanned underwater vehicle (UUV) designed for long-duration missions such as oceanographic research, naval operations, and especially antisubmarine warfare (ASW). Since an underwater glider is equipped with a wireless network and requires less energy during its missions, it would be an effective platform for future ASW, such as Intelligence, Surveillance, and Reconnaissance (ISR), and targeting and/or identifying the enemy.

ASW is a branch of undersea warfare (USW) conducted with the intention of destroying and neutralizing enemy submarines by using naval assets such as surface ships, submarines, and aircrafts. ASW's operational objectives are to deter the enemy from using its submarines effectively and to allow friendly forces to operate throughout the area of operations (AO). It is crucial for naval forces to accomplish maritime superiority and to establish dominance in the underwater environment simultaneously (DOD 2013, Chapter IV).

ASW is a vital naval operation because of the continuous development of submarines and underwater weapons. ASW, especially, has emerged as a more important issue for the Republic of Korea Navy (ROKN) since the ROK Ship *Cheonan* was sunk by the North Korea Navy's torpedo attack in 2010. Since then, the ROKN has been required to improve ASW capability. As part of these improvements, the underwater glider is expected to be a suitable platform for future ASW.

B. PROBLEM STATEMENT

An underwater glider could be beneficial to future ASW in the ROKN, but it is difficult to estimate its underwater trajectory precisely. To conduct ASW effectively, accurate localization of a glider is important because observed ocean data or the enemy target information can be more useful when the location of the data is precise. Localizing a glider's underwater position, however, is difficult and complex. The glider's velocity is limited compared to that of other UUVs due to its buoyancy-driven propulsion system. Typically, the horizontal velocity is about 0.4 ms^{-1} and the vertical velocity is about 0.2 ms^{-1}, which is the same order of magnitude as the ocean currents (Smith et al. 2010a). Thus, the glider's movement is strongly affected by the ocean currents. In addition, a glider does not have sensors for measuring its position and the subsurface ocean currents in real time (Smith et al. 2010b), and it can only receive a Global Positioning System (GPS) fixed position when it is located at sea surface. Consequently, given that some margin of error is common between the dead reckoning (DR) position (P_{dr} in Figure 1) and the real surfacing position (P_{gps} in Figure 1), knowing its actual underwater location is difficult.

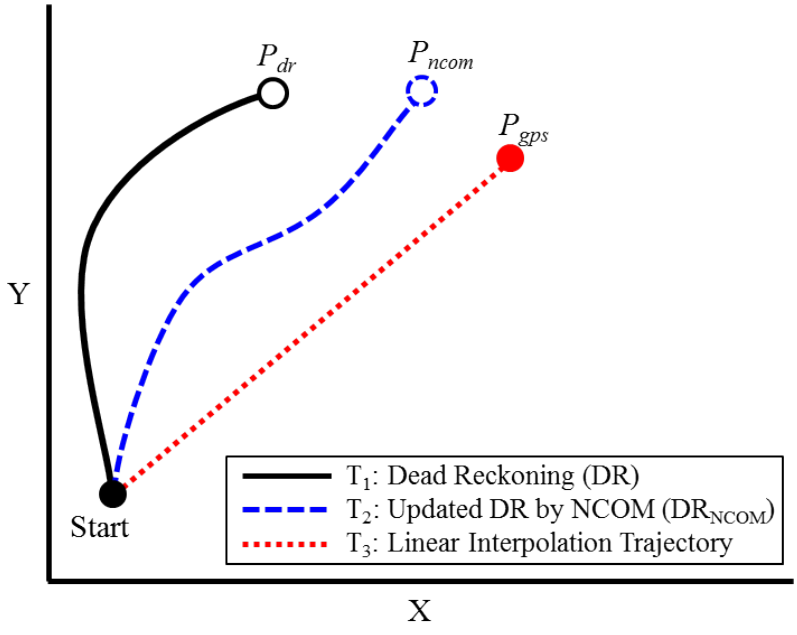

Figure 1. Schema of Glider Trajectories.

While improving the method for estimating a glider's underwater trajectory is important, it is a challenging task due to several errors in the existing methods. As of now, estimating a glider's trajectory is done by linear interpolation between actual surfaced positions (T_3 in Figure 1) or by improving the accuracy of its DR trajectories (T_1 in Figure 1). The former method, however, is not realistic because the position is estimated by dividing the distance between the real GPS fixed position by transit time, and the glider's direction and speed remain constant. In other words, the trajectory looks like a straight line. The latter method has two major types of error: inherent error and extraneous error. Inherent error can be caused by the glider's dynamic, mechanical, and measurement errors, such as heading, roll and pitch, and pressure. On the other hand, extraneous error can be caused by environmental factors, mainly the ocean currents. These errors have an effect on the estimation of DR trajectory.

C. HYPOTHESIS AND EXPLANATIONS

The accuracy for estimating a glider's underwater trajectory can be increased by correcting these errors with two major models: the glider's vehicle model and the ocean circulation model. The former is the solution to inherent error, and the latter is the solution to extraneous error. Recently, Wang et al. (2013) and Singh (2014) studied localization improvement for an underwater glider based on its vehicle model. Smith et al. (2010a,b) developed the algorithm for a glider's path planning and trajectory design by using ocean currents prediction model data. However, no localization method using the ocean currents prediction model data has been studied. Therefore, this study attempts to develop a better method for estimating a glider's optimal underwater trajectory based on the U.S. Navy Coastal Ocean Model (NCOM) prediction data, especially the Regional NCOM. Even though we can exploit advanced sensors as studied by Woithe et al. (2011) and Somers (2011) or additional reference UUVs as studied by Somers (2011), these methods require more resources and, therefore, more financial backing. Thus, this thesis focuses on the single glider operating situation without any advantage of additional equipment.

D. RESEARCH QUESTIONS

The primary research questions of this thesis are: "How can we estimate a glider's optimal underwater trajectory more accurately?" and "How does this study impact future ASW in the ROKN?"

As a part of the research process, the following subsidiary questions will be discussed:

- Why is the precisely estimated underwater trajectory of a glider important?
- What is the most influential factor in estimating the underwater trajectory of a glider?
- Which method can be used to correct a glider's underwater trajectory?
- How does the method in this thesis compare to the existing method?

E. BENEFITS OF STUDY

This study aims to provide a better method for estimating a glider's optimal underwater trajectory, focusing on the importance of the ocean currents. The precise estimation of a glider's trajectory would be useful for ASW. During a mission, a glider can collect ocean data, such as Conductivity, Temperature, and Depth (CTD). Moreover, a glider's navigational accuracy would be increased with well-estimated trajectories, and this improved navigational accuracy would help it to get more precise ocean data and to target information of the enemy. These precise and valuable ocean data are critical for calibrating sonar to ensure that it provides the most accurate underwater environment. ASW would be more effective with more accurate information on an enemy's target. As a result, by collecting and using these precise ocean data and target information, the Navy would be able to improve ASW capability, such as operating ISR, targeting, and/or attacking the enemy's underwater forces.

F. SCOPE AND METHODOLOGY

Since this study is limited, the research will not consider a glider's dynamic model, mechanics, and measurement errors. For this study, data on the Slocum Electric glider from a Naval Postgraduate School class field experiment and the Regional NCOM predictions at Monterey Bay from the Naval Oceanographic Office (NAVOCEANO) will be used to improve the method for estimating a glider's optimal underwater trajectory. Details of the background and the methods will be described in Chapter II and Chapter III.

For this thesis, generally, the methodology is as follows. First of all, this thesis provides background on currently used underwater gliders, their navigation scheme and limitations, and their DR algorithm and limitations by conducting a literature review. It also describes existing methods for estimating a underwater trajectory of a glider with a discussion of their limitations and provides background information on an underwater glider's dynamic model and its limitations.

Secondly, this thesis analyzes data on the Slocum Electric glider and the Regional NCOM predictions and details methods that will be developed in this study. The method development process is divided into two phases, and the second phase is divided into four steps. Phase One aims to prove the importance of the ocean currents in estimating a glider's trajectory by comparing the distance between P_{gps} and P_{dr} (d_1) to P_{gps} and P_{ncom} (d_2) in each dive (see Figure 2).

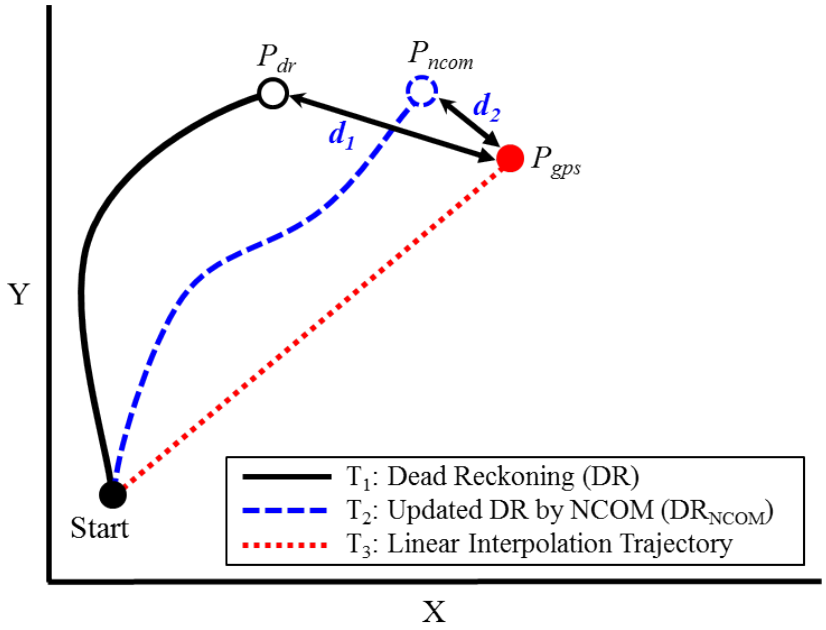

Figure 2. Schematic Presentation of the Phase One.

P_{gps} is obtained from the GPS fixed position information, and P_{dr} can be computed by a glider's DR algorithm. P_{ncom}, however, can be updated by adding position data of T_1 and the calculated water displacement from the Regional NCOM prediction data which can be computed by numerical integration, *simple composite trapezoidal rule*. After calculating the distance difference, we will determine how much the DR_{NCOM} (T_2) is improved than T_1 by comparing absolute ($d_2 - d_1$) and relative ($[d_1 - d_2]/d_1$) distance differences between the two trajectories.

Phase Two attempts to develop a better method for estimating a glider's optimal underwater trajectory by correcting T_1 trajectory with two different methods: *depth-averaged correction* and *depth-dependent correction*. In both methods, the glider's velocity is relative to the water velocity and its underwater position is calculated by the DR algorithm. Therefore, the only aspect that needs to be calculated for estimating the glider's underwater trajectory is the displacement of ocean water. By adding the calculated water displacement to the glider's DR position data and correcting errors against T_3, the corrected trajectory will be estimated more precisely. To calculate the glider's underwater position, it is assumed that the T_3 is a real estimated trajectory in

every dive because knowing a glider's actual underwater position is difficult and is limited. So the T_3 is used as an initial reference trajectory to match the depth and time-consequent location of the Regional NCOM prediction data with other trajectories in every correction method. The $T_{3,}$ however, is not a realistic trajectory. Thus, to compare precision of the depth-averaged correction method and the depth-dependent correction method, an optimal trajectory will be estimated by using iteration method from the corrected trajectory with the depth-dependent correction method.

The depth-averaged correction method is similar to the depth-averaged currents calculation method (see Chapter II). This method considers the averaged ocean currents during one dive. The water displacement at each time (t_n) is calculated linearly by dividing the total water displacement ($\Delta X^w, \Delta Y^w$) by time ratio at each time (t_n / t_N) (see Figure 3).

The depth-dependent correction method, however, is a new approach to correct error of trajectory. This method considers the ocean currents from the Regional NCOM prediction data, which have four-dimensional (4-D) variables, i.e., $\mathbf{U}_{ncom}(x, y, z, t)$: longitude and latitude, depth, and time, respectively. Therefore, the more precise water displacement can be calculated by considering the depth and time-consequent location and by using the simple trapezoidal rule (see Figure 4).

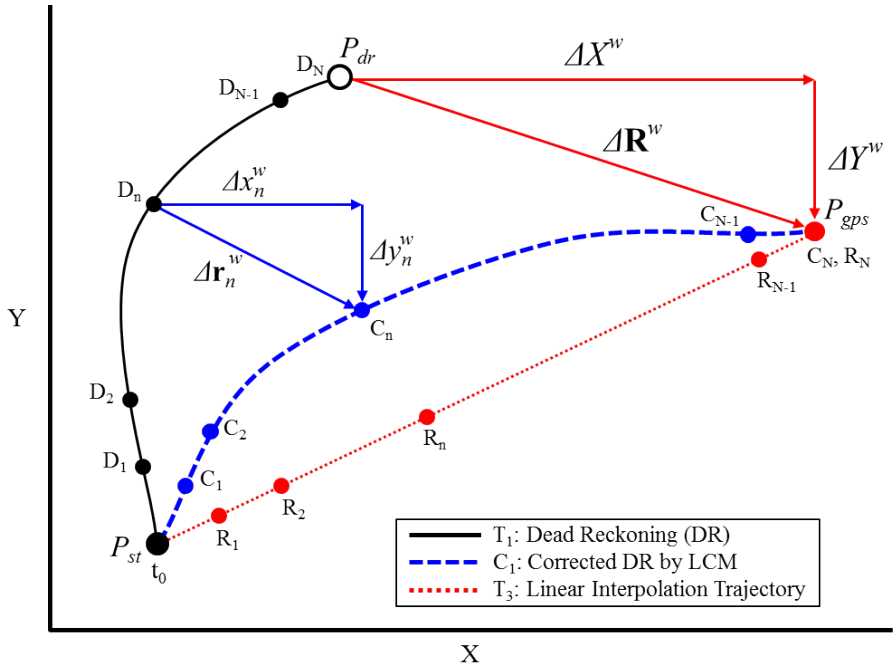

Figure 3. Downward Looking View of Glider's Trajectories with the Depth-averaged Correction Method.

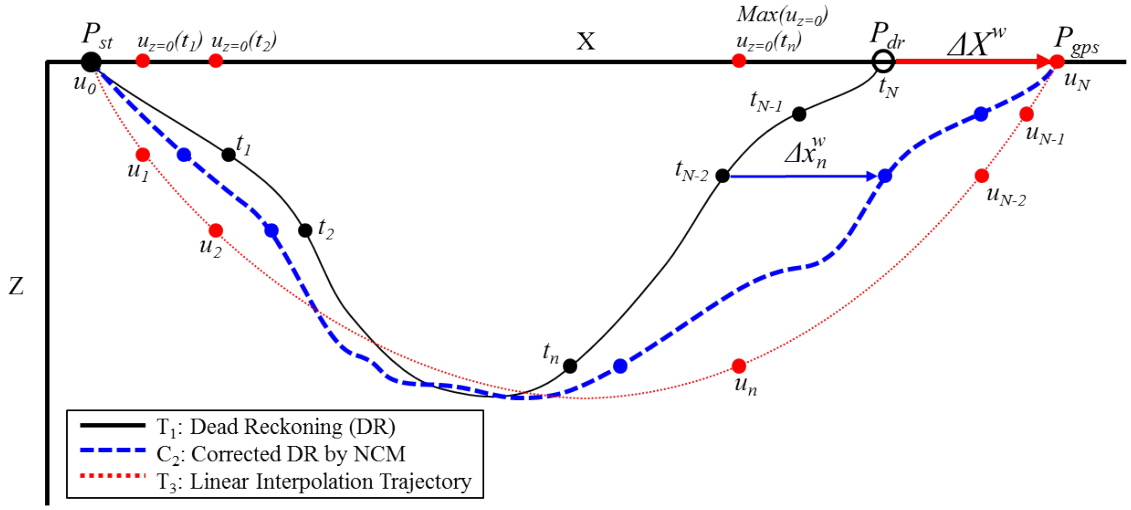

Figure 4. Lateral View of the Eastward Component of Glider's Trajectories with the Depth-dependent Correction Method.

The corrected trajectories are compared to each other to develop a better method in the following four steps, and more details of the methods in each phase and step will be discussed in Chapter III.

- In Step One, T_1 trajectory is corrected by using the depth-averaged correction method. The corrected trajectory is referred to as C_1. In this step, C_1 cannot be compared to T_3 because T_3 is not a real trajectory. Thus, only results of corrected trajectory will be shown.

- In Step Two, the T_1 trajectory is corrected by using the depth-dependent correction method. The corrected trajectory is referred to as C_2. In this step, the C_2 also cannot be compared to T_3 for the same reason as given in Step One. Thus, only results of the corrected trajectory will be shown.

- In Step Three, an optimal trajectory is estimated by using the iteration method with C_2. This optimal trajectory is referred to as C_3, which is expected to be closest to a real trajectory.

- In Step Four, two corrected trajectories are compared to an optimal trajectory (C_1 and C_3, C_2 and C_3) to determine which method is developed well.

Finally, this thesis discusses the results by comparing these corrected trajectories. Then, it details the relevance of findings to future ASW in the ROKN.

G. THESIS OUTLINE

The rest of this thesis is divided into four chapters. Chapter II provides background from a literature review. In Chapter III, a method development process for estimating a glider's optimal underwater trajectory will be detailed, followed by a description of the data set and field experiment information. Chapter IV analyzes the data and discusses the results of this study, and then it describes the relevance of these findings to the navy. Chapter V concludes the thesis and recommends future research areas.

THIS PAGE INTENTIONALLY LEFT BLANK

II. BACKGROUND

A more cost-effective and accurate localization method needs to be developed for the navigation systems of an underwater glider. A glider's navigation and localization accuracy are important. However, since an underwater glider is vulnerable to the ocean currents and lacks inexpensive and efficient localization sensors (Singh 2014), estimating its precise underwater position is challenging. For these reasons, many researches and studies have been done to develop a better method for increasing the accuracy of a glider's underwater position in recent decades.

Although the developed methods could get a more accurate underwater position than the traditional dead reckoning (DR) algorithm, they still have some limitations. Currently, three types of underwater glider are widely used: the Slocum, the Spray, and the Seaglider. They have roughly similar appearance features, but their navigation algorithms and localization methods are slightly different. Thus, their navigation algorithms and localization methods must be considered when generating a novel method for precise localization. Most of the previous studies developed methods by using the glider's vehicle model, and some studies measured the ocean currents with extra onboard sensors or localized the glider's position with additional equipment. The vehicle model-based methods, however, cannot fully consider the ocean current effects because they focus on improving the glider's attitude, state, and control. The methods using extra onboard sensors can measure the ocean currents in near real-time and compensate for error in improving a glider's navigation accuracy, but these sensors make a glider heavier and require more energy. Consequently, the glider's operation duration is shorter than it was before. The methods using multiple platforms like reference UUVs and acoustic-based network sensors (Paull et al. 2014) can localize the glider in near real-time, but they are expensive, and some equipment may be subjected to the ocean environment; for example, the ocean currents and bottom topography (Paull et al. 2014; Wang et al. 2013). Therefore, this study attempts to develop a more cost-effective and reliable method based on the ocean model.

The rest of this chapter explains the motivations for developing a novel method for estimating a glider's underwater trajectory by reviewing the glider's *6 Degrees of Freedom* (6 DOF) non-linear dynamic equations of motion and the existing model-based methods. The following section begins by presenting general descriptions of the three commonly-used underwater gliders, including their common navigation scheme and DR algorithm. Then, each glider's navigation algorithm and its limitations are detailed to provide background knowledge for developing a better method for estimating a glider's underwater position.

A. UNDERWATER GLIDERS

At the present time, three major types of underwater glider are commonly used: the Slocum (see Figure 5a) that was produced by the Teledyne Webb Research, the Spray (see Figure 5b) that was co-developed by Scripps Institution of Oceanography (SIO) and Woods Hole Oceanographic Institution (WHOI), and the Seaglider (see Figure 5c) that was developed by the University of Washington. Although these gliders have roughly similar appearance and operational characteristics, their navigational characteristics are slightly different. Such differences must be studied and considered to improve the method for estimating a glider's optimal underwater trajectory.

(a) (b) (c)

Figure 5. Three Types of Underwater Glider: (a) the Slocum (from Autonomous Undersea Vehicle Application Center [AUVAC] 2014, http://auvac.org/uploads/configuration/Slocum1.jpg); (b) the Spray (from AUVAC 2014, http://auvac.org/uploads/configuration/spray.jpg); (c) the Seaglider (from University of Washington 2014, http://www.washington.edu/news/files/2013/05/glider-500x3311.jpg).

1. General Descriptions

Commonly-used underwater gliders are small, cost-effective, and multifunctional UUV designed for high-endurance missions. They are approximately two meters long, weigh about 52 kilograms, and have a hull diameter of about 20–30 centimeters, so they are small enough to be handled by one to three persons (Davis et al. 2002). Due to the lack of propulsion system, they glide through the ocean by controlling their buoyancy using interior pumps and tanks and by controlling their attitude using two wings and a tail that are attached to their bodies (Graver 2005). Depending on their type and the purposed of their mission, gliders are designed to operate at the maximum depth of 200–1,500 meters. The Spray and the Seaglider are designed for deep, open-ocean operations, so they can dive at the maximum depth of 1,000–1,500 meters. The Slocum Electric, on the other hand, is optimized for shallow-water and coastal operations, and its maximum depth is 200 meters. The underwater gliders move forward at a horizontal average velocity of about 0.4 ms^{-1} with a saw-tooth vertical profile (see Figure 6). This forward movement is produced by changing the gliders' water displacement with a buoyancy engine (Schofield et al. 2007) and by converting their buoyancy into horizontal movement by a lift force, which is created from the gliders' wings (Bender et al. 2008).

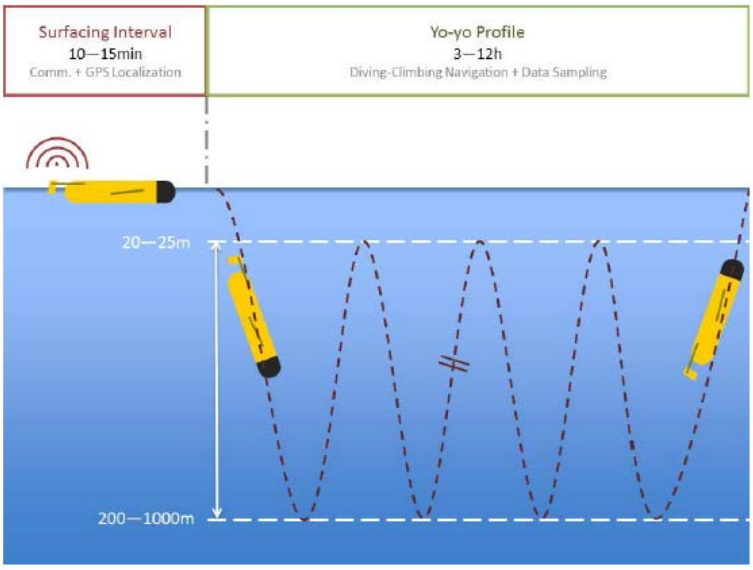

Figure 6. The Slocum's Saw-tooth Profile (from Hernandez et al. 2014).

A glider is more cost-effective than other UUVs and ships (Graver 2005). The glider's buoyancy-driven propulsion system allows it to have minimal velocity and thus expends less power than other kinds of UUVs. Therefore, it can observe and collect vast ocean data autonomously while it is conducting long-range and long-duration missions. In addition, a glider can receive commands remotely and transmit collected data in near real-time through a wireless telecommunication systems, such as Radio Frequency (RF) modem, Iridium satellite, Advanced Research and Global Observation Satellite (ARGOS), and tele-sonar modem (Webb et al. 2001) via antennas that are attached their body. For these reasons, the underwater glider can be used in various missions like ocean sampling and monitoring (Schofield et al. 2007), as well as naval applications such as ASW, maritime surveillance and reconnaissance.

a. Common Navigation Scheme

Although each glider has unique characteristics, the navigation scheme of the three widely-used gliders is roughly similar. Their navigation primarily relies on a GPS signal, magnetic compass, altimeter, and subsurface DR. When a glider locates at surface, its actual position is fairly precise because it can receive GPS fixed information. During the subsurface mission, however, its position information is not as accurate as the former situation due to the lack of GPS signals. Once the glider is diving into the ocean, it is gliding vertically with several upward and downward dives (see Figure 6), until it resurfaces (Merckelbach et al. 2008). During the dives, the glider measures parameters such as heading, pitch and roll, and depth change rate from the onboard sensors, i.e., attitude and pressure sensors (Singh 2014). Then, the glider estimates its underwater position by computing the parameters with the DR algorithm; the details of the DR algorithm will be described in the next section. After several dives, a glider's DR position (see position 1_a in Figure 7) is different from the actual measured surfacing position (see position 1 in Figure 7). This difference occurs due to the ocean currents and is commonly referred to as *depth-averaged currents*. The magnitude of depth-averaged currents can be calculated from the distance between the DR and actual surfacing positions, and the distance is divided by the subsurface transit time (Merckelbach et al. 2008).

A glider uses the depth-averaged currents by means of correcting the next waypoint to compensate for these errors, and this increases its navigation accuracy. Merckelbach et al. (2008) describe the Slocum's currents correction algorithm (see Figure 7), which is similar to the other gliders, and the details of each stage are described as follows.

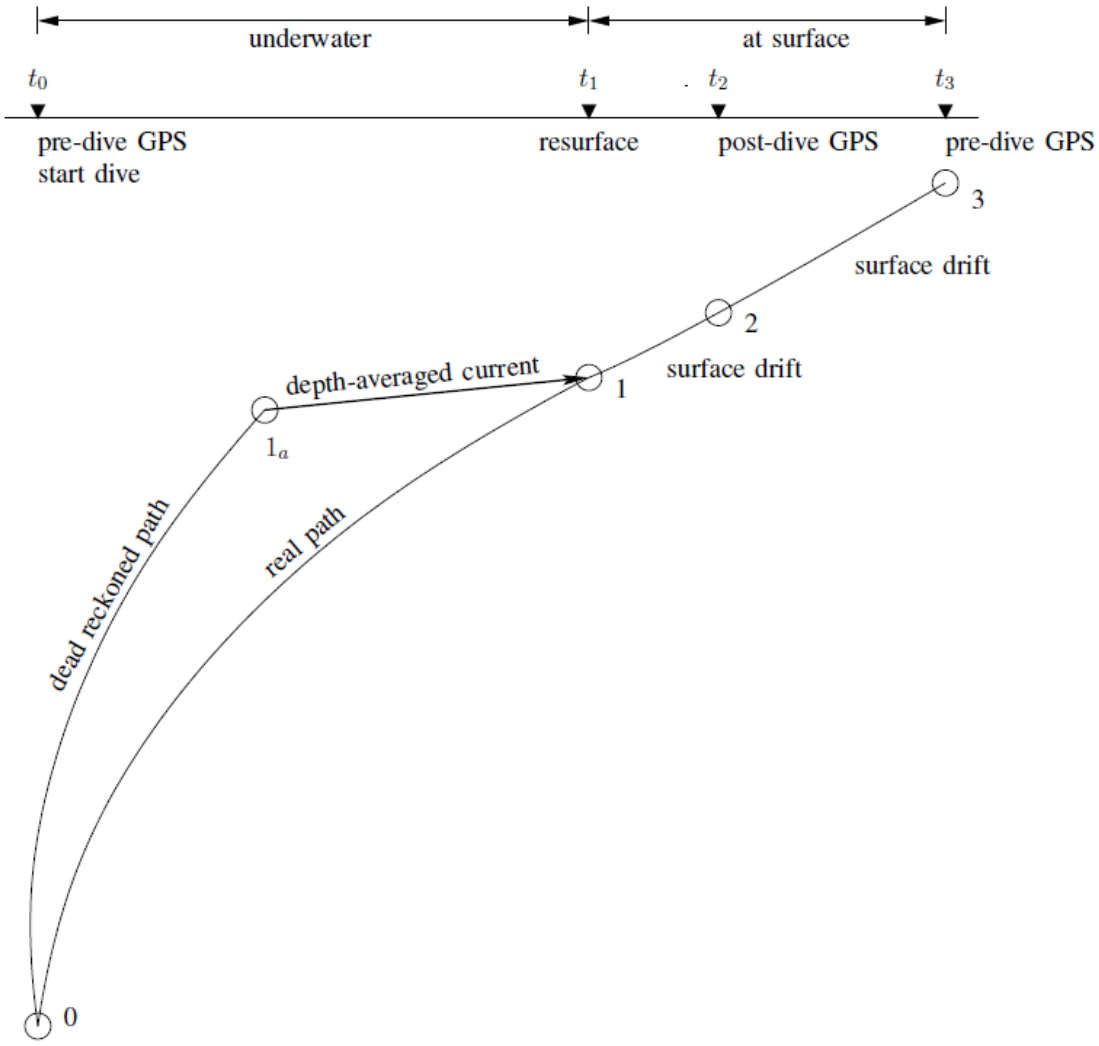

Figure 7. Schema of the Slocum's Currents Correction Algorithm (from Merckelbach et al. 2008).

- At stage 0, the Slocum prepares to dive underwater and obtains GPS fixed information.

- At stage 1, the Slocum resurfaces and prepares to receive GPS signals and commands for the next mission via telemetry communications. Note that after it has resurfaced, the Slocum is affected by surface currents until it receives GPS signals. So, its actual position cannot be calculated immediately but can be estimated. First, the surface current velocity can be estimated from the distance between position 2 and 3, divided by time between t_2 and t_3. And then, position 1 can be estimated from position 2 by using the surface current velocity with the elapsed time between t_1 and t_2.

- At stage 1_a, the Slocum's resurfacing location is estimated by DR algorithm.

- At stage 2, the Slocum obtains its first GPS fixed information after resurfacing.

- Finally, the Slocum prepares to dive again and obtains GPS fixed information prior to diving.

b. Dead Reckoning (DR) Algorithm

An underwater glider primarily uses the DR algorithm to estimate its underwater position and to increase its navigational accuracy. A glider's new position is estimated by the DR algorithm at about every four seconds of the control cycle (Woithe et al. 2011) using the internal navigation system. The estimated position is calculated from the glider's horizontal speed ($\mathbf{U}_g$) and heading (h) (Merckelbach et al. 2008), and the horizontal speed is derived from the pitch angle (θ) and depth change rate (d_g) that are measured by the onboard attitude and pressure sensors (Woithe et al. 2011). The attitude sensor measures the glider's pitch angle, roll, and heading, and the pressure sensor measures their depth. Woithe et al. (2011) present a simple calculation method to estimate a glider's underwater position and explain related parameters with the following equations.

The glider's horizontal speed ($\mathbf{U}_g$) is calculated from the depth change rate (d_g) and present pitch angle (θ) during one control cycle (Δt) (Woithe et al. 2011), as shown in Equation (1).

$$\mathbf{U}_g = \frac{d_g}{tan\theta} \tag{1}$$

Then, the glider's eastward (u) and northward (v) horizontal velocity are computed using the glider's horizontal speed, and the measured present heading (h), as shown in Equation (2) (Merckelbach et al. 2008).

$$\begin{aligned} u &= \mathbf{U}_g \sin h \\ v &= \mathbf{U}_g \cos h \end{aligned} \tag{2}$$

These components are integrated by the real-time difference (Δt) since the last control cycle, then converted to meters (Δx , Δy) as in Equation (3).

$$\begin{aligned} \Delta x &= u\ \Delta t \\ \Delta y &= v\ \Delta t \end{aligned} \tag{3}$$

Equation (4) represents the updated DR position ($\hat{x}$, $\hat{y}$) by adding the newly calculated location (Δx , Δy) with the previous one (x , y).

$$\begin{aligned} \hat{x} &= x + \Delta x \\ \hat{y} &= y + \Delta y \end{aligned} \tag{4}$$

Finally, the horizontal distance (d) during the present control cycle time (Δt) is calculated as shown Equation (5) (Woithe et al. 2011).

$$d = \sqrt{\Delta x^2 + \Delta y^2} \tag{5}$$

Even the glider's DR algorithm is a more accurate method for estimating the underwater position than a simple linear interpolation, but errors between real and DR position exist. The main error can be accounted for by the ocean currents. Some errors are made in the DR algorithm itself or are derived from the simplification of glider dynamics. Moreover, the others are parameter errors measured by onboard sensors.

2. The Slocum

The Slocum is a torpedo-shaped underwater glider, which consists of two different models: the Slocum Electric (see Figure 5a) and the Slocum Thermal (see Figure 8). The Slocum Electric is propelled by a battery-powered buoyancy engine and is optimized for shallow-water coastal operation (Davis et al. 2002) with various depth ranges of 4–200 meters, so it is equipped with a navigation system that can quickly change the horizontal and vertical movement (Webb et al. 2001). It can steer in a horizontal direction by using a tail fin rudder (Scholfield et al. 2007) with a turning circle of within about seven meters (Davis et al. 2002). Also it can rapidly change its buoyancy by pushing water in and out through a nozzle that is located in the nose by using a large-volume, single-stroke, piston pump (Davis et al. 2002). The Slocum G2, another type of the Slocum Electric, was developed recently. It can optionally be equipped with various onboard sensors which are already developed, and it is capable of operating with an additional depth of 350 meters, and 1,000 meters by changing some components like the buoyancy engine (Teledyne Webb Research 2014). As a result, the Slocum Electric has a multi-depth and multifunctional capability. It, on the other hand, would have a disadvantage of much poorer applicability than other gliders when it has the newly developed sensors installed. The Slocum Thermal is optimized for deep-water operation at a maximum depth of 1,200 meters and is propelled by heat from the ocean's thermal stratification (Rudnick et al. 2004).

Figure 8. The Slocum Thermal (from Teledyne Webb Research 2014, http://www.webbresearch.com/thermal.aspx).

The Slocum navigates using a simple DR algorithm, but this method has some limitations. Both the Slocum Electric and Thermal navigate between each GPS fixed position by calculating their heading and glide angle, and those parameters are maintained until they are recalculated (Bender et al. 2008). During the subsurface mission, the Slocum calculates its buoyancy, pitch angle, and vertical velocity to estimate its underwater position using the DR algorithm (Webb et al. 2001). The Slocum, however, does not estimate the ocean currents for calculating the underwater position (Bender et al. 2008), so its underwater trajectory is less precise.

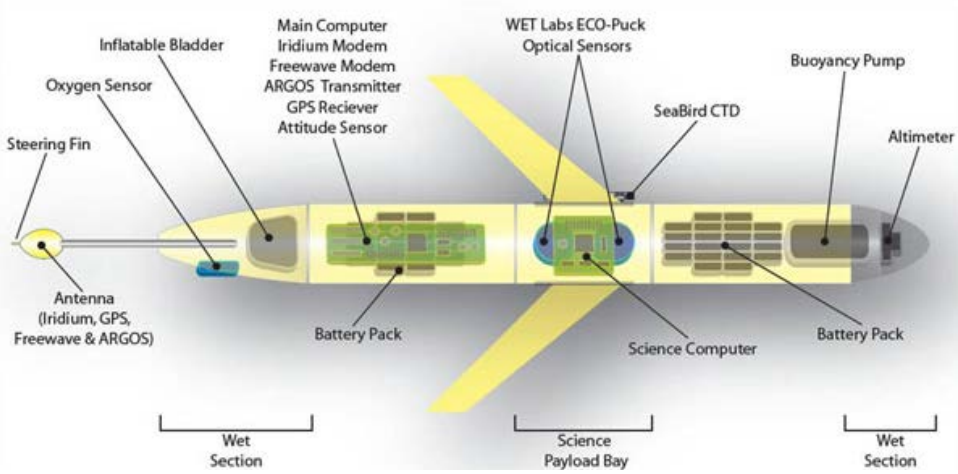

Figure 9. The Slocum Electric Interior (from AUVAC 2014, http://auvac.org/uploads/configuration/Glider_structure.jpg).

3. The Spray

Like the Slocum, the Spray is propelled by a battery-powered buoyancy engine, but its body is a nearly streamlined torpedo-shaped, so the Spray's water resistance is 50% less than the Slocum (Sherman et al. 2001). Its minimal water resistance allows the Spray to move quickly, using less energy to overcome the strong water currents. Additionally, the Spray is less affected by the strong ocean currents relative to the other gliders because it can control its roll precisely, thereby its attitude can be fixed well. It is optimized for deep-water operation (Rudnick et al. 2004) at a maximum depth of 1,500 meters. The Spray controls its attitude by using its internal batteries: the roll is controlled by moving them to the left or right, and the pitch is controlled by moving them to forward or backward (Sherman et al. 2001). This control method, however, could be inefficient because the Spray spends too much time doing so to change its path when operating in a coastal area containing many obstacles and where the depth change is complex.

To perform the mission, the Spray rolls 90 degrees at the surface to make one wing vertical (see Figure 10) for obtaining GPS fixes or communicating through Iridium satellite (Rudnick et al. 2004). After that, it uses a simple navigation algorithm to compute the heading and glide angle, which are required to reach a desired location from

its present position with the assumption of a constant pitch angle, heading, and angle of attack during its subsurface mission (Sherman et al. 2001).

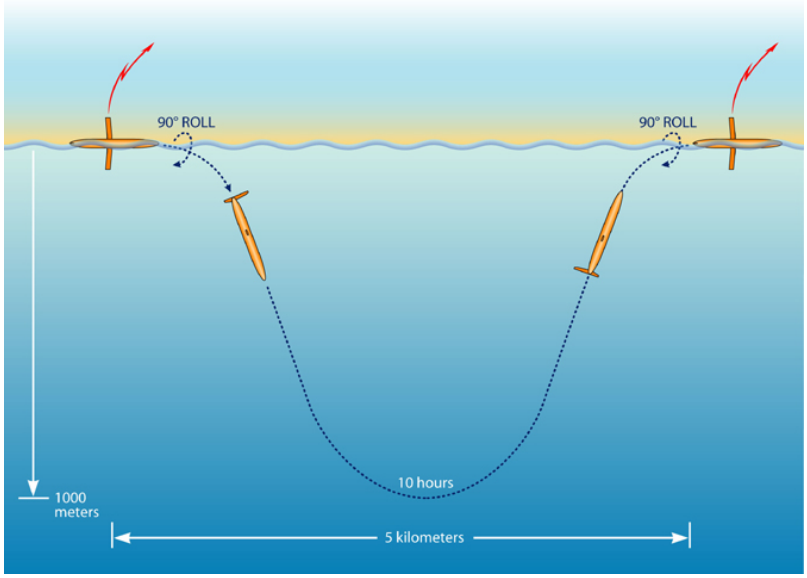

Figure 10. Schema of the Spray's Navigation Feature (from SIO 2014, http://spray.ucsd.edu/pub/rel/info/spray_description.php).

Like the Slocum, the Spray uses the DR algorithm for estimating its underwater trajectory, but this method is also less precise because it does not estimate the ocean currents. Therefore, it is difficult to navigate by following the preplanned path. The Spray, however, can compensate for some errors on its path by calculating the depth-averaged ocean currents information.

4. The Seaglider

The Seaglider is designed for deep-water missions like the Spray. Its fairing is enclosed in low-drag-shaped compressible fiberglass (Eriksen et al. 2001), which allows the glider to prevent loss of buoyancy resulting from its depth change. Thus, it can dive into deep-ocean by using less energy than other gliders which have an incompressible body (Davis et al. 2002). On the other hand, it is difficult to load additional equipment near the glider's body because the contraction and expansion of the body are repeated depending on the pressure during the subsurface mission. Moreover, the Seaglider can

only accommodate additional sensors near its wings due to its structural features, so it has less versatility than other gliders (Eriksen et al. 2001).

Unlike the Slocum and the Spray, the Seaglider has a unique ability to estimate the ocean currents by using a *Kalman Filter (KF)* algorithm to increase its navigational accuracy (Eriksen et al. 2001). The Seaglider automatically controls its direction to compensate for the navigational errors between the preplanned path and actual surfaced position based on the DR position and the indirectly measured speed of ocean currents by using the KF. By using the filter, the Seaglider can approach the prescribed position more precisely and expend less energy as well (Eriksen et al. 2001).

B. MODEL-BASED ESTIMATION OF A GLIDER'S UNDERWATER TRAJECTORY

Underwater glider's navigation and localization accuracy are important issues because they allow a glider to get spatiotemporally higher resolution data and to save energy consequent to its extended mission time. Precise localization of a glider is essential to obtain its navigational accuracy, but it is a challenging mission. This is because a glider can only receive GPS fixed position information when it is surfacing, and GPS signals cannot penetrate into the ocean, so a glider is highly dependent on its navigation algorithm to estimate its underwater position. In addition, due to its minimal velocity relative to the other UUVs, the attitude of a glider is strongly affected by the ocean currents, and thus localization of a glider is a complex task.

Most of the underwater gliders primarily use the traditional DR algorithm to increase their navigational accuracy. This method, however, still has limitations. First of all, a glider uses the depth-averaged currents to compensate for error and to set the next waypoint (Merckelbach et al. 2008), but this method is relatively inaccurate. Since the depth-averaged currents are estimated from the previous dive sequences in the previous mission area, those data are not coincident with the areas of the future mission. Therefore, the corrected waypoint by the depth-averaged currents would not be able to account for the real-time ocean currents fully. Second, the glider measures parameters by onboard sensors to use them for the DR algorithm, but measurement errors still exist. These errors

have a significant impact on the magnitude of parameters, which are determined by the glider's dynamic model and consequent localization. For these reasons, two types of methods can be considered to compensate for these errors. The first method considers a gilder's *vehicle model*, which determines the glider's position and orientation in 6 DOF. The six different motion components of the glider are measured by onboard sensors and are calculated by its dynamic equation of motion. Thus, the glider's more accurate position can be estimated by using the well-developed vehicle model and by reducing the measurement error. The second method considers the *environmental model*, especially the ocean currents, to compensate for errors from external forces and moments acting on the glider (Fossen 1994). This model considers the environmental disturbances—such as ocean currents, wind, and waves—that affect the glider's position and motion. These disturbances can be approximated by applying the principle of superposition and be added to the dynamic equation of motion.

Some of researches and studies (Graver et al. 2003; Graver 2005; Bender et al. 2008) discussed the dynamic equations of motion and parameter identification of underwater gliders in past years (Smith et al. 2010b). This section describes the 6 DOF non-linear dynamic equations of motion and discusses previous work for each model-based method to provide the background knowledge for developing a novel method for estimating a glider's optimal underwater trajectory.

1. 6 DOF Non-linear Dynamic Equations of Motion

A glider's dynamic model represents its motion by a system of equations corresponding to the 6 DOF, i.e., surge (u), sway (v), heave (w), roll (p), pitch (q), yaw (r), and a glider's position and orientation are determined by the 6 DOF (see Table 1). The first three DOF components represent the glider's *position and transitional motion*, and the last three DOF components indicate their *orientation and rotational motion* (Fossen 1994).

Table 1. Notation of 6 DOF for the Underwater Glider (after Fossen 1994).

DOF		Forces and Moments (Body-fixed)	Linear and Angular Velocities (Body-fixed)	Positions and Euler Angles (Earth-fixed)
1	Motions in the *x*-direction (surge)	X	u	x
2	Motions in the *y*-direction (sway)	Y	v	y
3	Motions in the *z*-direction (heave)	Z	w	z
4	Rotation about the *x*-axis (roll)	K	p	ϕ
5	Rotation about the *y*-axis (pitch)	M	q	θ
6	Rotation about the *z*-axis (yaw)	N	r	ψ

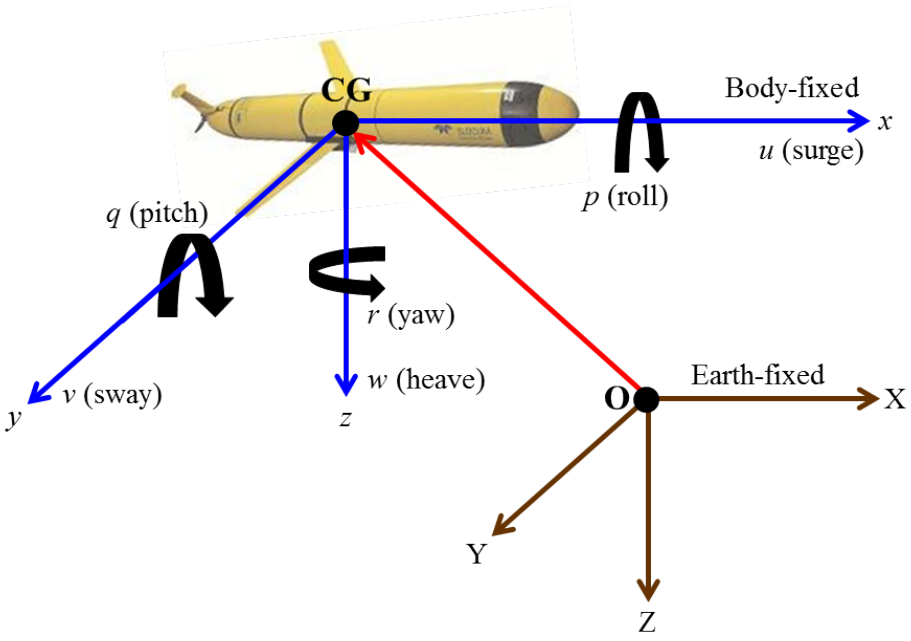

Figure 11. Earth-fixed and Body-fixed Coordinate Frames.

To develop the equations of motion, some following assumptions are required. First, the underwater glider behaves as a rigid body. Second, the Earth's rotation can be neglected because the motion of the Earth rarely has an impact on low-speed gliders. Thus, the Earth-fixed frame can be regarded as an inertial frame. With these assumptions, the glider's motion is described in two coordinate frames: the Earth-fixed frame and the body-fixed frame (see Figure 11). The origin of the Earth-fixed frame is the center of the

Earth (O), and the position and Euler angles of the glider are expressed relative to this reference frame. The origin of the body-fixed frame, on the other hand, is the center of the glider (CG), and the linear and angular velocities are expressed in this frame, and the motion of the body-fixed frame is represented relative to the Earth-fixed frame (Fossen 1994).

Fossen (1994) describes the general motion of the glider in 6 DOF as following vectors.

$$\boldsymbol{\eta} = [x, y, z, \phi, \theta, \psi]^T$$
$$\boldsymbol{\nu} = [u, v, w, p, q, r]^T$$
$$\boldsymbol{\tau} = [X, Y, Z, K, M, N]^T$$

Here, $\boldsymbol{\eta}$ indicates the position and Euler angles vector in the Earth-fixed frame, $\boldsymbol{\nu}$ means the linear and angular velocity vector in the body-fixed frame, and $\boldsymbol{\tau}$ denotes the forces and moments acting on the vehicle in the body-fixed frame. With these 6 DOF, the non-linear dynamic equation of motion can be obtained by considering the relationship between two coordinate frames (see Equation (6)).

$$M\frac{d\boldsymbol{\nu}}{dt} + C(\boldsymbol{\nu})\boldsymbol{\nu} + D(\boldsymbol{\nu})\boldsymbol{\nu} + g(\boldsymbol{\eta}) = \boldsymbol{\tau} \tag{6}$$

where

M : inertia matrix (including added mass)

C : matrix of Coriolis and centripetal terms (including added mass)

D : damping matrix

g : vector of gravitational forces and moments

$\boldsymbol{\tau}$: vector of control inputs

After that, the rigid-body equation of motion is derived by applying the *Newtonian* and *Lagrangian* mechanics, and the equation of translational (see Equation (7)) and rotational motion (see Equation (8)) is obtained by applying *Euler's First and Second Axioms*.

$$\begin{aligned} m[\dot{u} - vr + wq - x_G(q^2 + r^2) + y_G(pq - \dot{r}) + z_G(pr + \dot{q})] &= \mathrm{X} \\ m[\dot{v} - wp + ur - y_G(r^2 + p^2) + z_G(qr - \dot{p}) + x_G(qp + \dot{r})] &= Y \\ m[\dot{w} - uq + vp - z_G(p^2 + q^2) + x_G(rp - \dot{q}) + y_G(rq + \dot{p})] &= Z \end{aligned} \tag{7}$$

$$
\begin{aligned}
&I_x\dot{p} + (I_z - I_y)qr - (\dot{r} + pq)I_{xz} + (r^2 - q^2)I_{yz} + (pr - \dot{q})I_{xy} \\
&\qquad + m[y_G(\dot{w} - uq + vp) - z_G(\dot{v} - wp + ur)] = K \\
&I_y\dot{q} + (I_x - I_z)rp - (\dot{p} + qr)I_{xy} + (p^2 - r^2)I_{zx} + (qp - \dot{r})I_{yz} \\
&\qquad + m[z_G(\dot{u} - vr + wq) - x_G(\dot{w} - uq + vp)] = M \\
&I_z\dot{r} + (I_y - I_x)pq - (\dot{q} + rp)I_{yz} + (q^2 - p^2)I_{xy} + (rq - \dot{p})I_{zx} \\
&\qquad + m[x_G(\dot{v} - wp + ur) - y_G(\dot{u} - vr + wq)] = N
\end{aligned}
\tag{8}
$$

where

x_G, y_G, z_G : center of gravity

I_x, I_y, I_z : the moments of inertia about the *x*, *y*, *z* axes

I_{xy}, I_{xz}, I_{yz}: the products of inertia

The Equation (7) and Equation (8) can be re-expressed as the vectorial representation (see Equation (9)) by considering the glider's hydrodynamics and moments with *Radiation-induced forces* and *Froude-Kriloff and Diffraction forces* (Fossen 1994).

$$
M\frac{d\mathbf{v}}{dt} + C(\mathbf{v})\mathbf{v} + D(\mathbf{v})\mathbf{v} + g(\boldsymbol{\eta}) = \boldsymbol{\tau}_E + \boldsymbol{\tau} \tag{9}
$$

where

$M \triangleq M_{RB} + M_A$

$C(\mathbf{v}) \triangleq C_{RB}(\mathbf{v}) + C_A(\mathbf{v})$

$\boldsymbol{\tau}_E = \boldsymbol{\tau}_{current} + \boldsymbol{\tau}_{wind} + \boldsymbol{\tau}_{wave}$

$\boldsymbol{\tau}_E$: the environmental forces and moments acting on the vehicle

$\boldsymbol{\tau}$: the propulsion forces and moments

The left-hand side of Equation (9) expresses the glider's vehicle model, and the right-hand side of the equation describes the environmental effects through $\boldsymbol{\tau}_E$. More details of each equation's derivation and an explanation of terms are described in Fossen (1994).

2. Previous Works

This section describes previous works in developing methods for estimating the underwater trajectory of a glider based on each model.

a. Vehicle Model-Based Methods

As previously discussed, an underwater glider estimates its subsurface position with the DR algorithm by measuring pitch angle, heading, and depth change rate from its onboard sensors. During the long-duration missions, measurement errors of these parameters can cause inaccuracy in estimating a glider's underwater DR position. Since these measured parameters are derived from the glider's vehicle model, more accurate estimation can be obtained by developing the model (Wang et al. 2013).

Most of the studies consulted for this thesis developed methods for localization of a glider by using its vehicle model, but this model has some errors. Woithe et al. (2011) developed a method to improve the accuracy of the traditional DR algorithm by using a Doppler Velocity Log (DVL). DVL uses four or more beams of acoustic wave to track the seabed, and the glider's relative motion (u, v, w) is determined by measuring the Doppler-shifted returns from the seabed (Paull et al. 2014). Then, the glider's position is estimated by replacing the calculated velocity with traditionally calculated speeds for the DR process (Woithe et al. 2011). This method can estimate the glider's underwater position more precisely, but it has some drawbacks. Since the extra onboard sensors make the glider heavier and require onboard decision making and calculation (Smith et al. 2012), the glider requires more energy to operate and consequently its mission duration would be shortened. Furthermore, some sensors are expensive; for example, a DVL costs about $50,000, so this type of method is not cost effective. Also, since DVL estimates the glider's position by integrating its estimated velocity, the integrated data could result in cumulative errors. Singh (2014) attempted to improve the accuracy of the Slocum's underwater position by developing the glider's dynamic models based on the Extended Kalman Filter (EKF). This method, however, did not consider the ocean currents and glider's lateral motion as well. The EKF is optimized for non-linear process and measurement models. In addition, its prediction operation is fast, but updating the

measurement is slow because it uses matrix inversion (Paull et al. 2014). Thus, the error of the processing delay still exists.

The various filters, including the EKF, allow the gliders to estimate its position more accurately by estimating the glider's state. These filters, however, also have some disadvantages. The KF is an efficient recursive algorithm that can predict the glider's state of a dynamic system with measured input parameters (Rajendra and Jannett 2007) such as pitch angle and depth by the onboard sensors. Since the KF uses the measured input parameters, measurement errors by onboard sensors can occur, and the errors can be accumulated due to the glider's long mission time. Also, the KF has some time delays for data processing, as presented by Paull et al. (2014); thus the delayed data causes errors as well. Since a glider can only update parameters consequent to its position by using KF when it locates at surface, some gliders use other sensors like the Inertial Navigation System (INS) and DVL to compensate for some errors. INS uses accelerometers and gyroscopes to improve DR accuracy by integrating measurements, and DVL can measure the glider's velocity relative to the ground (Woithe et al. 2011). Even though using INS and DVL is more accurate than only using the KF algorithm, calibration and initial alignment errors can still exist (Rajendra and Jannett 2007). Therefore, it is essential for estimating a glider's precise position to measure input parameters accurately and to calibrate onboard sensors precisely when additional sensors are used. In addition, some errors can be reduced by making the glider surface frequently, but this would negatively impact the amount of ocean data collected during the underwater mission.

b. Environmental Model-Based Methods

The environmental model focuses on the effect of ocean currents for estimating a glider's position by combining the effects of currents with the parameters that are derived from the vehicle model. Since the glider is strongly affected by ocean currents, the precision of its position can be increased by obtaining more accurate underwater currents information.

Generally, two different methods can be used to obtain the ocean current information. One is measuring the *in-situ* ocean currents, using additional onboard sensors or instruments that are pre-installed at the area of interest. The other is using the ocean model data. The first method has some limitations for application to the underwater gliders. A glider can be equipped with additional current measurement sensors like the Acoustic Doppler Currents Profiler (ADCP) and DVL to measure the in-situ ocean currents for improving the accuracy of DR algorithm. DVL can calculate the ocean current velocity by computing the velocity of the ocean water and the seabed relative to the glider. ADCP also can be installed within the Slocum glider to estimate real-time ocean currents. These extra onboard sensors, however, have some drawbacks as discussed in the previous section. Moreover, the stability of ADCP has not been proven yet, and its related study is still ongoing.

Some previous studies applied the ocean model prediction data to plan a path and to design trajectories of the glider. Smith et al. (2010a, b) presented the effects of the ocean currents by applying the ocean model, especially, the Regional Ocean Modeling System (ROMS) prediction data to planning a path and designing the trajectory of the Slocum. Their simulations show that there was approximately a 50% reduction in the errors between the prescribed waypoint and the actual surfacing point by fusing ROMS and unscented Kalman Filter (UKF). As presented here, the previous studies considered the ocean currents from the ocean model prediction, but these studies developed the algorithm in planning a path or designing trajectories of the glider. To the best of our knowledge, no previous work exists for localization of a glider's underwater position using the ocean model predictions. Therefore, this thesis attempts to develop a novel method for estimating glider's underwater position using the ocean currents prediction data, especially from the Regional NCOM prediction.

c. Other Methods

Except the two model-based methods discussed in the previous two sections, some researches and experiments developed other methods to improve the accuracy of a glider's underwater position. But these studies tried to estimate the position by using

additional instruments like multiple UUVs and acoustic transponders and beacons (Paull et al. 2014). Somers (2011) studied the Doppler-based localization method by using multiple Autonomous Underwater Vehicles (AUVs), and Uffelen et al. (2013) studied the method using broadband acoustic signals. Even though these methods are able to estimate a glider's position more accurately, they are not cost-effective methods and do not consider the gliders' dynamic models. Therefore, the details of these methods will not be covered in this study.

C. CHAPTER SUMMARY

This chapter provided motivations for developing a novel method for estimating a glider's optimal underwater trajectory by reviewing general characteristics of widely-used gliders, including their common navigational scheme and DR algorithm, each glider's navigational features, and the existing model-based methods.

An underwater glider's position accuracy is important because the accuracy provides spatiotemporally higher resolution ocean data and allows the glider to save energy and time, as well. However, since the glider is susceptible to the ocean currents and lacks inexpensive and efficient localization sensors, estimating its precise underwater position is difficult.

The three widely-used underwater gliders, the Slocum, the Spray, and the Seaglider, have similar appearances and a common navigational scheme, but each one has unique features and navigational characteristics. All of them are propelled by a buoyancy-driven propulsion system and are designed for long range and duration missions. The Spray, the Seaglider, and the Slocum Thermal are optimized for deep-water missions. Conversely, the Slocum Electric was initially optimized for shallow-water coastal missions, but recently it became available for both shallow and deep water operations. The common navigational scheme of the underwater glider is mainly reliant on a GPS signal, altimeter, and DR algorithm. The DR algorithm is the most frequently used method to estimate a glider's underwater position. Even though the algorithm provides more accurate position estimation than the simple linear interpolation method, it has some margin of error. The main error is caused by the ocean currents, and another

error is derived from the DR algorithm itself or the simplification of the glider's dynamics. Also, other errors come from the parameters measured by onboard sensors that relate to the glider's dynamic model. The Seaglider uses the KF algorithm for compensating its navigation error by estimating the velocity of the ocean currents. The Slocum and the Spray, however, do not estimate the ocean currents, so their estimated underwater position is less precise than that of the Seaglider.

Many researches and studies have developed model-based methods for estimating a glider's underwater position in recent decades. These methods can be divided into two models: the vehicle model and the environmental model. Most of the studies focused on the vehicle model-based methods, and some of studies developed the environmental model-based methods by considering the ocean currents with additional onboard sensors and by localizing the glider's position with additional equipment. These developed methods can estimate the glider's underwater position more accurately than the traditional DR algorithm, but still have some limitations. First of all, most studies using the glider's vehicle model have limitations in explaining the effects of the ocean current because the model does not consider it. Secondly, the methods using extra onboard sensors make the glider heavier and require more energy for their missions, so the glider's operation duration would be shortened. Lastly, the methods using additional equipment require more financial backing, and the equipment is sometimes subjected to the complex ocean environment; for example, the ocean currents, bottom topography. Therefore, these methods are less cost-effective.

The Slocum would be a suitable platform for littoral operations due to its multi-depth capability, remarkable versatility, and navigational features (Teledyne Webb Research 2014). Although the Slocum has some advantages for littoral operations, it still has some navigational limitations. Thus, this study applies the Slocum Electric data to develop a more cost-effective and accurate localization method based on the ocean model for estimating a glider's optimal underwater trajectory. This novel method will be discussed in Chapter III.

THIS PAGE INTENTIONALLY LEFT BLANK

III. DATA SET AND METHODOLOGY

This chapter presents the methodology to develop a novel approach for estimating a glider's optimal underwater trajectory. It starts with a description of the Slocum Electric data set, providing general information on field experiments, and then discusses the Regional NCOM prediction data set. Finally, the chapter details the methodology.

Subsurface ocean currents must be considered when estimating the underwater position of a glider. Smith et al. (2010a) showed the effects of ocean currents in planning a path of the Slocum with observation of approximately a 50% reduction in surfacing errors by incorporating ROMS predictions. This result implies that the ocean model would be effective in estimating a glider's underwater position. If real-time ocean currents information is available, a glider's underwater position could be estimated more accurately, but it is difficult to obtain the information because of the lack of in-situ measurement sensors. The glider must be equipped with extra onboard sensors like ADCP for measuring the ocean currents, and additional instruments must be pre-installed in the area of interest to measure the ocean currents or to estimate the glider's position in near-real time. Before installation of additional instruments for ocean current measurement, we propose a novel method for estimating a glider's underwater position by incorporating the Regional NCOM prediction data. For the purpose of this study, it is assumed that no errors exist in the Regional NCOM data and the measured parameters from onboard sensors, and the ocean currents structure of the Regional NCOM is similar with that of in-situ ocean currents. In addition, this study does not consider the dynamic or mechanical errors of the glider.

A. DATA SETS

To develop the novel method, two data sets are used: the Slocum Electric data set and the Regional NCOM data set. The Slocum data set is foundational, providing the trajectory information that needs to be corrected. A subset of the Regional NCOM data, the ocean currents prediction data, is used to correct the inaccurate trajectory.

1. The Slocum Electric Data

The Slocum Electric (hereafter referred to as the Slocum) data are essential for estimating its underwater position. The data are obtained from a Naval Postgraduate School class field experiment. During the field experiment one Slocum was deployed at Monterey Bay (see Figure 12) for three days, from January 30, 2014, to February 1, 2014.

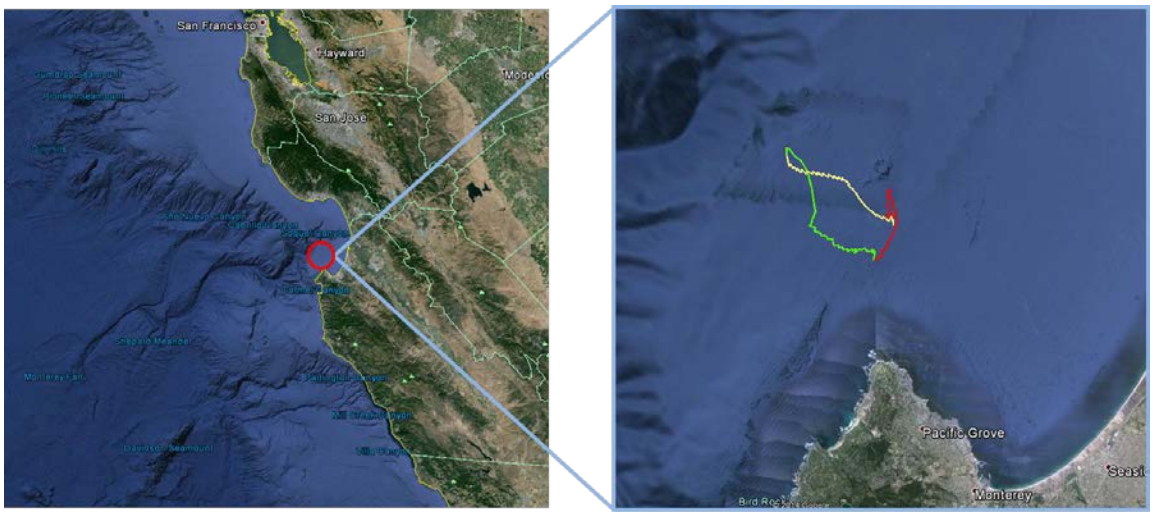

Figure 12. Experiment Area and Trajectories of the Slocum (after Google Earth).

Actually, this field experiment was not intended only for this study, but fortunately, both the Slocum and Regional NCOM data match in time and location, so these data are suitable for this study. During the three days of deployment time, the Slocum performed 68 dives. The average straight distance of DR trajectory was about 362 meters, with a minimum of 112 meters and maximum of 623 meters, depending on the prescribed depth and location. The average time of a single dive was about 20.5 minutes, and the average time of staying at surface was about 10 to 15 minutes. In addition, the average of maximum depth was about 95 meters, with maximum depth of about 198 meters. After finishing the three-day mission, the Slocum's basic navigation data were processed with MATLAB. The data included time; pressure; CTD; and the data for three main positions, i.e., GPS fixed position, DR position, and linear interpolation position. To estimate the glider's optimal underwater trajectory, we assume that there are

no errors in DR trajectory. Also, we do not consider surface drift, so we only attempt to estimate the underwater trajectory for each dive.

2. The Regional NCOM Data

NCOM is a free-surface general circulation model (Ngodock and Carrier 2014) based primarily on two existing ocean circulation models, the Princeton Ocean Model (POM) (Martin et al. 2009) and the Sigma/Z-level Model (SZM) (Martin et al., 1998). It is also based on primitive-equation and using the hydrostatic, Boussinesq, and incompressible approximations (Martin et al. 2009). NCOM is a real-time data-assimilating global ocean nowcast and forecast system. It has been developed at the Naval Research Laboratory (NRL) and transitioned to the NAVOCEANO to support naval operations, operational activities, and other researches (Rhodes et al. 2002). It has been used in global- and basin-scale circulation applications (Barron et al. 2003, 2004; Kara et al. 2006).

NCOM has two types of model: the Global and the Regional model. The Global NCOM (GNCOM), however, has been replaced by the operational Global HYbrid Coordinate Ocean Model (HYCOM) (Ocean Prediction Center (OPC) 2014). HYCOM has a horizontal resolution of 1/12 degree (about 9 kilometers) (Metzger et al. 2014) and 40 depth levels, and it uses hybrid (isopycnal/sigma/z-level) coordinates in the vertical (National Oceanic and Atmospheric Administration (NOAA) 2014). The HYCOM data consist of sea surface temperature (SST), sea surface height (SSH), eastward and northward currents and subsurface temperature and salinity (NOAA 2014; NRL 2014). HYCOM assimilates data from satellite and in-situ observation, using the Navy Coupled Ocean Data Assimilation (NCODA) system (NRL 2014). HYCOM provides boundary conditions to the Regional NCOM (NOAA 2014). The Regional NCOM includes the U.S. East coast, the Southern California coast, Hawaiian coasts, and the Gulf of Mexico and Caribbean Seas (OPC 2014).

In this thesis, the Regional NCOM data of Southern California coast are used. This data set has a high resolution of 1/30 degree, about 3.6 kilometers. Every day, the U.S. Navy produces a seven-day forecast (Metzger et al. 2014) of the Regional NCOM.

The data is updated at 00Z with the four-day (96 hours) forecast and three-hour increments (NOAA 2014). The Regional NCOM has the grid data which consist of many variables, especially the time; position (longitude and latitude); depth; and the eastward (u_{ncom}) and northward (v_{ncom}) component of ocean current velocity. Even though the Regional NCOM has high resolution data, it requires being reprocessed to match with the Slocum data. After the processing is done, these data can be applied to our novel method. Details of data processing of the Regional NCOM are described in the following section.

a. Data Processing of the Regional NCOM

The Slocum data is point data, while the Regional NCOM data is grid data (see Figure 13), so data processing is required to match both data sets with time and location.

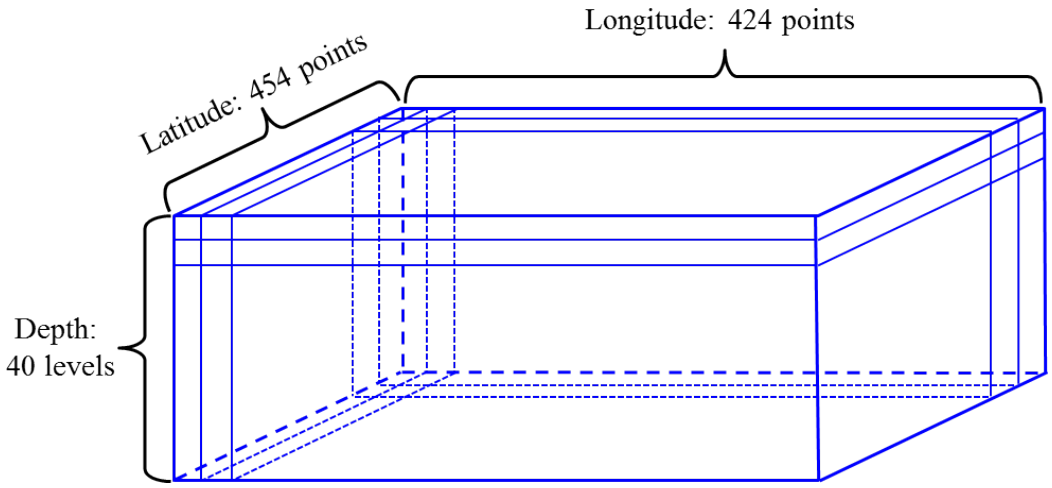

Figure 13. Schema of Grid Data of the Regional NCOM for One Step Time Interval.

The water velocity of Regional NCOM is divided into eastward (u_{ncom}) and northward (v_{ncom}) components, and these components depend on the 4-D variables: longitude, latitude, depth, and time. The time duration of prediction is three hours in one data file. Given every three-hour time interval, the longitude is about 14 degrees long (from 110˚54’ W to 125˚00’ W) dividing linearly by 424 points, and the latitude is about 15 degrees long (from 25˚00’ N to 40˚06’ N) dividing linearly by 454 points, which

means the resolution of position data is 1/30 degree, about 3.6 kilometers. The depth data is divided non-linearly by 40 levels from surface to 5,000 meters. The first 20 steps are from surface to 100 meters, and then the depth is rapidly increasing to maximum depth. Given this original Regional NCOM data, we use linear interpolation for the data processing to match both the Slocum and the Regional NCOM data,

$$f(t_i) = \left[f(t_{N-1}) \frac{t_N - t_i}{t_N - t_{N-1}} \right] + \left[f(t_N) \frac{t_i - t_{N-1}}{t_N - t_{N-1}} \right], \; i = 1, 2, \cdots, N-1, N \tag{10}$$

Now, an example of the method for calculating u at specific time is presented. Let us compute the data of u at time 10:00 with the same position and depth. Since the time interval is three hours, choose two boundary times, 9:00 and 12:00, which include 10:00. If the velocity at 9:00 and 12:00 are 0.5 ms^{-1} and 0.3 ms^{-1}, respectively, the velocity at 10:00 can be calculated as follows.

$$u(10) = \left[0.5 \frac{12-10}{12-9} \right] + \left[0.3 \frac{10-9}{12-9} \right]$$
$$= 0.5 \frac{2}{3} + 0.3 \frac{1}{3} \approx 0.4333 \, ms^{-1}$$

This linear interpolation method is applied to all data sets.

B. METHODOLOGY

In this section, a novel method will be developed through two phases. Phase One proves the importance of the ocean currents by comparing distance d_1 to d_2. d_1 is the distance between the actual resurfaced position (P_{gps}) and final estimated position (P_{dr}) of DR trajectories (T_1), and d_2 is the distance between P_{gps} and the final estimated position (P_{ncom}) of updated DR trajectories (T_2). We also refer to this trajectory as DR_{NCOM}. DR_{NCOM} trajectory is obtained from T_1 by combining its DR position data and the Regional NCOM data with the *simple composite trapezoidal rule*, which is a type of numerical integration.

Phase Two develops a novel correction method to estimate the glider's optimal underwater trajectory by correcting with the depth-averaged and depth-dependent correction methods and by using the simple composite trapezoidal rule. Both correction

methods would increase precision for estimating the glider's trajectory, but to develop a better method, they will be compared. The depth-averaged correction method idea is originated from the depth-average currents calculation method. The depth-averaged correction method calculates the water displacement by dividing the total distance of error ($\Delta X^w, \Delta Y^w$) by time ratio (t_n/t_N) between total transit time (t_N) and at each time (t_n). Since this method corrects the trajectory by linearly calculating the water displacement, we refer to it as the Linear Correction Method (LCM). The depth-dependent correction method is a novel approach for estimating a glider's trajectory, correcting the trajectory by using the spatiotemporally dependent ocean prediction data. Unlike the depth-averaged correction method, this method calculates the water displacement by using the ocean currents prediction data that depend on the depth and time consequent to the location, so the solution cannot be calculated linearly. Thus, we referred to it as the Non-linear Correction Method (NCM).

For this study, the Phase Two is divided into four steps. In Step One and Two, the corrected trajectories by two correction methods are described. In Step Three, an optimal trajectory is estimated, and the corrected trajectories are compared to the optimal trajectory in Step Four. Since this study focuses only on the impact of the ocean currents instead of other factors like the glider's dynamic, mechanics, and measurements, these errors are neglected.

1. Phase One: Proof of the Ocean Effects on Localization

The purpose of this section is to prove the hypothesis that the underwater position of a glider is strongly affected by the ocean currents, and its position estimation can be improved by applying the ocean model prediction data. Once this hypothesis is proven, the Regional NCOM prediction data will be applied to estimating the glider's optimal underwater trajectory in Section 2.

To verify the hypothesis, we compare the distance between the resurfaced and estimated final positions (P_{dr}, P_{ncom}, and P_{gps}) of each trajectory (T_1, T_2, and T_3) in each dive. These trajectories are defined as follows: The first trajectory (T_1) is calculated from the traditional DR algorithm of the glider as we described in Chapter II. The second

trajectory (T_2) is updated by combining the glider's position data on T_1 with the water displacement that is calculated from the Regional NCOM data on T_3 by numerical integration. The third trajectory (T_3) is calculated by linear interpolation between two GPS fixed positions in each dive. Though the linear interpolation is not realistic, this trajectory is used to estimate T_2. Since the glider's actual underwater position cannot be known, we assume the glider follows T_3. In addition, since the time of each point on T_1 and T_3 can be matched, the water velocity of the Regional NCOM data at each position on T_3 also can be used to estimate the water displacement consequent the position of T_2. T_1 and T_3 are calculated from the glider's algorithm, so they are set as reference trajectories to estimate the T_2. To estimate the position of T_2, both the glider's displacement and the water displacement are required to be calculated. The glider's displacement was already calculated from the DR algorithm, but the water displacement is required to be calculated. Since the Regional NCOM prediction data are grid data, the linear interpolation is used to match the time and depth with each point on T_1 as described in Section A. P_{gps} on T_3 is merely obtained from the GPS fixed information. With these three resurfaced positions, we compared the distance between P_{dr} and P_{gps} (d_1) to P_{ncom} and P_{gps} (d_2).

Generally, the displacement ($\mathbf{R}_n$) of marine vehicles can be simply calculated by integration with their velocity ($\mathbf{U}(t)$) during the transit time (t_n).

$$\mathbf{R}_n = \int_{t_0}^{t_n} \mathbf{U}(t)\, dt, \qquad n = 1, 2, \cdots, N-1, N \tag{11}$$

Since the glider's underwater velocity ($\mathbf{U}_g(t)$) is relative to the ocean currents' velocity ($\mathbf{U}_{ncom}(t)$), their total underwater velocity ($\mathbf{U}_{tot}(t)$) can be expressed as

$$\mathbf{U}(t) = \mathbf{U}_{tot}(t) = \mathbf{U}_g(t) + \mathbf{U}_{ncom}(t) \tag{12}$$

By substituting $\mathbf{U}_{tot}(t)$ in Equation (12) into Equation (11), the glider's underwater displacement can be estimated analytically by *numerical integration*

$$\mathbf{R}_n = \int_{t_0}^{t_n} \mathbf{U}_{tot}(t)\, dt = \int_{t_0}^{t_n} \mathbf{U}_g(t)\, dt + \int_{t_0}^{t_n} \mathbf{U}_{ncom}(t)\, dt \tag{13}$$

In this study, however, displacement of the glider can be estimated without calculation because its displacement ($\int_{t_0}^{t_n} \mathbf{U}_g(t)\,dt$) is already calculated as longitude and latitude, and thus, the only thing required to calculate is the water displacement ($\int_{t_0}^{t_n} \mathbf{U}_{ncom}(t)\,dt$). In this study, the analytical solution can be simply calculated as a numerical solution by using the *composite trapezoidal rule,*

$$\begin{aligned}\int_{t_0}^{t_N} \mathbf{U}_{ncom}(t)\,dt &= \int_{t_0}^{t_1} \mathbf{U}_{ncom}(t)\,dt + \int_{t_1}^{t_2} \mathbf{U}_{ncom}(t)\,dt + \cdots + \int_{t_{N-1}}^{t_N} \mathbf{U}_{ncom}(t)\,dt \\ &= \frac{h}{2}\left(\mathbf{U}_0 + \mathbf{U}_1\right) + \frac{h}{2}\left(\mathbf{U}_1 + \mathbf{U}_2\right) + \cdots + \frac{h}{2}\left(\mathbf{U}_{N-1} + \mathbf{U}_N\right) \\ &= \frac{h}{2}\left(\mathbf{U}_0 + 2\mathbf{U}_1 + 2\mathbf{U}_2 + \cdots + 2\mathbf{U}_{N-1} + \mathbf{U}_N\right), \quad h = \frac{t_N - t_0}{N}\end{aligned} \tag{14}$$

This rule can be used when the value of each time interval (Δt) is constant, but Δt in this study is not constant. However, the mean values of the time interval and the velocity difference between each point are small: $\overline{\Delta t} = 4.346\,\text{sec}$, $\overline{u} = 2.06\times10^{-6}\,ms^{-1}$, $\overline{v} = -1.55\times10^{-5}\,ms^{-1}$, respectively, so the error would be small. Therefore, the simple *composite trapezoidal rule* can be applied to calculate the water displacement expressed as

$$\begin{aligned}\int_{t_0}^{t_N} \mathbf{U}_{ncom}(t)\,dt &= \int_{t_0}^{t_1} \mathbf{U}_{ncom}(t)\,dt + \cdots + \int_{t_{N-1}}^{t_N} \mathbf{U}_{ncom}(t)\,dt \\ &= \frac{\Delta t_1}{2}\left(\mathbf{U}_0 + \mathbf{U}_1\right) + \cdots + \frac{\Delta t_N}{2}\left(\mathbf{U}_{N-1} + \mathbf{U}_N\right), \quad \Delta t_i = t_i - t_{i-1}\ (i = 1, 2, \cdots, N)\end{aligned} \tag{15}$$

Generally, a glider's two-dimensional (2-D) movement consists of eastward (x) and northward (y) components, so does the water displacement. Also, water velocity ($\mathbf{U}_{ncom}$) consists of eastward (u_{ncom}) and northward (v_{ncom}) components corresponding to the water displacement ($\delta x_i^w, \delta y_i^w$) at each time interval (Δt_i),

$$\begin{aligned}\delta x_i^w &= \int_{t_{i-1}}^{t_i} u_{ncom}(t)\,dt \simeq \frac{\Delta t_i}{2}(u_{i-1} + u_i), \quad \Delta t_i = t_i - t_{i-1} \\ \delta y_i^w &= \int_{t_{i-1}}^{t_i} v_{ncom}(t)\,dt \simeq \frac{\Delta t_i}{2}(v_{i-1} + v_i), \quad \Delta t_i = t_i - t_{i-1}\end{aligned} \tag{16}$$

Then, the water displacement at time t_n will be

$$\Delta x_n^w = \sum_{i=1}^{n} \delta x_i^w$$
$$\Delta y_n^w = \sum_{i=1}^{n} \delta y_i^w \tag{17}$$

Since the unit of calculated water displacement in Equation (17) is meters, it is required to be converted into units of degree by using Equation (18) to estimate the underwater position of T_2. Note that we assume the one degree in both longitude and latitude as 110 kilometers, i.e., 1.1×10^5 meters.

$$lon_n^w = \Delta x_n^w / (1.1\times10^5)$$
$$lat_n^w = \Delta y_n^w / (1.1\times10^5) \tag{18}$$

Then, each position of T_2 can be obtained by adding the water displacement to the longitude and latitude of the glider displacement. Finally, the glider's underwater position, which is updated by the Regional NCOM prediction, can be obtained as

$$lon_n^{ncom} = lon_n^{dr} + lon_n^w, \qquad n = 1, 2, \cdots, N-1, N$$
$$lat_n^{ncom} = lat_n^{dr} + lat_n^w, \qquad n = 1, 2, \cdots, N-1, N \tag{19}$$

where lon_n^{dr}, lon_n^{ncom} and lat_n^{dr}, lat_n^{ncom} are the longitude and latitude of T_1 and T_2 at each time (t_n). To calculate the distance d_1 and d_2, first calculate the distance with longitude and latitude by using the distance formula; then convert the unit of distance from degrees to meters.

Let the longitude and latitude of P_{gps}, P_{dr}, and P_{ncom} be lon_{gps}; lon_{dr}; lon_{ncom}; lat_{gps}; lat_{dr}; and lat_{ncom}, respectively. Then each distance d_1 and d_2 is calculated as

$$d_1 = \sqrt{(lon_{gps} - lon_{dr})^2 + (lat_{gps} - lat_{dr})^2}\ (1.1\times10^5)$$
$$d_2 = \sqrt{(lon_{gps} - lon_{ncom})^2 + (lat_{gps} - lat_{ncom})^2}\ (1.1\times10^5) \tag{20}$$

After calculating the distance d_1 and d_2, compare the result to prove how well estimated the trajectory is by considering the ocean model prediction data.

2. Phase Two: Trajectory Correction Method Development

To develop a novel method for estimating a glider's optimal underwater trajectory, two correction methods are developed: *the Depth-averaged Correction Method,* which is referred to as *the Linear Correction Method (LCM)* and *the Depth-dependent Correction Method*, which is referred to as *the Non-linear Correction Method (NCM).* Newly corrected trajectories would be produced by combining DR trajectory with the ocean model prediction data. These corrected trajectories will be developed in the first two steps, and an optimal trajectory will be estimated in Step Three. Then two corrected trajectories will be compared to the optimal trajectory in Step Four to determine how well the methods are developed.

a. Depth-Averaged Correction Method: Linear Correction Method (LCM)

The depth-averaged correction is not a newly developed method, but the application of this method to estimate a glider's underwater trajectory would be a new attempt. This method's inspiration is derived from the depth-averaged currents calculation method. Thus, this method is similar to the calculation method of the depth-averaged currents. Figure 3 promotes a better understanding of this method.

When the glider resurfaces after each dive, P_{gps} is the only exact position, and P_{dr} is the estimated position by the DR algorithm. Thus, a position error between P_{gps} and P_{dr} occurs. Since the DR algorithm uses only the glider's velocity, which is relative to the water velocity, and does not consider the ocean currents, the total distance ($\Delta\mathbf{R}^w$) of the error accounts for the ocean current effects, i.e., the water displacement. Therefore, more precise estimation of the glider's underwater trajectory would be obtained by adding the ocean currents displacement to the DR position. The total water displacement consists of eastward (ΔX^w) and northward (ΔY^w) components, and the glider's total transition time is (t_N). Before detailing the method, let us assume that the glider's actual underwater trajectory follows on the linear interpolation trajectory (T_3) because no one knows the actual underwater trajectory of the glider. With this assumption, it is possible to calculate the water displacement (Δx_n^w, Δy_n^w) at each time (t_n) by using the depth-averaged

correction method. The water displacement at each time can be simply calculated from the total water displacement ($\Delta X^w, \Delta Y^w$) divided by the time ratio between the total transit time and at each time (t_n/t_N). Then, the water displacement at each time can be expressed linearly as

$$\begin{aligned} \Delta x_n^w &= \Delta X^w \frac{t_n}{t_N}, \quad n = 1, 2, \cdots, N-1, N \\ \Delta y_n^w &= \Delta Y^w \frac{t_n}{t_N}, \quad n = 1, 2, \cdots, N-1, N \end{aligned} \tag{21}$$

Since the water displacement is calculated linearly consequent to the estimated position, we refer to this method as the Linear Correction Method. As in the first phase, since the unit of each DR position data (lon_n^{dr}, lat_n^{dr}) is degrees and the unit of water displacement is meters, the latter needs to be converted to degrees (lon_n^{cor}, lat_n^{cor}) by

$$\begin{aligned} lon_n^{cor} &= \Delta x_n^w / (1.1 \times 10^5) \\ lat_n^{cor} &= \Delta y_n^w / (1.1 \times 10^5) \end{aligned} \tag{22}$$

Then, the estimated underwater position of the glider (lon_n^{est}, lat_n^{est}) at each time can be expressed as

$$\begin{aligned} lon_n^{est} &= lon_n^{dr} + lon_n^{cor} \\ lat_n^{est} &= lat_n^{dr} + lat_n^{cor} \end{aligned} \tag{23}$$

We can estimate the glider's underwater position using this simple and fast correction method. This method, however, does not consider the actual ocean currents since the real position cannot be obtained. Moreover, it calculates the water displacement linearly and does not consider the ocean currents' dependence on depth and time. Therefore, the more precise method using depth-dependent correction will be discussed in the following section.

b. Depth-Dependent Correction Method: Non-linear Correction Method (NCM)

Depth-dependent correction is a novel method which considers the spatiotemporal effects of the ocean current, so it is expected that a more precise underwater position of the glider would be estimated with this method. Like the depth-averaged correction

method, the depth-dependent correction method considers the effects of ocean current, but the latter uses the spatiotemporally dependent data of ocean model prediction to estimate more precise water displacement rather than the depth-averaged water displacement for estimating a glider's underwater trajectory. Also, the assumption that the glider's actual underwater trajectory follows on the linear interpolation trajectory is still valid. The primary difference between the two methods is the calculation method of the water displacement. The depth-averaged correction method calculates the water displacement linearly by multiplying total displacement ($\Delta X^w, \Delta Y^w$) by time ratio (t_n / t_N) at each time (t_n) as shown in Equation (21). The depth-dependent correction method, on the other hand, calculates the water displacement by using the Regional NCOM prediction data, which is dependent on the depth of the glider (z) at each time-consequent location. Since this method calculates the water displacement spatiotemporally, the solution is not linear. Therefore, we refer to this method as the Non-linear Correction Method (NCM).

In this method, Equation (11) to Equation (13) can be applied to estimate the glider's underwater position, and the glider's subsurface displacement is also calculated by the DR algorithm with the Slocum data. Thus, the only aspect that needs to be calculated is the water displacement. The water displacement ($\Delta \mathbf{r}_n^w$) at time (t_n) is calculated from the Regional NCOM data on T_3 by

$$\Delta \mathbf{r}_n^w = \int_{t_0}^{t_n} \mathbf{U}_{ncom}(t)\, dt, \qquad n = 1, 2, \cdots, N-1, N \tag{24}$$

The Regional NCOM prediction data have 4-D variables, i.e., $\mathbf{U}_{ncom}(x, y, z, t)$, and the water velocity consists of the eastward (u_{ncom}) and the northward (v_{ncom}) component, as already mentioned in Section 1 in this chapter. In this section, however, we will only present the method to calculate eastward displacement. The northward displacement can be calculated by substituting v_{ncom} with u_{ncom} in each equation. The water displacement can be simply calculated by the simple composite trapezoidal rule of numerical integration, which is the same as in Equation (16) and Equation (17).

Therefore, the water displacement of the eastward component (Δx_n^w) at time (t_n) is calculated as

$$\Delta x_n^w = \int_{t_0}^{t_n} u_{ncom}(t)\, dt \simeq \sum_{i=1}^{n}\left[\frac{\Delta t_i}{2}(u_{i-1}+u_i)\right] = \sum_{i=1}^{n}\left(u_i^{ncom}\Delta t_i\right), \quad \text{where } u_i^{ncom} = \frac{u_{i-1}+u_i}{2} \text{ and } \Delta t_i = t_i - t_{i-1} \tag{25}$$

In Equation (25), however, the depth-dependent water velocity of the Regional NCOM prediction data is required to calculate the water displacement, using the depth-dependent correction method. In addition, the water velocity of the Regional NCOM prediction data depends on the time-consequent location, so the eastward component of the water velocity can be expressed as $u_i^{ncom}(z_i, t_i)$. Even though the depth-dependent water velocity is used to correct the trajectory, the corrected trajectory would not follow the real trajectory, and the final position of the corrected trajectory would not match with P_{gps}, like T_2 in Figure 2. Therefore, some equations for correcting the water velocity will be discussed to match the final position, and thus to correct the trajectory more precisely.

The eastward component of the water velocity of the Regional NCOM prediction data at each time can be expressed in three parts as

$$u_i^{ncom}(z_i, t_i) = \frac{u_i^{ncom}(z_i, t_i)}{u_i^{ncom}(0, t_i)} \frac{u_i^{ncom}(0, t_i)}{u_{\max}} u_{\max} \quad \text{where } u_{\max} = \max\left[u_i^{ncom}(0, t_i)\right], i = 1, 2, \cdots, N \tag{26}$$

The first part of the right-hand side shows the velocity ratio between the surface and the glider's depth at time t_i, and the second part presents the surface velocity ratio between the position of maximum surface velocity during transit time of one dive (t_N) and the position of the glider at time t_i. We refer to these two parts as *z factor* (f_i^z), and *t factor* (f_i^t), respectively.

$$f_i^z = \frac{u_i^{ncom}(z_i, t_i)}{u_i^{ncom}(0, t_i)},\ f_n^t = \frac{u_i^{ncom}(0, t_i)}{u_{\max}} \quad \text{then, } u_i^{ncom}(z_i, t_i) = f_i^z f_n^t u_{\max} \tag{27}$$

The third part indicates the maximum surface velocity during the transit time of one dive, and the maximum velocity has a constant value. If the value of maximum velocity is the same as shown Equation (26), the corrected trajectory would be exactly same with the results of the Phase One. Thus, the velocity of the Regional NCOM data for trajectory correction will be redefined more realistically as

$$u_i^{cor}(z_i, t_i) = f_i^z f_i^t u_{\max}^{cor} \tag{28}$$

Moreover, since no one knows the actual trajectory of the glider consequent the value of the maximum surface velocity, a new equation that does not use the maximum surface water velocity is required. For this study, it is assumed that there is no error between the ocean current structure of in-situ data and that of the Regional NCOM prediction data. Given this assumption, we can apply z factor and t factor to correct the trajectory. Let the total eastward water displacement at final position (t_N) during one dive be ΔX^w. Substitution of Equation (28) into Equation (25) leads to

$$\Delta X^w = \sum_{i=1}^{N} u_i^{cor}(z_i, t_i)\Delta t_i = \left(\sum_{i=1}^{N} f_i^z f_i^t \Delta t_i \right) u_{\max}^{cor} \tag{29}$$

After that, the maximum surface velocity to correct the trajectory is re-expressed as

$$u_{\max}^{cor} = \frac{\Delta X^w}{\sum_{i=1}^{N} f_i^z f_i^t \Delta t_i} \tag{30}$$

Similarly, the water displacement of each trajectory at time t_n is given by

$$\Delta x_n^w = \sum_{i=1}^{n} u_i^{cor}(z_i, t_i)\Delta t_i = \left(\sum_{i=1}^{n} f_i^z f_i^t \Delta t_i \right) u_{\max}^{cor} \tag{31}$$

Finally, the water displacement of each trajectory at time t_n can be re-expressed as

$$\Delta x_n^w = \Delta X^w \frac{\sum_{i=1}^{n} f_i^z f_i^t \Delta t_i}{\sum_{i=1}^{N} f_i^z f_i^t \Delta t_i} \tag{32}$$

After calculating the corrected water displacement, processing for estimating the glider's underwater trajectory is the same with the LCM as shown in Equation (22) and Equation (23).

c. Application to Four Steps

This section describes the application of two developed correction methods to DR trajectory correction. In first two steps, DR trajectory is corrected by using two correction methods without comparing because there is no reference trajectory to determine improvement of estimated trajectory. In Step Three, an optimal trajectory is estimated as a reference trajectory by using iteration method, incorporating the depth-dependent correction method. Then, two corrected trajectories are compared to a reference trajectory in Step Four. By comparing these three trajectories, it would be possible to determine which correction method is better for estimating a glider's optimal underwater trajectory. The brief explanation of each step is as follows.

(1) Step One: The Depth-averaged Correction with DR

In this step, DR trajectory (T_1) is corrected using the depth-averaged correction method. The schema of this method is the same as shown in Figure 3. This corrected trajectory is referred to as C_1. The C_1 is expected to be a less accurate trajectory than other corrected trajectory.

(2) Step Two: Depth-dependent Correction with DR

In this step, T_1 is corrected using the depth-dependent correction method. The schema of this method is the same as shown in Figure 4. This corrected trajectory is referred to as C_2. C_2 is expected to be a more accurate trajectory than C_1.

(3) Step Three: Optimal Trajectory Development using Iteration Method with the C_2

In this step, more precise trajectory of the glider is estimated by iterating the C_2 until relative error converges to 10^{-5}. This corrected trajectory is referred to as C_3. C_3 is expected to be the most precise trajectory among the three trajectories. Thus, it is also referred to as an optimal trajectory.

(4) Step Four: Comparison Three corrected Trajectories

In this step, two corrected trajectories will be compared to an optimal trajectory (C_1 and C_3, C_2 and C_3) to determine which correction method is more precise for estimating a glider's optimal underwater trajectory.

C. CHAPTER SUMMARY

To increase the precision of a glider's trajectory, a novel method was developed by applying the Regional NCOM data through two phases and four subset steps in Phase Two.

In Phase One, we attempted to show the influence of ocean currents by applying the Regional NCOM data to the DR trajectory. In Phase Two, we aimed to develop two correction methods: the depth-averaged and the depth-dependent correction methods for estimating the glider's optimal underwater trajectory. Even though both correction methods consider the ocean currents, the former corrects the glider's trajectory linearly; and this linear correction method would be relatively less accurate. Thus, to correct trajectory more precisely, we developed the latter method. Since the latter method considers the ocean currents dependence on depth and time-consequent location, it could estimate a glider's underwater trajectory more accurately than the former one. With these two developed methods, we corrected the DR trajectory by applying them to two different steps. Then, two correction methods are evaluated by comparing two corrected trajectories to an optimal trajectory. In Chapter IV, the results of these correction methods will be analyzed by comparing the corrected trajectories.

IV. RESULTS AND DISCUSSION

This chapter provides results of this study, analyzing corrected trajectories by applying the two correction methods that were described in Chapter III. Detailed results of each phase and step will be discussed, as well as the relevance of this study to the ROKN.

A. RESULTS

The analysis is divided into two subsections. In the first section, the DR (T_1) and the DR_{NCOM} (T_2) trajectories are compared to each other to show that the Regional NCOM prediction data have an impact on improving the accuracy of a glider's DR trajectory. After obtaining updated trajectories, the distances between final points of each trajectory P_{gps} and P_{dr} (d_1), P_{gps} and P_{ncom} (d_2) are compared to each other. In the second section, it is determined which method is a better correction method for estimating a glider's optimal underwater trajectory throughout the four steps. Step One deals with results of DR trajectories, which are corrected by the depth-averaged correction method (C_1). Step Two provides results of DR trajectories, which are corrected by the depth-dependent correction method (C_2). Since there is no actual trajectory that can compare with the C_1 and C_2 to prove their estimation precision, an optimized trajectory (C_3) is estimated. After obtaining the C_3, the C_1 and the C_2 are compared to C_3 to determine which method is a better.

1. Result of Phase One

This section presents the importance of the ocean current effects in estimating a glider's underwater trajectory by comparing the distance between d_1 and d_2 for each dive. Figure 14 shows an example of the results, and more figures of results are shown in Appendix A. Distance d_1 and d_2 are calculated by using Equation (20). These two distances are then compared by calculating absolute differences ($d_2 - d_1$) and relative differences ($[d_1 - d_2]/d_1$). However, before comparing these distances' differences, results of distance d_1 and d_2 are analyzed statistically as shown in Table 2.

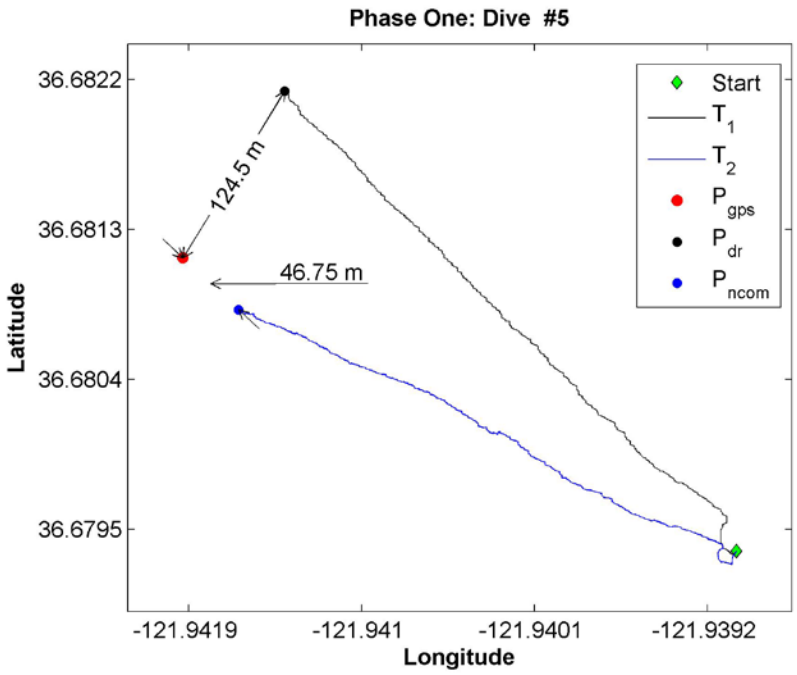

Figure 14. An Example Result of Phase One: Downward Looking View of DR and DR_{NCOM} Trajectories.

Table 2. Statistical Analysis of Distance d_1 and d_2.

Distance	d_1 (P_{gps} - P_{dr})	d_2 (P_{gps} - P_{ncom})
Mean	168.895 m	62.970 m
Minimum	38.421 m	7.219 m
Maximum	295.417 m	264.922 m
Median	167.170 m	50.697 m
Standard Deviation	66.147 m	40.196 m

Since T_1 was estimated by the traditional DR algorithm without considering the ocean current effects, the values of d_1 were larger than those of d_2. Next, the absolute and relative improvements of T_2 compared to T_1 were calculated for each dive. As shown in Figure 15, by applying the Regional NCOM prediction data, most of the T_2 trajectories improved by 97.18% compared to the T_1 trajectories. These results were similar to those of previous work from Smith et al. (2010a).

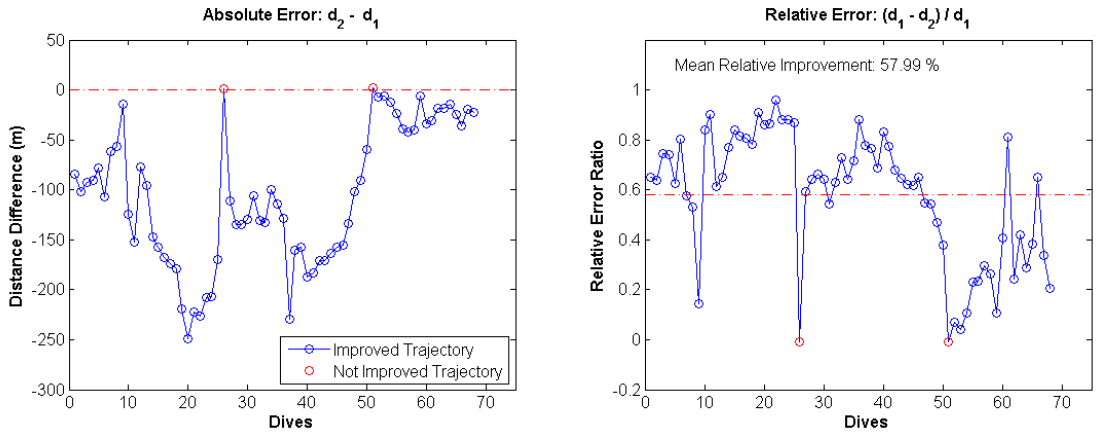

Figure 15. Absolute and Relative Differences between d_1 and d_2.

In addition, the statistical analysis of both absolute and relative differences between d_1 and d_2 was provided in Table 3. The mean of absolute difference was -105.93 meters, and its standard deviation was 69.21 meters. The root mean square (RMS) of distance difference was 126.25 meters. Furthermore, the T_2 improved by 58.0% in terms of mean relative distance difference, 25.9% in terms of standard deviation, and 63.4% in terms of RMS. These results are enough to account for the ocean current effect in estimating a glider's underwater trajectory. Based on these results, Phase Two attempted to develop a novel method for estimating a glider's optimal underwater trajectory by applying the Regional NCOM to the DR trajectory.

Table 3. Statistical Analysis of the Absolute and Relative Differences between d_1 and d_2.

Differences	Absolute Values	Relative Ratio
Improvement	97.06 %	
Mean	-105.93 m	0.5799
Standard Deviation	69.21 m	0.2588
RMS	126.25 m	0.6343

2. Results of Phase Two

This section discusses the results of applying two correction methods to the DR (T_1) trajectory in four steps. In the first two steps, two different corrected trajectories, the DR trajectory corrected by the depth-averaged correction method (C_1) and the DR trajectory corrected by the depth-dependent correction method (C_2), were estimated. Then, to compare these two correction methods, an optimal trajectory (C_3) was estimated by using the iteration method from C_2 until the relative error converges to less than 10^{-5} with the Regional NCOM prediction data. Finally, the C_1 and C_2 were compared to C_3 to determine which correction method is better for estimating a glider's underwater trajectory more precisely.

a. Step One: DR Trajectory Corrected by the Depth-Averaged Correction Method

Step One provides the results of the depth-averaged correction method when applied to the DR trajectory (T_1). Generally, since this method corrected trajectory linearly, the shape of the corrected trajectory (C_1) looked similar to T_1. Moreover, the length of the C_1 was shorter than the original T_1. Figure 16 shows an example of the results, and more figures of results are shown in Appendix A.

b. Step Two: DR Trajectory Corrected by the Depth-Dependent Correction Method

Step Two provides results of the depth-dependent correction method when applied to the DR trajectory (T_1) (see Figure 17). Actually, this step was supposed to deal with the DR_{NCOM} trajectory (T_2), but the results of this correction method for T_1 and T_2 are theoretically the same because T_2 is updated from T_1 by considering the depth-dependent Regional NCOM prediction data. Thus, T_1 could be used directly without any additional processing to compensate for the ocean current effects, which was done in Phase One. Therefore, T_2 did not need to be corrected with either of the two correction methods in this study. The mathematical proof is presented in Appendix B due to its complexity.

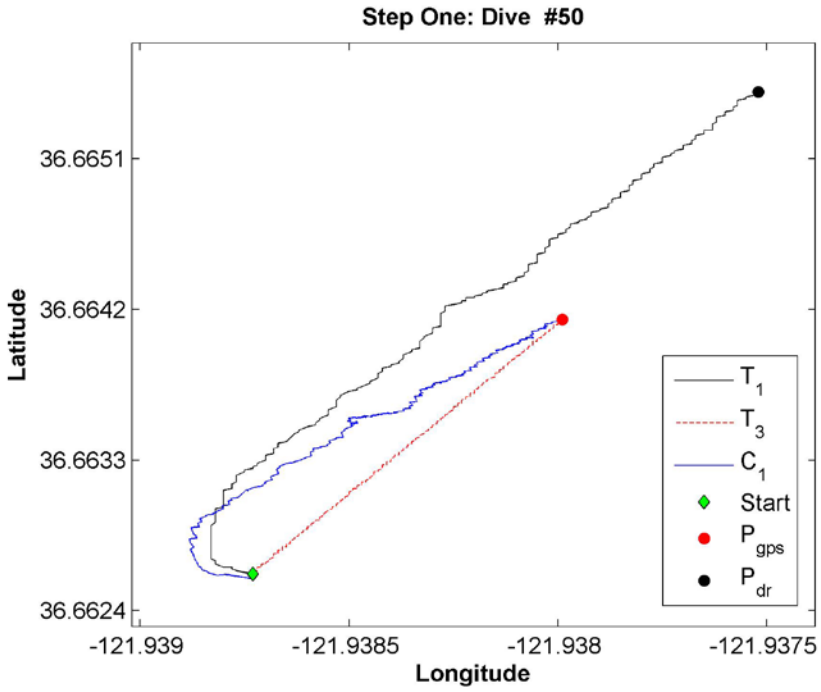

Figure 16. The Result of Step One: Downward Looking View of the T_1, the T_3, and the C_1 with the Depth-averaged Correction Method.

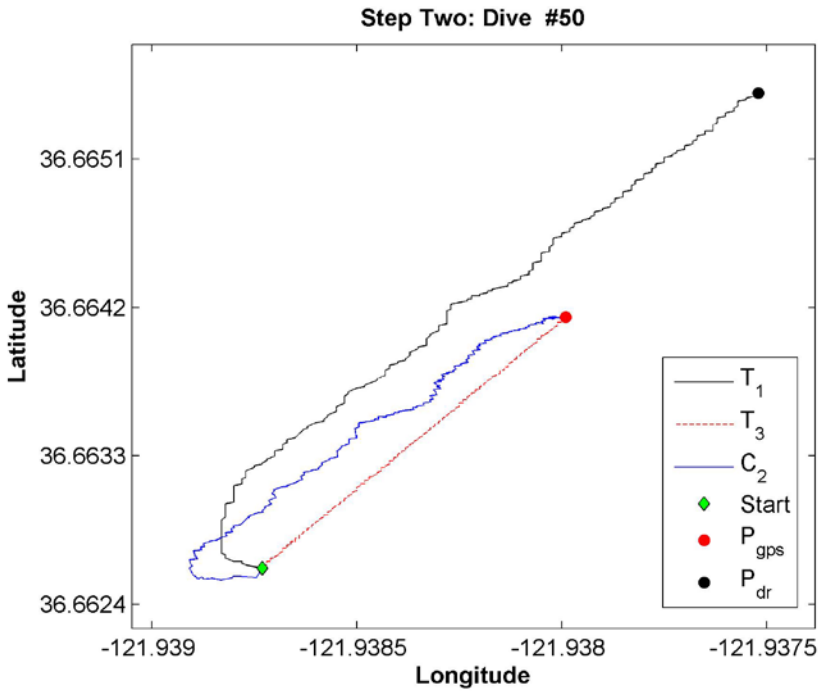

Figure 17. The Result of Step Two: Downward Looking View of the T_1, the T_3, and the C_2 with the Depth-dependent Correction.

Unlike the depth-averaged correction method, the depth-dependent correction method corrected trajectory nonlinearly using the Regional NCOM prediction data, which depends on the depth, time-consequent location. Since this method corrected T_1, the shape of the corrected trajectory (C_2) might look similar to T_1, but C_2 was more meandering than C_1 due to the dependence of the Regional NCOM prediction data. In addition to the example result of Step Two that is shown in Figure 17, more figures of results are shown in Appendix A.

Both C_1 and C_2 appear to be more accurate than the original T_1, but this result is inconclusive. It cannot be determined which trajectory, C_1 or C_2, was estimated more precisely due to the lack of a glider's actual trajectory information. At this time, results suggest that C_2 was estimated better than T_1 using the depth-averaged correction method by incorporating the Regional NCOM prediction data. It is, however, difficult to determine which trajectory was more precisely compared to the real trajectory.

c. Step Three: Optimal Trajectory Development by Using Iteration Method from the C_2

To address the problems caused in the previous two steps, an optimal trajectory was developed as a reference point for comparison to determine a better correction method. It is not an easy way to estimate an optimal trajectory because there is less information: the linearly interpolated trajectory (T_3), which is not a real trajectory, between each GPS fixed position, the corrected DR trajectory with the depth-dependent correction method (C_2), and the Regional NCOM prediction data as the ocean currents information. Furthermore, since the Regional NCOM prediction data is not exactly same with the real ocean currents velocity, it is assumed that the ocean currents structure of the Regional NCOM is similar to that of the in-situ. Given these data and assumption, an optimal trajectory was estimated from C_2 by using the iteration method (see Figure 18).

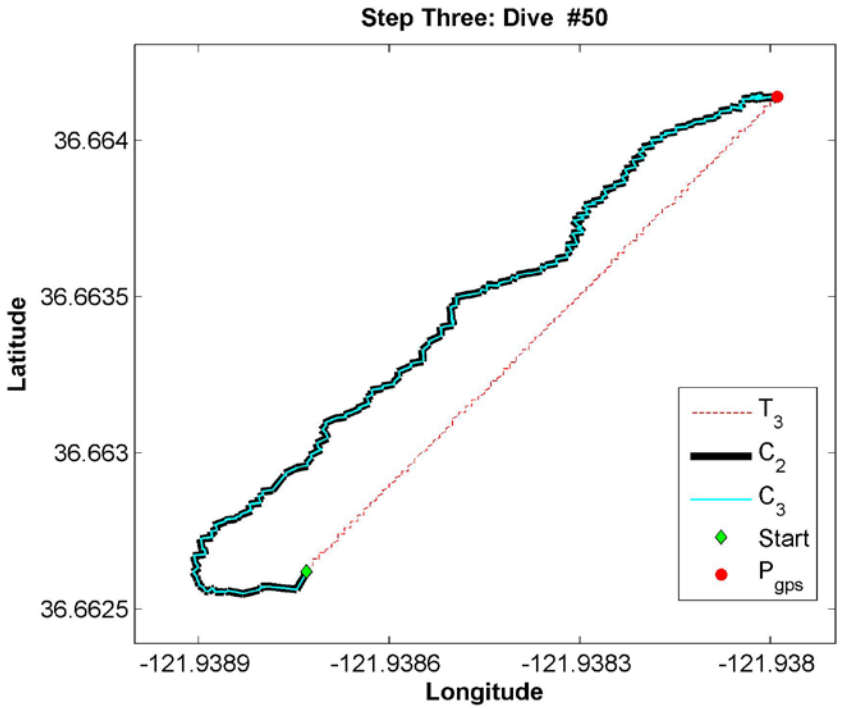

Figure 18. The Result of Step Three: Downward Looking View of C_2 and its Iterated Trajectory, C_3.

In this section, the relative error calculation method and the procedure of the iteration method will be explained briefly. The details of the iteration method are presented in Appendix C, and more figures of results are shown in Appendix A.

First, the relative error calculation method is explained as follows. Let the reference and iterated trajectory be T_m, T_{m+1}, the sum of distance difference between two trajectories be D_m, and the total length of the reference trajectory be L_m at each step. Then the relative error (E_{rel}) at each step can be calculated by dividing D_m by L_m as shown in Equation (33).

$$E_{rel} = D_m / L_m, \quad m = 1, 2, \cdots, M-1, M \tag{33}$$

Now, the procedure of the iteration method will be explained. In the first step, it is assumed that the initial reference trajectory is T_3, and then the C_2 is estimated from T_1 by applying the depth-dependent correction method against the distance difference between P_{dr} and P_{gps} (ΔX^w, see Figure 4). The used Regional NCOM prediction data are obtained

from each point on T_3. After estimating the C_2, the relative error is computed by using Equation (33), but this step is not included in the iteration step.

After the first step, C_2 becomes a reference trajectory, and the Regional NCOM prediction data is obtained from each point on C_2 as in the first step. Then T_1 is corrected again by using the depth-dependent correction method against the same distance difference ΔX^w as the first step. This time is regarded as the first iteration. After the first iteration, the relative error is calculated. If the value of relative error is less than 10^{-5}, the iteration is finished, and the final trajectory, which is estimated by the iteration method, would be the C_3.

In this study, the mean iteration steps were 3.088 with the maximum of eight steps, and the mean relative error at Step One, Two, and Three was 0.387, 0.001, and 0.003, respectively. Table 4 provides the statistical results of the iteration method.

Table 4. Statistical Analysis of the Iteration Method.

Relative Error	First Step	Second Step	Third Step
Mean	0.387	0.001	0.003
Minimum	0.002	1.309×10^{-6}	0.000
Maximum	20.056	0.448	0.193
Median	0.034	0.059	0.023
Standard Deviation	2.431	9.646×10^{-5}	3.972×10^{-7}

Even though an optimal trajectory can be estimated with iteration method, the precision of the trajectory is not guaranteed. For the purpose of this study, however, it is assumed that C_3 is the most similar trajectory to a real trajectory.

d. Step Four: Comparison of Three Types of Corrected Trajectories

This section provides results of comparison between two types of corrected trajectory, C_1 and C_2, to an estimated optimal trajectory, C_3, to determine which correction method is better for estimating a glider's optimal underwater trajectory. Figure 19 presents comparison of these three trajectories, and more figures of results can be seen in Appendix A.

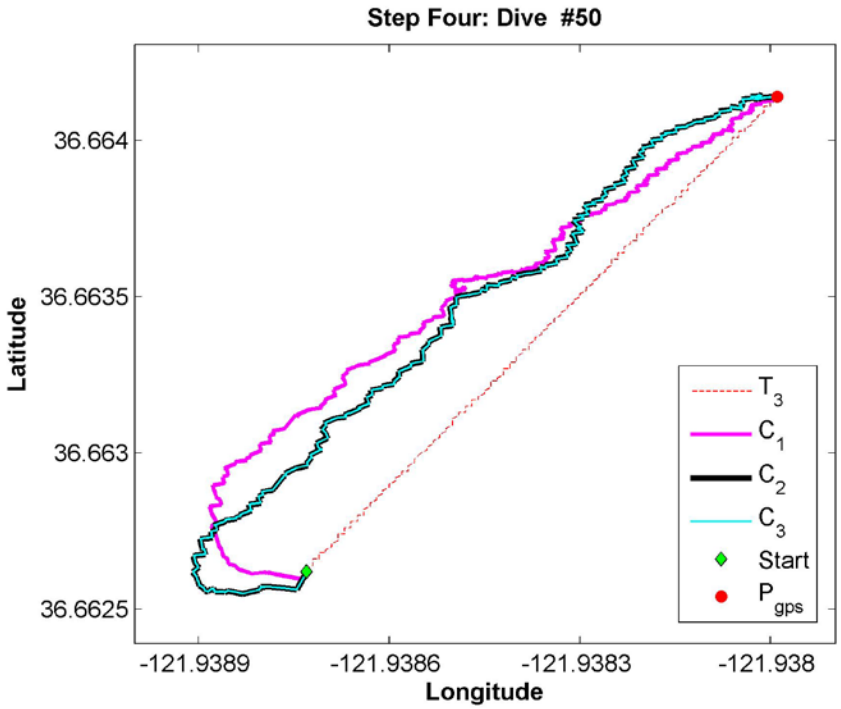

Figure 19. Downward Looking View of Three Types of Corrected Trajectory.

Given these three trajectories, the RMS of distance difference between C_1 and C_3 (d_3), C_2 and C_3 (d_4) for each dive was calculated to determine a better method. Table 5 provides statistical analysis of the RMS of distance d_3 [RMS (d_3)] and d_4 [RMS (d_4)] for total dives, and Figure 20 shows absolute and relative differences between RMS (d_3) and RMS (d_4).

Table 5. Statistical Analysis of the RMS (d_3) and RMS (d_4) for Total Dives.

RMS of Distance	d_3 (C_1 - C_3)	d_4 (C_2 - C_3)
Mean	9.890 m	1.034 m
Minimum	1.195 m	0.003 m
Maximum	80.536 m	59.100 m
Median	6.316 m	0.052 m
Standard Deviation	11.052 m	7.168 m

From the Table 5, all values of RMS (d_4) are less than RMS (d_3), which means the C_2 was more close to the C_3. In addition, from Figure 20, it can be said that the C_2 was better estimated than C_1 by comparing the absolute and relative differences between RMS (d_3) and RMS (d_4).

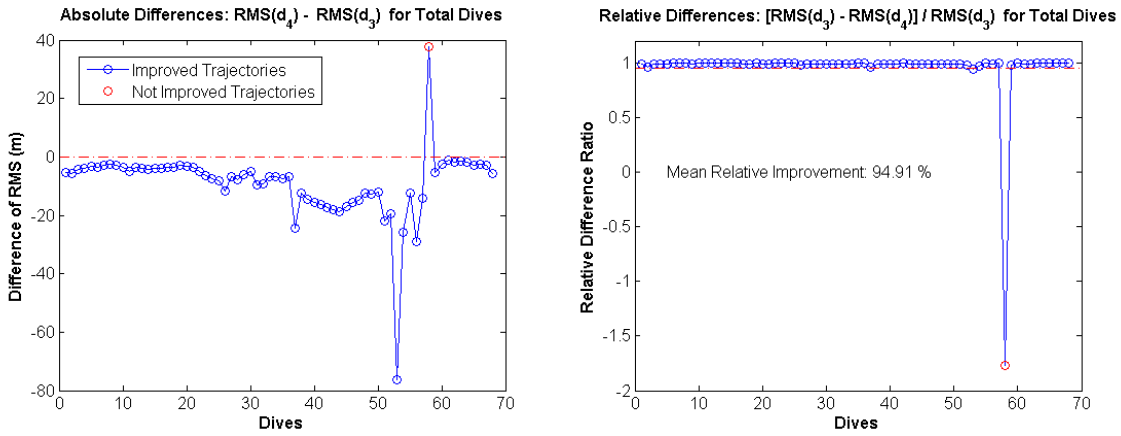

Figure 20. Absolute and Relative Differences between RMS (d_3) and RMS (d_4) for Total Dives.

Table 6 provides statistical analysis of the maximum distance of d_3 and d_4 for total dives. Like the analysis of RMS of distance, all values of d_3 are larger than those of d_4. This also means C_2 was closer to C_3.

Table 6. Statistical Analysis of the Maximum Distance of d_3 and d_4 for Total Dives.

Maximum Distance	d_3 (C_1 - C_3)	d_4 (C_2 - C_3)
Mean	16.052 m	2.142 m
Minimum	1.912 m	0.005 m
Maximum	142.648 m	123.491 m
Median	10.070 m	0.095 m
Standard Deviation	19.354 m	14.987 m

In addition to the statistical analysis, Figure 21 describes the maximum distance of d_3 and d_4 for total dives. Only four of the data of d_4 were longer than one meter, but no data of d_3 was less than one meter.

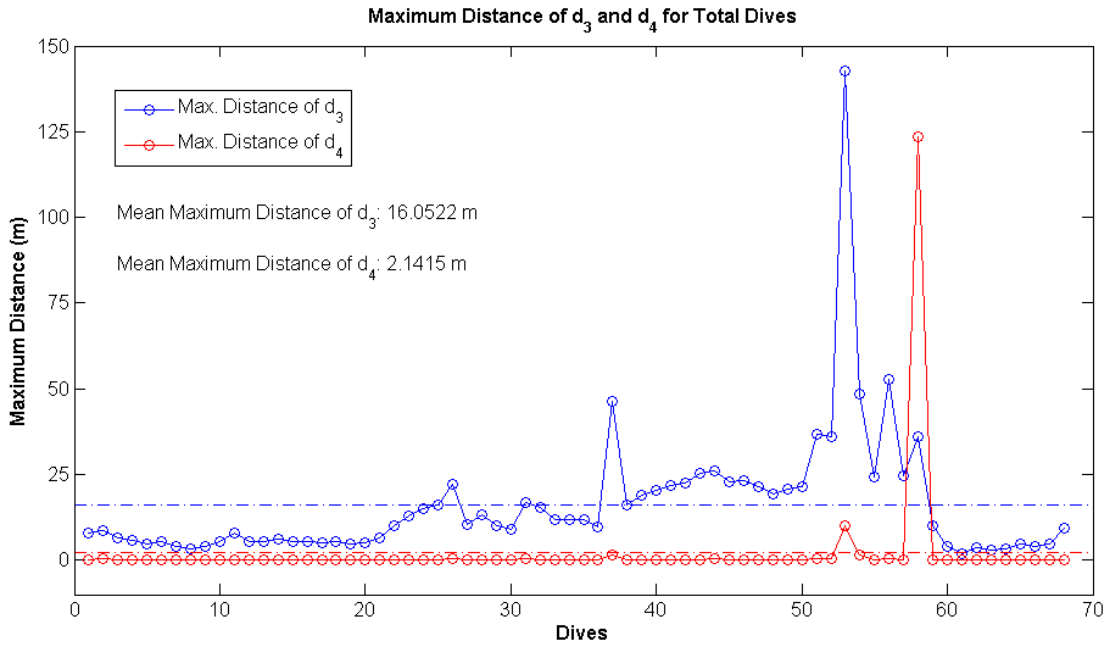

Figure 21. Maximum Distance of d_3 and d_4 for Total Dives.

By comparing these results, the tentative conclusion can be expressed that C_2, which was corrected by the depth-dependent correction method, was estimated more precisely than C_1, which was corrected by the depth-averaged correction method.

Now, a controversial issue can be argued as to which trajectory was estimated more precisely between C_2 and C_3. It is expected that C_3 would be more precise than C_2 because C_3 was estimated by the iteration method by considering the Regional NCOM prediction data, which depends on the depth and time-consequent location, on the corrected trajectories. Even though the iteration method makes the trajectory more precise than without iteration, the depth-dependent correction method would be more efficient than the iteration method because the iteration method is complex and difficult to deal with, so it would take more processing time to estimate C_3 requires than that to

estimate C_2. Furthermore, the distance difference between C_2 and C_3 was minimal. Therefore, if the time cost of data processing is larger than the distance difference cost, it is expected that the depth-dependent correction method without combining with the iteration method would be an efficient and precise enough method for estimating a glider's optimal underwater trajectory.

B. DISCUSSION

This section discusses the relevance of findings in this study to the ROKN. It is divided into three parts: advantages of an underwater glider in ASW, relevance of findings to ASW, and relevance to future ASW in the ROKN. The first section describes three high-level advantages of the underwater glider in ASW: cost-effectiveness, various mission capabilities, and risk reduction. The second section discusses relevance of findings to ASW by reviewing the U.S. Navy Unmanned Undersea Vehicle Master Plan (UUVMP) (DON 2004) and by applying four Sub-Pillar missions to the underwater glider in ASW. An optimally estimated trajectory would be beneficial to operating ISR in the area of interest, detecting and identifying the enemy's bottoming submarine, enhancing and supporting tactical oceanography by providing spatiotemporally high resolution ocean data, and providing communication and localization information. Finally, we discuss the relevance of these findings to future ASW by reviewing ASW threats to the ROKN and by suggesting recommendations for using the underwater glider for ASW in the ROKN.

1. Advantages of the Underwater Glider in ASW

An underwater glider has primarily been used for oceanographic research with data collection or environment monitoring. Recently, however, there is an increasing tendency to take advantage of the glider in naval operations, especially, ASW. Some UUVs were already used in previous naval operations; for example, the REMUS was employed for mine countermeasures (MCM) operations during Operation Iraqi Freedom (Clegg and Peterson 2003). However, the glider has not been deployed in real-time combat operations yet, and the development of the glider's capability and concept of operations (CONOPs) for ASW is still ongoing. Even though the glider needs to be

improved in various fields, it is expected that the glider will be an effective platform in the future ASW due to their various high-level advantages as follows.

a. Cost Effectiveness

An underwater glider is designed for long-duration and long-range missions. Its propulsion system requires less energy, and it is cheaper than ships or other marine vehicles, which perform similar missions. Thus, its low cost allows multiple gliders to be deployed and to patrol in a broader area than other ships. Furthermore, they can collect more spatiotemporally vast ocean data than existing ocean observation ships or instruments. For these reasons, the underwater glider is cost-effective platform.

b. Various Mission Capabilities

A glider can be equipped with additional sensors for various missions; for example, acoustic sonar for ISR, side scan sonar (SSS) for detecting a bottoming submarine, and some optic sensors for detecting and identifying unknown underwater targets. Even though installing additional sensors shortens a glider's mission time, the navy could benefit from a glider's mission capabilities. This is because a glider can cover wider mission area and perform for a longer time with less cost than presently used ships or other marine vehicles. In addition, the glider's cost-effectiveness allows multiple gliders to be deployed simultaneously. For example, a fleet of gliders would be able to act as an intelligence network by gathering underwater target information simultaneously. By doing so, they can provide more precise target information, so that the ASW capability would be increased. Moreover, multiple gliders can act as communication nodes with other platforms such as surface ships, submarines, and other UUVs in the subsurface area. For these reasons, a glider's ASW capability effectiveness would be increased.

c. Risk Reduction

Even though an underwater glider has various mission capabilities, it is still required to deploy manned platforms to accomplish the ROKN's mission more effectively. Manned platforms, however, have an ever-present danger when they perform

missions in a hazardous operation environment like a shallow-water, mine burial area. Since an underwater glider is an unmanned vehicle and is operated autonomously, manned platforms can be replaced by the glider in such perilous AO; for example, explosive ordnance disposal (EOD) and mine localization. Especially, the glider could be a safe platform when performing ASW operations because it is relatively quieter than other UUVs due to its buoyancy-driven engine. The quietness makes the glider generate less self-noise so it has superior detection ability when it attempts to detect underwater targets by using acoustics. Furthermore, the quietness makes the enemy have more difficulty detecting a glider. Therefore, an underwater glider would be able to perform its mission more safely and it offers more opportunity to accomplish its mission more successfully.

2. Relevance of Findings to ASW

The following two subsections discuss the relevance of findings from this study to ASW in the ROKN. The first subsection outlines the overview of the U.S. Navy UUVMP to provide the background of the UUV's nine Sub-Pillar missions based on the Sea Power 21 pillars. The second subsection discusses the relevance of findings to ASW related to the UUVs' mission capabilities mentioned in the Master Plan. This section constrains the area of cover to four capabilities related to ASW: ISR; Littoral ASW; Tactical Oceanography; and Communication/Navigation Network Nodes (CN3).

a. Overview of the U.S. Navy UUVMP

The U.S. Navy UUVMP (hereafter referred to as UUVMP) is an updated UUVMP based on the 2000 UUVMP. It was updated due to changes in various fields in the U.S. Navy: technology, platforms, and other factors (DON 2004). The UUVMP classifies the high-priority missions based on the four Sea Power 21 pillars: *Sea Shield*, *Sea Strike*, *Sea Base*, and *FORCEnet* (DON 2004). Then, these four pillars are divided by UUV missions into nine sub-pillar missions as shown in Figure 22, and the details of each mission are described in the Master Plan. However, not all sub-pillar missions can be performed by an underwater glider due to its minimal velocity and limited payload.

For these reasons, we will discuss the relevance of findings related to only some of those capabilities in ASW operations: ISR; Littoral ASW; Tactical Oceanography; and CN3.

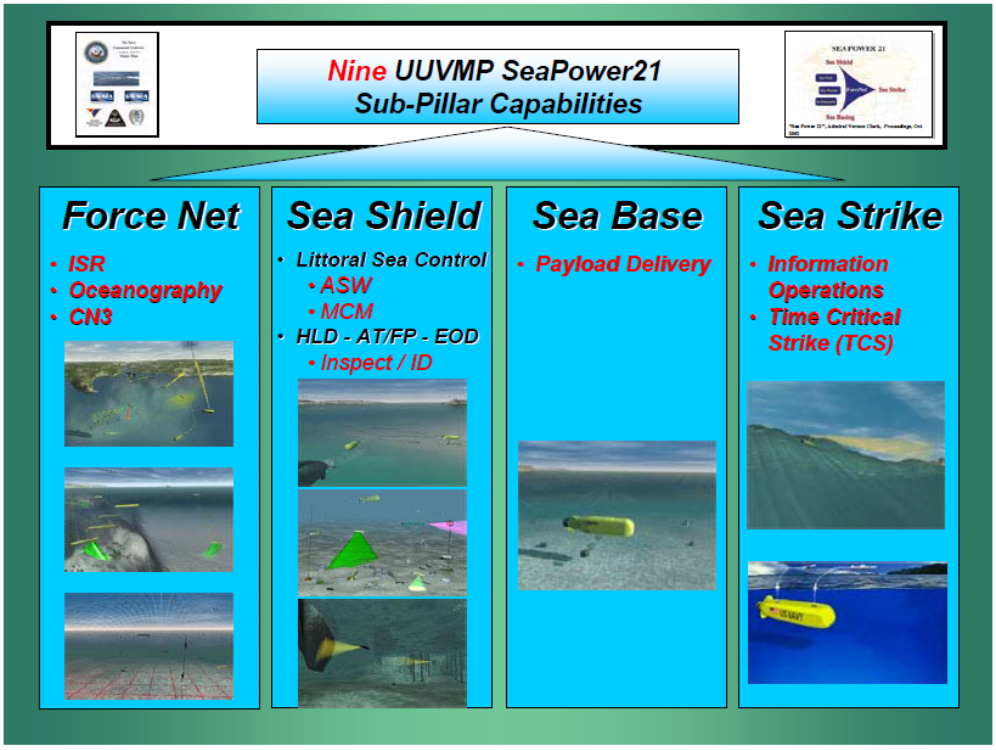

Figure 22. Sea Power 21 Nine Sub-Pillar Capabilities (from DON 2004).

b. Relevance Related to the UUVMP

In this section, the relevance of findings to the ROKN that relate to the UUVMP and ASW operations will be detailed in four sub-pillar missions as follows.

(1) ISR

ISR is an essential operation in ASW. The ISR mission consists of intelligence gathering, target detection and localization, and mapping (DON 2004). An underwater glider can be used for persistent and clandestine ISR, and it can perform the mission effectively with high-endurance and long-range capabilities, its ability to operate in shallow water and coastal areas, and its autonomous features (DON 2004). The glider can patrol a friendly harbor or coastal area near the high-value infrastructures. Even though

the glider is limited in its ability to attack an enemy submarine directly due to its minimal velocity and limited payload, it can provide more precise and reliable target information in the area of interest. Thus, the ROKN can get the target information more precisely and prevent the enemy from infiltrating into friendly territory. This precise information makes the navy spend less effort to detect, to identify, and to attack the enemy underwater forces in ASW.

(2) Littoral ASW

The U.S. Navy Task Force ASW has instituted a new focus on littoral ASW and described three major categories in ASW as follows (DON 2004):

"Hold at Risk": monitoring all the submarines that exit a port or transit a checkpoint, "Maritime Shield": clearing and maintaining a large Carrier or Expeditionary Strike Group (CSG or ESG) operation area free of threat submarines, and "Protected Passage": clearing and maintaining a route for an ESG from one operating area to another free of threat submarines.

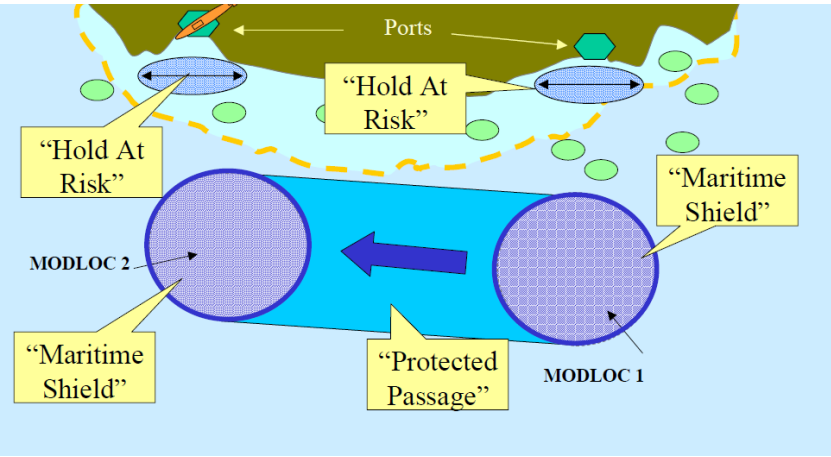

Figure 23. Schema of Task Force ASW Three Major Categories (from DON 2004).

An underwater glider can offer some support in the second and third categories but is more suitable for "Hold at Risk" missions due to the glider's restricted velocity (DON 2004). The glider can perform the "Hold at Risk" mission more effectively by

connecting communication with other platforms and by providing longer detection range (DON 2004), estimating its location precisely consequent the enemy location. Moreover, since the glider can operate in shallower water and closer to shore than other platforms, it can establish an early warning barrier. This early warning barrier allows friendly manned platforms to stay in a safe area away from the enemy's detection or hazardous environment and to focus on preparing the next mission after the glider detects and identifies some underwater objects. Even though the UUVMP analyzed and determined to be suitable for this "Hold at Risk" mission was a large vehicle class of UUV, we think that an underwater glider also would be able to accomplish the mission with some limitations.

In addition to the "Hold at Risk" mission, a glider would be able to detect and identify the enemy underwater forces when they are sitting on the seabed. Such a mission could be performed more effectively by using SSS-like mine localization. The detected target information would be more precise when a glider's position consequent the target position is estimated precisely. By doing so, a commander can evaluate the target quickly and make the right decision so that ASW operation would be performed effectively.

(3) Tactical Oceanography

Knowing the environment feature of AO is an essential component in ASW. An underwater glider can collect spatiotemporally high-resolution ocean data during a long-term mission, and these data provide maritime domain awareness (MDA) (DON 2007) and intelligence preparation of the operational environment (IPOE). These collected data can be used for increasing ocean model prediction precision and antisubmarine warfare tactical decision aids (TDAs) to support and to optimize operational planning and asset management (DON 2004). Thus, the location where these data are collected is very important. These spatiotemporally high-resolution ocean data can be obtained by calculating from the glider's precise underwater trajectory. For example, CTD and some optical data, which are collected accurately and persistently, would optimize the oceanographic characteristic of AO to help with understanding environmental conditions that impact the operational effectiveness in ASW.

(4) CN3

An underwater glider has restricted CN3 capabilities due to its payload limitation. Operators, however, still can take some advantage of the glider's CN3 capabilities. Communication is an essential factor in battle, but it is limited in a subsurface mission area due to the acoustic wave's characteristics: attenuation, refraction, and reflection. Although a glider is limited in providing long-range communication between subsurface forces, it can act as a network node as previously mentioned in Section 1. Furthermore, multiple gliders can act as communication nodes with other platforms such as surface ships, submarines, and other UUVs in the subsurface area.

An even more important feature is that an underwater glider can provide underwater target location information. This target location information would be precise when the glider's underwater trajectory is estimated precisely. In addition, a fleet of gliders would be able to gather underwater target information simultaneously. Thus, they can provide more precise target information than when a single glider operates. For these reasons, a glider's ASW capability effectiveness would be increased.

3. Relevance to Future ASW in the ROKN

This section discusses relevance to future ASW in the ROKN by reviewing ASW threats to the ROKN and providing future recommendations for ASW in the ROKN. The first section describes the force power and organization of the North Korea Navy's underwater forces, which are the most threatening underwater forces to the ROKN. The second section provides some future recommendations for ASW in the ROKN to overcome present limitations in the ASW platform aspect.

a. ASW Threats to the ROKN

Even though ASW operation was conducted by the ROKN a bit later than by other navies, it has been become an important naval operation since the Korean War. The most threatening forces to the ROKN are the North Korea Navy's underwater forces. The North Korea Navy has about 70 underwater forces, which consist of R class and Sang-O

class submarines and Yono class submersible vessels, as shown in Figure 24 (Government of the Republic of Korea 2011; MND 2013).

(a) (b) (c)

Figure 24. Underwater Forces of The North Korea Navy: (a) R class Submarine; (b) Sang-O class Submarine; (c) Yono class submersible vehicles (from Government of the Republic of Korea, 2011).

Their mission is a sea line of communication (SLOC) interdiction, mine laying, attack surface ships, and supporting the infiltration of special warfare units (MND 2013). In fact, North Korea has been continuing several underwater infiltrations and provocations since the Korean War. Recently, on March 26, 2010, in a tragic incident, the ROK Ship Cheonan was sunk in a surprise torpedo attack by North Korea Navy's small submarine (MND 2010). In addition, North Korea continues making and developing new submarines and underwater weapons in order to augment the underwater forces as asymmetrical capabilities (MND 2013). Therefore, such underwater forces of North Korea pose the greatest threat to the ROKN's ASW operation.

The lessons from the review of ASW threat, the potential power of submarines, and the importance of effort and resources in ASW to counter them were learned. ASW will not disappear as long as enemy submarines are present, and they will continue to be developed and pose the most threats. Therefore, the ROKN who is faced with these threats must develop active and forward-looking countermeasures in order not to repeat the failures which were demonstrated in the past.

b. Future Recommendations to ASW in the ROKN

An effective platform development could be considered as a part of improving ASW capability in the ROKN. Currently, various types of ASW platforms are being

operated in the ROKN: surface ships, submarines, aircrafts (see Figure 25). These platforms, however, have some limitations—such as shortage of platform numbers, time available of platform, and limited manpower and budget compared to AO—that must be overcome. Since an underwater glider has various advantages as mentioned in Section 1, it can be used to compensate for these limitations. Thus, an underwater glider is expected to be applied to conduct effective ASW operations in the near future. The types of glider could be selected depending on detailed missions and the environment. If a glider is to be used for long-term missions like collecting ocean data and conducting ISR near the deep and open ocean, the Spray or the Seaglider, which are optimized for deep-water operations, would be a proper platform. On the other hand, if a glider is to be used for short-term missions like littoral ASW, including ISR near the shallow or coastal ocean, the Slocum Electric, which is optimized for shallow-water operations, would be a suitable platform.

(a) (b) (c) (d)

Figure 25. Currently Operating Platforms for ASW in the ROKN: (a) Surface Ship (DDG) (from MND 2014, https://www.flickr.com/photos /kormnd/7445969416/in/photolist-fq14Rx-fq14Hp-fq14T4-fq151H-ckWcsd-NAzrw-ckYxi3-ktTP6w-9sTYsu-ajkxJd-mB5CqH-cHudGY-dU98Hp-dUeKiU-dUeKpE-dU98yV-dUeKt5-dU98De-dUeKkm-498nUX); (b) Submarine (214 Class) (from Center for International Maritime Security [CIMSEC] 2014, http://cimsec.org/wp-content/ uploads/2014/02/Type_214_Conventional_Attack_Submarine-672x372.jpg); (c) Antisubmarine Patrol Aircraft (P-3C) (from Aviation WA 2014, http://www.aviationwa.org.au/wp-content/uploads /2014/05/20140417_950905_Lockheed_P-3C-III+_Orion_Keith_Anderson_2.jpg); (d) Antisubmarine Helicopter (LYNX) (from the ROKN 2014, http://cfile25.uf.tistory.com/image /177CF81C4B1F334A2B8922).

Future ASW CONOPs would be network centric warfare (NCW) based on Command, Control, Communications, Computers, and ISR (C4ISR). Even though a present glider is equipped with telecommunication systems, its capability is limited

during the subsurface time. However, if a fleet of gliders forms an intelligence network, they would be able to provide more precise and useful information. Additionally, if there is no network sensor near a mission area, a glider can act as a network node itself between the glider and both the subsurface and surface platforms. Consequently, ASW operation capability would be doubled with the development of the communication system between a glider and operators and other types of platforms.

Such a beneficial underwater glider would be an effective future ASW platform in the ROKN. The ROKN is, however, in the early stages of developing its glider. Moreover, operating the glider is not simple compared to other ocean observation instruments. Unlike these other instruments, the glider considers the operation environment and requires more effort from its operators to receive collected data and to command missions. Thus, the ROKN needs to develop CONOPs, as well as manpower for operation and maintenance. Therefore, to take advantages of the glider in ASW, the ROKN should train its operators, develop its infrastructure, and systematically prepare for operating the underwater glider.

C. CHAPTER SUMMARY

In this chapter, we discussed the results of corrected trajectory by applying our two correction methods, the depth-averaged and the depth-dependent correction method, and the iteration method. By using these methods, the glider's underwater trajectories were corrected and its optimal trajectories, which act as reference trajectories, were obtained as well. Then, we could compare corrected trajectories to an optimal trajectory at each dive to determine which correction method is better. From the comparison among these three trajectories, we could get a tentative conclusion that the novel method, the depth-dependent correction method, is more efficient and precise enough to estimate the glider's optimal underwater trajectory.

Based on these finding from this study, we discussed the relevance of findings to the ROKN by describing advantages of the underwater glider and by reviewing the UUVMP. The underwater glider has three high-level advantages in ASW: cost effectiveness, various mission capabilities, and risk reduction. With these advantages, the

glider can accomplish various naval operations, especially ASW operations. To discuss the relevance of these findings to the ROKN, the UUVMP was reviewed to get the background on UUVs' sub-pillar capabilities. However, since a glider is limited in velocity and payload, only four capabilities, i.e., ISR, Littoral ASW, Tactical Oceanography, and CN3, were covered in this study. Even though a glider still has some limitations in performing these four missions, it is expected that a glider would be able to contribute to increased ASW capability effectiveness. Finally, we reviewed ASW threats to the ROKN to propose future recommendations. An underwater glider would be an effective platform that can solve the limited ASW platform problem in the future ROKN. A glider's telecommunication system would allow the glider to perform more effectively in ASW related to NCW. A glider could be a network node, and a fleet of gliders would be able to provide more precise intelligence. To improve efficiency of a glider, different types of gliders must be considered with their mission type and the ocean environment. In addition, since a glider is not developed well enough to apply to naval operation in the ROKN, professional and systematic preparation is required to take advantage of the underwater glider in ASW.

V. CONCLUSIONS AND FUTURE RESEARCH

This chapter concludes the thesis by summarizing the results of the method developed by the thesis, by discussing limitations of this study, and by suggesting future research.

A. CONCLUSIONS

This study was intended to develop a novel method for estimating a glider's optimal underwater trajectory, considering the ocean current effects. A precisely estimated trajectory would be beneficial for ocean observation and naval applications. Estimating a glider's underwater trajectory is, however, a challenging task because a glider's navigational accuracy is limited during the subsurface missions. Its DR algorithm does not consider the ocean current effects, and the submerged glider is limited in its ability to receive GPS fix information. In addition, a glider lacks inexpensive and efficient onboard sensors to measure ocean currents. For these reasons, developing a new cost-efficient and reliable method is needed.

Two methods were developed to solve this challenging problem by applying the Regional NCOM data to the traditional DR trajectory. Two corrected trajectories (C_1 and C_2) were compared to an optimal trajectory (C_3), which was estimated by using the depth-dependent correction method and incorporating the iteration method. Since no one knows the real trajectory, it was assumed that C_3 is the most precisely estimated trajectory. This trajectory, however, requires more time than C_2 to process the data of the glider and the ocean model data, and the iteration method itself is lengthy and difficult to understand. Moreover, the distance difference between C_2 and C_3 is minimal. Thus, the depth-dependent correction method without using the iteration method would be a more efficient and sufficiently precise correction method.

Given that the depth-dependent correction method is reliable in estimating a glider's optimal underwater trajectory, an underwater glider could be more beneficial for ocean observation and naval applications. A glider can collect spatiotemporally higher-resolution ocean data by performing persistent ocean sampling, and the collected data

would be more valuable if the glider's estimated underwater positions are precise. Furthermore, the precisely estimated underwater trajectory of a glider would have a great impact on ASW; for example, performing ISR, detecting and identifying the enemy target, using multiple gliders to form a communication system by acting as network nodes and providing precise intelligence, and supporting tactical oceanography.

Although a glider has many advantages in ASW, operating it is more difficult and complex than operating other ocean monitoring instruments. Thus, more professional and systematic preparation is required to apply a glider to future naval operations.

B. LIMITATIONS AND FUTURE RESEARCH

To further the research presented in this paper, several future research areas are suggested. First of all, since the C_3 was not an actual trajectory, the result of this study was a tentative conclusion. Thus, to estimate a more precise trajectory and to verify our novel method, a glider's real underwater trajectory information must be obtained by using additional sensors like ADCP or DVL (see Figure 26). Then, we can compare the C_3 to the real trajectory to determine which correction method is more suitable.

(a) (b)

Figure 26. (a) Sentinel ADCP (from Teledyne RD Instruments 2014, http://www.rdinstruments.com/images/web_sentinel1105.jpg); (b) Explorer DVL (from Teledyne RD Instruments 2014, http://www.rdinstruments.com/images/explorer_pa_pd2.jpg).

Second, this study used limited data. The Slocum conducted a total of 68 dives for a three-day deployment, and the length of each dive was short, with 362 meters of average straight DR trajectory distance. It was a relatively short experiment compared to

previous works. For example, Smith et al. (2010a) used the Slocum data, which were obtained from a month-long deployment with an average trajectory length of two kilometers and more than 200 times of surfacing. However, since our particular experiment was not originally intended for this study, it was uncontrollable. Generally, an underwater glider is designed for long-range and long-duration missions. Thus, we need to research more realistically to determine the suitability of our novel method by using data from long-range and long-duration missions.

Third, this study used relatively low resolution of the Regional NCOM data. Our average dive length was 362 meters, but the resolution of the Regional NCOM data set was 1/30 degree (about 3.6 kilometers). Generally, we can say that 1/30 degree is high resolution because the Global HYCOM has 1/12 degree (about nine kilometers), but it was actually a relatively low resolution to the glider's dive length. Velocity change of the ocean currents in one grid cell of the Regional NCOM data was not sensitive, and each dive length was included in one grid cell of the Regional NCOM data. Thus, the velocity effect on estimating trajectory was small. If the resolution of the ocean velocity is high in one grid cell of the Regional NCOM data, the trajectory could be estimated more precisely. Some NCOM prediction data sets have higher resolution, less than one kilometer. Thus, research would be able to attempt to determine whether an optimal trajectory can be estimated by using both higher resolution data and our correction methods. If the two correction methods can be applied to this situation, operators would get better trajectory estimation.

Finally, this study only considered the ocean current effects. The position of an underwater glider is, however, determined by both vehicle and environment models as we discussed in Chapter II. Thus, it is expected that a more precise trajectory can be estimated by considering both the ocean current and a glider's vehicle model effects. Some previous research studied the glider's dynamic model effects without considering the ocean current effects, but more expansive research would incorporate the two effects simultaneously. Even though this recommended future research is complex and requires more time, it would be able to estimate a more precise trajectory.

THIS PAGE INTENTIONALLY LEFT BLANK

APPENDIX A: RESULTS OF TRAJECTORY ESTIMATION

A. PHASE ONE: DR AND DR_{NCOM} TRAJECTORIES

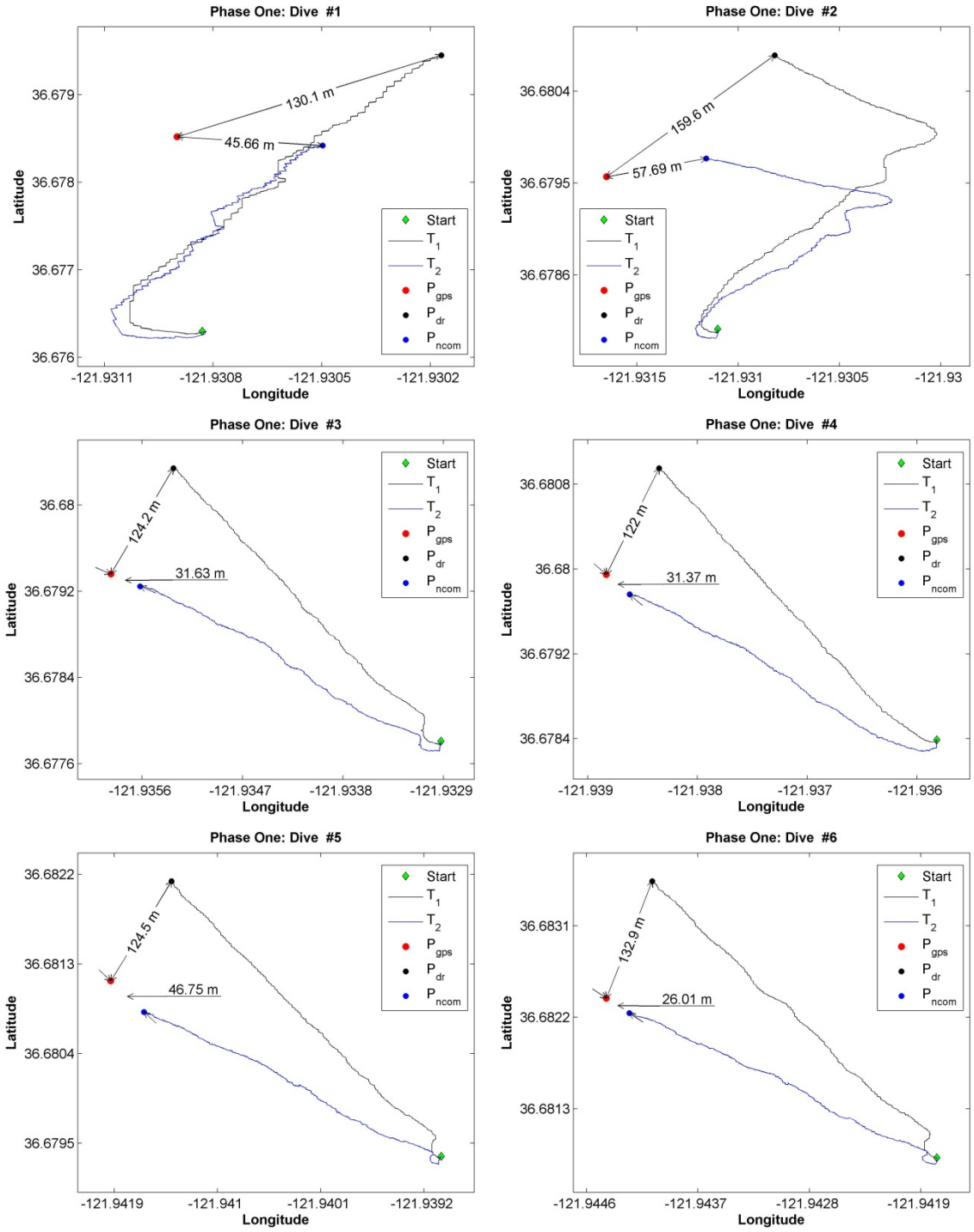

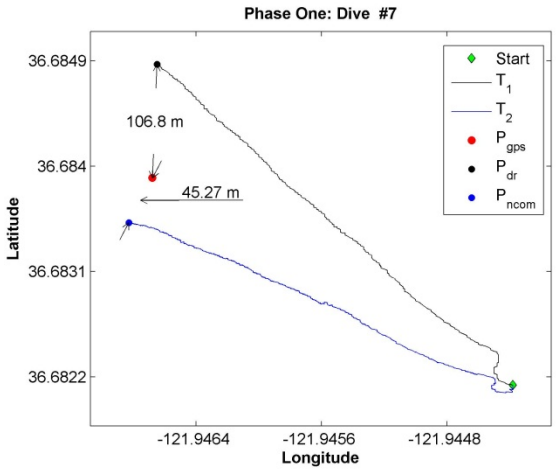
Phase One: Dive #7
Start
T_1
T_2
P_{gps}
P_{dr}
P_{ncom}
106.8 m
45.27 m
36.6849
36.684
36.6831
36.6822
Latitude
-121.9464
-121.9456
-121.9448
Longitude

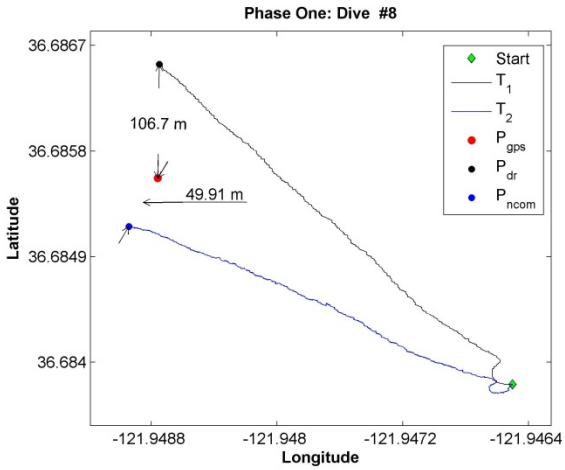
Phase One: Dive #8
Start
T_1
T_2
P_{gps}
P_{dr}
P_{ncom}
106.7 m
49.91 m
36.6867
36.6858
36.6849
36.684
Latitude
-121.9488
-121.948
-121.9472
-121.9464
Longitude

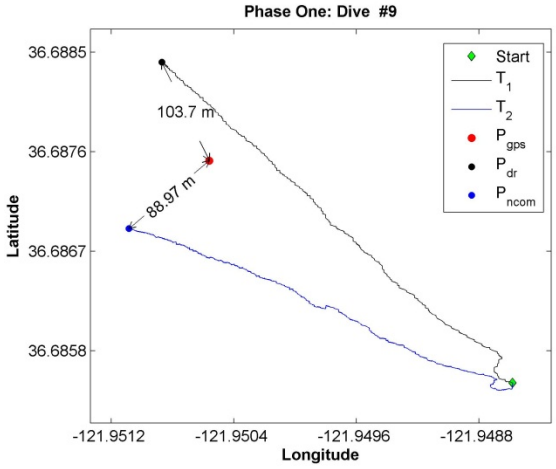
Phase One: Dive #9
Start
T_1
T_2
P_{gps}
P_{dr}
P_{ncom}
103.7 m
88.97 m
36.6885
36.6876
36.6867
36.6858
Latitude
-121.9512
-121.9504
-121.9496
-121.9488
Longitude

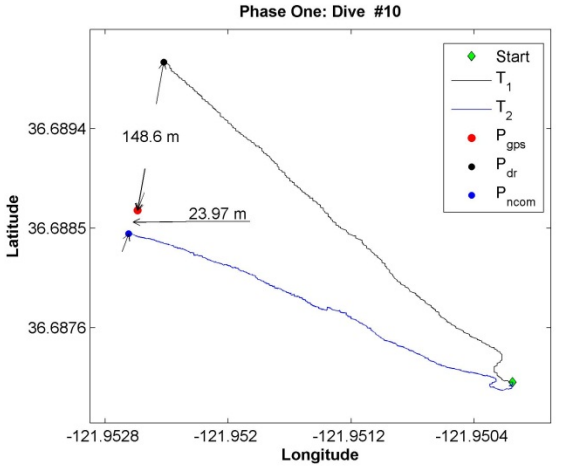
Phase One: Dive #10
Start
T_1
T_2
P_{gps}
P_{dr}
P_{ncom}
148.6 m
23.97 m
36.6894
36.6885
36.6876
Latitude
-121.9528
-121.952
-121.9512
-121.9504
Longitude

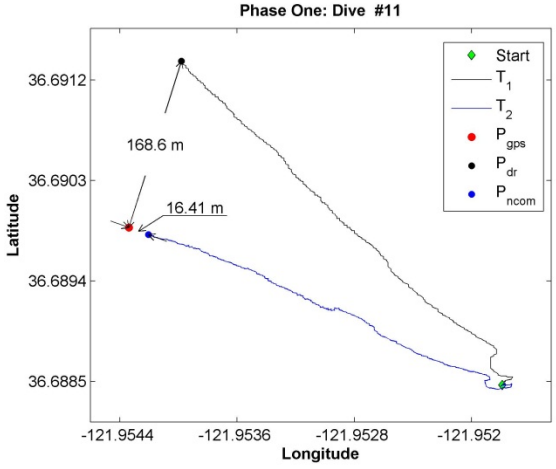
Phase One: Dive #11
Start
T_1
T_2
P_{gps}
P_{dr}
P_{ncom}
168.6 m
16.41 m
36.6912
36.6903
36.6894
36.6885
Latitude
-121.9544
-121.9536
-121.9528
-121.952
Longitude

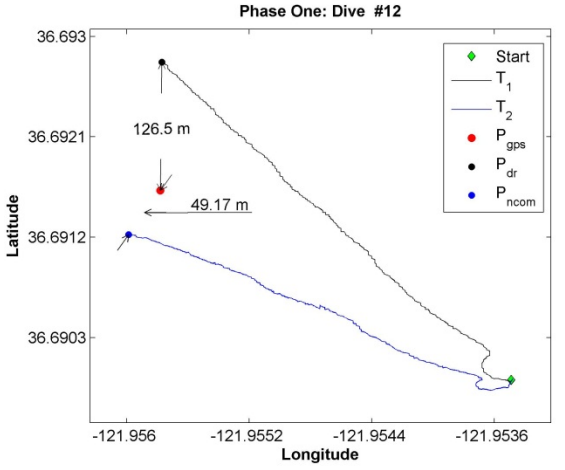
Phase One: Dive #12
Start
T_1
T_2
P_{gps}
P_{dr}
P_{ncom}
126.5 m
49.17 m
36.693
36.6921
36.6912
36.6903
Latitude
-121.956
-121.9552
-121.9544
-121.9536
Longitude

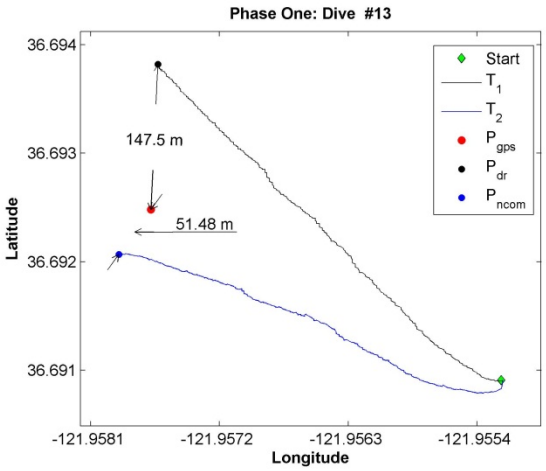
Phase One: Dive #13
Start
T_1
T_2
P_{gps}
P_{dr}
P_{ncom}
147.5 m
51.48 m
36.694
36.693
36.692
36.691
Latitude
-121.9581
-121.9572
-121.9563
-121.9554
Longitude

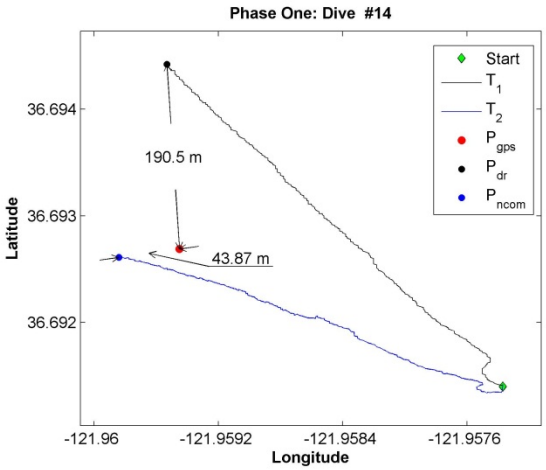
Phase One: Dive #14
Start
T_1
T_2
P_{gps}
P_{dr}
P_{ncom}
190.5 m
43.87 m
36.694
36.693
36.692
Latitude
-121.96
-121.9592
-121.9584
-121.9576
Longitude

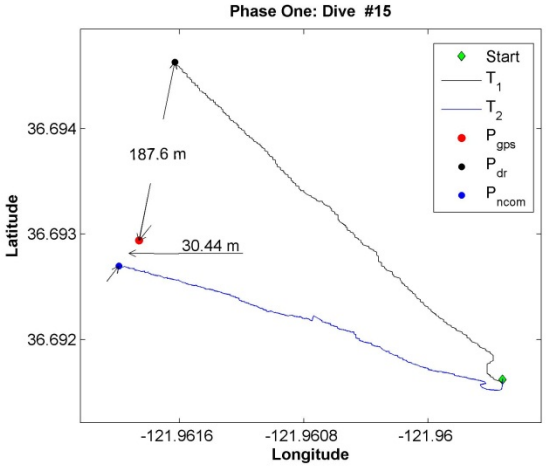
Phase One: Dive #15
Start
T_1
T_2
P_{gps}
P_{dr}
P_{ncom}
187.6 m
30.44 m
36.694
36.693
36.692
Latitude
-121.9616
-121.9608
-121.96
Longitude

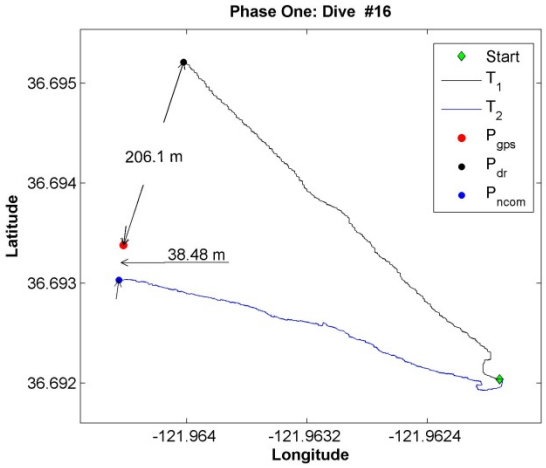
Phase One: Dive #16
Start
T_1
T_2
P_{gps}
P_{dr}
P_{ncom}
206.1 m
38.48 m
36.695
36.694
36.693
36.692
Latitude
-121.964
-121.9632
-121.9624
Longitude

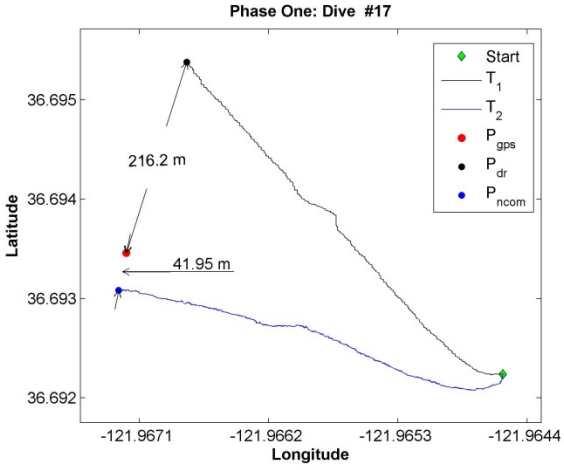
Phase One: Dive #17
Start
T_1
T_2
P_{gps}
P_{dr}
P_{ncom}
216.2 m
41.95 m
36.695
36.694
36.693
36.692
Latitude
-121.9671
-121.9662
-121.9653
-121.9644
Longitude

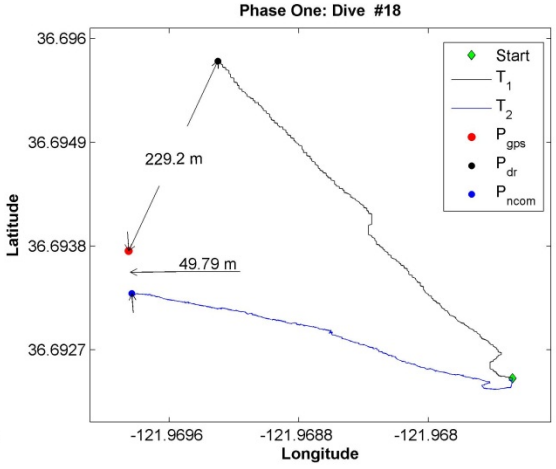
Phase One: Dive #18
Start
T_1
T_2
P_{gps}
P_{dr}
P_{ncom}
229.2 m
49.79 m
36.696
36.6949
36.6938
36.6927
Latitude
-121.9696
-121.9688
-121.968
Longitude

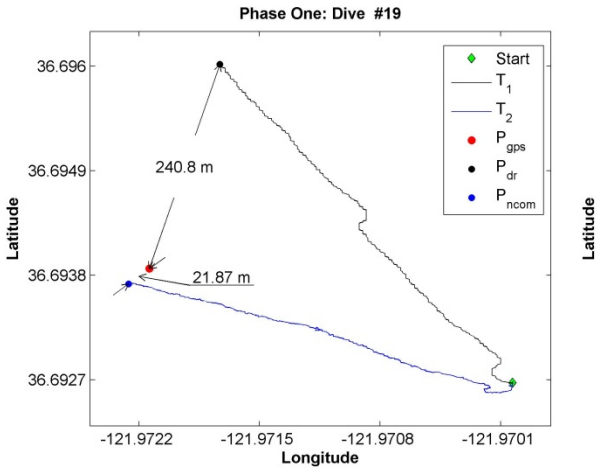
Phase One: Dive #19
Start
T_1
T_2
P_{gps}
P_{dr}
P_{ncom}
240.8 m
21.87 m
36.696
36.6949
36.6938
36.6927
Latitude
-121.9722
-121.9715
-121.9708
-121.9701
Longitude

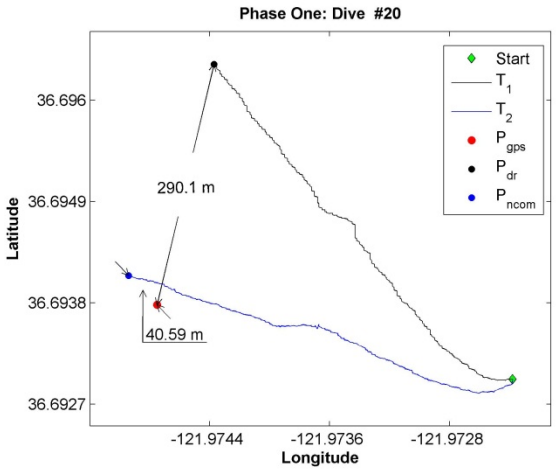
Phase One: Dive #20
Start
T_1
T_2
P_{gps}
P_{dr}
P_{ncom}
290.1 m
40.59 m
36.696
36.6949
36.6938
36.6927
Latitude
-121.9744
-121.9736
-121.9728
Longitude

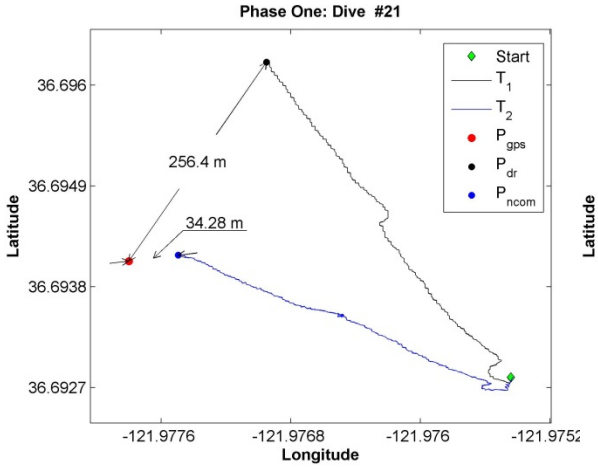
Phase One: Dive #21
Start
T_1
T_2
P_{gps}
P_{dr}
P_{ncom}
256.4 m
34.28 m
36.696
36.6949
36.6938
36.6927
Latitude
-121.9776
-121.9768
-121.976
Longitude

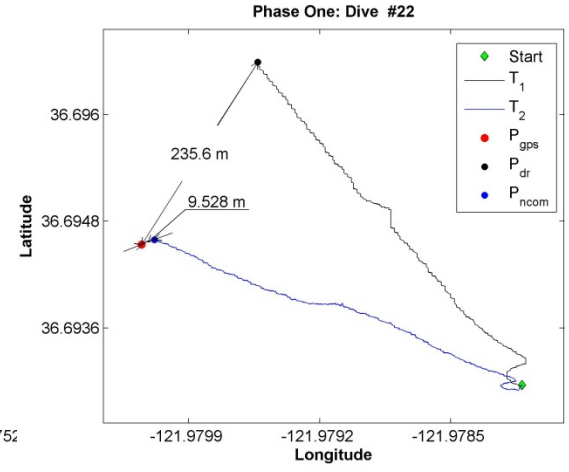
Phase One: Dive #22
Start
T_1
T_2
P_{gps}
P_{dr}
P_{ncom}
235.6 m
9.528 m
36.696
36.6948
36.6936
Latitude
-121.9799
-121.9792
-121.9785
Longitude

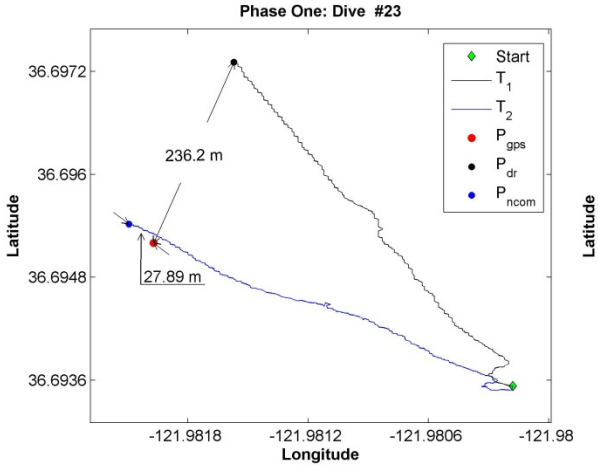
Phase One: Dive #23
Start
T_1
T_2
P_{gps}
P_{dr}
P_{ncom}
236.2 m
27.89 m
36.6972
36.696
36.6948
36.6936
Latitude
-121.9818
-121.9812
-121.9806
Longitude

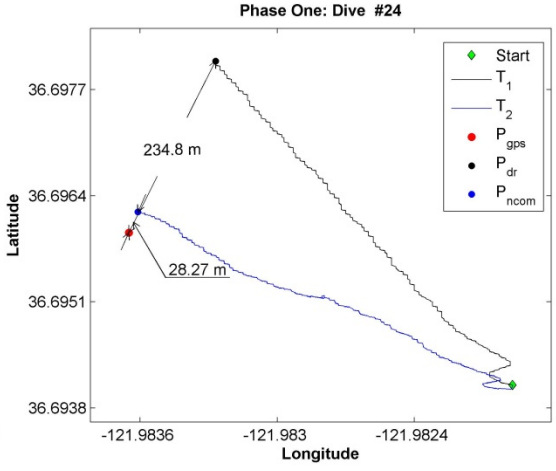
Phase One: Dive #24
Start
T_1
T_2
P_{gps}
P_{dr}
P_{ncom}
234.8 m
28.27 m
36.6977
36.6964
36.6951
36.6938
Latitude
-121.9836
-121.983
-121.9824
Longitude

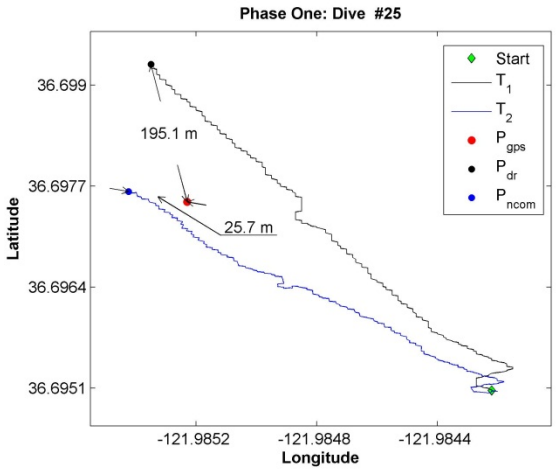
Phase One: Dive #25
Start
T_1
T_2
P_{gps}
P_{dr}
P_{ncom}
195.1 m
25.7 m
36.699
36.6977
36.6964
36.6951
Latitude
-121.9852
-121.9848
-121.9844
Longitude

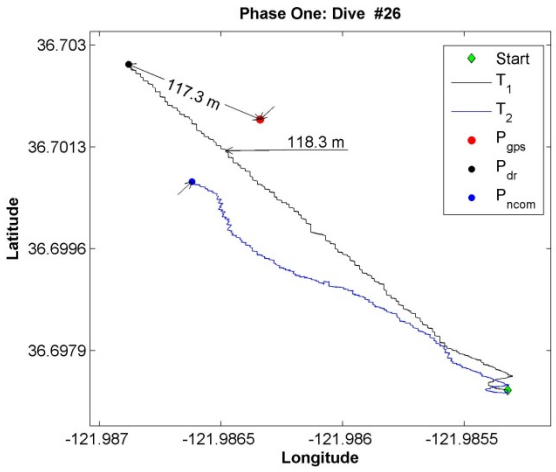
Phase One: Dive #26
Start
T_1
T_2
P_{gps}
P_{dr}
P_{ncom}
117.3 m
118.3 m
36.703
36.7013
36.6996
36.6979
Latitude
-121.987
-121.9865
-121.986
-121.9855
Longitude

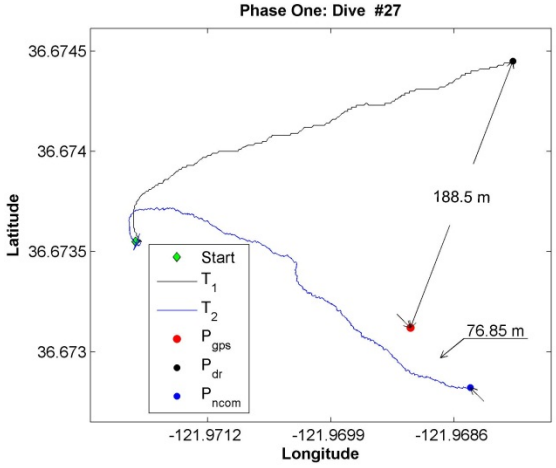
Phase One: Dive #27
Start
T_1
T_2
P_{gps}
P_{dr}
P_{ncom}
188.5 m
76.85 m
36.6745
36.674
36.6735
36.673
Latitude
-121.9712
-121.9699
-121.9686
Longitude

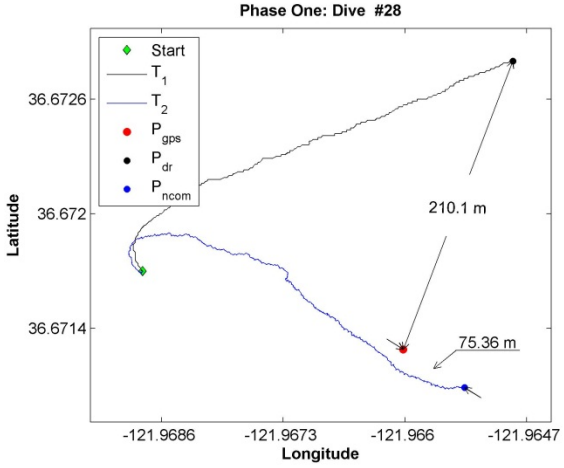
Phase One: Dive #28
Start
T_1
T_2
P_{gps}
P_{dr}
P_{ncom}
210.1 m
75.36 m
36.6726
36.672
36.6714
Latitude
-121.9686
-121.9673
-121.966
-121.9647
Longitude

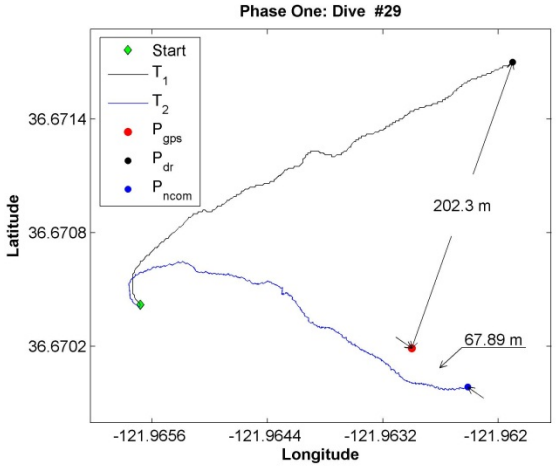
Phase One: Dive #29
Start
T_1
T_2
P_{gps}
P_{dr}
P_{ncom}
202.3 m
67.89 m
36.6714
36.6708
36.6702
Latitude
-121.9656
-121.9644
-121.9632
-121.962
Longitude

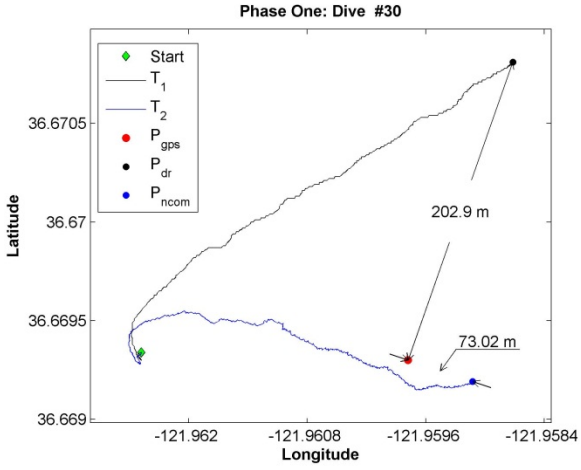
Phase One: Dive #30
Start
T_1
T_2
P_{gps}
P_{dr}
P_{ncom}
202.9 m
73.02 m
36.6705
36.67
36.6695
36.669
Latitude
-121.962
-121.9608
-121.9596
-121.9584
Longitude

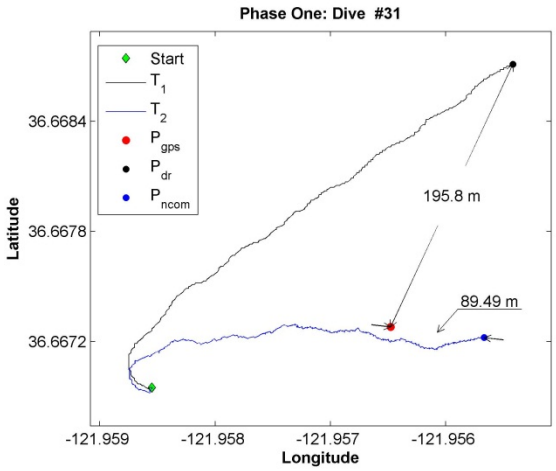
Phase One: Dive #31
Start
T_1
T_2
P_{gps}
P_{dr}
P_{ncom}
195.8 m
89.49 m
Latitude
Longitude
36.6684
36.6678
36.6672
-121.959
-121.958
-121.957
-121.956

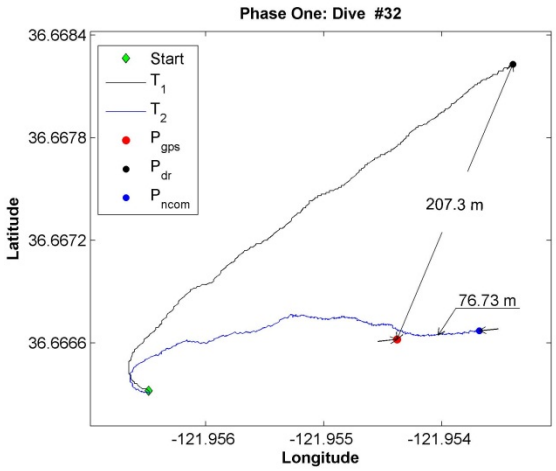
Phase One: Dive #32
Start
T_1
T_2
P_{gps}
P_{dr}
P_{ncom}
207.3 m
76.73 m
Latitude
Longitude
36.6684
36.6678
36.6672
36.6666
-121.956
-121.955
-121.954

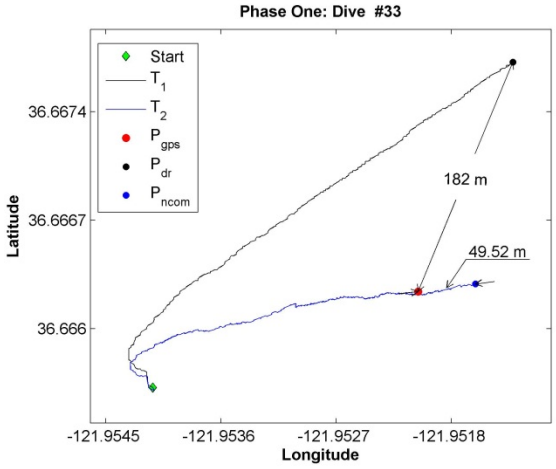
Phase One: Dive #33
Start
T_1
T_2
P_{gps}
P_{dr}
P_{ncom}
182 m
49.52 m
Latitude
Longitude
36.6674
36.6667
36.666
-121.9545
-121.9536
-121.9527
-121.9518

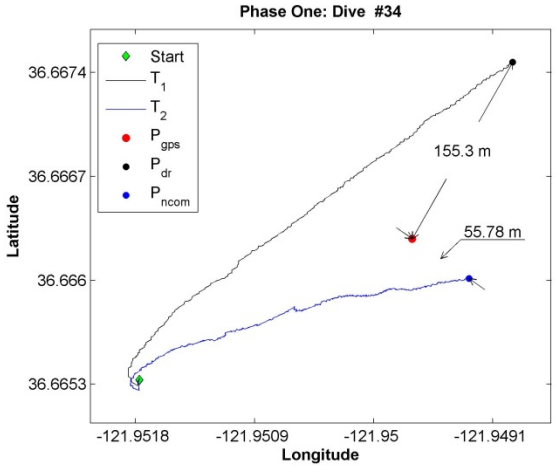
Phase One: Dive #34
Start
T_1
T_2
P_{gps}
P_{dr}
P_{ncom}
155.3 m
55.78 m
Latitude
Longitude
36.6674
36.6667
36.666
36.6653
-121.9518
-121.9509
-121.95
-121.9491

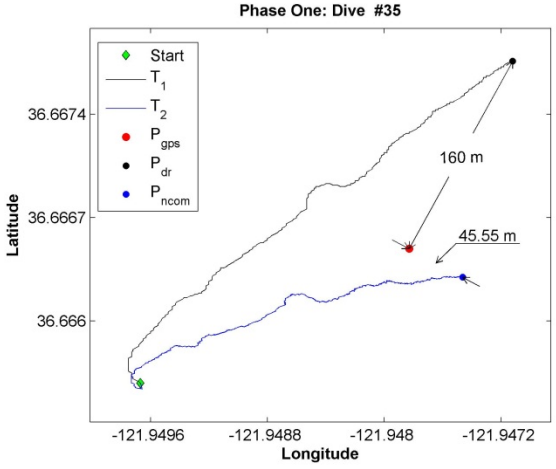
Phase One: Dive #35
Start
T_1
T_2
P_{gps}
P_{dr}
P_{ncom}
160 m
45.55 m
Latitude
Longitude
36.6674
36.6667
36.666
-121.9496
-121.9488
-121.948
-121.9472

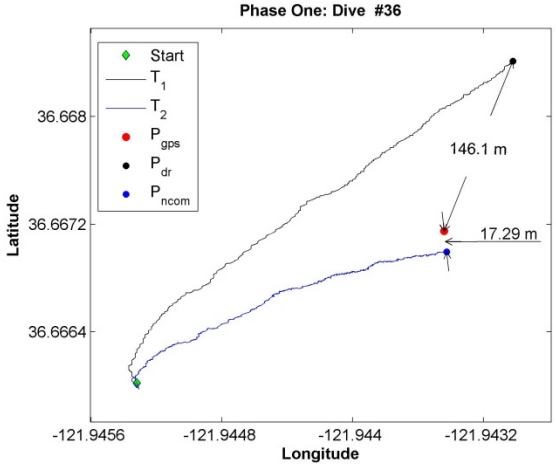
Phase One: Dive #36
Start
T_1
T_2
P_{gps}
P_{dr}
P_{ncom}
146.1 m
17.29 m
Latitude
Longitude
36.668
36.6672
36.6664
-121.9456
-121.9448
-121.944
-121.9432

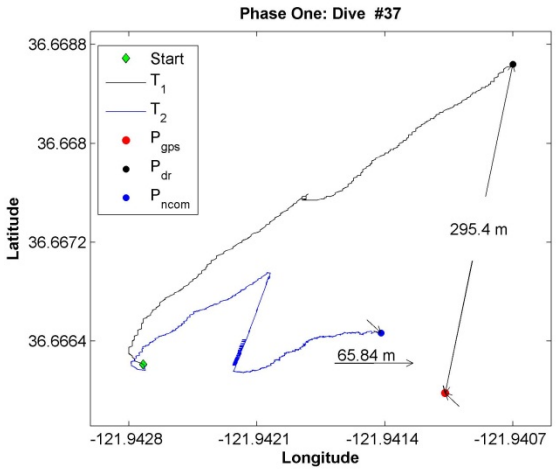
Phase One: Dive #37
Start
T_1
T_2
P_{gps}
P_{dr}
P_{ncom}
295.4 m
65.84 m
Latitude
Longitude
36.6688
36.668
36.6672
36.6664
-121.9428
-121.9421
-121.9414
-121.9407

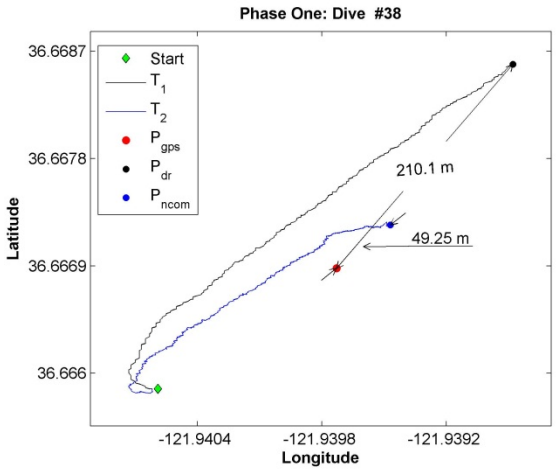
Phase One: Dive #38
Start
T_1
T_2
P_{gps}
P_{dr}
P_{ncom}
210.1 m
49.25 m
Latitude
Longitude
36.6687
36.6678
36.6669
36.666
-121.9404
-121.9398
-121.9392

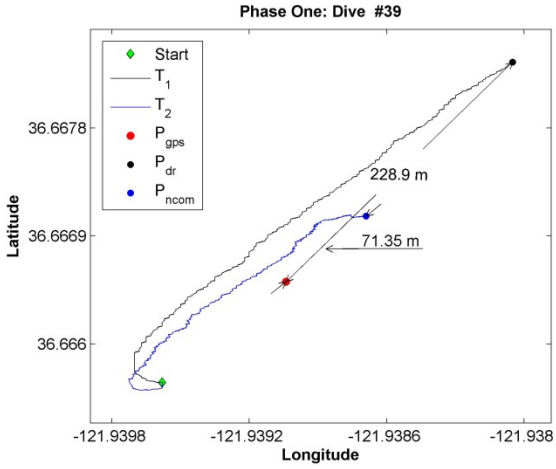
Phase One: Dive #39
Start
T_1
T_2
P_{gps}
P_{dr}
P_{ncom}
228.9 m
71.35 m
Latitude
Longitude
36.6678
36.6669
36.666
-121.9398
-121.9392
-121.9386
-121.938

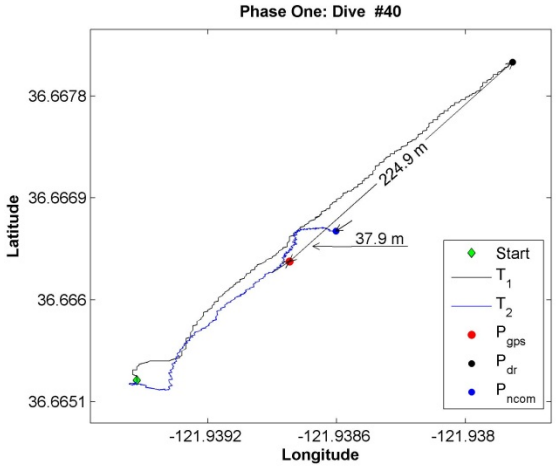
Phase One: Dive #40
Start
T_1
T_2
P_{gps}
P_{dr}
P_{ncom}
224.9 m
37.9 m
Latitude
Longitude
36.6678
36.6669
36.666
36.6651
-121.9392
-121.9386
-121.938

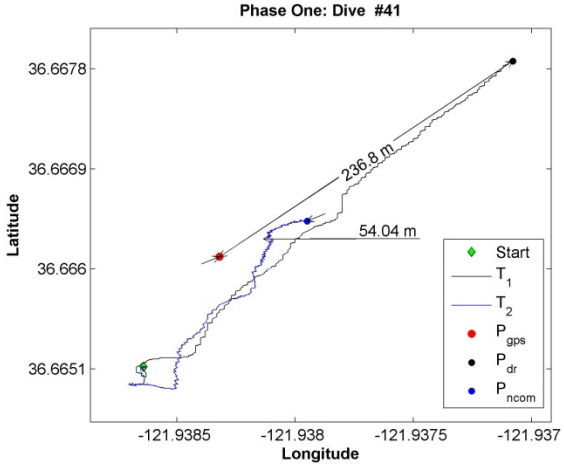
Phase One: Dive #41
Start
T_1
T_2
P_{gps}
P_{dr}
P_{ncom}
236.8 m
54.04 m
Latitude
Longitude
36.6678
36.6669
36.666
36.6651
-121.9385
-121.938
-121.9375
-121.937

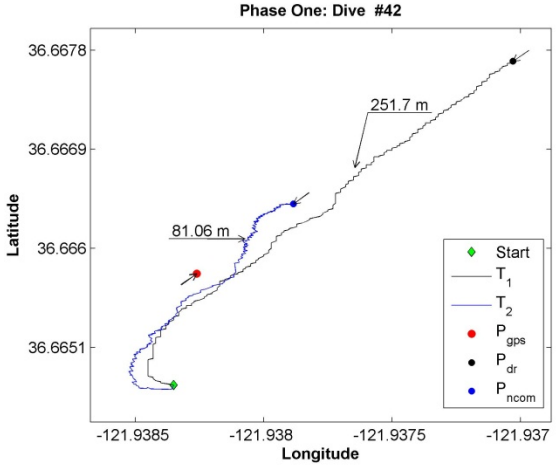
Phase One: Dive #42
Start
T_1
T_2
P_{gps}
P_{dr}
P_{ncom}
251.7 m
81.06 m
Latitude
Longitude
36.6678
36.6669
36.666
36.6651
-121.9385
-121.938
-121.9375
-121.937

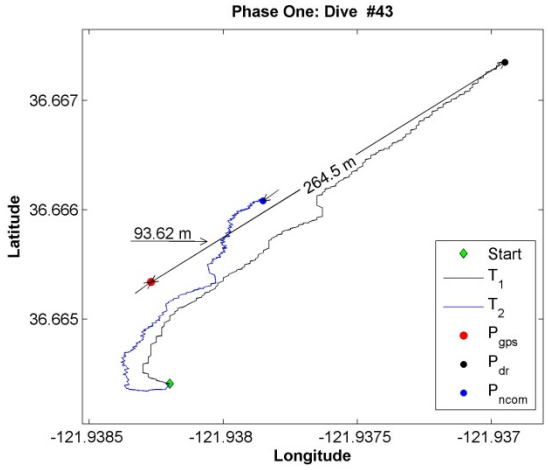
Phase One: Dive #43
36.667
36.666
36.665
Latitude
93.62 m
264.5 m
Start
T_1
T_2
P_{gps}
P_{dr}
P_{ncom}
-121.9385
-121.938
-121.9375
-121.937
Longitude

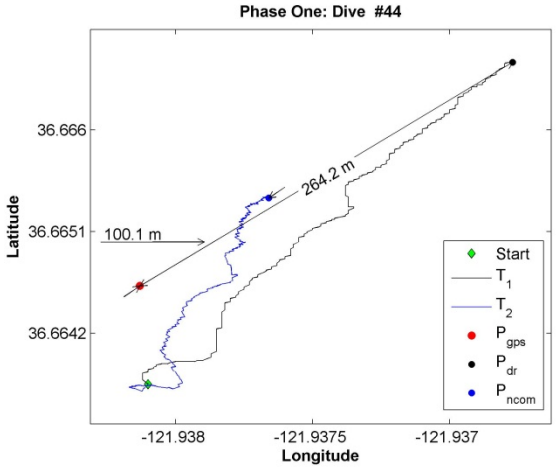
Phase One: Dive #44
36.666
36.6651
36.6642
Latitude
100.1 m
264.2 m
Start
T_1
T_2
P_{gps}
P_{dr}
P_{ncom}
-121.938
-121.9375
-121.937
Longitude

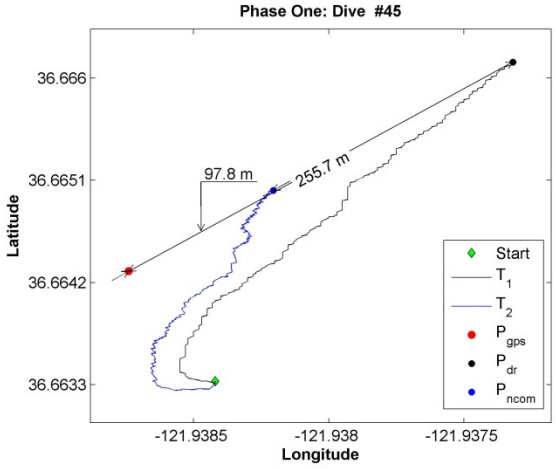
Phase One: Dive #45
36.666
36.6651
36.6642
36.6633
Latitude
97.8 m
255.7 m
Start
T_1
T_2
P_{gps}
P_{dr}
P_{ncom}
-121.9385
-121.938
-121.9375
Longitude

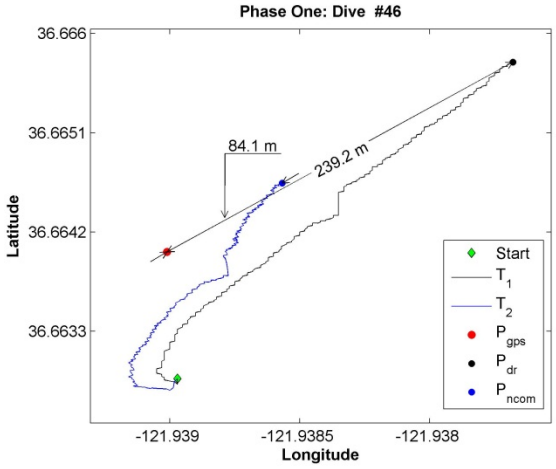
Phase One: Dive #46
36.666
36.6651
36.6642
36.6633
Latitude
84.1 m
239.2 m
Start
T_1
T_2
P_{gps}
P_{dr}
P_{ncom}
-121.939
-121.9385
-121.938
Longitude

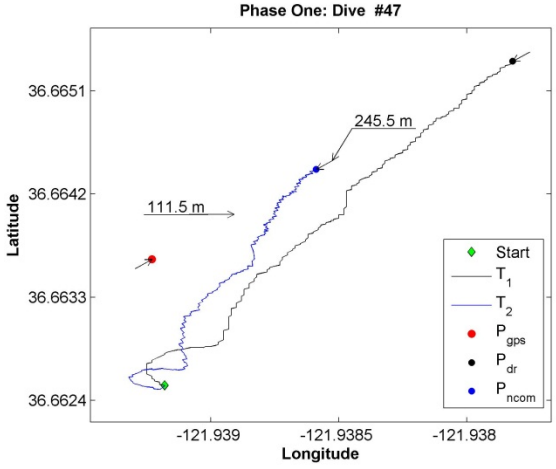
Phase One: Dive #47
36.6651
36.6642
36.6633
36.6624
Latitude
111.5 m
245.5 m
Start
T_1
T_2
P_{gps}
P_{dr}
P_{ncom}
-121.939
-121.9385
-121.938
Longitude

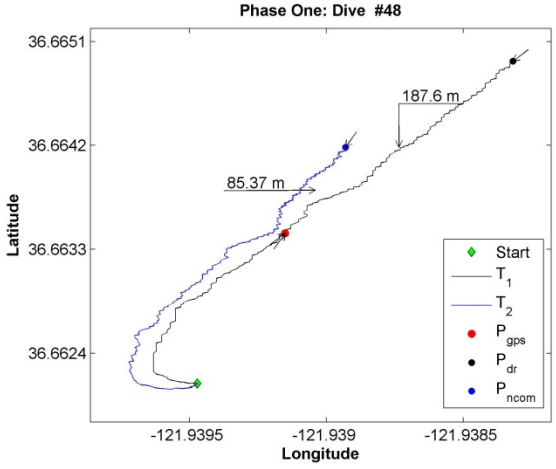
Phase One: Dive #48
36.6651
36.6642
36.6633
36.6624
Latitude
187.6 m
85.37 m
Start
T_1
T_2
P_{gps}
P_{dr}
P_{ncom}
-121.9395
-121.939
-121.9385
Longitude

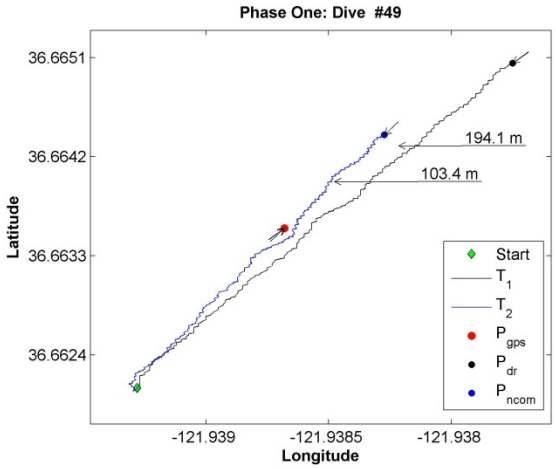
Phase One: Dive #49
36.6651
36.6642
36.6633
36.6624
Latitude
-121.939
-121.9385
-121.938
Longitude
194.1 m
103.4 m
Start
T1
T2
Pgps
Pdr
Pncom

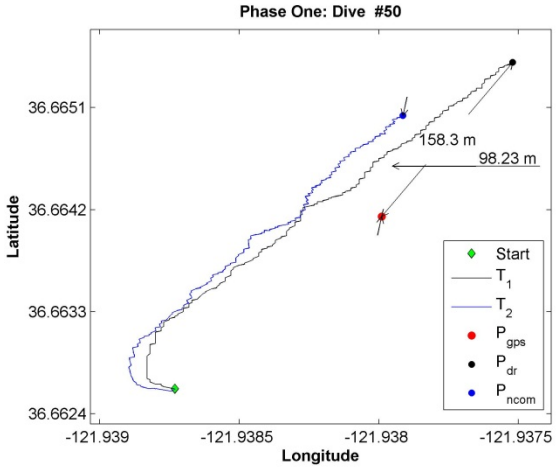
Phase One: Dive #50
36.6651
36.6642
36.6633
36.6624
Latitude
-121.939
-121.9385
-121.938
-121.9375
Longitude
158.3 m
98.23 m
Start
T1
T2
Pgps
Pdr
Pncom

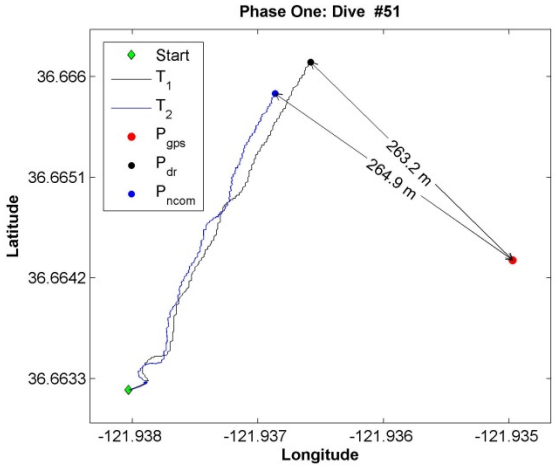
Phase One: Dive #51
36.666
36.6651
36.6642
36.6633
Latitude
-121.938
-121.937
-121.936
-121.935
Longitude
263.2 m
264.9 m
Start
T1
T2
Pgps
Pdr
Pncom

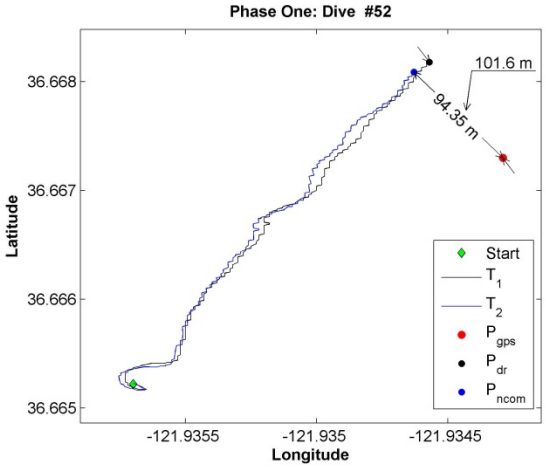
Phase One: Dive #52
36.668
36.667
36.666
36.665
Latitude
-121.9355
-121.935
-121.9345
Longitude
101.6 m
94.35 m
Start
T1
T2
Pgps
Pdr
Pncom

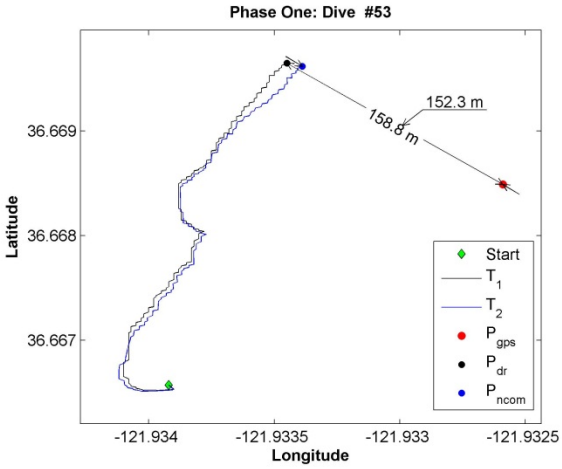
Phase One: Dive #53
36.669
36.668
36.667
Latitude
-121.934
-121.9335
-121.933
-121.9325
Longitude
152.3 m
158.8 m
Start
T1
T2
Pgps
Pdr
Pncom

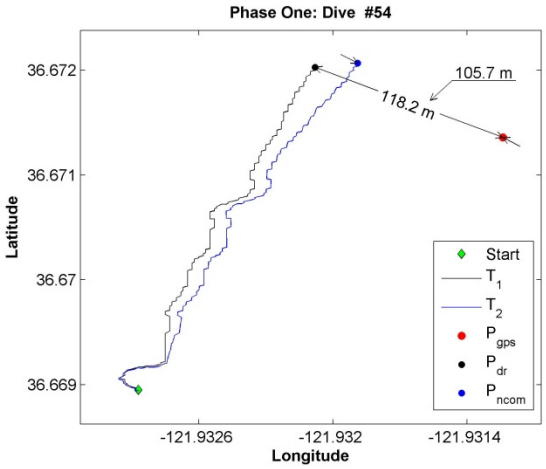
Phase One: Dive #54
36.672
36.671
36.67
36.669
Latitude
-121.9326
-121.932
-121.9314
Longitude
105.7 m
118.2 m
Start
T1
T2
Pgps
Pdr
Pncom

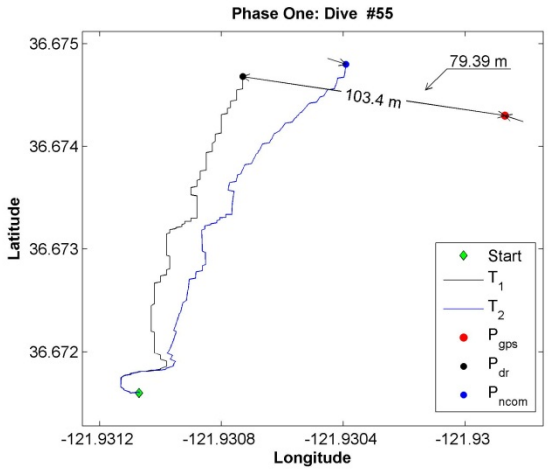
Phase One: Dive #55
79.39 m
103.4 m
Start
T_1
T_2
P_{gps}
P_{dr}
P_{ncom}
Latitude
Longitude
36.675
36.674
36.673
36.672
-121.9312
-121.9308
-121.9304
-121.93

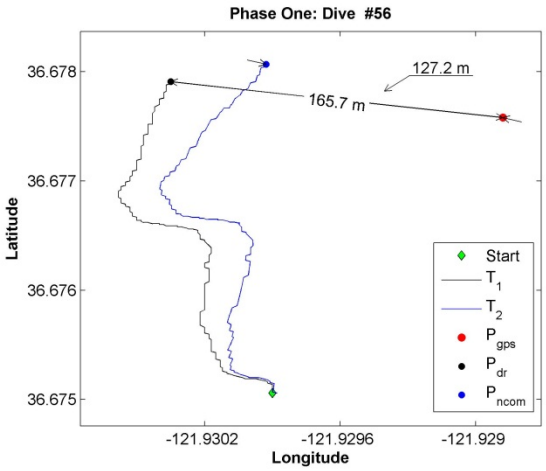
Phase One: Dive #56
127.2 m
165.7 m
Start
T_1
T_2
P_{gps}
P_{dr}
P_{ncom}
Latitude
Longitude
36.678
36.677
36.676
36.675
-121.9302
-121.9296
-121.929

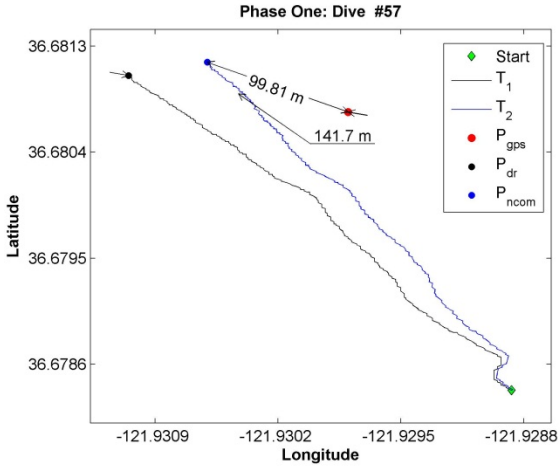
Phase One: Dive #57
99.81 m
141.7 m
Start
T_1
T_2
P_{gps}
P_{dr}
P_{ncom}
Latitude
Longitude
36.6813
36.6804
36.6795
36.6786
-121.9309
-121.9302
-121.9295
-121.9288

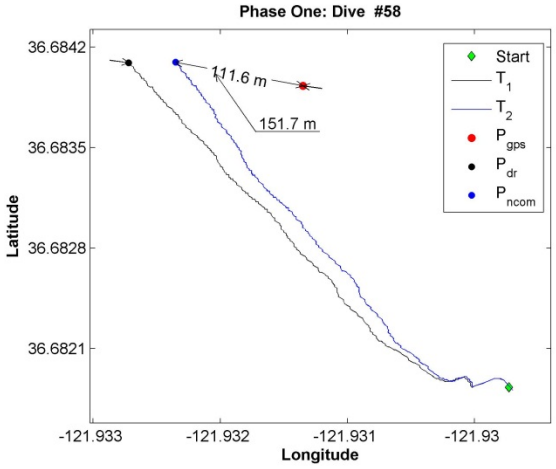
Phase One: Dive #58
111.6 m
151.7 m
Start
T_1
T_2
P_{gps}
P_{dr}
P_{ncom}
Latitude
Longitude
36.6842
36.6835
36.6828
36.6821
-121.933
-121.932
-121.931
-121.93

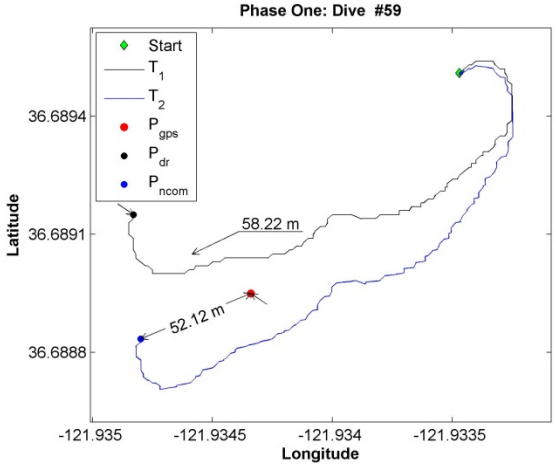
Phase One: Dive #59
58.22 m
52.12 m
Start
T_1
T_2
P_{gps}
P_{dr}
P_{ncom}
Latitude
Longitude
36.6894
36.6891
36.6888
-121.935
-121.9345
-121.934
-121.9335

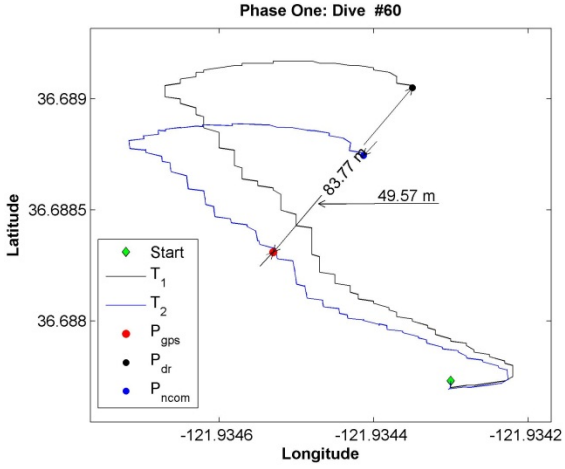
Phase One: Dive #60
83.77 m
49.57 m
Start
T_1
T_2
P_{gps}
P_{dr}
P_{ncom}
Latitude
Longitude
36.689
36.6885
36.688
-121.9346
-121.9344
-121.9342

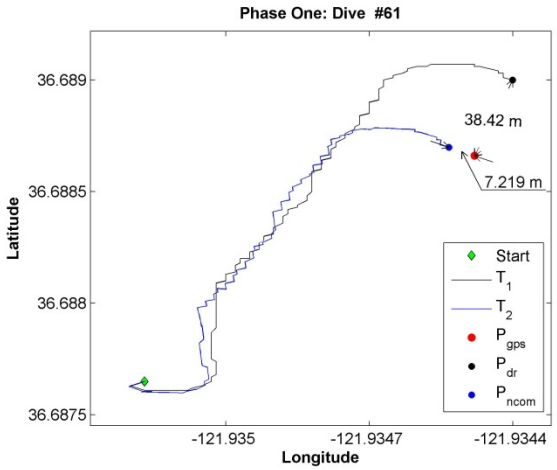
Phase One: Dive #61
36.689
36.6885
36.688
36.6875
Latitude
-121.935
-121.9347
-121.9344
Longitude
38.42 m
7.219 m
Start
T1
T2
Pgps
Pdr
Pncom

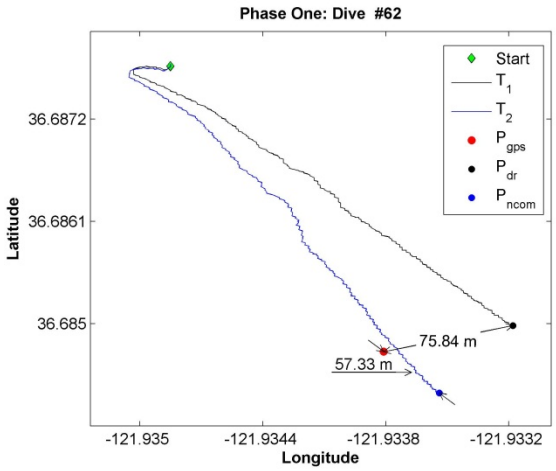
Phase One: Dive #62
36.6872
36.6861
36.685
Latitude
-121.935
-121.9344
-121.9338
-121.9332
Longitude
75.84 m
57.33 m
Start
T1
T2
Pgps
Pdr
Pncom

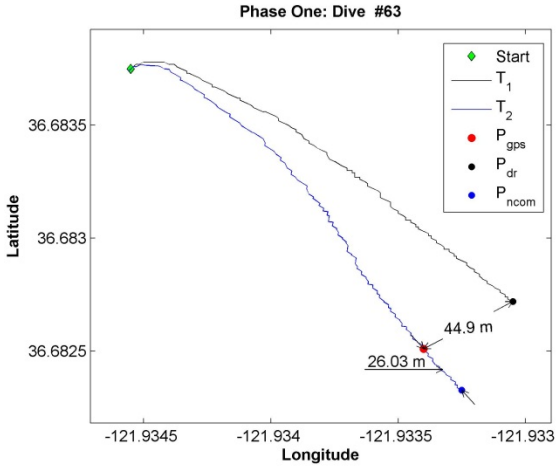
Phase One: Dive #63
36.6835
36.683
36.6825
Latitude
-121.9345
-121.934
-121.9335
-121.933
Longitude
44.9 m
26.03 m
Start
T1
T2
Pgps
Pdr
Pncom

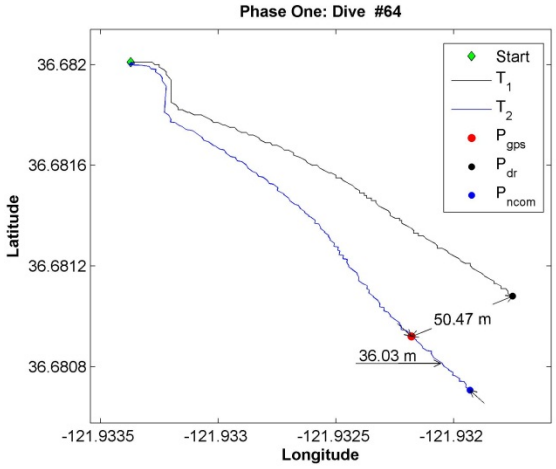
Phase One: Dive #64
36.682
36.6816
36.6812
36.6808
Latitude
-121.9335
-121.933
-121.9325
-121.932
Longitude
50.47 m
36.03 m
Start
T1
T2
Pgps
Pdr
Pncom

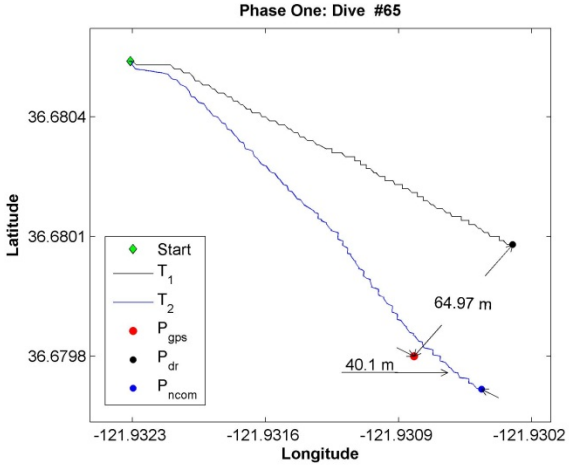
Phase One: Dive #65
36.6804
36.6801
36.6798
Latitude
-121.9323
-121.9316
-121.9309
-121.9302
Longitude
64.97 m
40.1 m
Start
T1
T2
Pgps
Pdr
Pncom

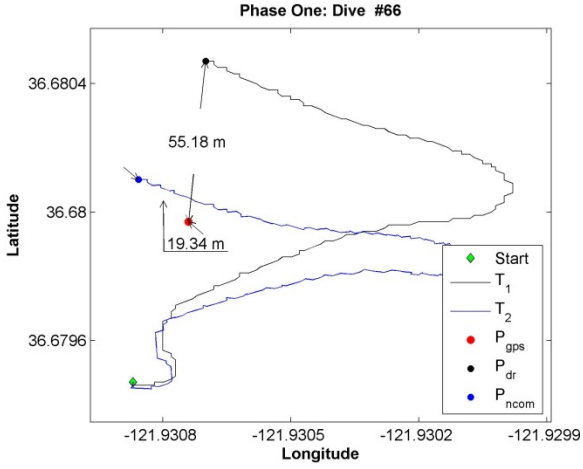
Phase One: Dive #66
36.6804
36.68
36.6796
Latitude
-121.9308
-121.9305
-121.9302
-121.9299
Longitude
55.18 m
19.34 m
Start
T1
T2
Pgps
Pdr
Pncom

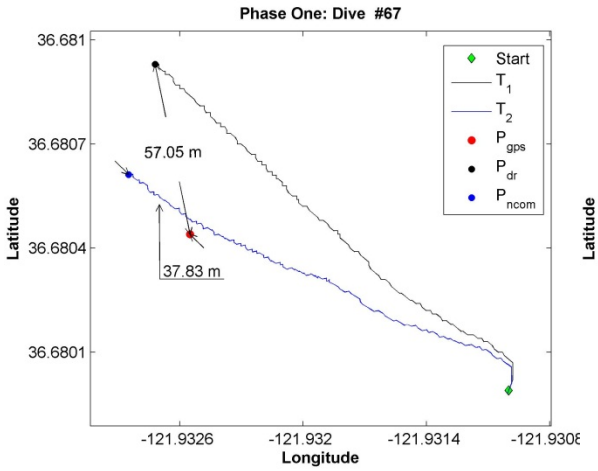
Phase One: Dive #67
Start
T_1
T_2
P_{gps}
P_{dr}
P_{ncom}
57.05 m
37.83 m
36.681
36.6807
36.6804
36.6801
Latitude
-121.9326
-121.932
-121.9314
-121.9308
Longitude

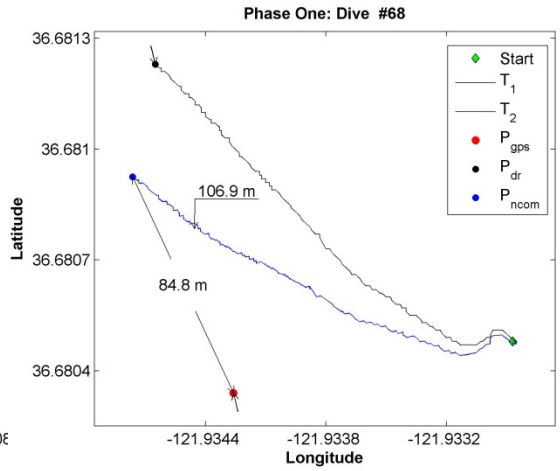
Phase One: Dive #68
Start
T_1
T_2
P_{gps}
P_{dr}
P_{ncom}
106.9 m
84.8 m
36.6813
36.681
36.6807
36.6804
Latitude
-121.9344
-121.9338
-121.9332
Longitude

B. STEP ONE: DR TRAJECTORIES WITH DEPTH-AVERAGED CORRECTION METHOD

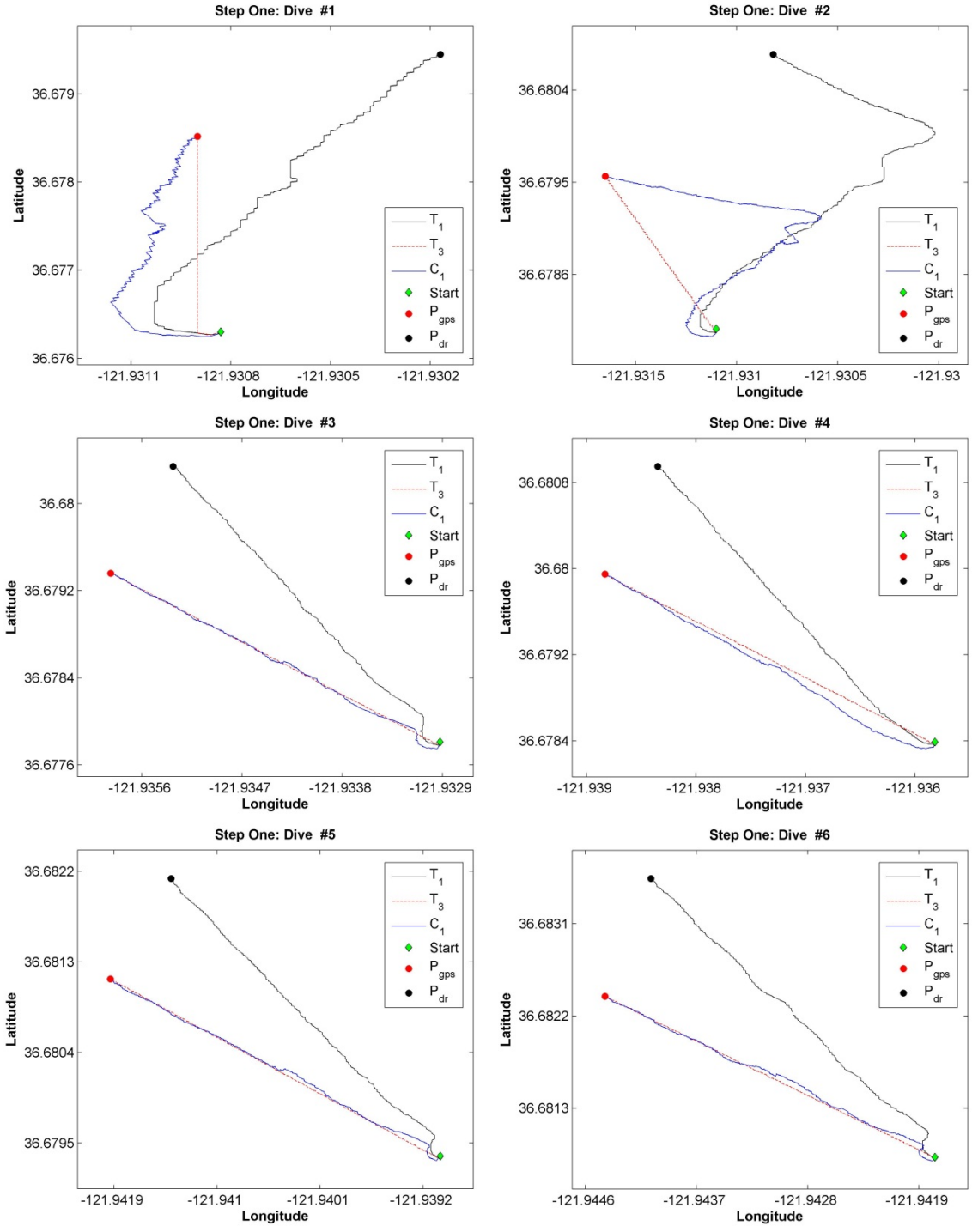

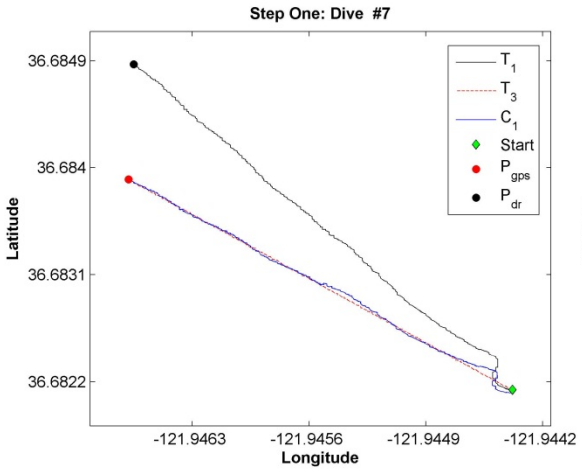
Step One: Dive #7
36.6849
36.684
36.6831
36.6822
Latitude
-121.9463
-121.9456
-121.9449
-121.9442
Longitude
T1
T3
C1
Start
Pgps
Pdr

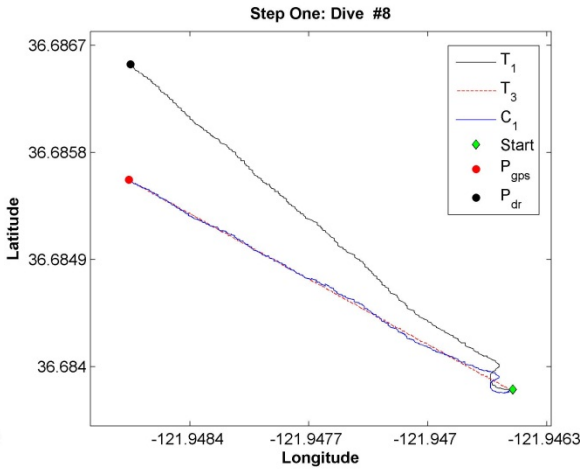
Step One: Dive #8
36.6867
36.6858
36.6849
36.684
Latitude
-121.9484
-121.9477
-121.947
-121.9463
Longitude
T1
T3
C1
Start
Pgps
Pdr

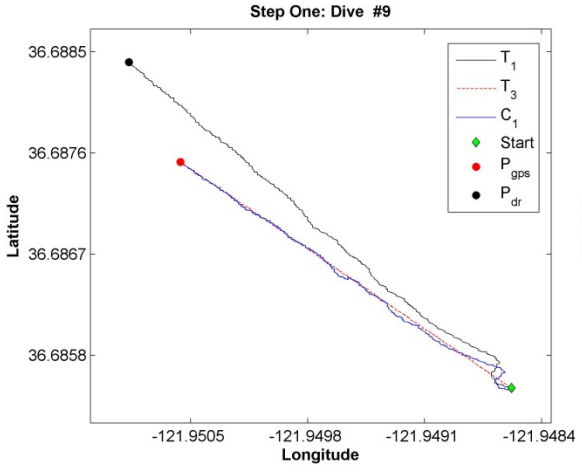
Step One: Dive #9
36.6885
36.6876
36.6867
36.6858
Latitude
-121.9505
-121.9498
-121.9491
-121.9484
Longitude
T1
T3
C1
Start
Pgps
Pdr

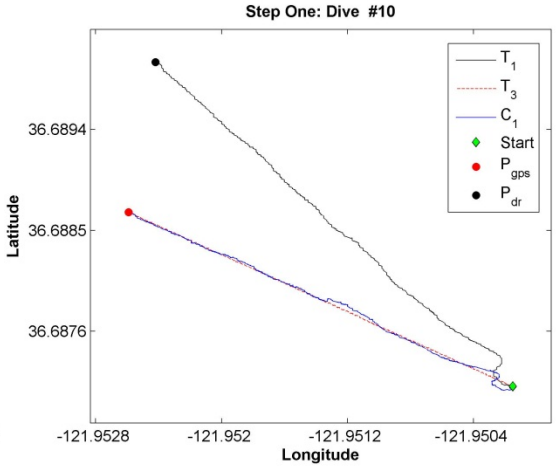
Step One: Dive #10
36.6894
36.6885
36.6876
Latitude
-121.9528
-121.952
-121.9512
-121.9504
Longitude
T1
T3
C1
Start
Pgps
Pdr

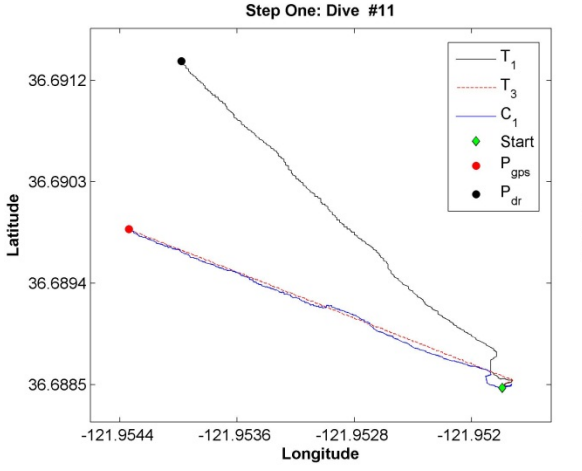
Step One: Dive #11
36.6912
36.6903
36.6894
36.6885
Latitude
-121.9544
-121.9536
-121.9528
-121.952
Longitude
T1
T3
C1
Start
Pgps
Pdr

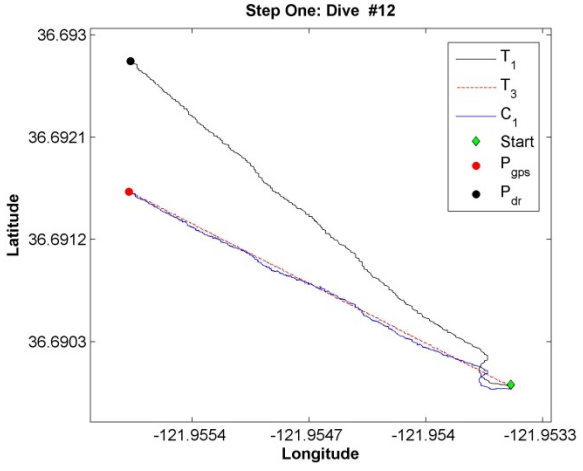
Step One: Dive #12
36.693
36.6921
36.6912
36.6903
Latitude
-121.9554
-121.9547
-121.954
-121.9533
Longitude
T1
T3
C1
Start
Pgps
Pdr

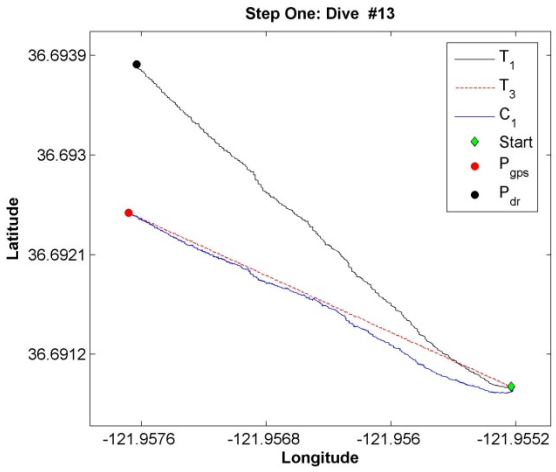
Step One: Dive #13
36.6939
36.693
36.6921
36.6912
Latitude
-121.9576
-121.9568
-121.956
-121.9552
Longitude
T1
T3
C1
Start
Pgps
Pdr

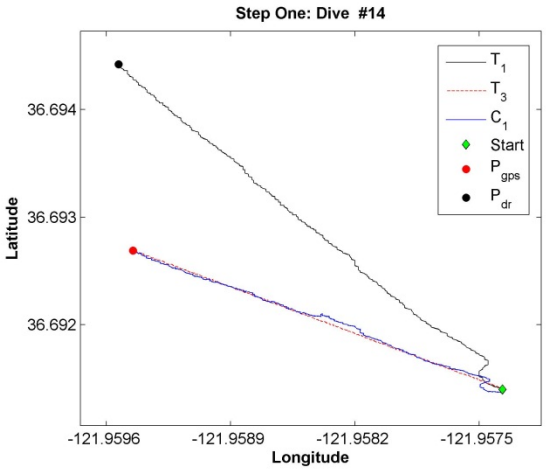
Step One: Dive #14
36.694
36.693
36.692
Latitude
-121.9596
-121.9589
-121.9582
-121.9575
Longitude
T1
T3
C1
Start
Pgps
Pdr

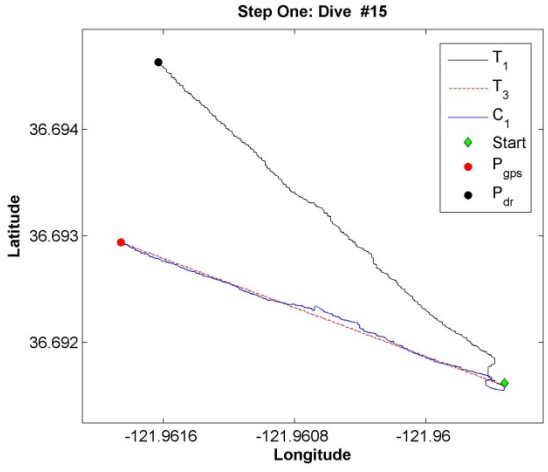
Step One: Dive #15
36.694
36.693
36.692
Latitude
-121.9616
-121.9608
-121.96
Longitude
T1
T3
C1
Start
Pgps
Pdr

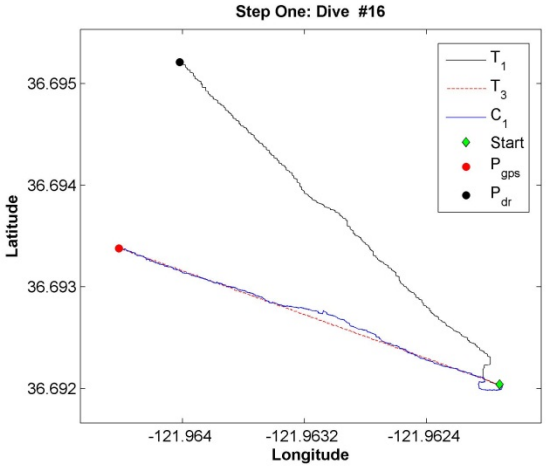
Step One: Dive #16
36.695
36.694
36.693
36.692
Latitude
-121.964
-121.9632
-121.9624
Longitude
T1
T3
C1
Start
Pgps
Pdr

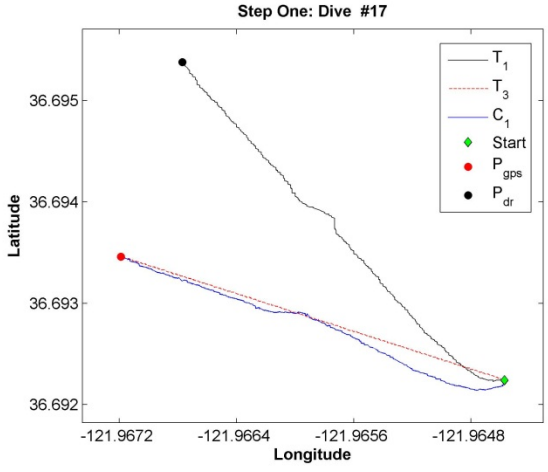
Step One: Dive #17
36.695
36.694
36.693
36.692
Latitude
-121.9672
-121.9664
-121.9656
-121.9648
Longitude
T1
T3
C1
Start
Pgps
Pdr

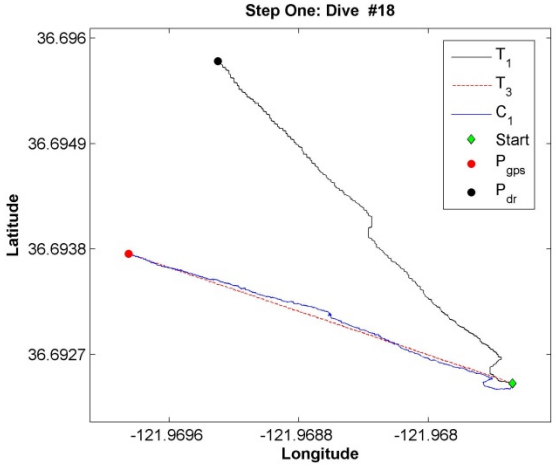
Step One: Dive #18
36.696
36.6949
36.6938
36.6927
Latitude
-121.9696
-121.9688
-121.968
Longitude
T1
T3
C1
Start
Pgps
Pdr

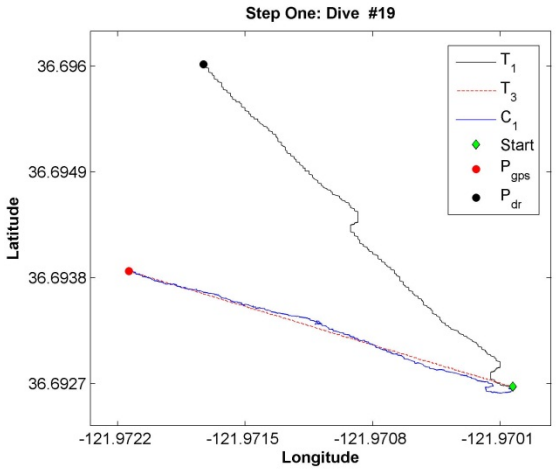
Step One: Dive #19
T1
T3
C1
Start
Pgps
Pdr
36.696
36.6949
36.6938
36.6927
Latitude
-121.9722
-121.9715
-121.9708
-121.9701
Longitude

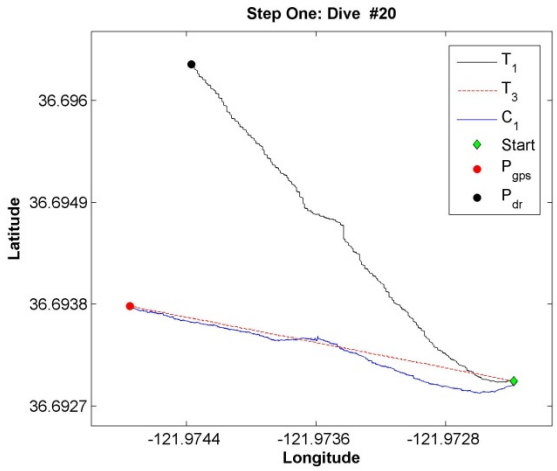
Step One: Dive #20
T1
T3
C1
Start
Pgps
Pdr
36.696
36.6949
36.6938
36.6927
Latitude
-121.9744
-121.9736
-121.9728
Longitude

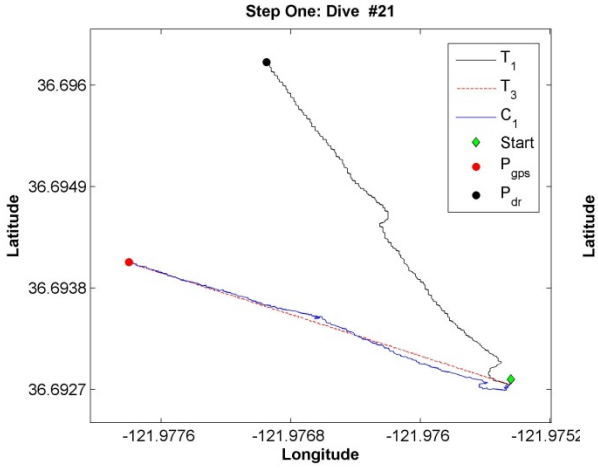
Step One: Dive #21
T1
T3
C1
Start
Pgps
Pdr
36.696
36.6949
36.6938
36.6927
Latitude
-121.9776
-121.9768
-121.976
Longitude

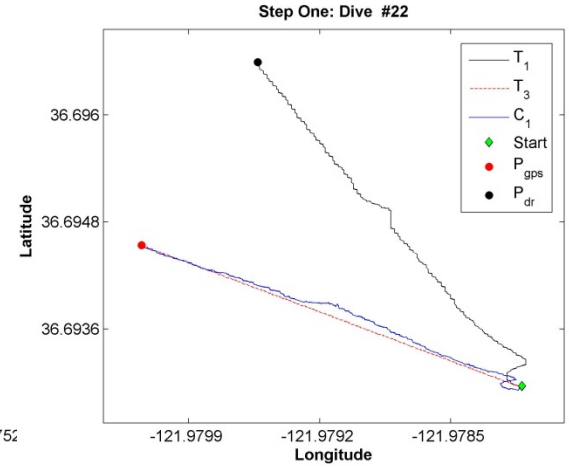
Step One: Dive #22
T1
T3
C1
Start
Pgps
Pdr
36.696
36.6948
36.6936
Latitude
-121.9799
-121.9792
-121.9785
Longitude

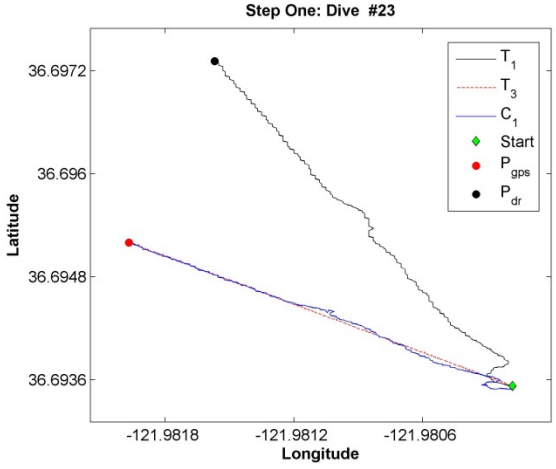
Step One: Dive #23
T1
T3
C1
Start
Pgps
Pdr
36.6972
36.696
36.6948
36.6936
Latitude
-121.9818
-121.9812
-121.9806
Longitude

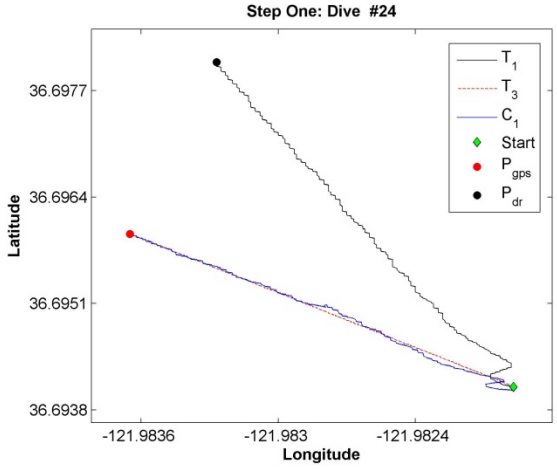
Step One: Dive #24
T1
T3
C1
Start
Pgps
Pdr
36.6977
36.6964
36.6951
36.6938
Latitude
-121.9836
-121.983
-121.9824
Longitude

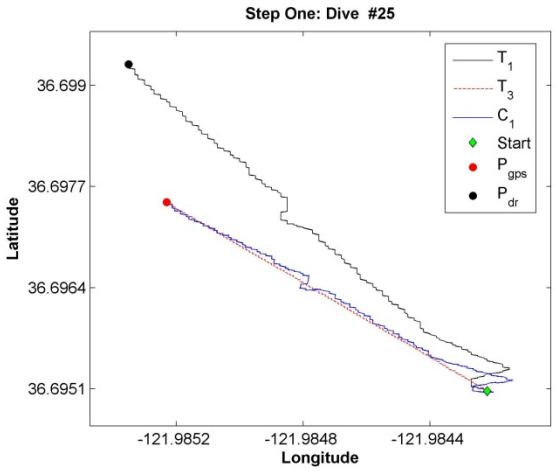
Step One: Dive #25
Latitude
Longitude
36.699
36.6977
36.6964
36.6951
-121.9852
-121.9848
-121.9844
T1
T3
C1
Start
Pgps
Pdr

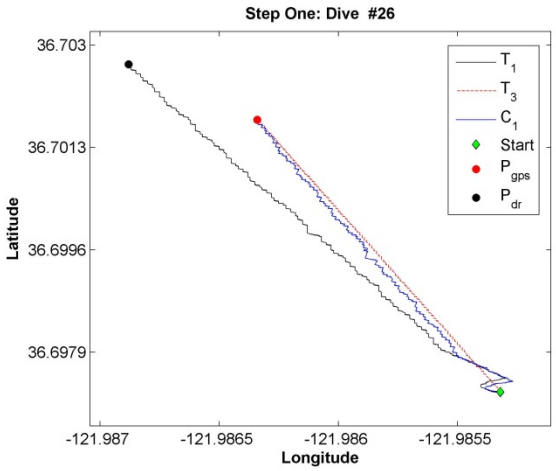
Step One: Dive #26
Latitude
Longitude
36.703
36.7013
36.6996
36.6979
-121.987
-121.9865
-121.986
-121.9855
T1
T3
C1
Start
Pgps
Pdr

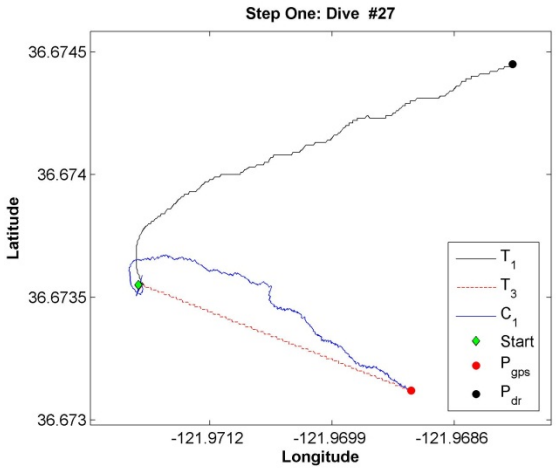
Step One: Dive #27
Latitude
Longitude
36.6745
36.674
36.6735
36.673
-121.9712
-121.9699
-121.9686
T1
T3
C1
Start
Pgps
Pdr

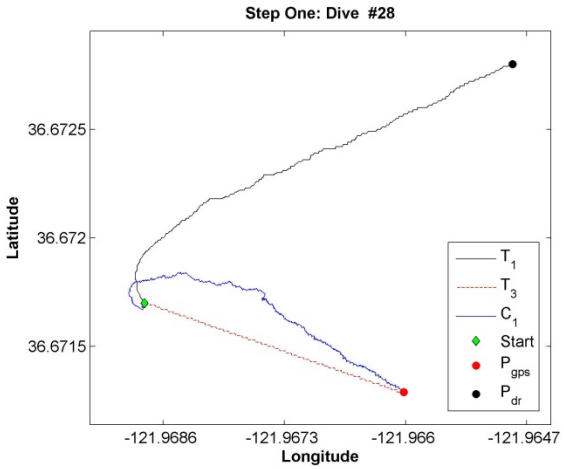
Step One: Dive #28
Latitude
Longitude
36.6725
36.672
36.6715
-121.9686
-121.9673
-121.966
-121.9647
T1
T3
C1
Start
Pgps
Pdr

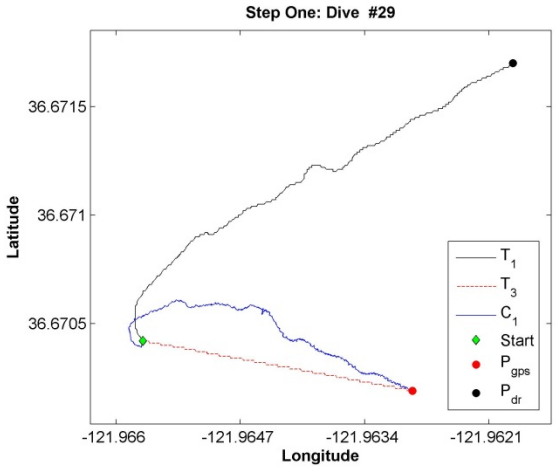
Step One: Dive #29
Latitude
Longitude
36.6715
36.671
36.6705
-121.966
-121.9647
-121.9634
-121.9621
T1
T3
C1
Start
Pgps
Pdr

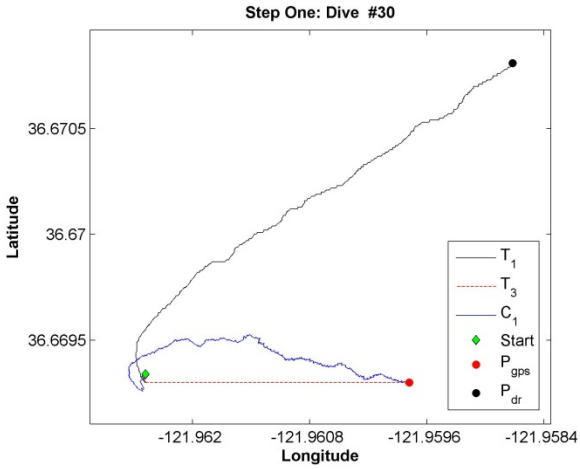
Step One: Dive #30
Latitude
Longitude
36.6705
36.67
36.6695
-121.962
-121.9608
-121.9596
-121.9584
T1
T3
C1
Start
Pgps
Pdr

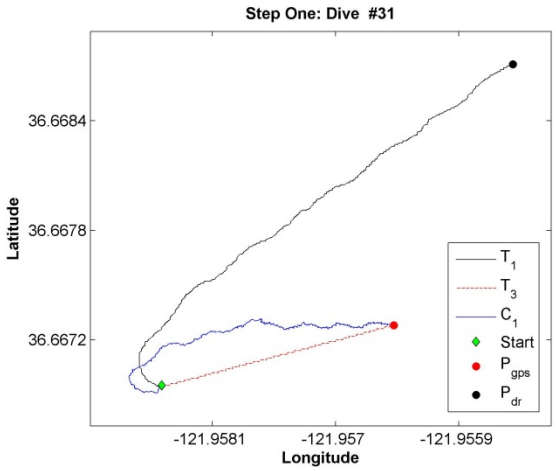
Step One: Dive #31
Latitude
Longitude
36.6684
36.6678
36.6672
-121.9581
-121.957
-121.9559
T1
T3
C1
Start
Pgps
Pdr

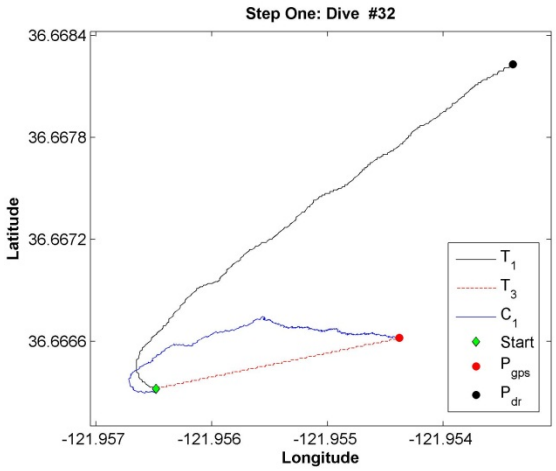
Step One: Dive #32
Latitude
Longitude
36.6684
36.6678
36.6672
36.6666
-121.957
-121.956
-121.955
-121.954
T1
T3
C1
Start
Pgps
Pdr

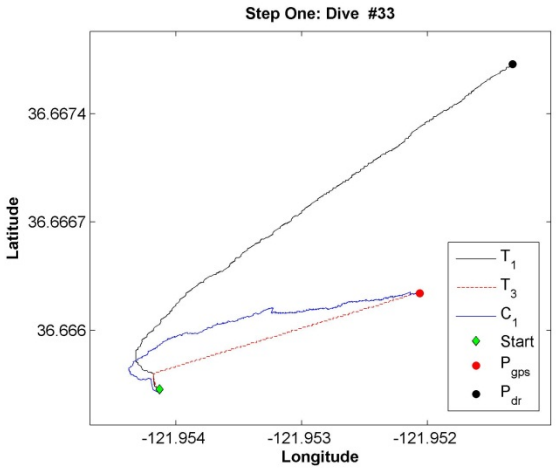
Step One: Dive #33
Latitude
Longitude
36.6674
36.6667
36.666
-121.954
-121.953
-121.952
T1
T3
C1
Start
Pgps
Pdr

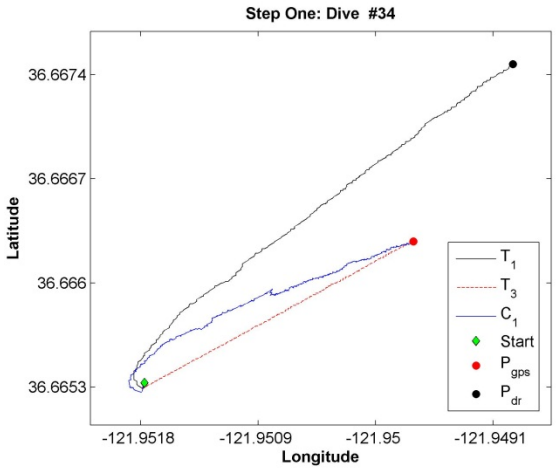
Step One: Dive #34
Latitude
Longitude
36.6674
36.6667
36.666
36.6653
-121.9518
-121.9509
-121.95
-121.9491
T1
T3
C1
Start
Pgps
Pdr

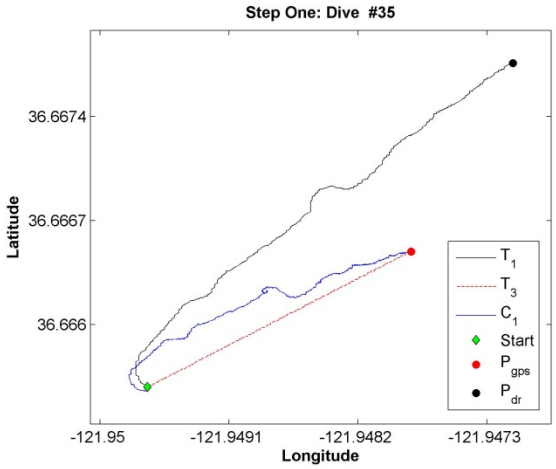
Step One: Dive #35
Latitude
Longitude
36.6674
36.6667
36.666
-121.95
-121.9491
-121.9482
-121.9473
T1
T3
C1
Start
Pgps
Pdr

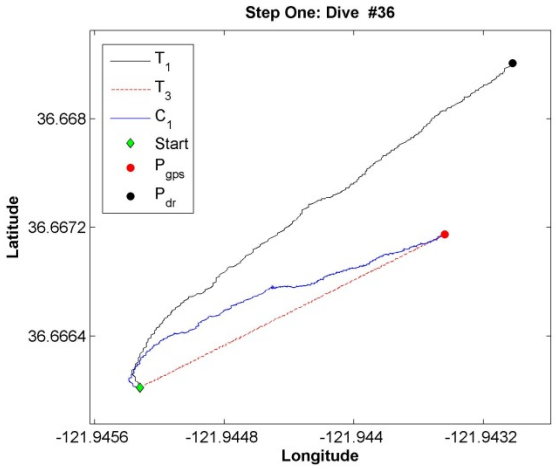
Step One: Dive #36
Latitude
Longitude
36.668
36.6672
36.6664
-121.9456
-121.9448
-121.944
-121.9432
T1
T3
C1
Start
Pgps
Pdr

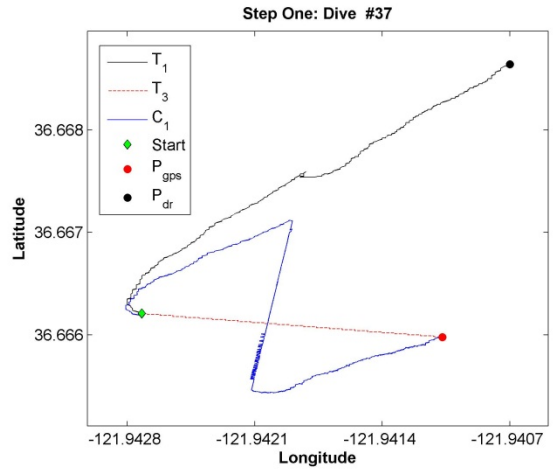
Step One: Dive #37
T1
T3
C1
Start
Pgps
Pdr
36.668
36.667
36.666
Latitude
-121.9428
-121.9421
-121.9414
-121.9407
Longitude

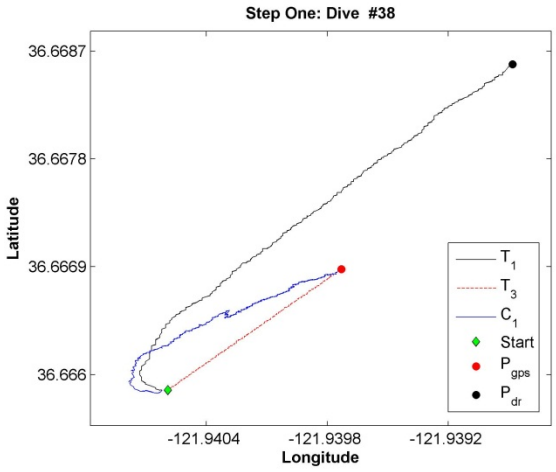
Step One: Dive #38
36.6687
36.6678
36.6669
36.666
Latitude
T1
T3
C1
Start
Pgps
Pdr
-121.9404
-121.9398
-121.9392
Longitude

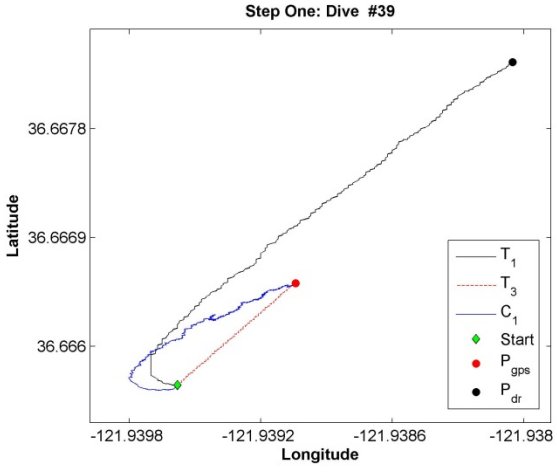
Step One: Dive #39
36.6678
36.6669
36.666
Latitude
T1
T3
C1
Start
Pgps
Pdr
-121.9398
-121.9392
-121.9386
-121.938
Longitude

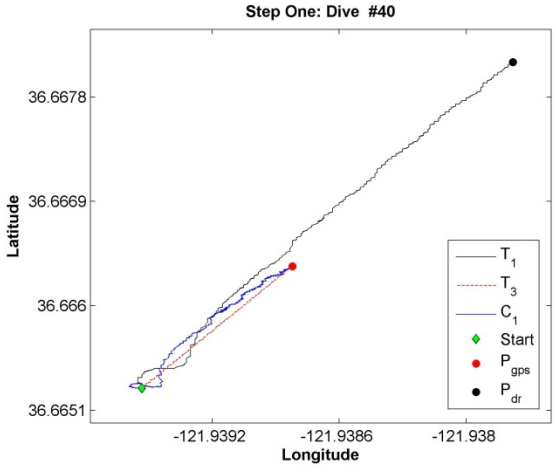
Step One: Dive #40
36.6678
36.6669
36.666
36.6651
Latitude
T1
T3
C1
Start
Pgps
Pdr
-121.9392
-121.9386
-121.938
Longitude

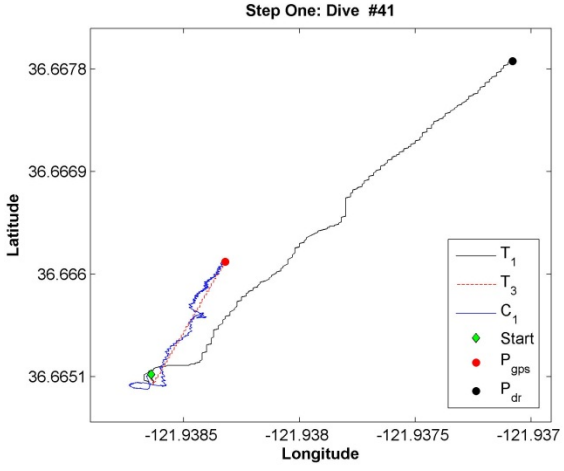
Step One: Dive #41
36.6678
36.6669
36.666
36.6651
Latitude
T1
T3
C1
Start
Pgps
Pdr
-121.9385
-121.938
-121.9375
-121.937
Longitude

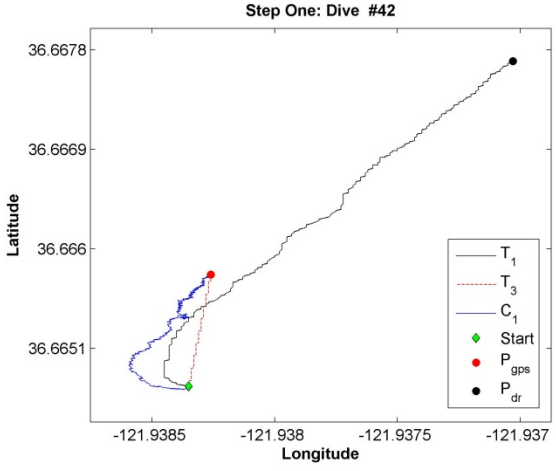
Step One: Dive #42
36.6678
36.6669
36.666
36.6651
Latitude
T1
T3
C1
Start
Pgps
Pdr
-121.9385
-121.938
-121.9375
-121.937
Longitude

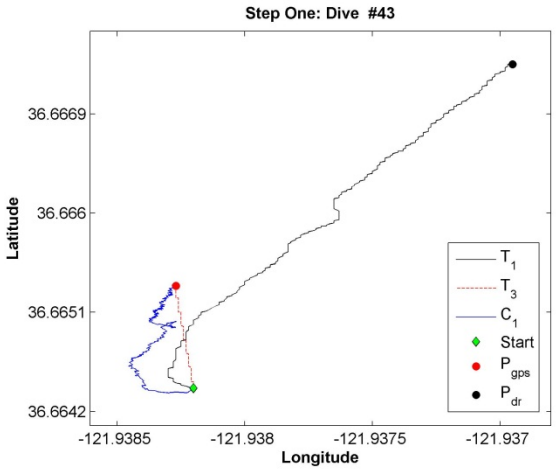
Step One: Dive #43
Latitude
Longitude
36.6669
36.666
36.6651
36.6642
-121.9385
-121.938
-121.9375
-121.937
T1
T3
C1
Start
Pgps
Pdr

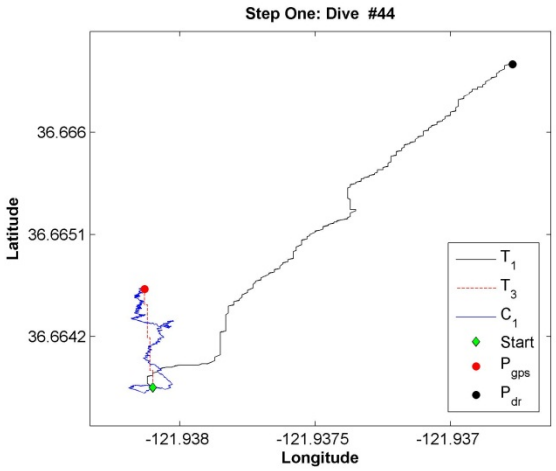
Step One: Dive #44
Latitude
Longitude
36.666
36.6651
36.6642
-121.938
-121.9375
-121.937
T1
T3
C1
Start
Pgps
Pdr

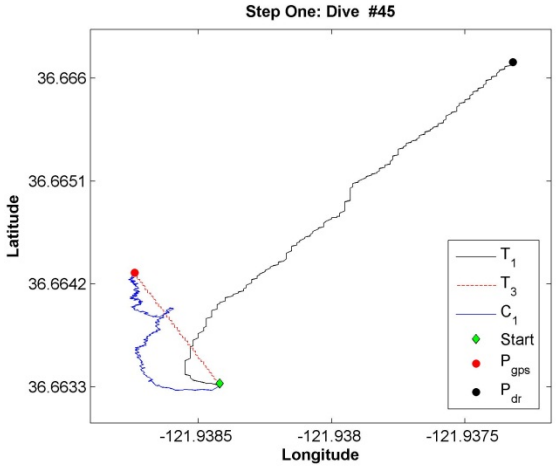
Step One: Dive #45
Latitude
Longitude
36.666
36.6651
36.6642
36.6633
-121.9385
-121.938
-121.9375
T1
T3
C1
Start
Pgps
Pdr

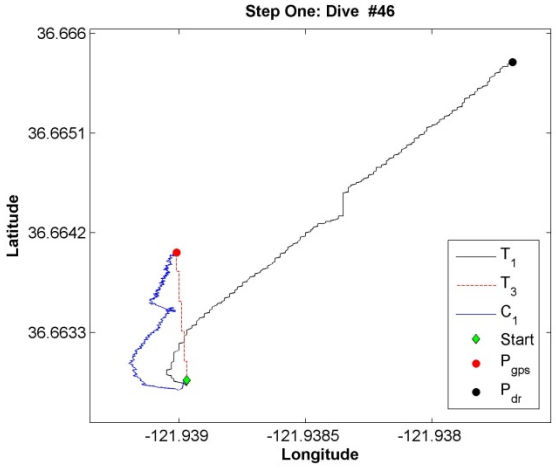
Step One: Dive #46
Latitude
Longitude
36.666
36.6651
36.6642
36.6633
-121.939
-121.9385
-121.938
T1
T3
C1
Start
Pgps
Pdr

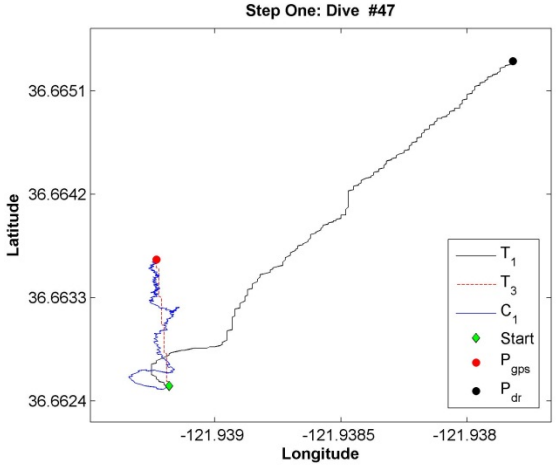
Step One: Dive #47
Latitude
Longitude
36.6651
36.6642
36.6633
36.6624
-121.939
-121.9385
-121.938
T1
T3
C1
Start
Pgps
Pdr

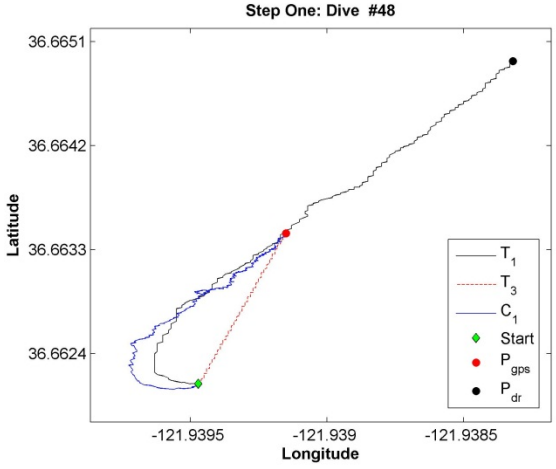
Step One: Dive #48
Latitude
Longitude
36.6651
36.6642
36.6633
36.6624
-121.9395
-121.939
-121.9385
T1
T3
C1
Start
Pgps
Pdr

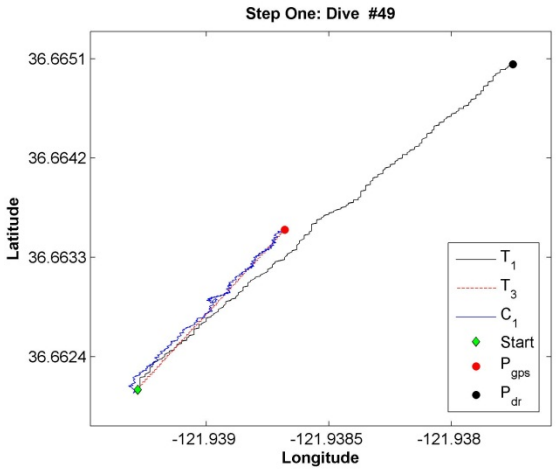
Step One: Dive #49
36.6651
36.6642
36.6633
36.6624
Latitude
-121.939
-121.9385
-121.938
Longitude
T1
T3
C1
Start
Pgps
Pdr

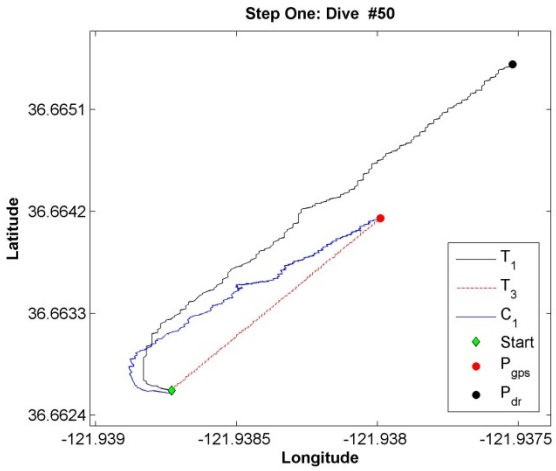
Step One: Dive #50
36.6651
36.6642
36.6633
36.6624
Latitude
-121.939
-121.9385
-121.938
-121.9375
Longitude
T1
T3
C1
Start
Pgps
Pdr

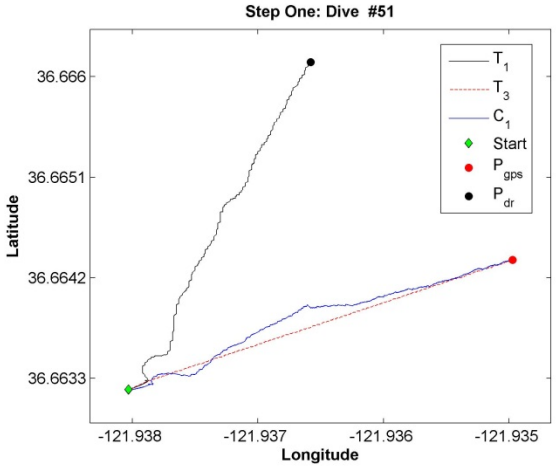
Step One: Dive #51
36.666
36.6651
36.6642
36.6633
Latitude
-121.938
-121.937
-121.936
-121.935
Longitude
T1
T3
C1
Start
Pgps
Pdr

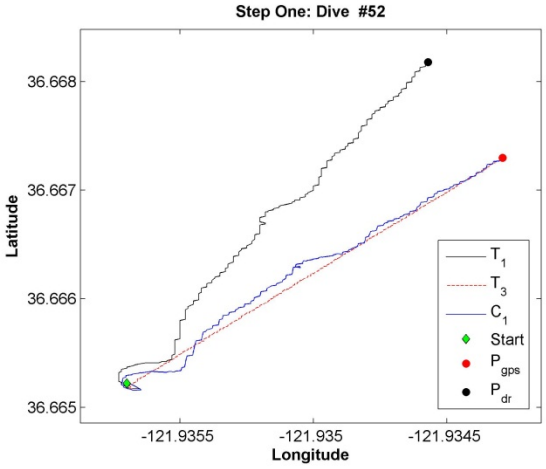
Step One: Dive #52
36.668
36.667
36.666
36.665
Latitude
-121.9355
-121.935
-121.9345
Longitude
T1
T3
C1
Start
Pgps
Pdr

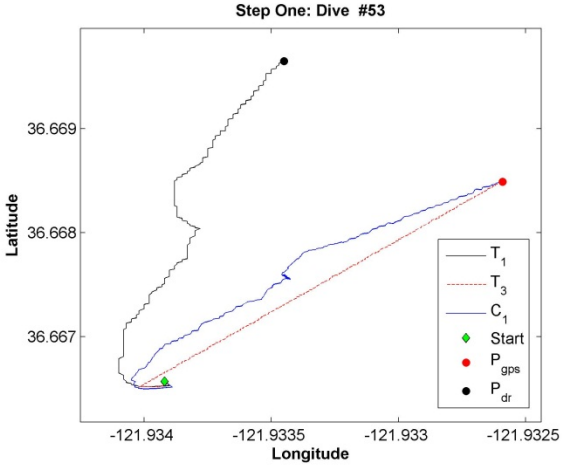
Step One: Dive #53
36.669
36.668
36.667
Latitude
-121.934
-121.9335
-121.933
-121.9325
Longitude
T1
T3
C1
Start
Pgps
Pdr

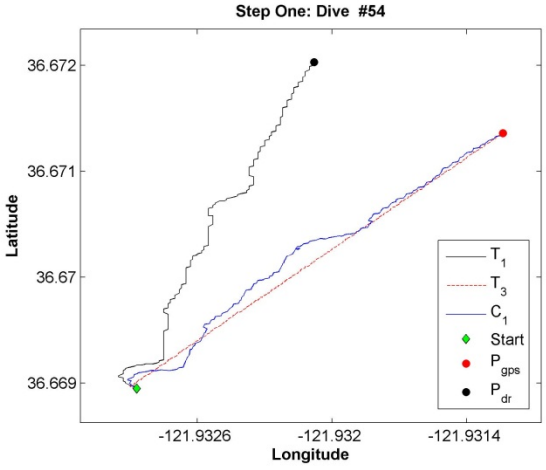
Step One: Dive #54
36.672
36.671
36.67
36.669
Latitude
-121.9326
-121.932
-121.9314
Longitude
T1
T3
C1
Start
Pgps
Pdr

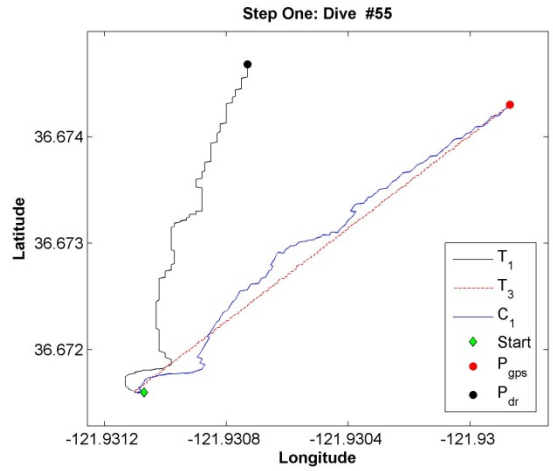
Step One: Dive #55
Latitude
Longitude
36.674
36.673
36.672
-121.9312
-121.9308
-121.9304
-121.93
T1
T3
C1
Start
Pgps
Pdr

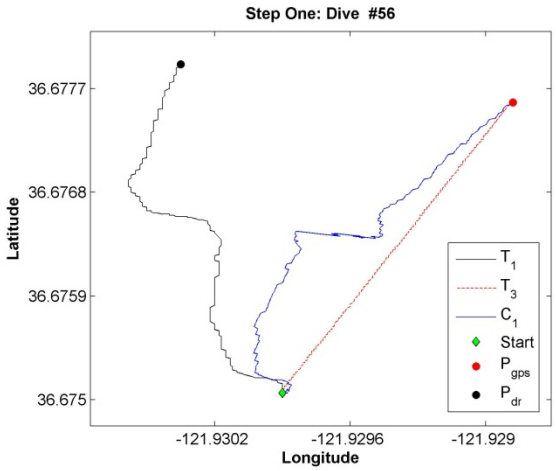
Step One: Dive #56
Latitude
Longitude
36.6777
36.6768
36.6759
36.675
-121.9302
-121.9296
-121.929
T1
T3
C1
Start
Pgps
Pdr

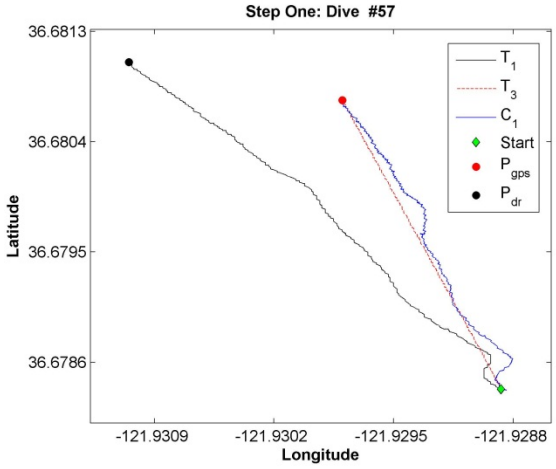
Step One: Dive #57
Latitude
Longitude
36.6813
36.6804
36.6795
36.6786
-121.9309
-121.9302
-121.9295
-121.9288
T1
T3
C1
Start
Pgps
Pdr

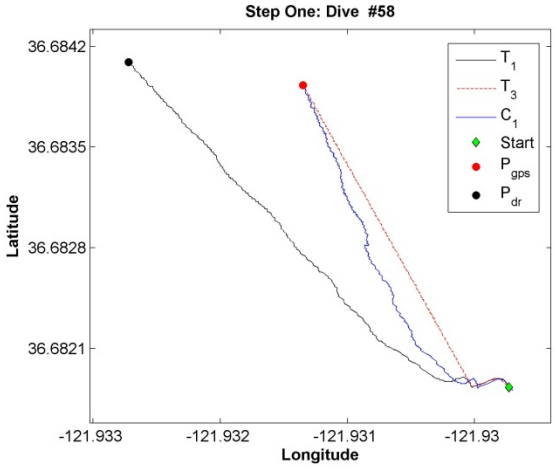
Step One: Dive #58
Latitude
Longitude
36.6842
36.6835
36.6828
36.6821
-121.933
-121.932
-121.931
-121.93
T1
T3
C1
Start
Pgps
Pdr

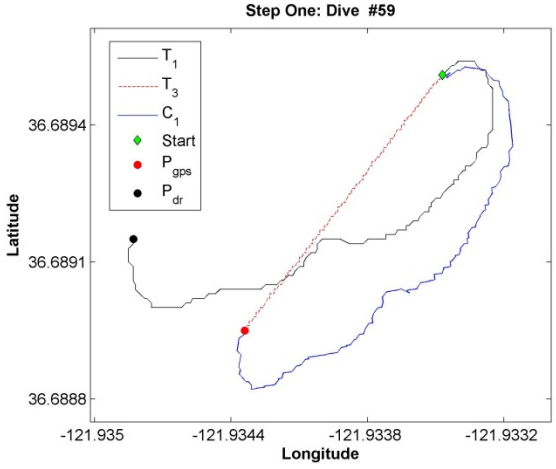
Step One: Dive #59
Latitude
Longitude
36.6894
36.6891
36.6888
-121.935
-121.9344
-121.9338
-121.9332
T1
T3
C1
Start
Pgps
Pdr

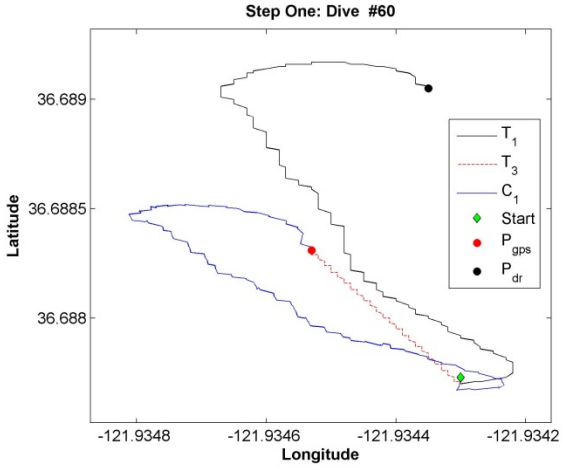
Step One: Dive #60
Latitude
Longitude
36.689
36.6885
36.688
-121.9348
-121.9346
-121.9344
-121.9342
T1
T3
C1
Start
Pgps
Pdr

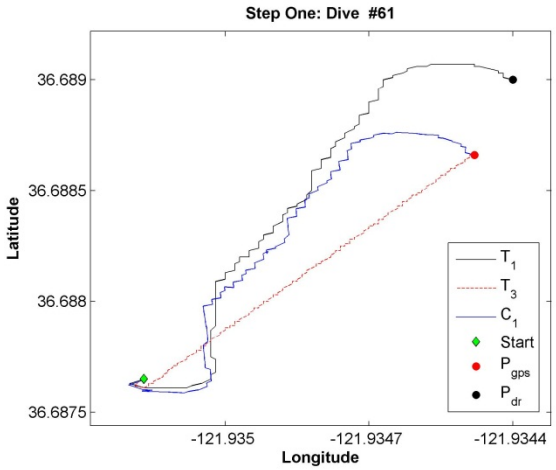
Step One: Dive #61
Latitude
Longitude
36.689
36.6885
36.688
36.6875
-121.935
-121.9347
-121.9344
T1
T3
C1
Start
Pgps
Pdr

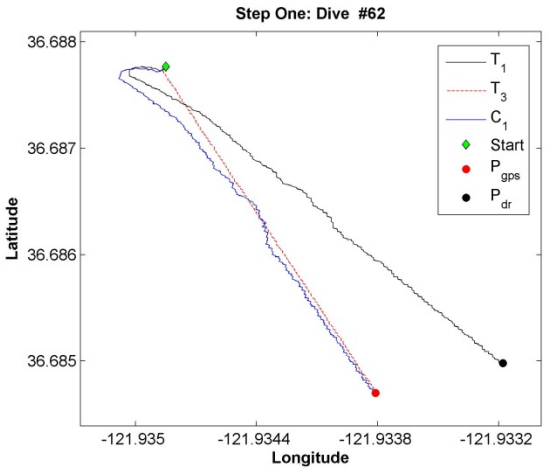
Step One: Dive #62
Latitude
Longitude
36.688
36.687
36.686
36.685
-121.935
-121.9344
-121.9338
-121.9332
T1
T3
C1
Start
Pgps
Pdr

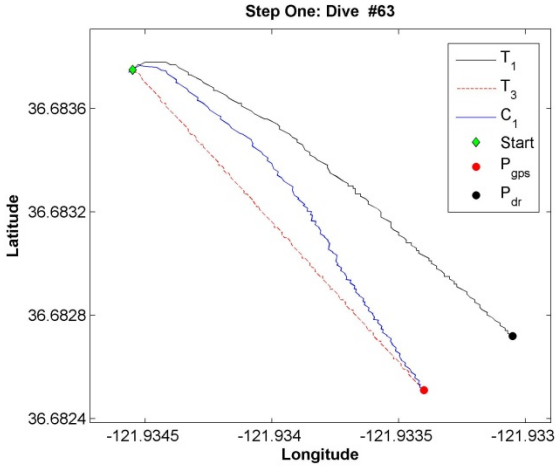
Step One: Dive #63
Latitude
Longitude
36.6836
36.6832
36.6828
36.6824
-121.9345
-121.934
-121.9335
-121.933
T1
T3
C1
Start
Pgps
Pdr

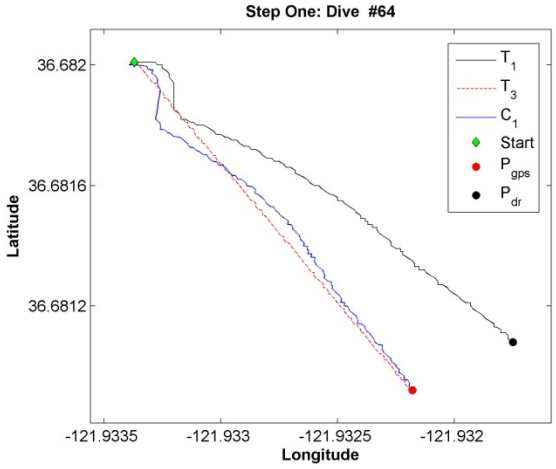
Step One: Dive #64
Latitude
Longitude
36.682
36.6816
36.6812
-121.9335
-121.933
-121.9325
-121.932
T1
T3
C1
Start
Pgps
Pdr

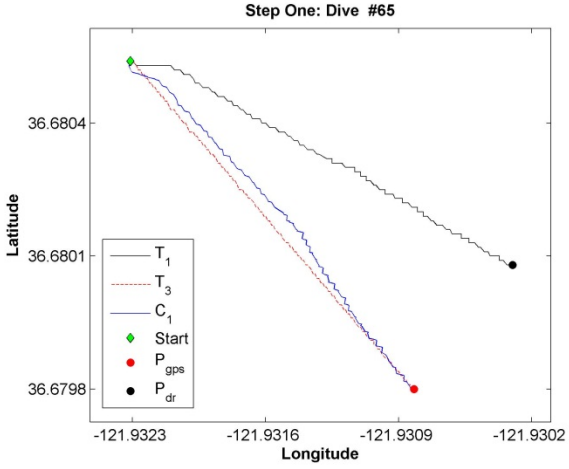
Step One: Dive #65
Latitude
Longitude
36.6804
36.6801
36.6798
-121.9323
-121.9316
-121.9309
-121.9302
T1
T3
C1
Start
Pgps
Pdr

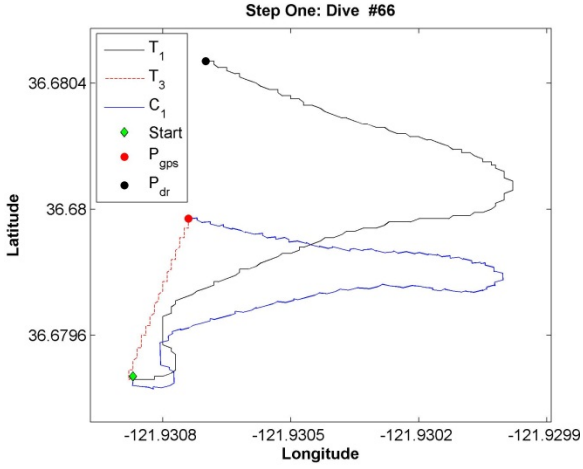
Step One: Dive #66
Latitude
Longitude
36.6804
36.68
36.6796
-121.9308
-121.9305
-121.9302
-121.9299
T1
T3
C1
Start
Pgps
Pdr

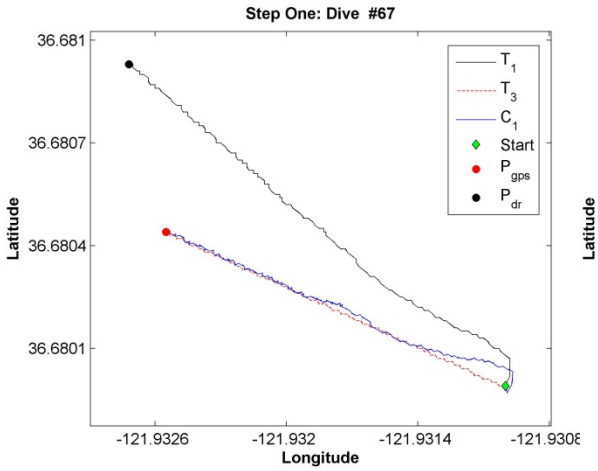
Step One: Dive #67
36.681
36.6807
36.6804
36.6801
Latitude
-121.9326
-121.932
-121.9314
-121.9308
Longitude
T1
T3
C1
Start
Pgps
Pdr

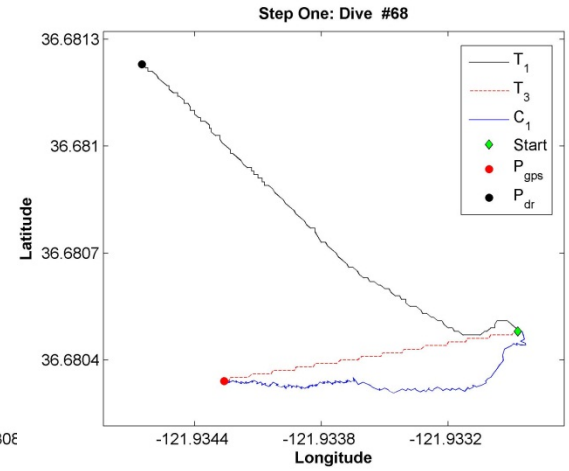
Step One: Dive #68
36.6813
36.681
36.6807
36.6804
Latitude
-121.9344
-121.9338
-121.9332
Longitude
T1
T3
C1
Start
Pgps
Pdr

C. STEP TWO: DR TRAJECTORIES WITH DEPTH-DEPENDENT CORRECTION METHOD

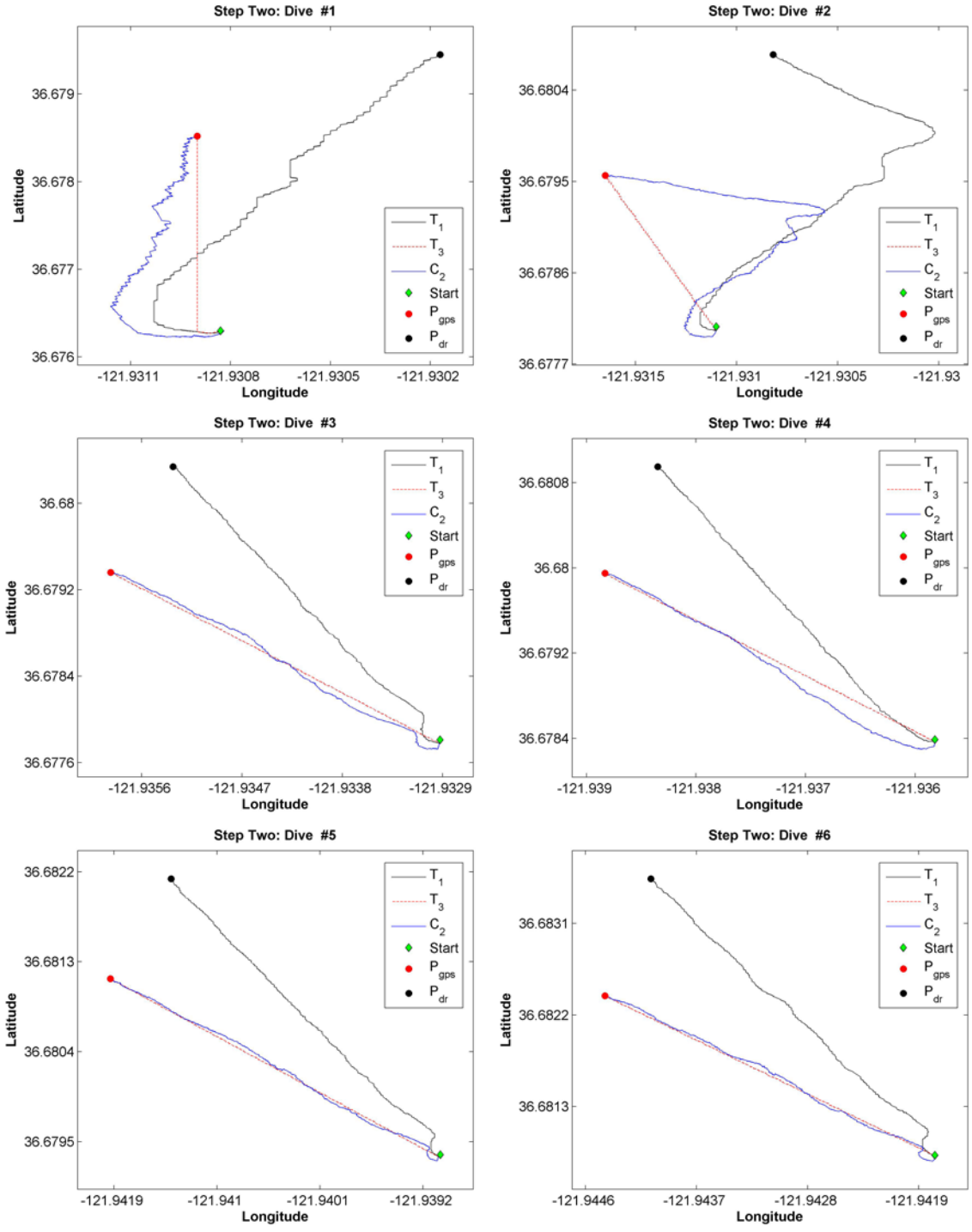

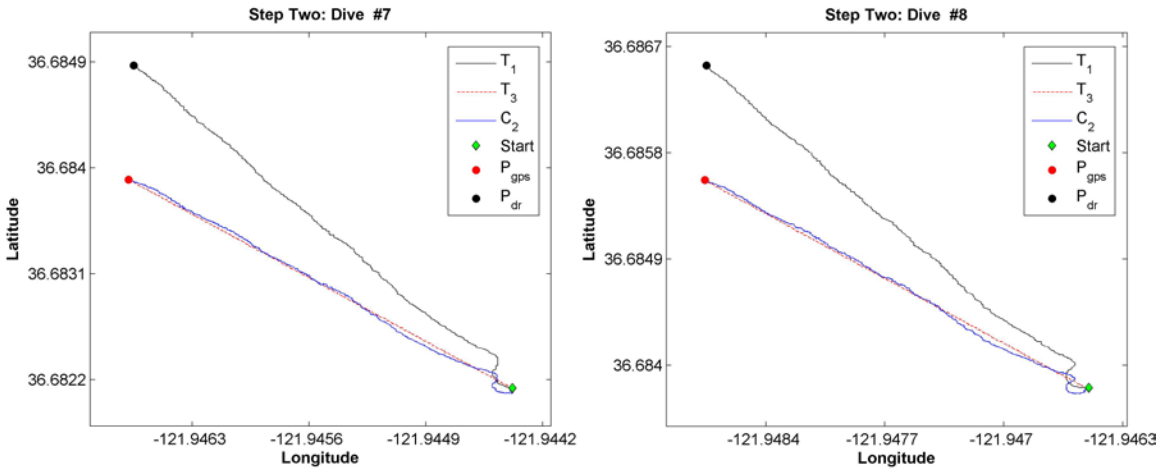
Step Two: Dive #7
Latitude
Longitude
36.6849
36.684
36.6831
36.6822
-121.9463
-121.9456
-121.9449
-121.9442
T1
T3
C2
Start
Pgps
Pdr

Step Two: Dive #8
Latitude
Longitude
36.6867
36.6858
36.6849
36.684
-121.9484
-121.9477
-121.947
-121.9463
T1
T3
C2
Start
Pgps
Pdr

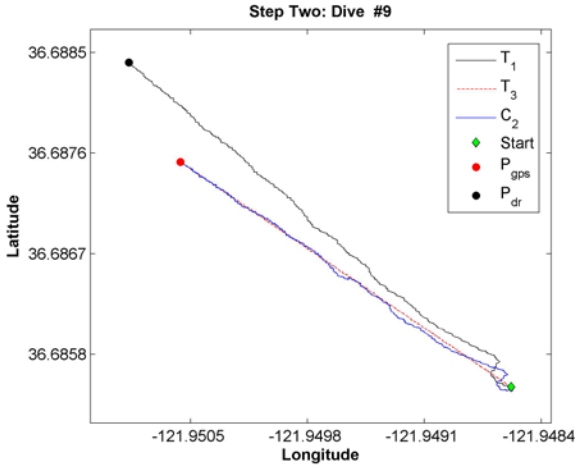
Step Two: Dive #9
Latitude
Longitude
36.6885
36.6876
36.6867
36.6858
-121.9505
-121.9498
-121.9491
-121.9484
T1
T3
C2
Start
Pgps
Pdr

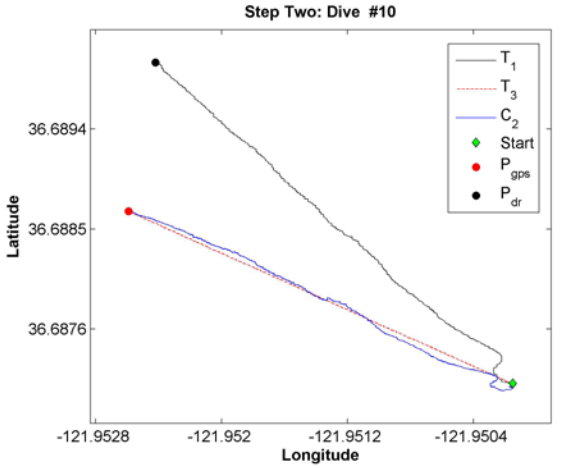
Step Two: Dive #10
Latitude
Longitude
36.6894
36.6885
36.6876
-121.9528
-121.952
-121.9512
-121.9504
T1
T3
C2
Start
Pgps
Pdr

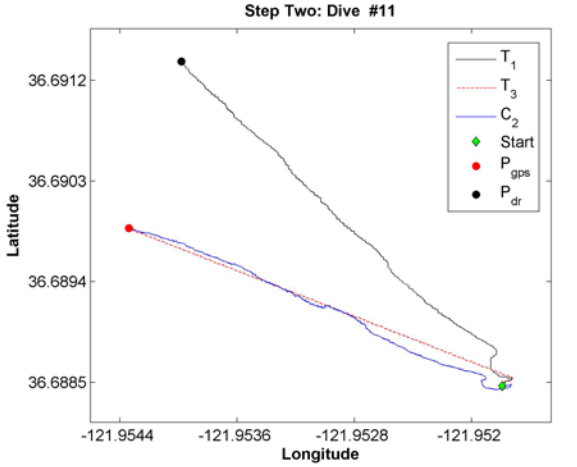
Step Two: Dive #11
Latitude
Longitude
36.6912
36.6903
36.6894
36.6885
-121.9544
-121.9536
-121.9528
-121.952
T1
T3
C2
Start
Pgps
Pdr

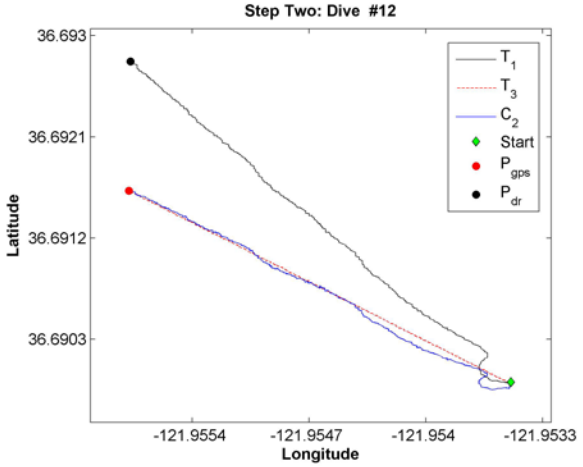
Step Two: Dive #12
Latitude
Longitude
36.693
36.6921
36.6912
36.6903
-121.9554
-121.9547
-121.954
-121.9533
T1
T3
C2
Start
Pgps
Pdr

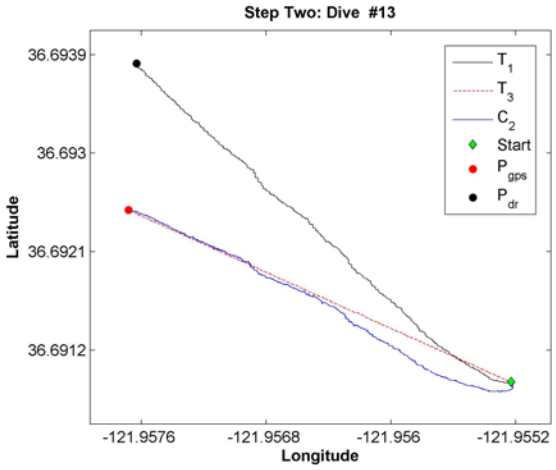
Step Two: Dive #13
T1
T3
C2
Start
Pgps
Pdr
36.6939
36.693
36.6921
36.6912
Latitude
-121.9576
-121.9568
-121.956
-121.9552
Longitude

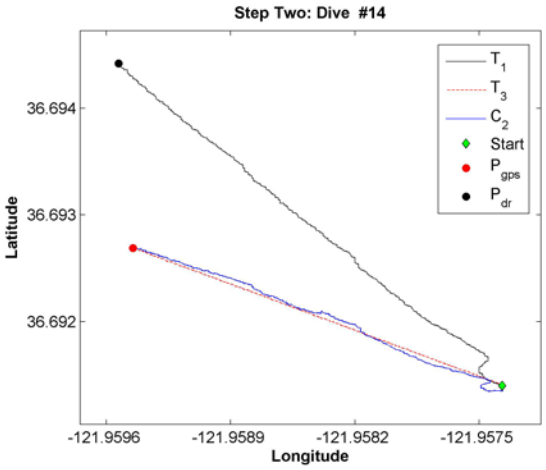
Step Two: Dive #14
T1
T3
C2
Start
Pgps
Pdr
36.694
36.693
36.692
Latitude
-121.9596
-121.9589
-121.9582
-121.9575
Longitude

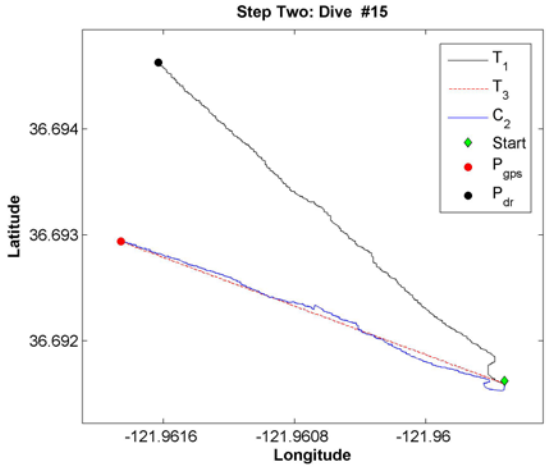
Step Two: Dive #15
T1
T3
C2
Start
Pgps
Pdr
36.694
36.693
36.692
Latitude
-121.9616
-121.9608
-121.96
Longitude

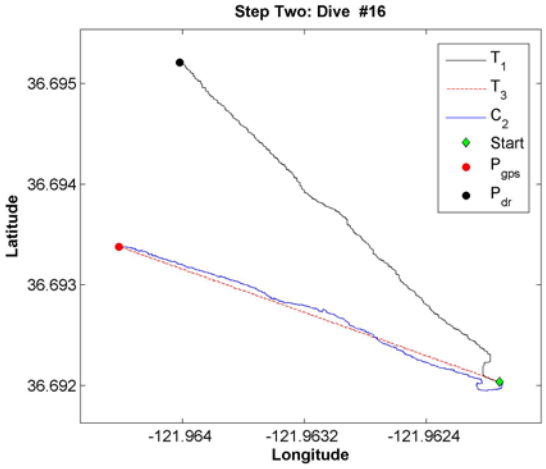
Step Two: Dive #16
T1
T3
C2
Start
Pgps
Pdr
36.695
36.694
36.693
36.692
Latitude
-121.964
-121.9632
-121.9624
Longitude

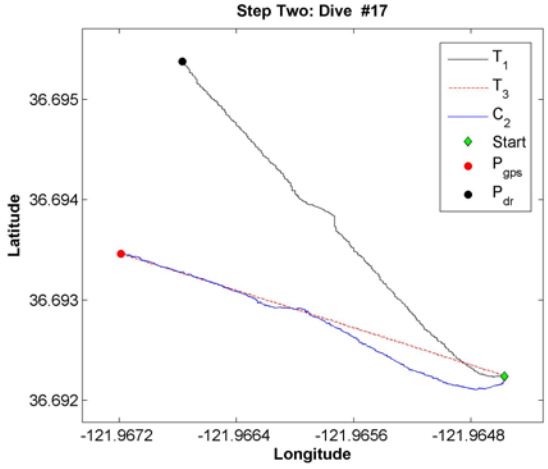
Step Two: Dive #17
T1
T3
C2
Start
Pgps
Pdr
36.695
36.694
36.693
36.692
Latitude
-121.9672
-121.9664
-121.9656
-121.9648
Longitude

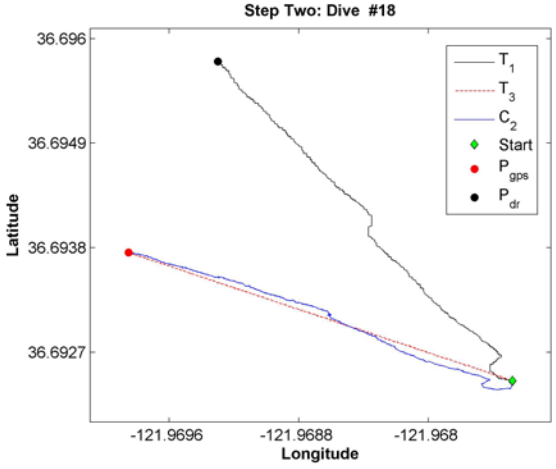
Step Two: Dive #18
T1
T3
C2
Start
Pgps
Pdr
36.696
36.6949
36.6938
36.6927
Latitude
-121.9696
-121.9688
-121.968
Longitude

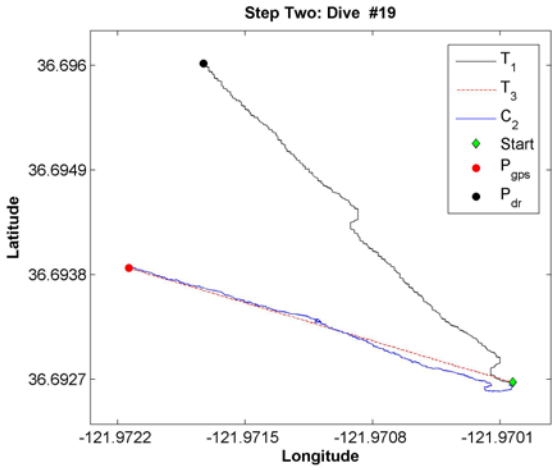
Step Two: Dive #19
T1
T3
C2
Start
Pgps
Pdr
Latitude
36.696
36.6949
36.6938
36.6927
-121.9722
-121.9715
-121.9708
-121.9701
Longitude

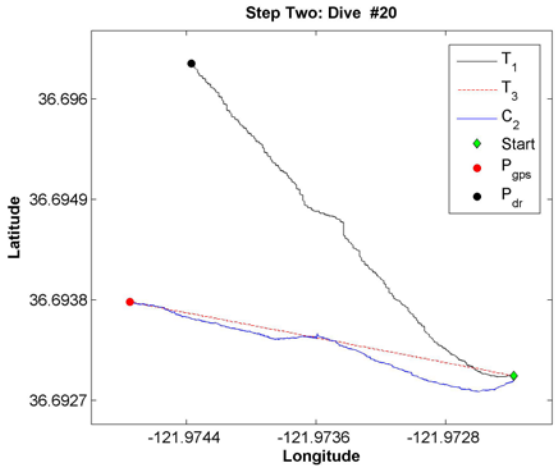
Step Two: Dive #20
T1
T3
C2
Start
Pgps
Pdr
Latitude
36.696
36.6949
36.6938
36.6927
-121.9744
-121.9736
-121.9728
Longitude

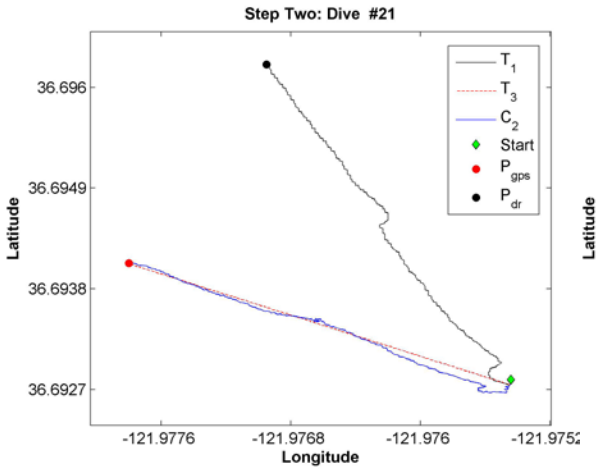
Step Two: Dive #21
T1
T3
C2
Start
Pgps
Pdr
Latitude
36.696
36.6949
36.6938
36.6927
-121.9776
-121.9768
-121.976
Longitude

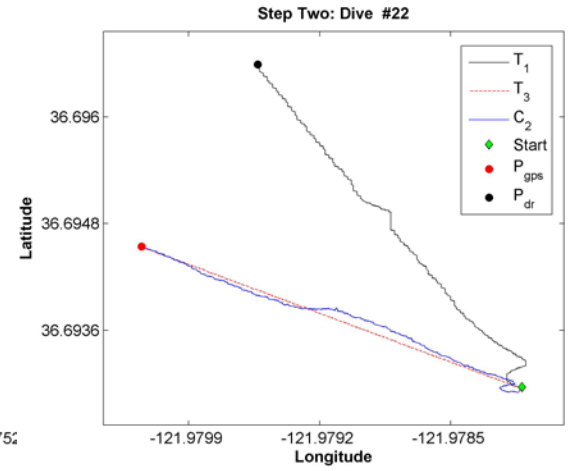
Step Two: Dive #22
T1
T3
C2
Start
Pgps
Pdr
Latitude
36.696
36.6948
36.6936
-121.9799
-121.9792
-121.9785
Longitude

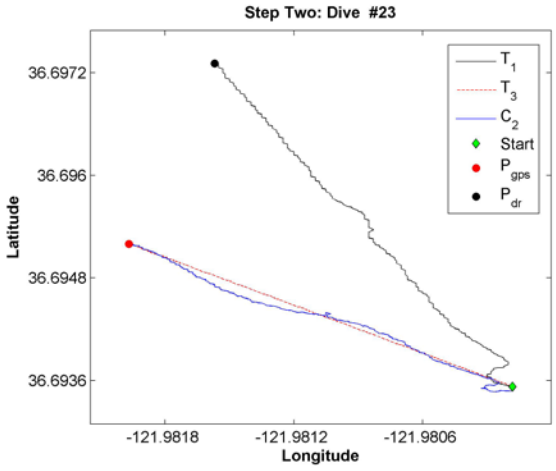
Step Two: Dive #23
T1
T3
C2
Start
Pgps
Pdr
Latitude
36.6972
36.696
36.6948
36.6936
-121.9818
-121.9812
-121.9806
Longitude

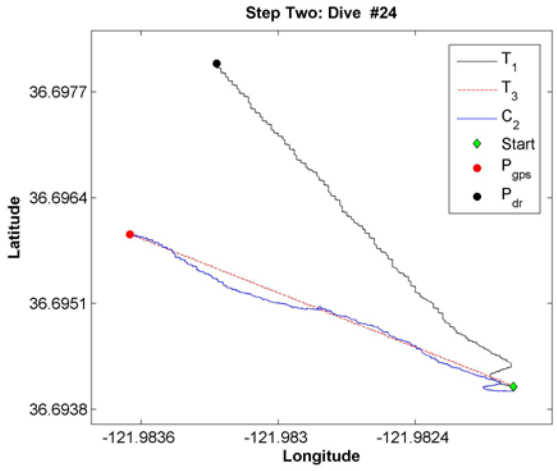
Step Two: Dive #24
T1
T3
C2
Start
Pgps
Pdr
Latitude
36.6977
36.6964
36.6951
36.6938
-121.9836
-121.983
-121.9824
Longitude

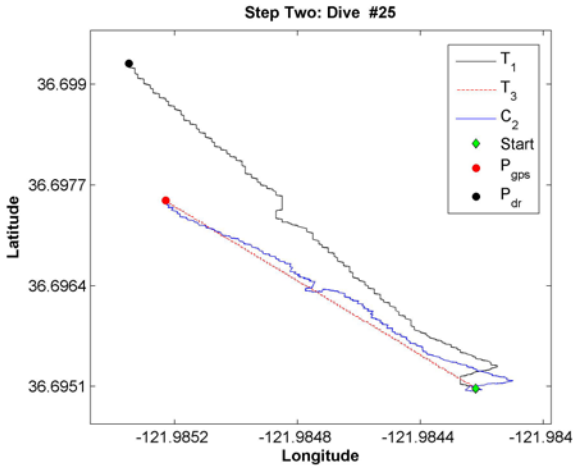
Step Two: Dive #25
Latitude
Longitude
36.699
36.6977
36.6964
36.6951
-121.9852
-121.9848
-121.9844
-121.984
T1
T3
C2
Start
Pgps
Pdr

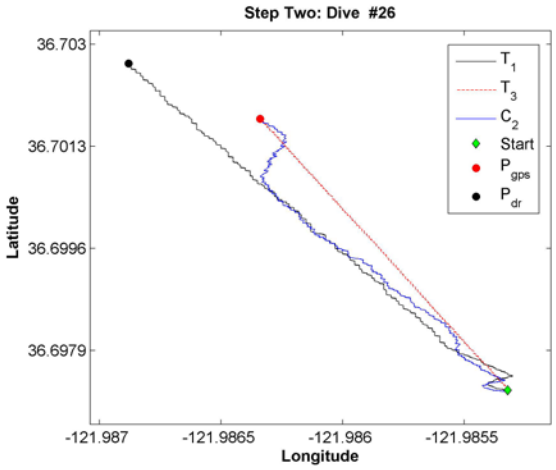
Step Two: Dive #26
Latitude
Longitude
36.703
36.7013
36.6996
36.6979
-121.987
-121.9865
-121.986
-121.9855
T1
T3
C2
Start
Pgps
Pdr

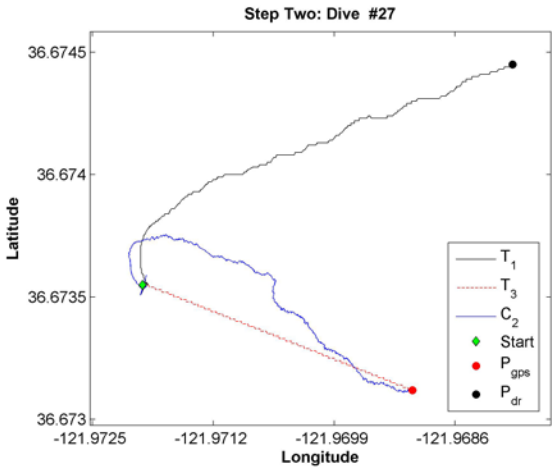
Step Two: Dive #27
Latitude
Longitude
36.6745
36.674
36.6735
36.673
-121.9725
-121.9712
-121.9699
-121.9686
T1
T3
C2
Start
Pgps
Pdr

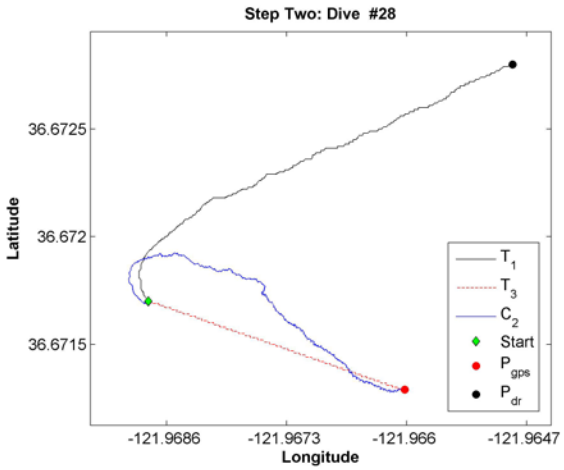
Step Two: Dive #28
Latitude
Longitude
36.6725
36.672
36.6715
-121.9686
-121.9673
-121.966
-121.9647
T1
T3
C2
Start
Pgps
Pdr

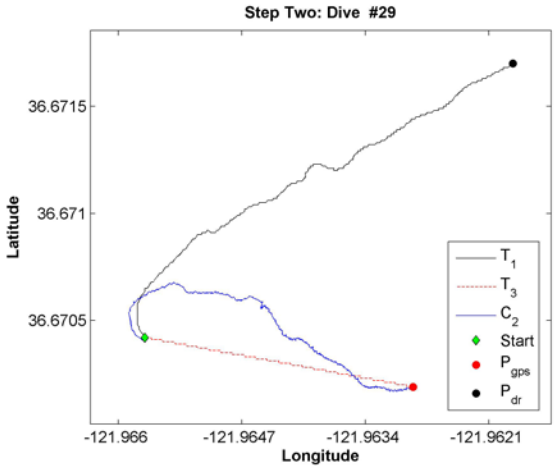
Step Two: Dive #29
Latitude
Longitude
36.6715
36.671
36.6705
-121.966
-121.9647
-121.9634
-121.9621
T1
T3
C2
Start
Pgps
Pdr

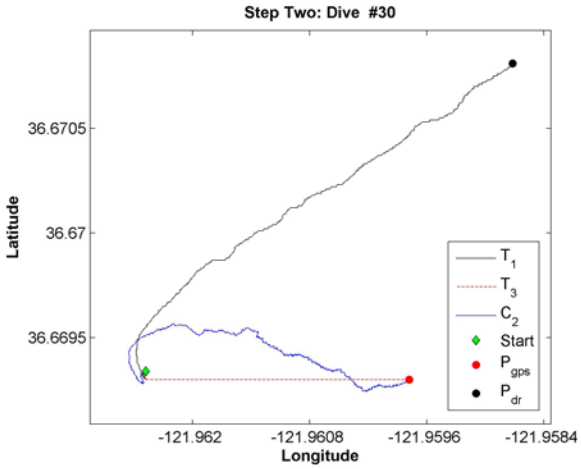
Step Two: Dive #30
Latitude
Longitude
36.6705
36.67
36.6695
-121.962
-121.9608
-121.9596
-121.9584
T1
T3
C2
Start
Pgps
Pdr

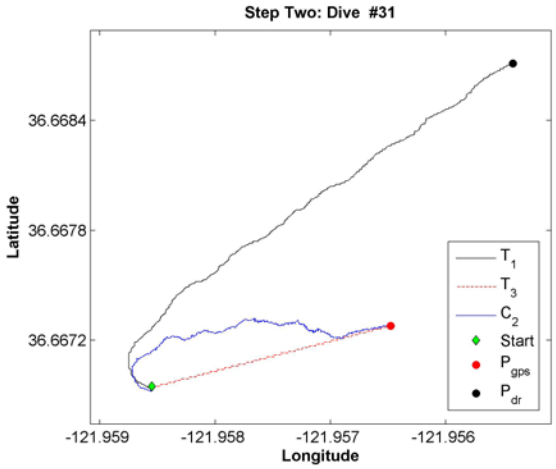
Step Two: Dive #31
Latitude
Longitude
36.6684
36.6678
36.6672
-121.959
-121.958
-121.957
-121.956
T1
T3
C2
Start
Pgps
Pdr

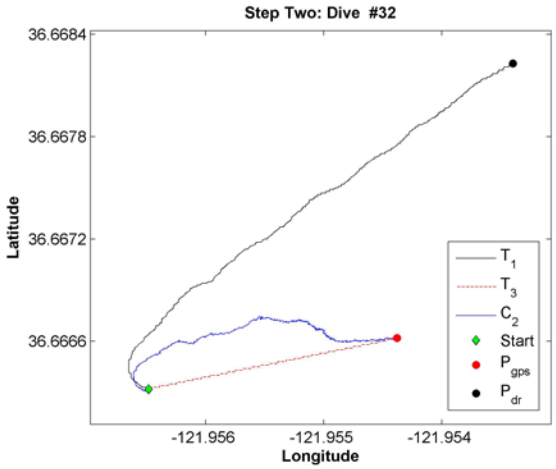
Step Two: Dive #32
Latitude
Longitude
36.6684
36.6678
36.6672
36.6666
-121.956
-121.955
-121.954
T1
T3
C2
Start
Pgps
Pdr

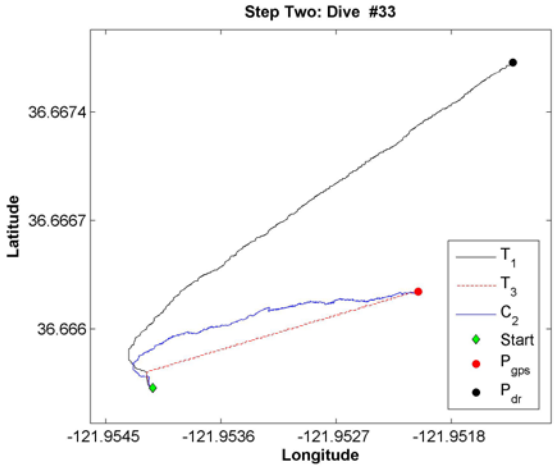
Step Two: Dive #33
Latitude
Longitude
36.6674
36.6667
36.666
-121.9545
-121.9536
-121.9527
-121.9518
T1
T3
C2
Start
Pgps
Pdr

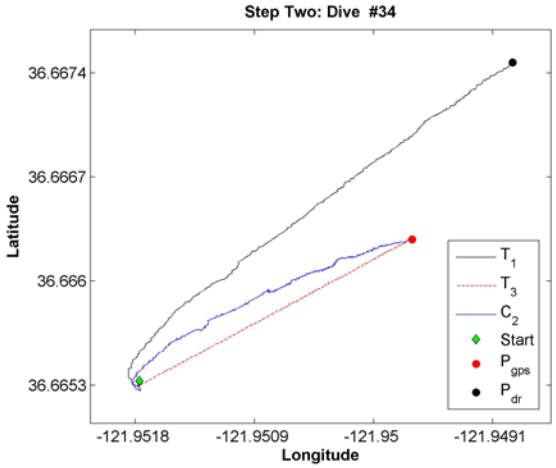
Step Two: Dive #34
Latitude
Longitude
36.6674
36.6667
36.666
36.6653
-121.9518
-121.9509
-121.95
-121.9491
T1
T3
C2
Start
Pgps
Pdr

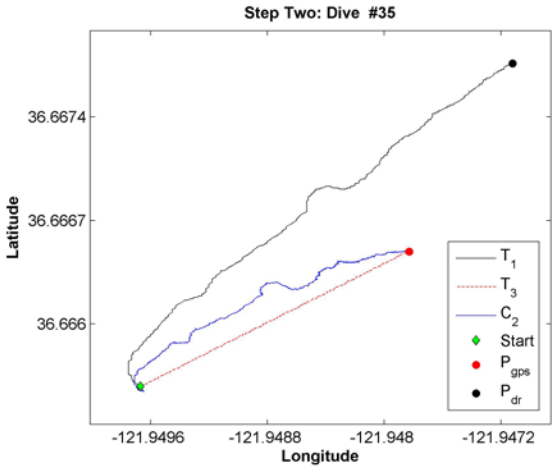
Step Two: Dive #35
Latitude
Longitude
36.6674
36.6667
36.666
-121.9496
-121.9488
-121.948
-121.9472
T1
T3
C2
Start
Pgps
Pdr

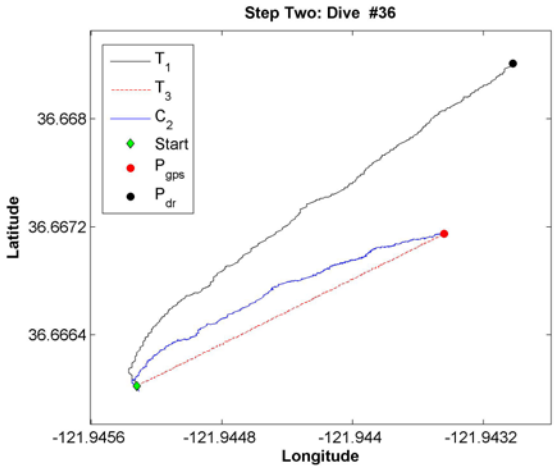
Step Two: Dive #36
Latitude
Longitude
36.668
36.6672
36.6664
-121.9456
-121.9448
-121.944
-121.9432
T1
T3
C2
Start
Pgps
Pdr

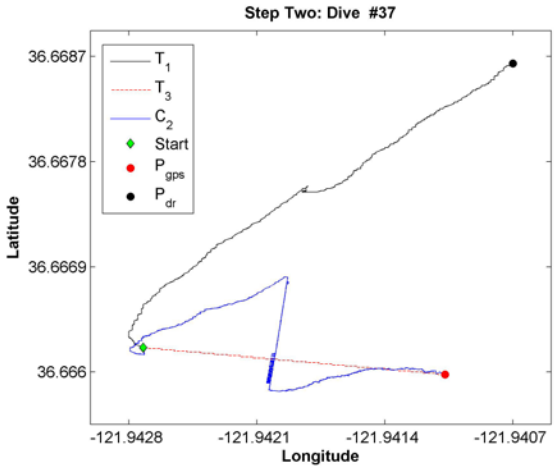
Step Two: Dive #37
Latitude
Longitude
36.6687
36.6678
36.6669
36.666
-121.9428
-121.9421
-121.9414
-121.9407
T1
T3
C2
Start
Pgps
Pdr

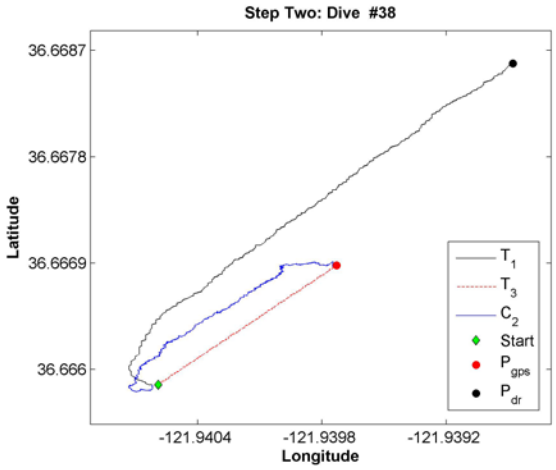
Step Two: Dive #38
Latitude
Longitude
36.6687
36.6678
36.6669
36.666
-121.9404
-121.9398
-121.9392
T1
T3
C2
Start
Pgps
Pdr

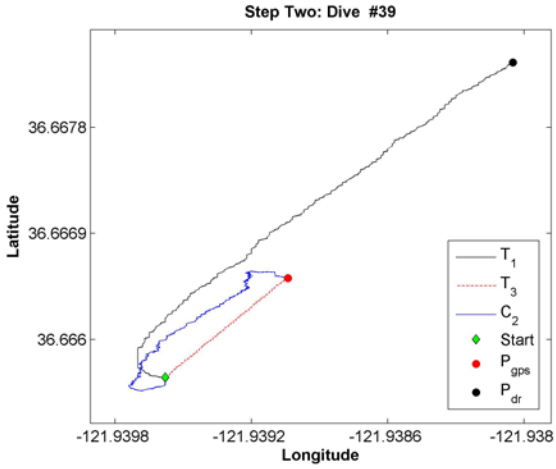
Step Two: Dive #39
Latitude
Longitude
36.6678
36.6669
36.666
-121.9398
-121.9392
-121.9386
-121.938
T1
T3
C2
Start
Pgps
Pdr

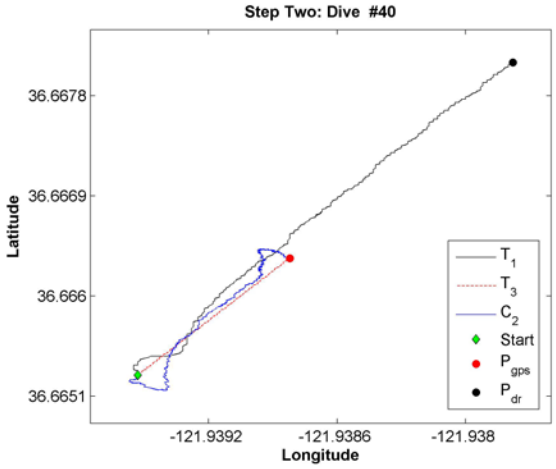
Step Two: Dive #40
Latitude
Longitude
36.6678
36.6669
36.666
36.6651
-121.9392
-121.9386
-121.938
T1
T3
C2
Start
Pgps
Pdr

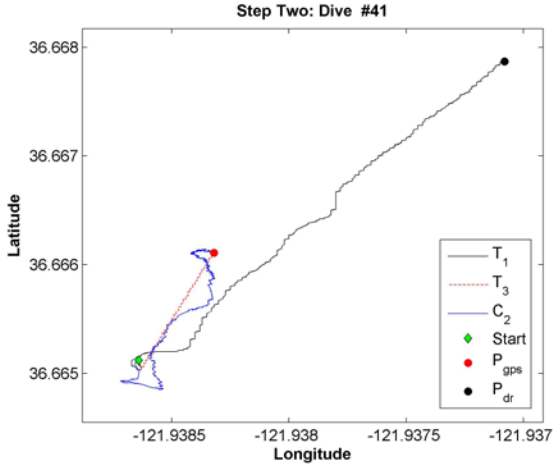
Step Two: Dive #41
Latitude
Longitude
36.668
36.667
36.666
36.665
-121.9385
-121.938
-121.9375
-121.937
T1
T3
C2
Start
Pgps
Pdr

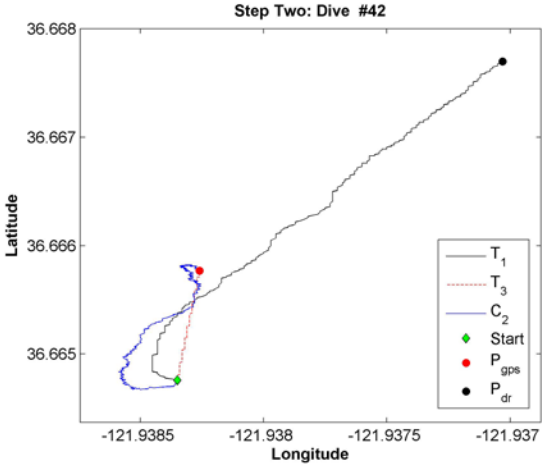
Step Two: Dive #42
Latitude
Longitude
36.668
36.667
36.666
36.665
-121.9385
-121.938
-121.9375
-121.937
T1
T3
C2
Start
Pgps
Pdr

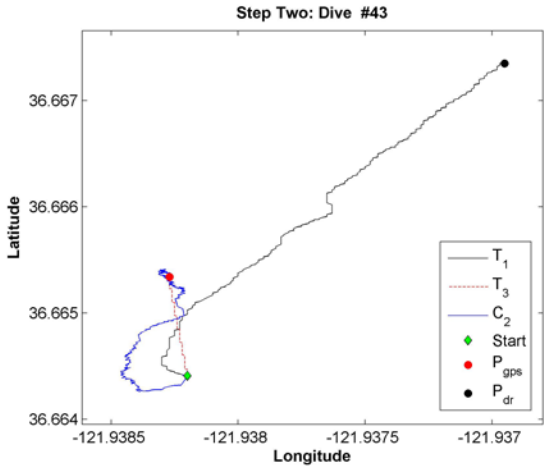
Step Two: Dive #43
Latitude
Longitude
36.667
36.666
36.665
36.664
-121.9385
-121.938
-121.9375
-121.937
T1
T3
C2
Start
Pgps
Pdr

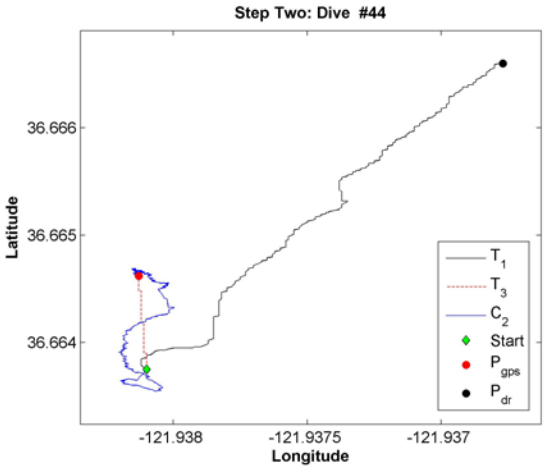
Step Two: Dive #44
Latitude
Longitude
36.666
36.665
36.664
-121.938
-121.9375
-121.937
T1
T3
C2
Start
Pgps
Pdr

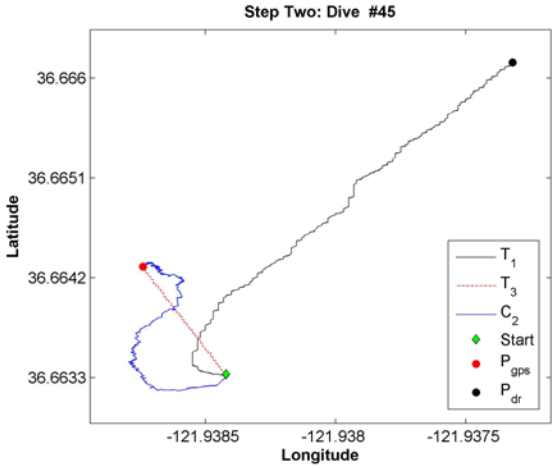
Step Two: Dive #45
Latitude
Longitude
36.666
36.6651
36.6642
36.6633
-121.9385
-121.938
-121.9375
T1
T3
C2
Start
Pgps
Pdr

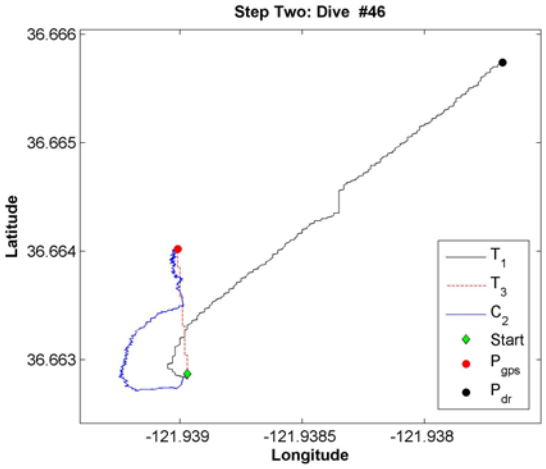
Step Two: Dive #46
Latitude
Longitude
36.666
36.665
36.664
36.663
-121.939
-121.9385
-121.938
T1
T3
C2
Start
Pgps
Pdr

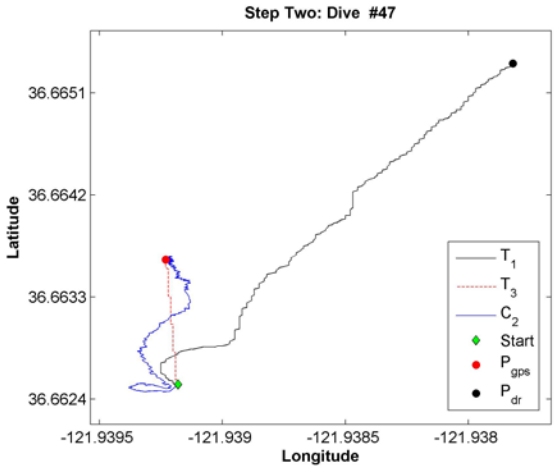
Step Two: Dive #47
Latitude
Longitude
36.6651
36.6642
36.6633
36.6624
-121.9395
-121.939
-121.9385
-121.938
T1
T3
C2
Start
Pgps
Pdr

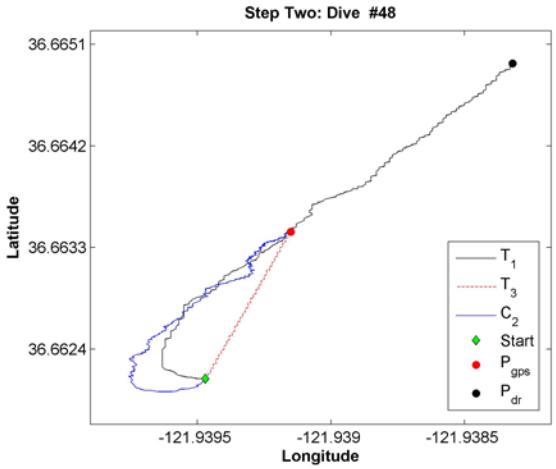
Step Two: Dive #48
Latitude
Longitude
36.6651
36.6642
36.6633
36.6624
-121.9395
-121.939
-121.9385
T1
T3
C2
Start
Pgps
Pdr

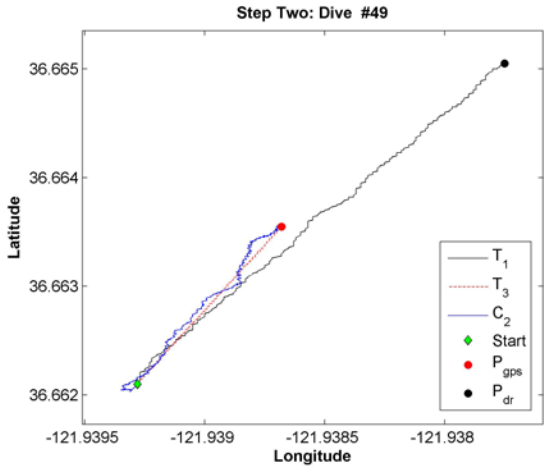
Step Two: Dive #49
Latitude
Longitude
36.665
36.664
36.663
36.662
-121.9395
-121.939
-121.9385
-121.938
T1
T3
C2
Start
Pgps
Pdr

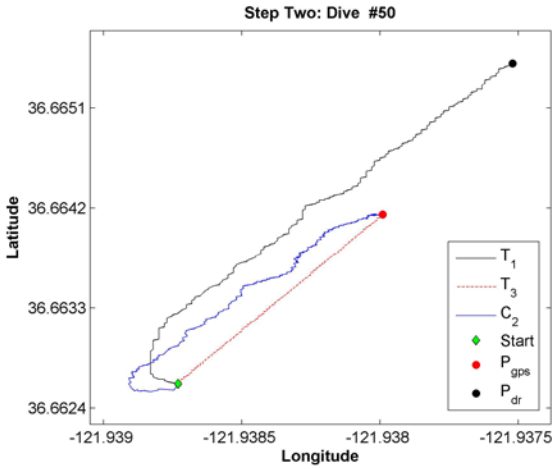
Step Two: Dive #50
Latitude
Longitude
36.6651
36.6642
36.6633
36.6624
-121.939
-121.9385
-121.938
-121.9375
T1
T3
C2
Start
Pgps
Pdr

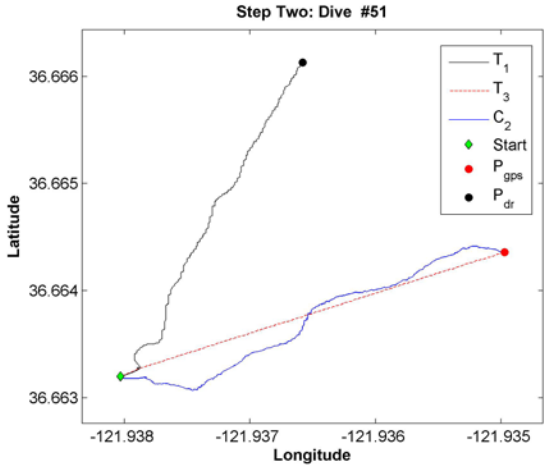
Step Two: Dive #51
Latitude
Longitude
36.666
36.665
36.664
36.663
-121.938
-121.937
-121.936
-121.935
T1
T3
C2
Start
Pgps
Pdr

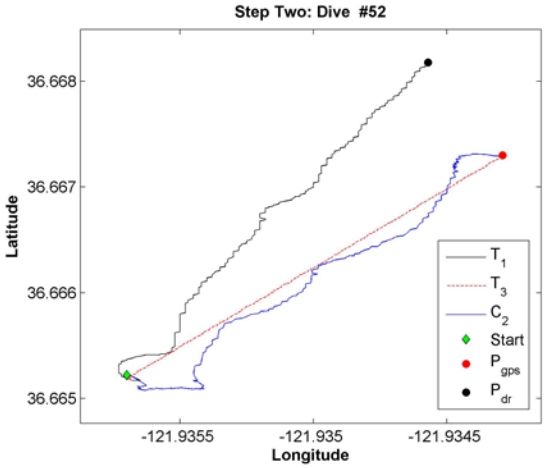
Step Two: Dive #52
Latitude
Longitude
36.668
36.667
36.666
36.665
-121.9355
-121.935
-121.9345
T1
T3
C2
Start
Pgps
Pdr

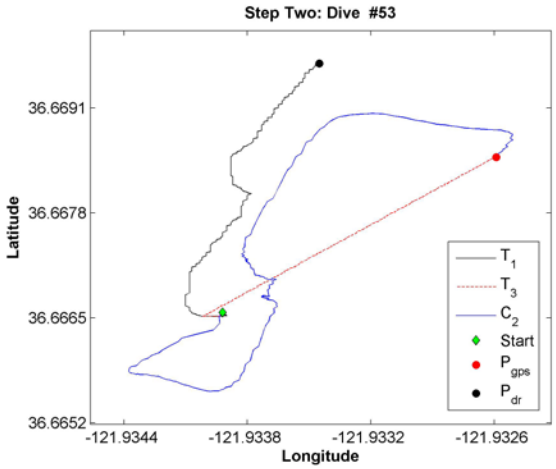
Step Two: Dive #53
Latitude
Longitude
36.6691
36.6678
36.6665
36.6652
-121.9344
-121.9338
-121.9332
-121.9326
T1
T3
C2
Start
Pgps
Pdr

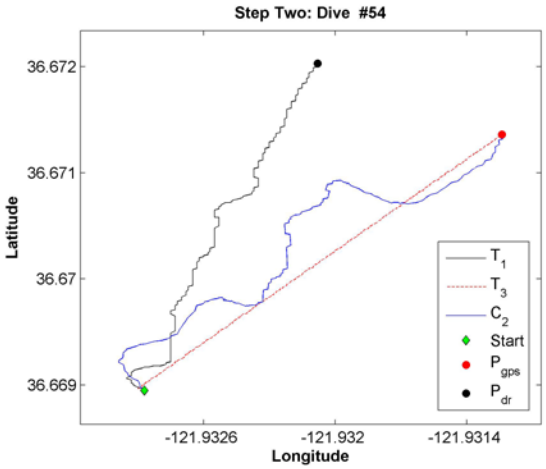
Step Two: Dive #54
Latitude
Longitude
36.672
36.671
36.67
36.669
-121.9326
-121.932
-121.9314
T1
T3
C2
Start
Pgps
Pdr

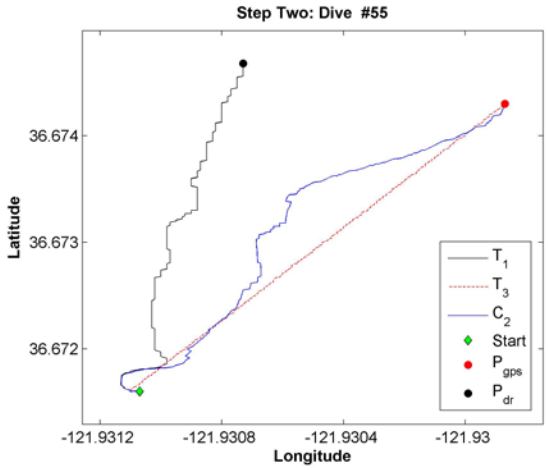
Step Two: Dive #55
Latitude
Longitude
36.674
36.673
36.672
-121.9312
-121.9308
-121.9304
-121.93
T1
T3
C2
Start
Pgps
Pdr

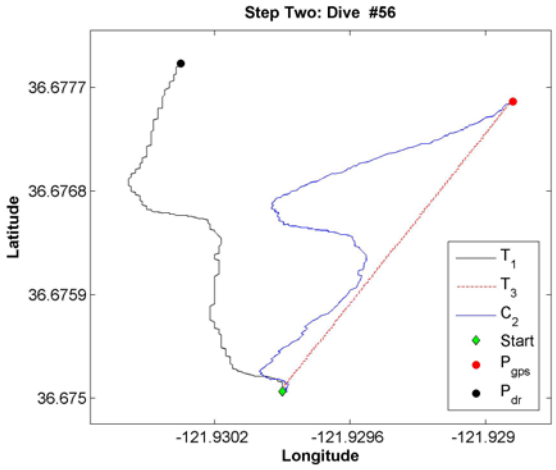
Step Two: Dive #56
Latitude
Longitude
36.6777
36.6768
36.6759
36.675
-121.9302
-121.9296
-121.929
T1
T3
C2
Start
Pgps
Pdr

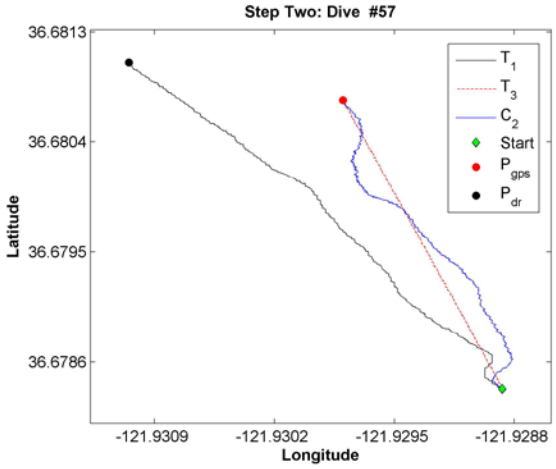
Step Two: Dive #57
Latitude
Longitude
36.6813
36.6804
36.6795
36.6786
-121.9309
-121.9302
-121.9295
-121.9288
T1
T3
C2
Start
Pgps
Pdr

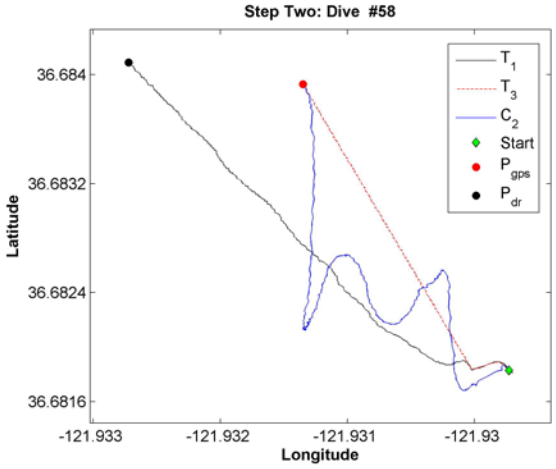
Step Two: Dive #58
Latitude
Longitude
36.684
36.6832
36.6824
36.6816
-121.933
-121.932
-121.931
-121.93
T1
T3
C2
Start
Pgps
Pdr

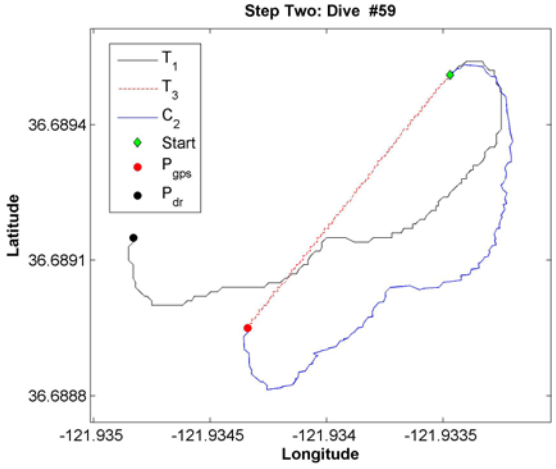
Step Two: Dive #59
Latitude
Longitude
36.6894
36.6891
36.6888
-121.935
-121.9345
-121.934
-121.9335
T1
T3
C2
Start
Pgps
Pdr

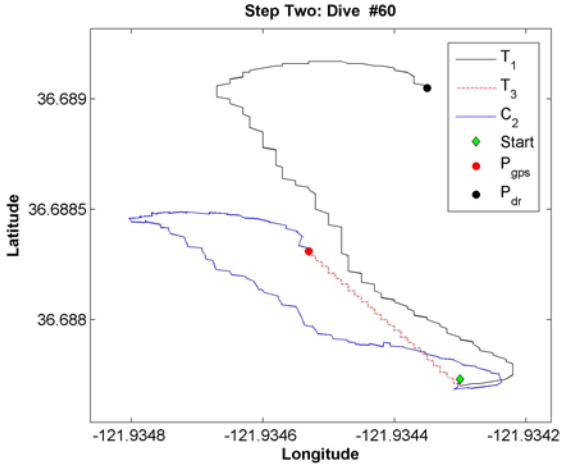
Step Two: Dive #60
Latitude
Longitude
36.689
36.6885
36.688
-121.9348
-121.9346
-121.9344
-121.9342
T1
T3
C2
Start
Pgps
Pdr

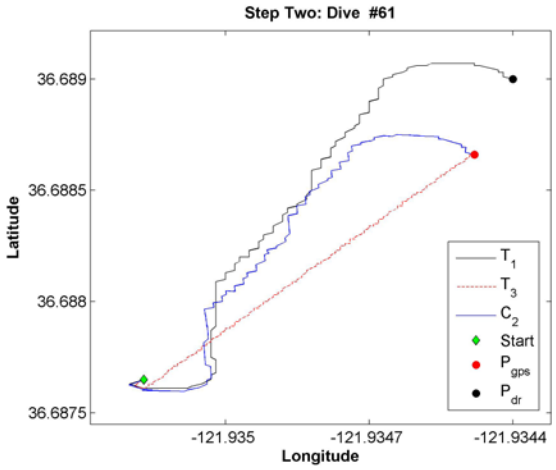
Step Two: Dive #61
Latitude
Longitude
36.689
36.6885
36.688
36.6875
-121.935
-121.9347
-121.9344
T1
T3
C2
Start
Pgps
Pdr

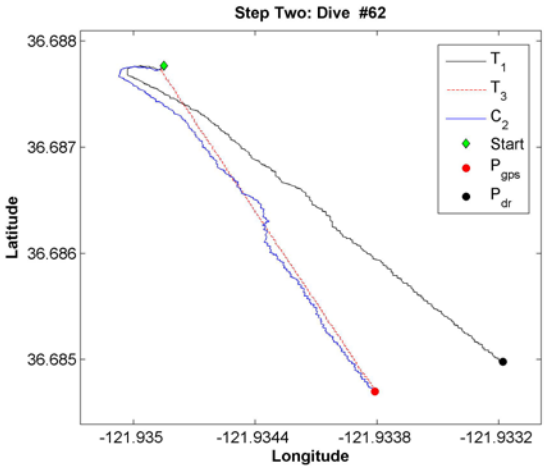
Step Two: Dive #62
Latitude
Longitude
36.688
36.687
36.686
36.685
-121.935
-121.9344
-121.9338
-121.9332
T1
T3
C2
Start
Pgps
Pdr

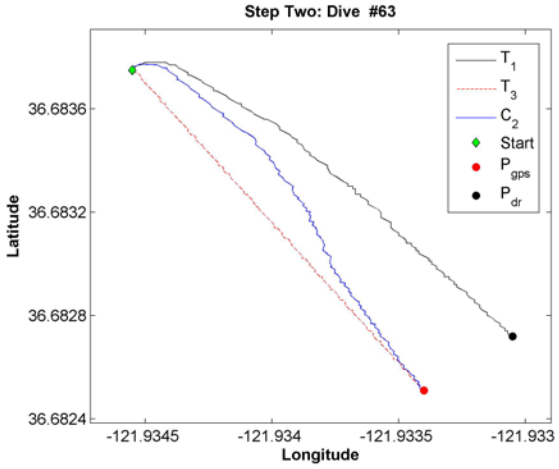
Step Two: Dive #63
Latitude
Longitude
36.6836
36.6832
36.6828
36.6824
-121.9345
-121.934
-121.9335
-121.933
T1
T3
C2
Start
Pgps
Pdr

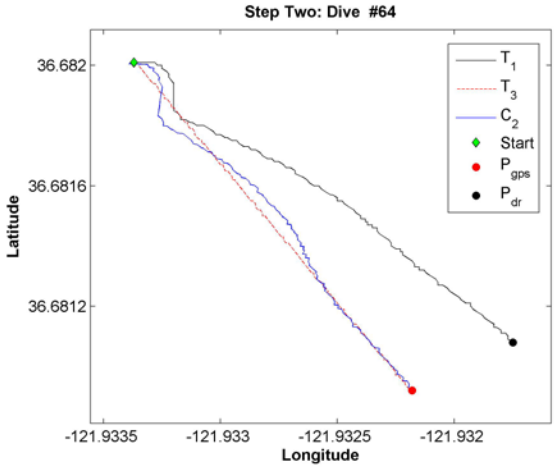
Step Two: Dive #64
Latitude
Longitude
36.682
36.6816
36.6812
-121.9335
-121.933
-121.9325
-121.932
T1
T3
C2
Start
Pgps
Pdr

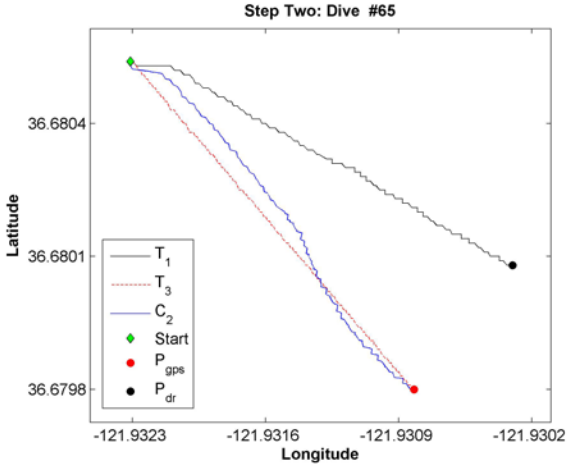
Step Two: Dive #65
Latitude
Longitude
36.6804
36.6801
36.6798
-121.9323
-121.9316
-121.9309
-121.9302
T1
T3
C2
Start
Pgps
Pdr

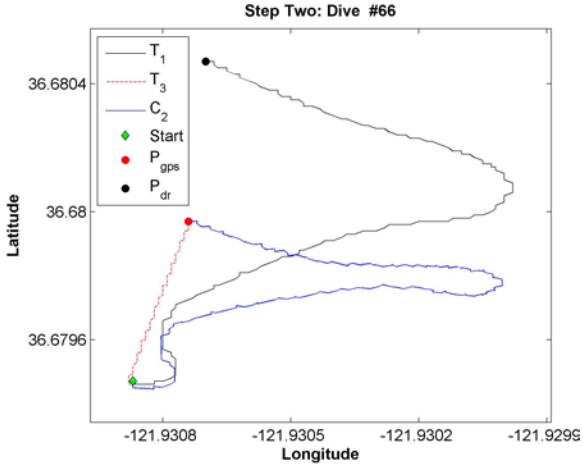
Step Two: Dive #66
Latitude
Longitude
36.6804
36.68
36.6796
-121.9308
-121.9305
-121.9302
-121.9299
T1
T3
C2
Start
Pgps
Pdr

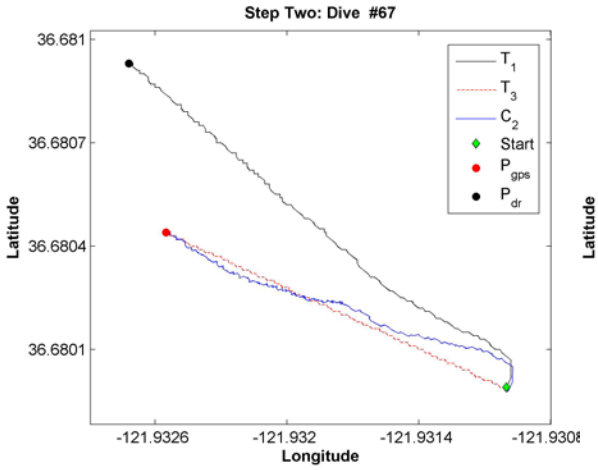
Step Two: Dive #67
36.681
36.6807
36.6804
36.6801
Latitude
-121.9326
-121.932
-121.9314
-121.9308
Longitude
T1
T3
C2
Start
Pgps
Pdr

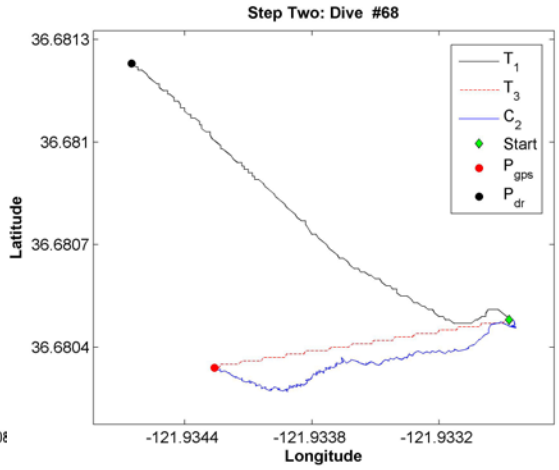
Step Two: Dive #68
36.6813
36.681
36.6807
36.6804
Latitude
-121.9344
-121.9338
-121.9332
Longitude
T1
T3
C2
Start
Pgps
Pdr

D. STEP THREE: ESTIMATED OPTIMAL TRAJECTORIES FROM C_2 BY USING ITERATION METHOD

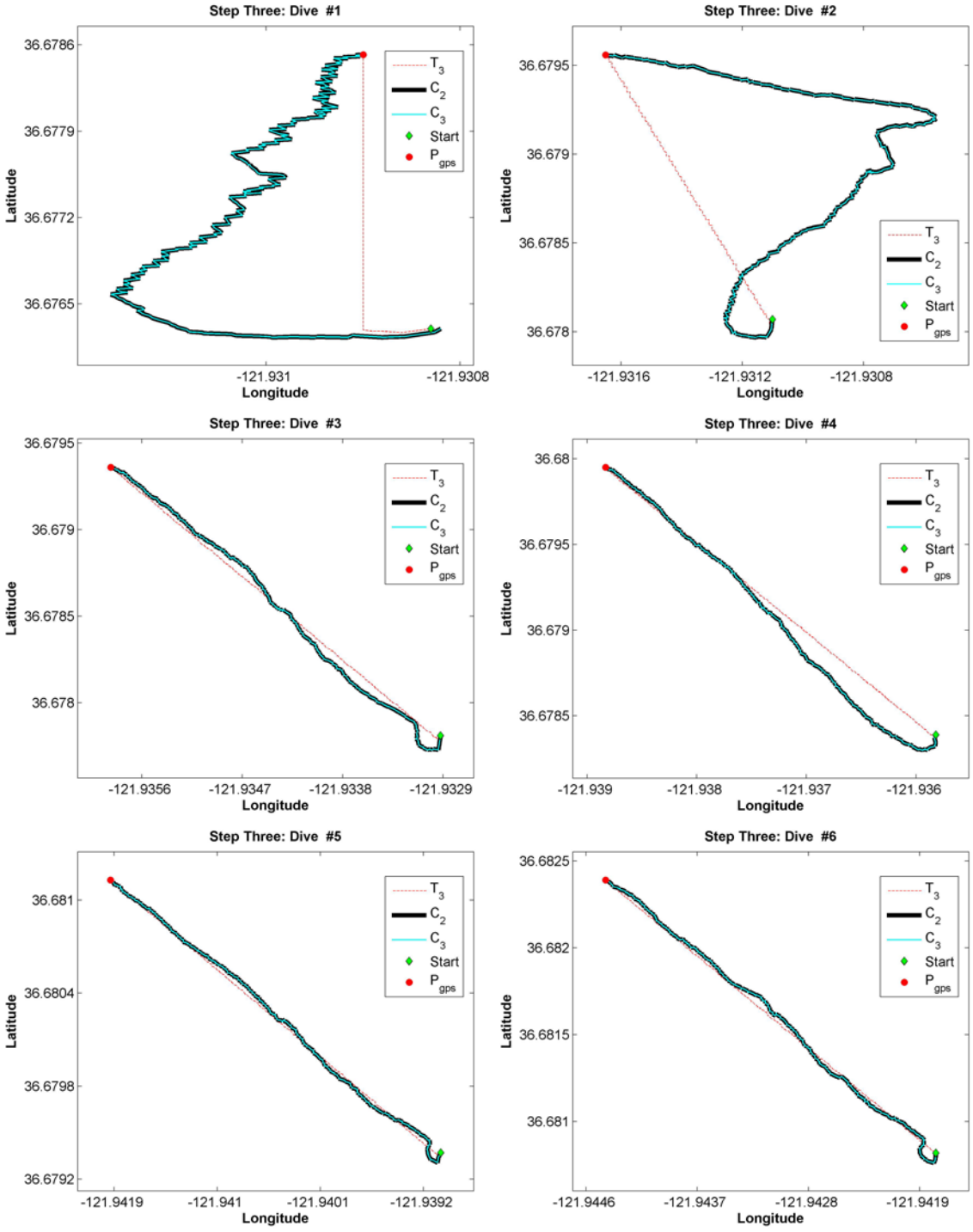

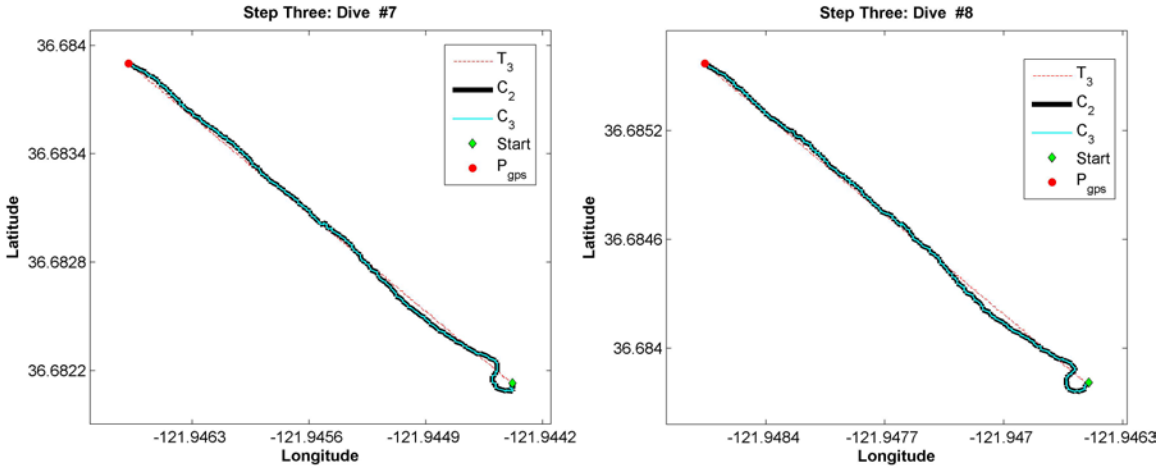
Step Three: Dive #7
Latitude
Longitude
36.684
36.6834
36.6828
36.6822
-121.9463
-121.9456
-121.9449
-121.9442
T3
C2
C3
Start
Pgps

Step Three: Dive #8
Latitude
Longitude
36.6852
36.6846
36.684
-121.9484
-121.9477
-121.947
-121.9463
T3
C2
C3
Start
Pgps

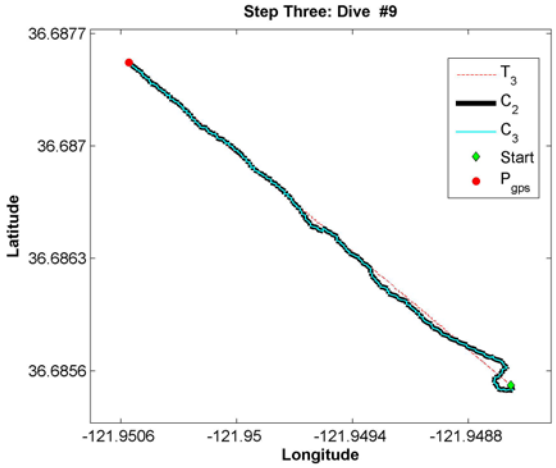
Step Three: Dive #9
Latitude
Longitude
36.6877
36.687
36.6863
36.6856
-121.9506
-121.95
-121.9494
-121.9488
T3
C2
C3
Start
Pgps

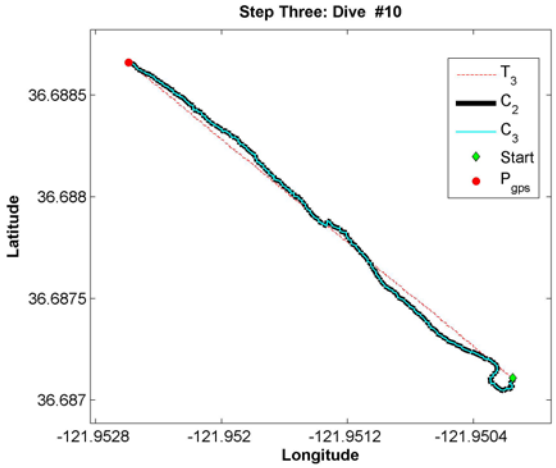
Step Three: Dive #10
Latitude
Longitude
36.6885
36.688
36.6875
36.687
-121.9528
-121.952
-121.9512
-121.9504
T3
C2
C3
Start
Pgps

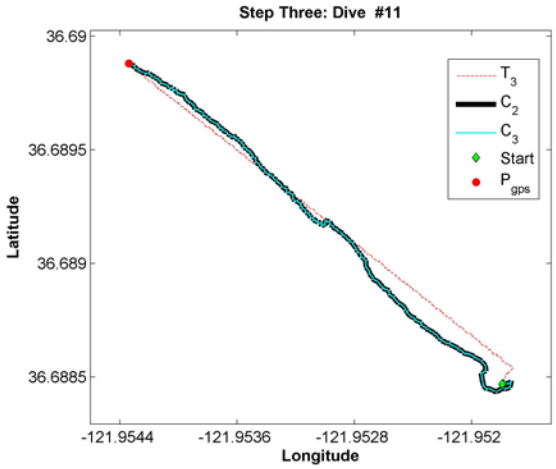
Step Three: Dive #11
Latitude
Longitude
36.69
36.6895
36.689
36.6885
-121.9544
-121.9536
-121.9528
-121.952
T3
C2
C3
Start
Pgps

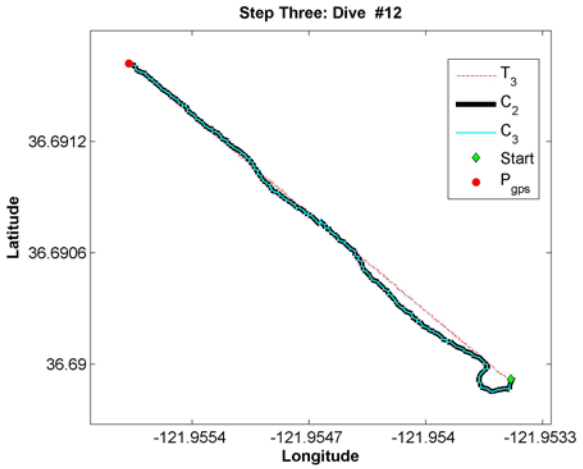
Step Three: Dive #12
Latitude
Longitude
36.6912
36.6906
36.69
-121.9554
-121.9547
-121.954
-121.9533
T3
C2
C3
Start
Pgps

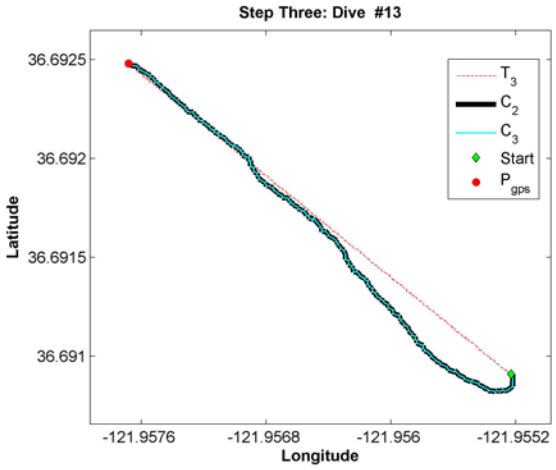
Step Three: Dive #13
36.6925
36.692
36.6915
36.691
Latitude
-121.9576
-121.9568
-121.956
-121.9552
Longitude
T3
C2
C3
Start
Pgps

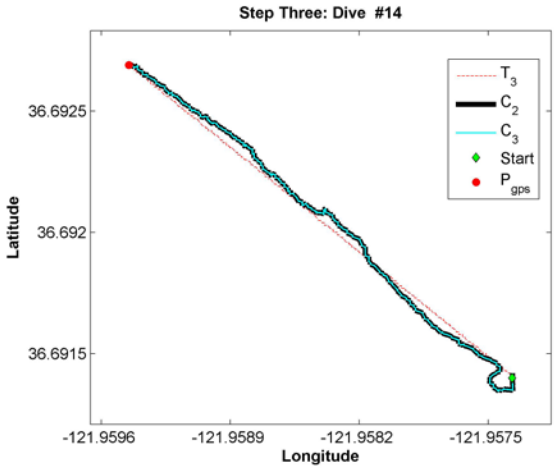
Step Three: Dive #14
36.6925
36.692
36.6915
Latitude
-121.9596
-121.9589
-121.9582
-121.9575
Longitude
T3
C2
C3
Start
Pgps

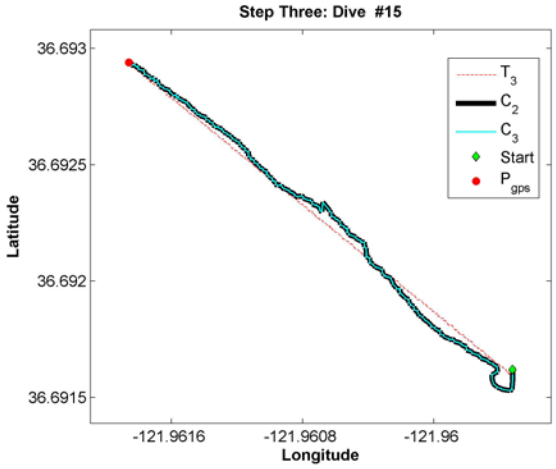
Step Three: Dive #15
36.693
36.6925
36.692
36.6915
Latitude
-121.9616
-121.9608
-121.96
Longitude
T3
C2
C3
Start
Pgps

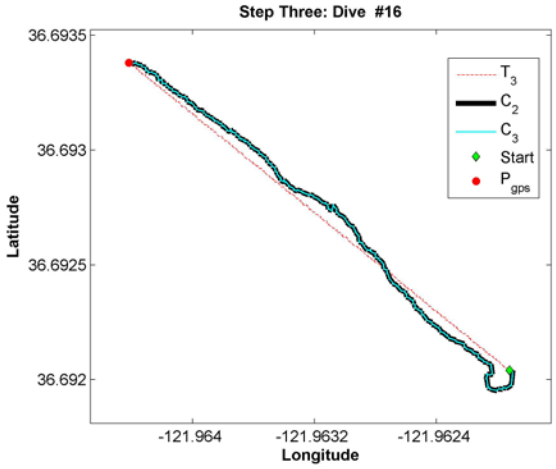
Step Three: Dive #16
36.6935
36.693
36.6925
36.692
Latitude
-121.964
-121.9632
-121.9624
Longitude
T3
C2
C3
Start
Pgps

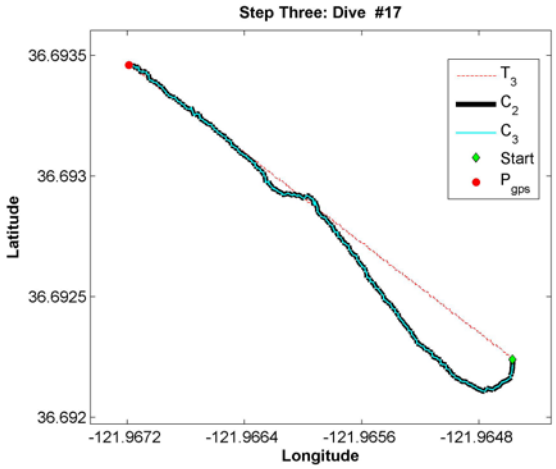
Step Three: Dive #17
36.6935
36.693
36.6925
36.692
Latitude
-121.9672
-121.9664
-121.9656
-121.9648
Longitude
T3
C2
C3
Start
Pgps

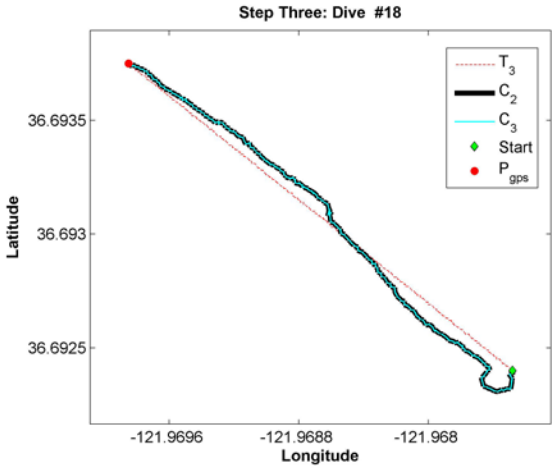
Step Three: Dive #18
36.6935
36.693
36.6925
Latitude
-121.9696
-121.9688
-121.968
Longitude
T3
C2
C3
Start
Pgps

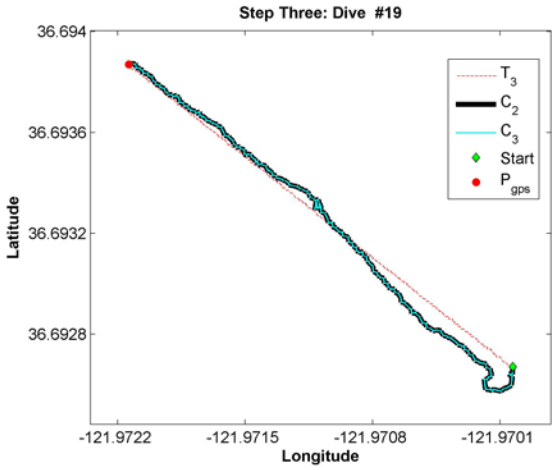
Step Three: Dive #19
36.694
36.6936
36.6932
36.6928
Latitude
-121.9722
-121.9715
-121.9708
-121.9701
Longitude
T3
C2
C3
Start
Pgps

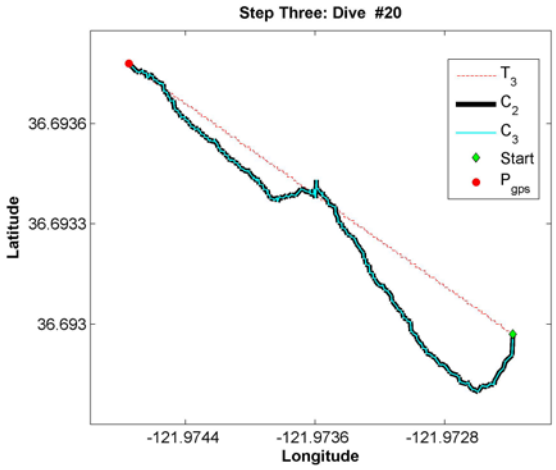
Step Three: Dive #20
36.6936
36.6933
36.693
Latitude
-121.9744
-121.9736
-121.9728
Longitude
T3
C2
C3
Start
Pgps

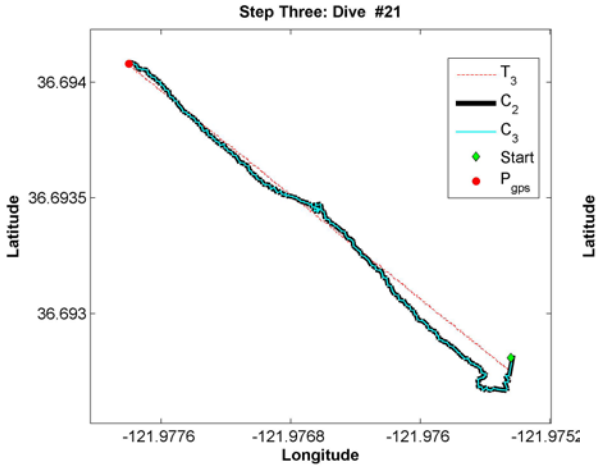
Step Three: Dive #21
36.694
36.6935
36.693
Latitude
-121.9776
-121.9768
-121.976
Longitude
T3
C2
C3
Start
Pgps

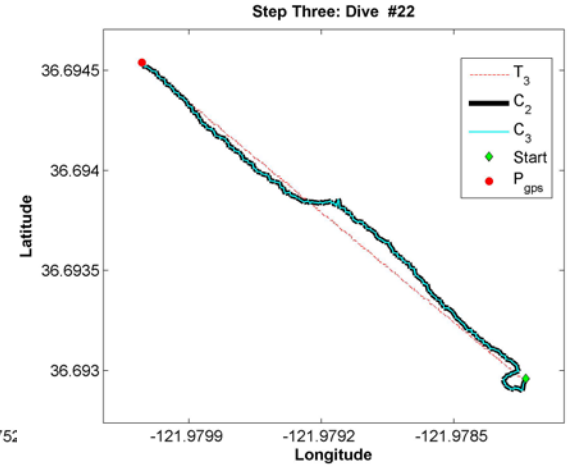
Step Three: Dive #22
36.6945
36.694
36.6935
36.693
Latitude
-121.9799
-121.9792
-121.9785
Longitude
T3
C2
C3
Start
Pgps

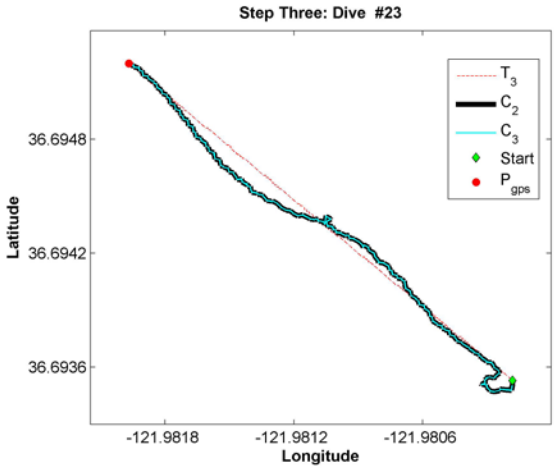
Step Three: Dive #23
36.6948
36.6942
36.6936
Latitude
-121.9818
-121.9812
-121.9806
Longitude
T3
C2
C3
Start
Pgps

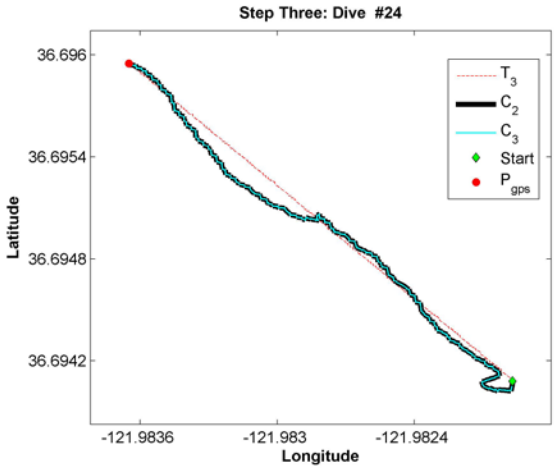
Step Three: Dive #24
36.696
36.6954
36.6948
36.6942
Latitude
-121.9836
-121.983
-121.9824
Longitude
T3
C2
C3
Start
Pgps

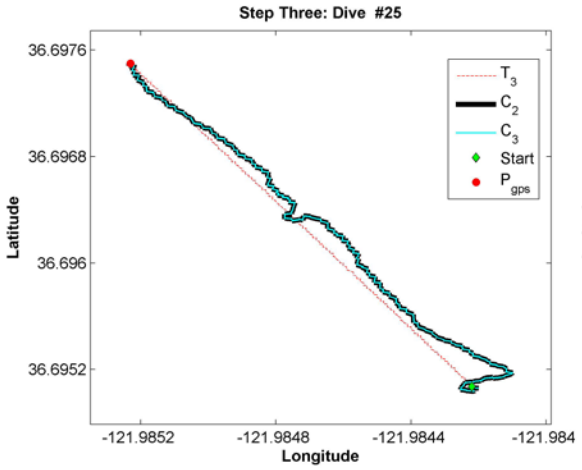
Step Three: Dive #25
36.6976
36.6968
36.696
36.6952
Latitude
-121.9852
-121.9848
-121.9844
-121.984
Longitude
T3
C2
C3
Start
Pgps

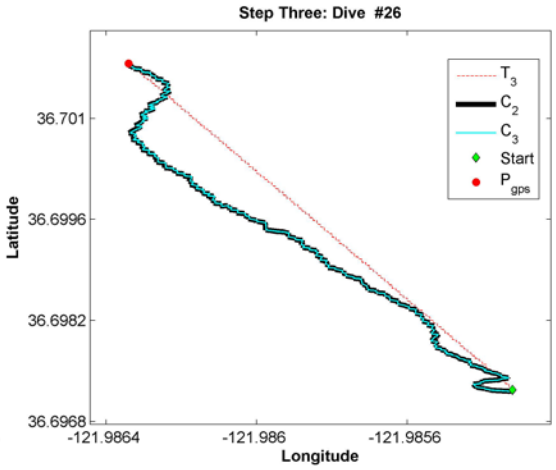
Step Three: Dive #26
36.701
36.6996
36.6982
36.6968
Latitude
-121.9864
-121.986
-121.9856
Longitude
T3
C2
C3
Start
Pgps

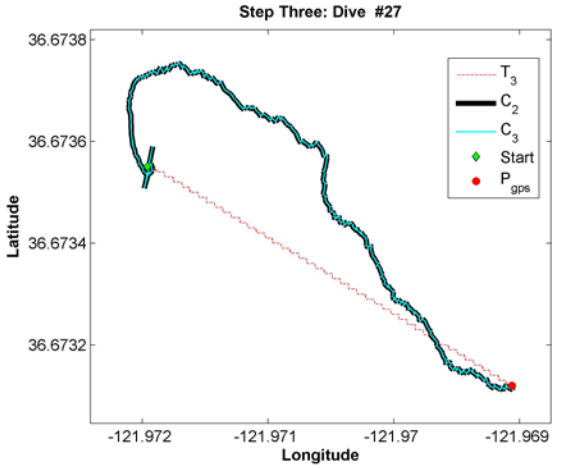
Step Three: Dive #27
36.6738
36.6736
36.6734
36.6732
Latitude
-121.972
-121.971
-121.97
-121.969
Longitude
T3
C2
C3
Start
Pgps

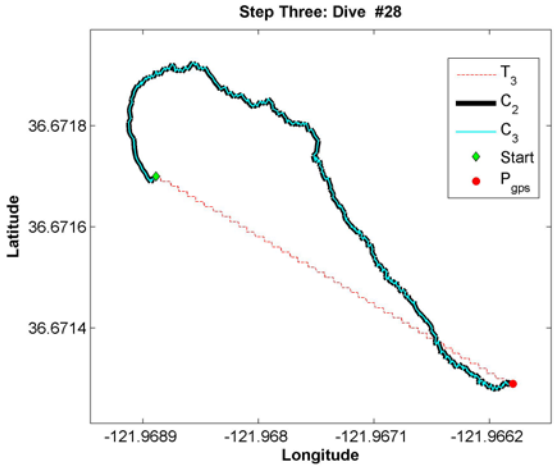
Step Three: Dive #28
36.6718
36.6716
36.6714
Latitude
-121.9689
-121.968
-121.9671
-121.9662
Longitude
T3
C2
C3
Start
Pgps

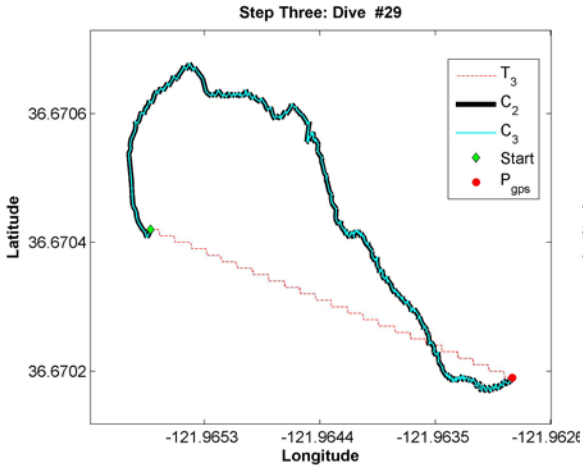
Step Three: Dive #29
36.6706
36.6704
36.6702
Latitude
-121.9653
-121.9644
-121.9635
-121.962
Longitude
T3
C2
C3
Start
Pgps

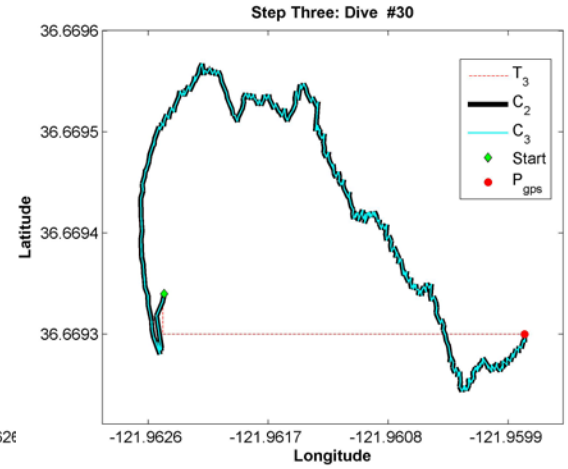
Step Three: Dive #30
36.6696
36.6695
36.6694
36.6693
Latitude
-121.9626
-121.9617
-121.9608
-121.9599
Longitude
T3
C2
C3
Start
Pgps

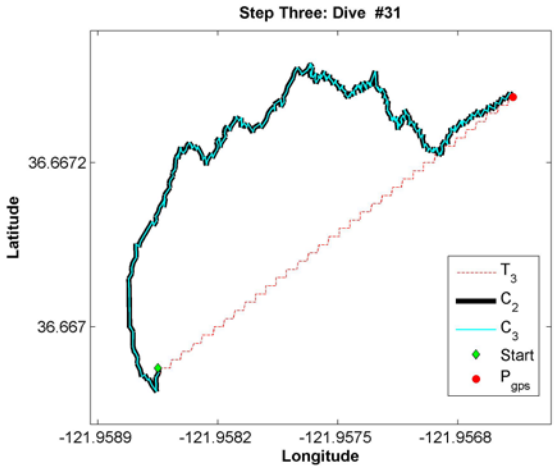
Step Three: Dive #31
Latitude
36.6672
36.667
-121.9589
-121.9582
-121.9575
-121.9568
Longitude
T3
C2
C3
Start
Pgps

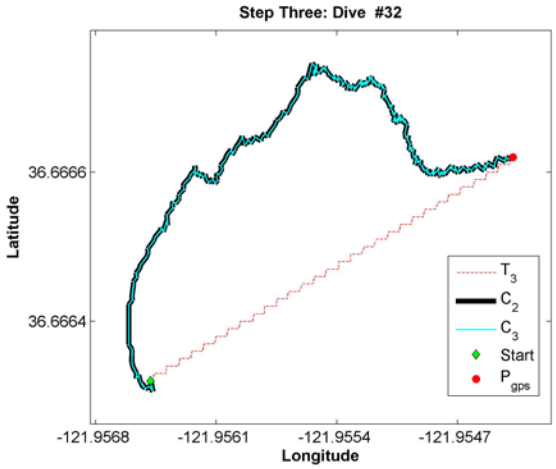
Step Three: Dive #32
Latitude
36.6666
36.6664
-121.9568
-121.9561
-121.9554
-121.9547
Longitude
T3
C2
C3
Start
Pgps

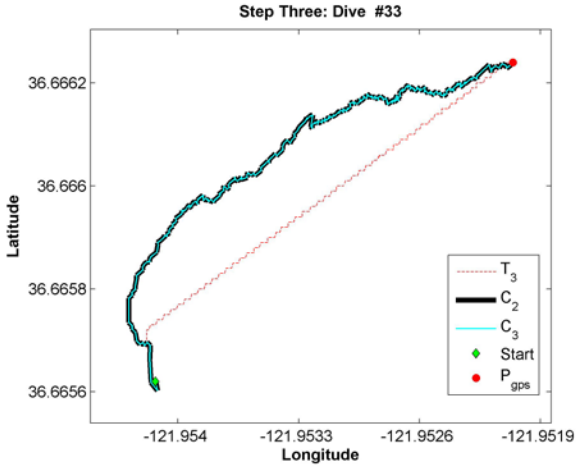
Step Three: Dive #33
Latitude
36.6662
36.666
36.6658
36.6656
-121.954
-121.9533
-121.9526
-121.9519
Longitude
T3
C2
C3
Start
Pgps

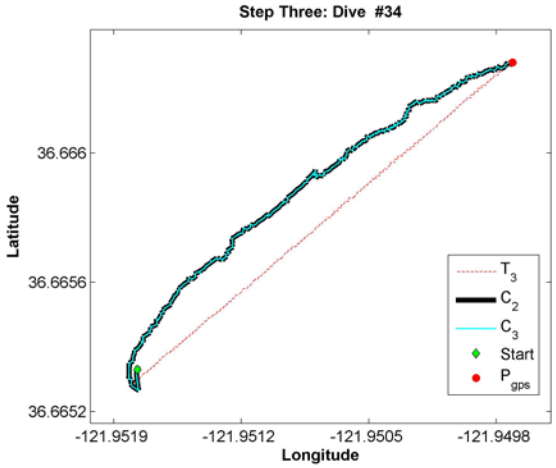
Step Three: Dive #34
Latitude
36.666
36.6656
36.6652
-121.9519
-121.9512
-121.9505
-121.9498
Longitude
T3
C2
C3
Start
Pgps

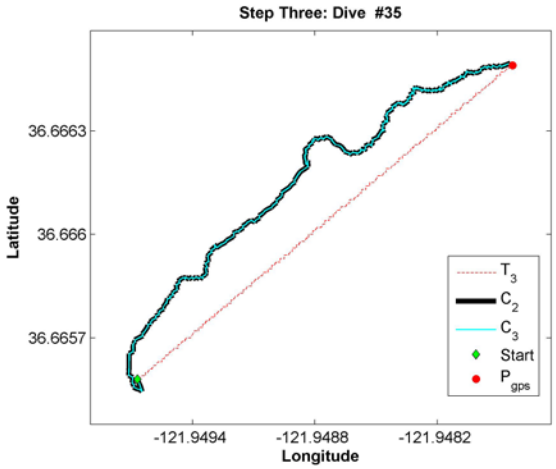
Step Three: Dive #35
Latitude
36.6663
36.666
36.6657
-121.9494
-121.9488
-121.9482
Longitude
T3
C2
C3
Start
Pgps

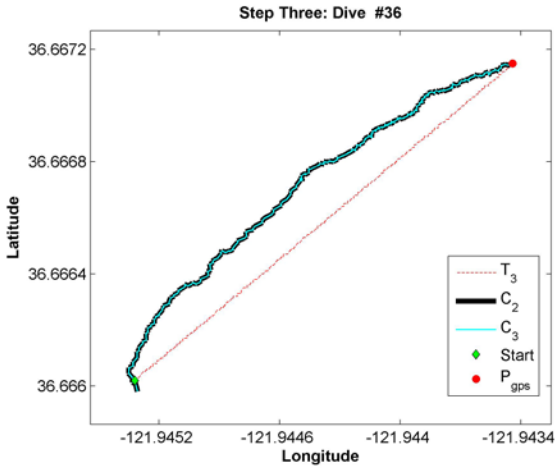
Step Three: Dive #36
Latitude
36.6672
36.6668
36.6664
36.666
-121.9452
-121.9446
-121.944
-121.9434
Longitude
T3
C2
C3
Start
Pgps

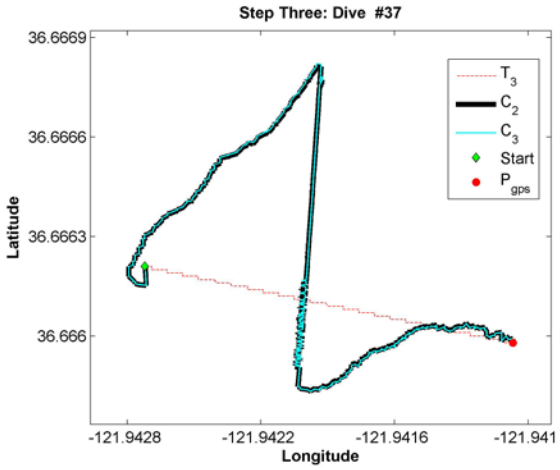
Step Three: Dive #37
36.6669
36.6666
36.6663
36.666
Latitude
-121.9428
-121.9422
-121.9416
-121.941
Longitude
T3
C2
C3
Start
Pgps

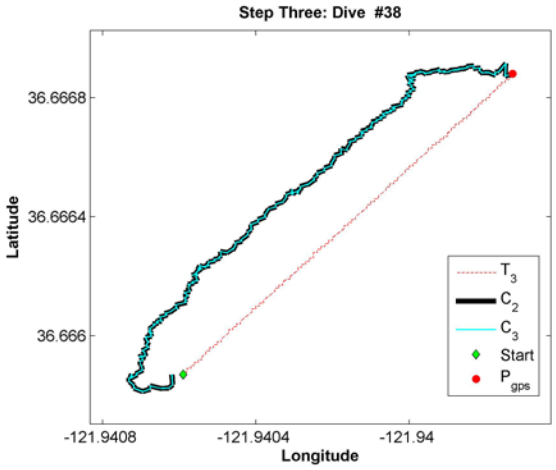
Step Three: Dive #38
36.6668
36.6664
36.666
Latitude
-121.9408
-121.9404
-121.94
Longitude
T3
C2
C3
Start
Pgps

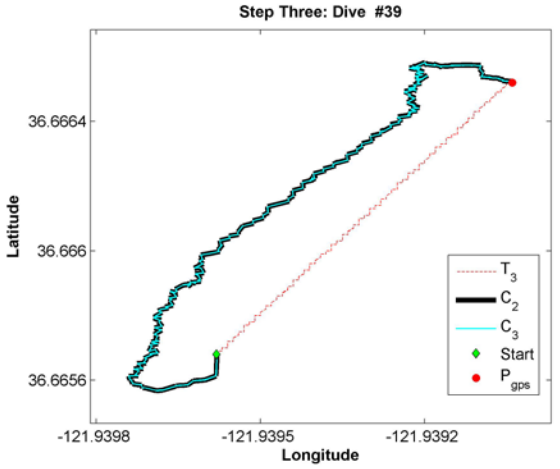
Step Three: Dive #39
36.6664
36.666
36.6656
Latitude
-121.9398
-121.9395
-121.9392
Longitude
T3
C2
C3
Start
Pgps

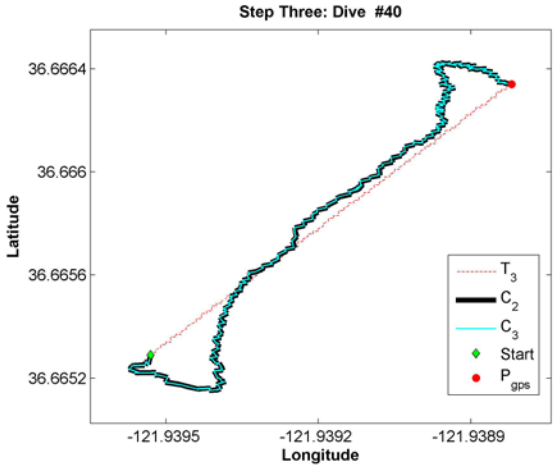
Step Three: Dive #40
36.6664
36.666
36.6656
36.6652
Latitude
-121.9395
-121.9392
-121.9389
Longitude
T3
C2
C3
Start
Pgps

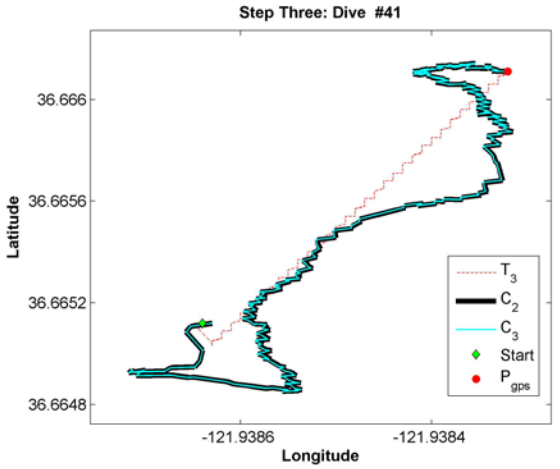
Step Three: Dive #41
36.666
36.6656
36.6652
36.6648
Latitude
-121.9386
-121.9384
Longitude
T3
C2
C3
Start
Pgps

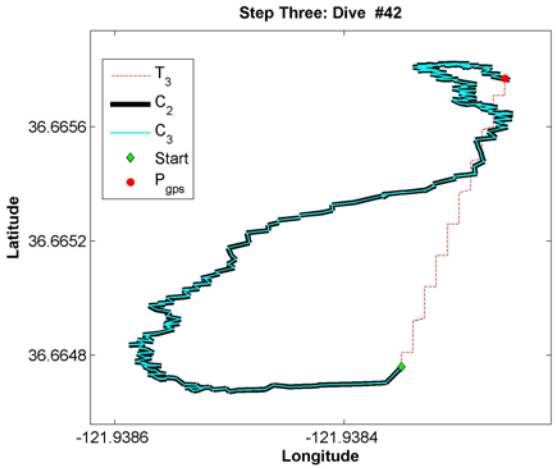
Step Three: Dive #42
36.6656
36.6652
36.6648
Latitude
-121.9386
-121.9384
Longitude
T3
C2
C3
Start
Pgps

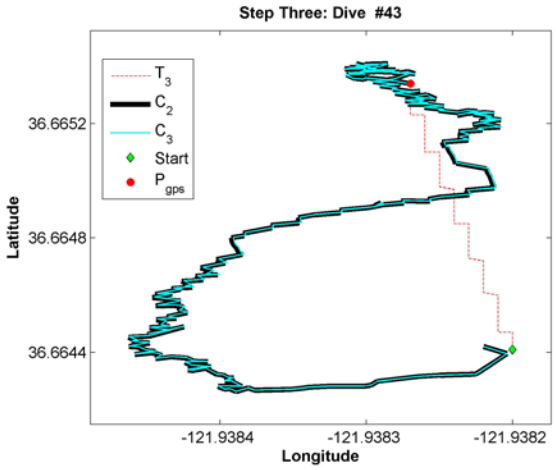
Step Three: Dive #43
T3
C2
C3
Start
Pgps
36.6652
36.6648
36.6644
Latitude
-121.9384
-121.9383
-121.9382
Longitude

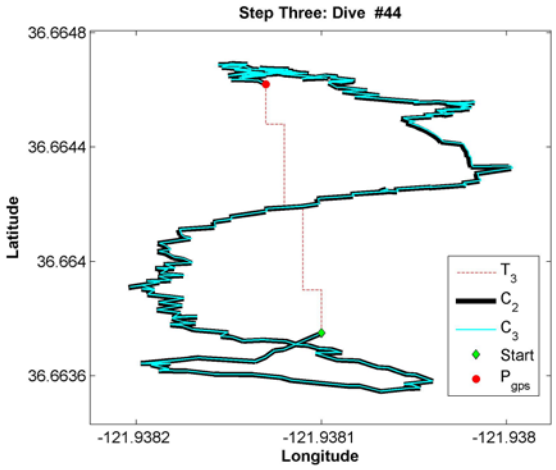
Step Three: Dive #44
36.6648
36.6644
36.664
36.6636
Latitude
T3
C2
C3
Start
Pgps
-121.9382
-121.9381
-121.938
Longitude

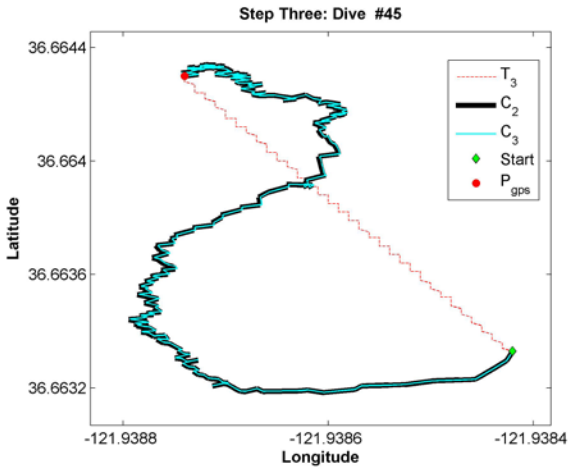
Step Three: Dive #45
36.6644
36.664
36.6636
36.6632
Latitude
T3
C2
C3
Start
Pgps
-121.9388
-121.9386
-121.9384
Longitude

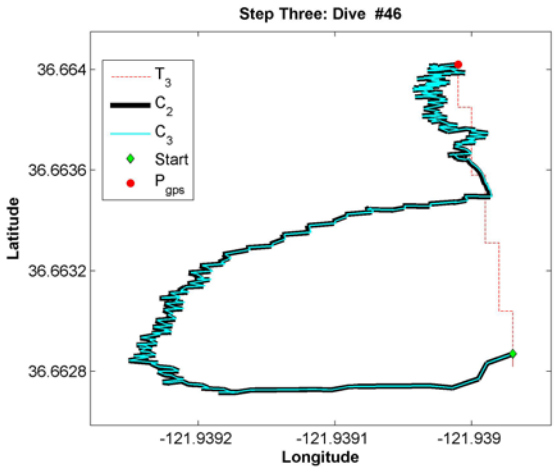
Step Three: Dive #46
36.664
36.6636
36.6632
36.6628
Latitude
T3
C2
C3
Start
Pgps
-121.9392
-121.9391
-121.939
Longitude

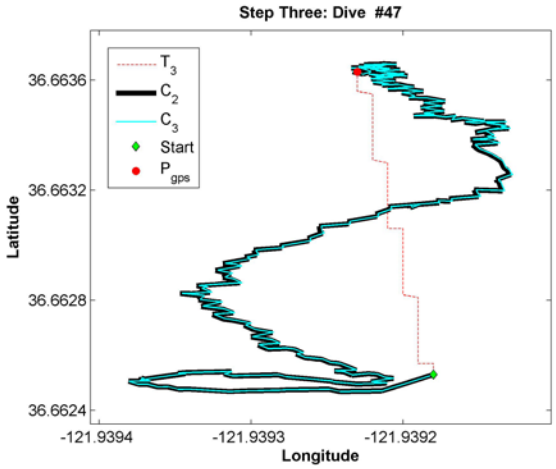
Step Three: Dive #47
36.6636
36.6632
36.6628
36.6624
Latitude
T3
C2
C3
Start
Pgps
-121.9394
-121.9393
-121.9392
Longitude

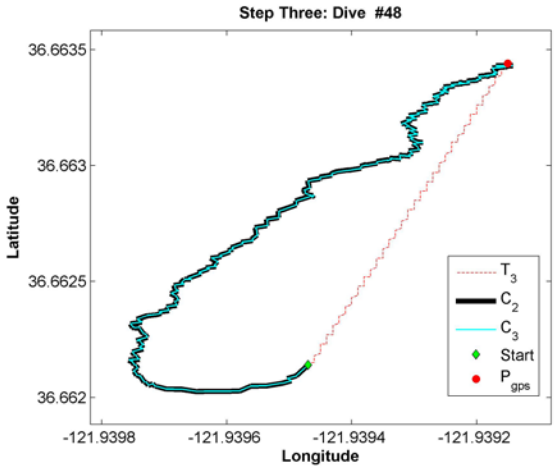
Step Three: Dive #48
36.6635
36.663
36.6625
36.662
Latitude
T3
C2
C3
Start
Pgps
-121.9398
-121.9396
-121.9394
-121.9392
Longitude

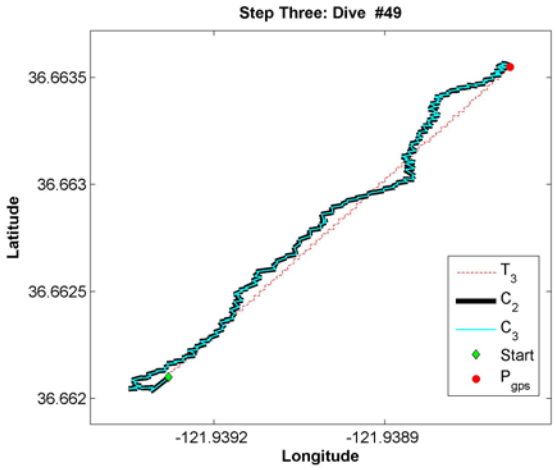
Step Three: Dive #49
Latitude
Longitude
36.6635
36.663
36.6625
36.662
-121.9392
-121.9389
T3
C2
C3
Start
Pgps

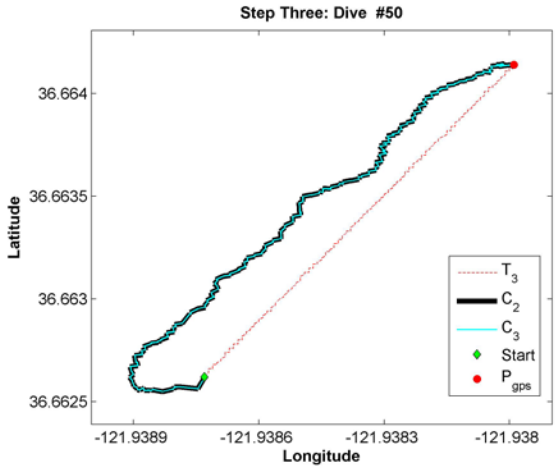
Step Three: Dive #50
Latitude
Longitude
36.664
36.6635
36.663
36.6625
-121.9389
-121.9386
-121.9383
-121.938
T3
C2
C3
Start
Pgps

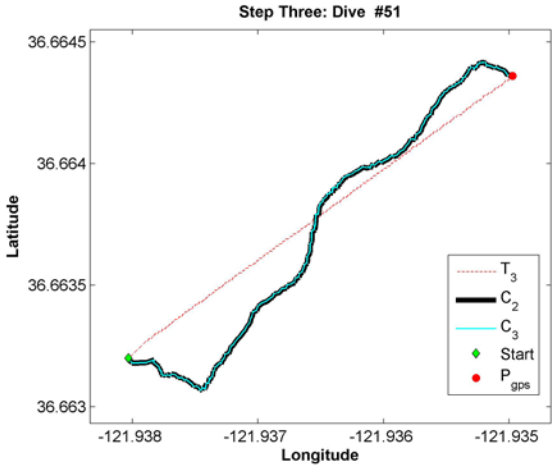
Step Three: Dive #51
Latitude
Longitude
36.6645
36.664
36.6635
36.663
-121.938
-121.937
-121.936
-121.935
T3
C2
C3
Start
Pgps

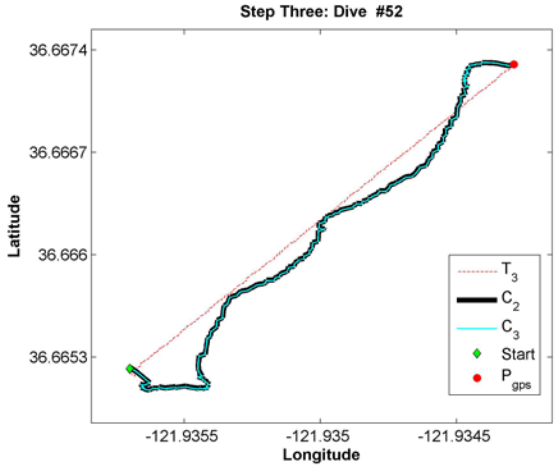
Step Three: Dive #52
Latitude
Longitude
36.6674
36.6667
36.666
36.6653
-121.9355
-121.935
-121.9345
T3
C2
C3
Start
Pgps

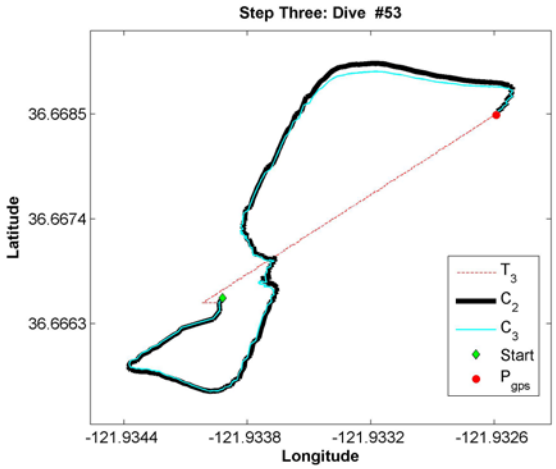
Step Three: Dive #53
Latitude
Longitude
36.6685
36.6674
36.6663
-121.9344
-121.9338
-121.9332
-121.9326
T3
C2
C3
Start
Pgps

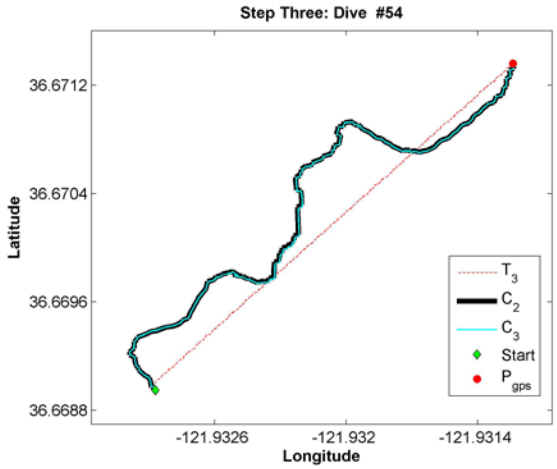
Step Three: Dive #54
Latitude
Longitude
36.6712
36.6704
36.6696
36.6688
-121.9326
-121.932
-121.9314
T3
C2
C3
Start
Pgps

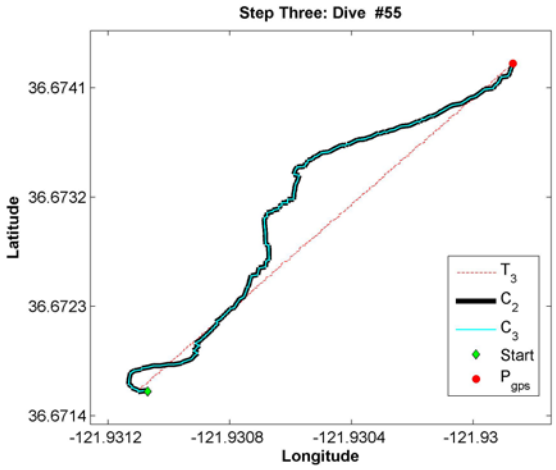
Step Three: Dive #55
36.6741
36.6732
36.6723
36.6714
Latitude
-121.9312
-121.9308
-121.9304
-121.93
Longitude
T3
C2
C3
Start
Pgps

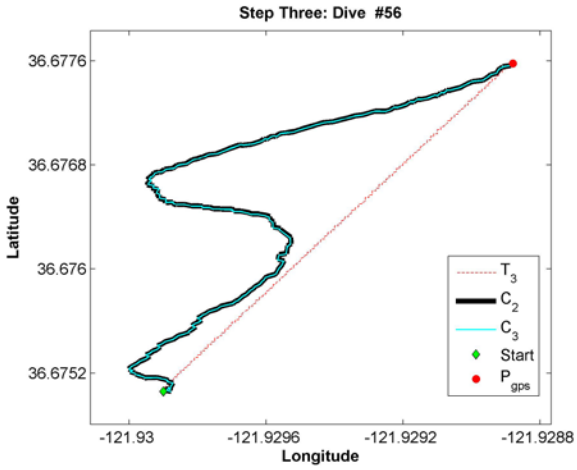
Step Three: Dive #56
36.6776
36.6768
36.676
36.6752
Latitude
-121.93
-121.9296
-121.9292
-121.9288
Longitude
T3
C2
C3
Start
Pgps

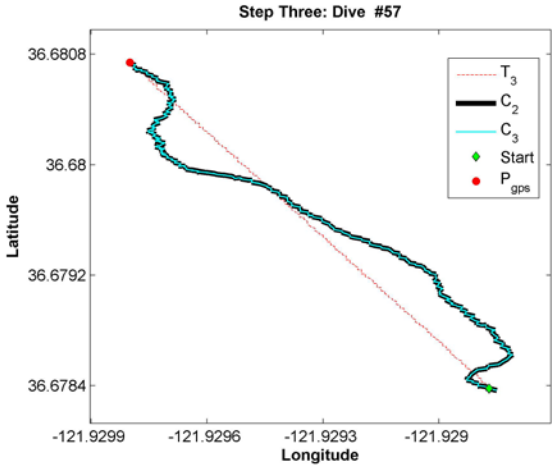
Step Three: Dive #57
36.6808
36.68
36.6792
36.6784
Latitude
-121.9299
-121.9296
-121.9293
-121.929
Longitude
T3
C2
C3
Start
Pgps

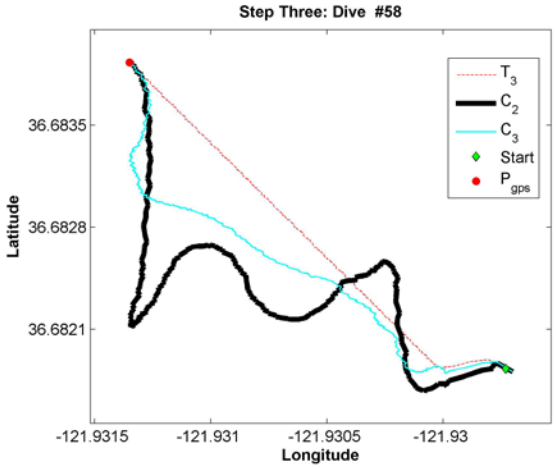
Step Three: Dive #58
36.6835
36.6828
36.6821
Latitude
-121.9315
-121.931
-121.9305
-121.93
Longitude
T3
C2
C3
Start
Pgps

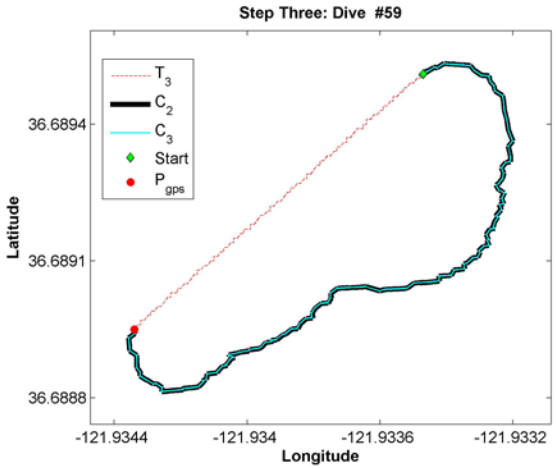
Step Three: Dive #59
36.6894
36.6891
36.6888
Latitude
-121.9344
-121.934
-121.9336
-121.9332
Longitude
T3
C2
C3
Start
Pgps

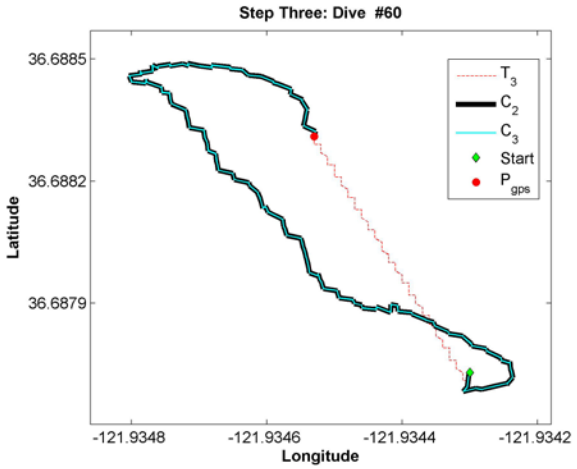
Step Three: Dive #60
36.6885
36.6882
36.6879
Latitude
-121.9348
-121.9346
-121.9344
-121.9342
Longitude
T3
C2
C3
Start
Pgps

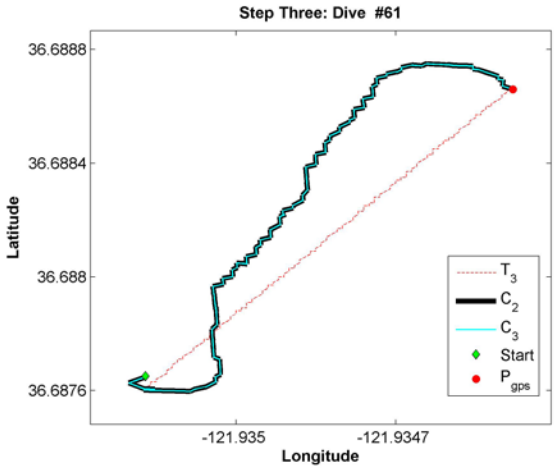
Step Three: Dive #61
36.6888
36.6884
36.688
36.6876
Latitude
-121.935
-121.9347
Longitude
T3
C2
C3
Start
Pgps

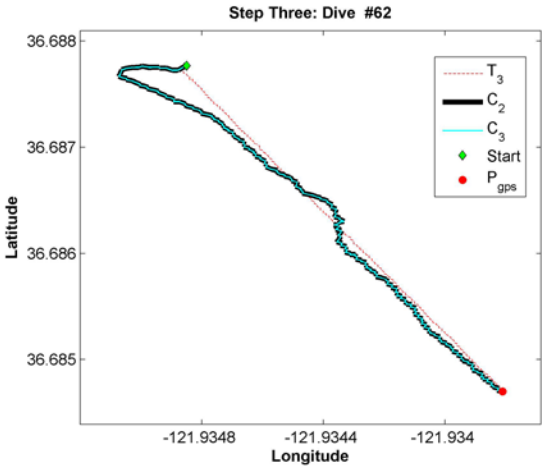
Step Three: Dive #62
36.688
36.687
36.686
36.685
Latitude
-121.9348
-121.9344
-121.934
Longitude
T3
C2
C3
Start
Pgps

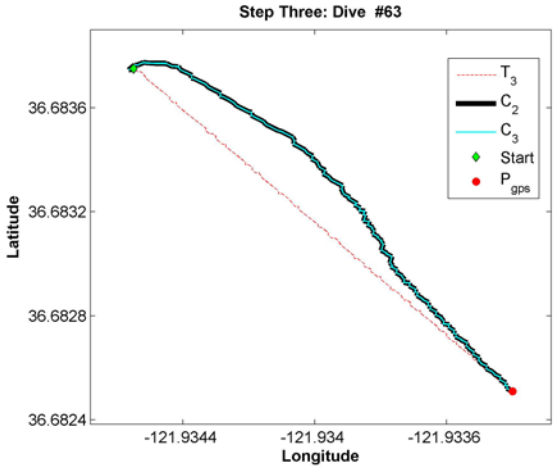
Step Three: Dive #63
36.6836
36.6832
36.6828
36.6824
Latitude
-121.9344
-121.934
-121.9336
Longitude
T3
C2
C3
Start
Pgps

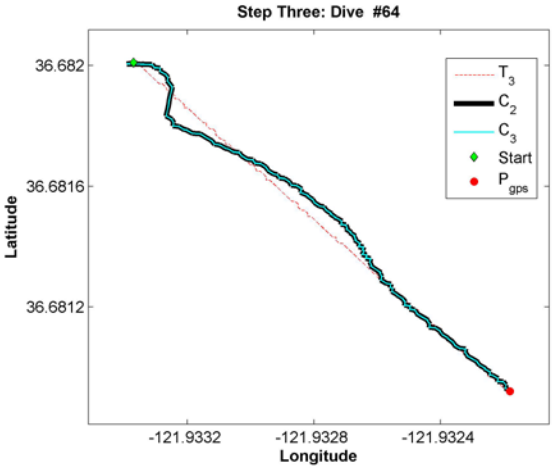
Step Three: Dive #64
36.682
36.6816
36.6812
Latitude
-121.9332
-121.9328
-121.9324
Longitude
T3
C2
C3
Start
Pgps

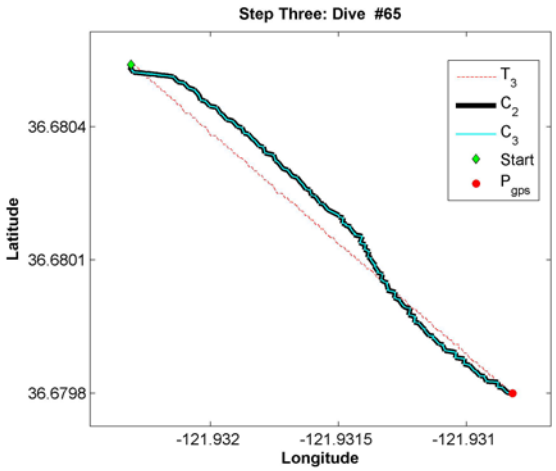
Step Three: Dive #65
36.6804
36.6801
36.6798
Latitude
-121.932
-121.9315
-121.931
Longitude
T3
C2
C3
Start
Pgps

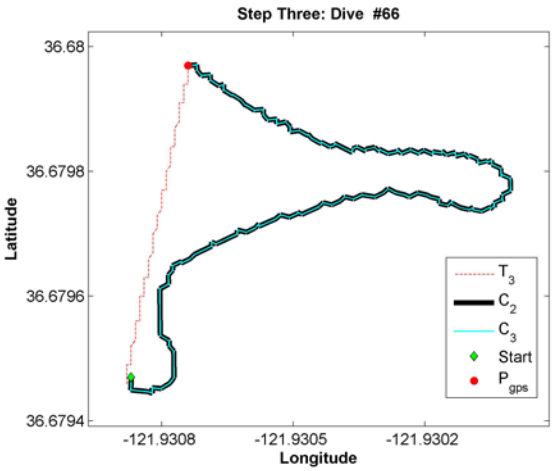
Step Three: Dive #66
36.68
36.6798
36.6796
36.6794
Latitude
-121.9308
-121.9305
-121.9302
Longitude
T3
C2
C3
Start
Pgps

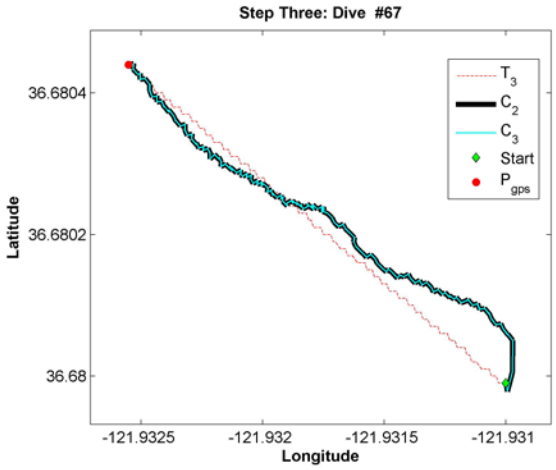
Step Three: Dive #67
36.6804
36.6802
36.68
Latitude
-121.9325
-121.932
-121.9315
-121.931
Longitude
T3
C2
C3
Start
Pgps

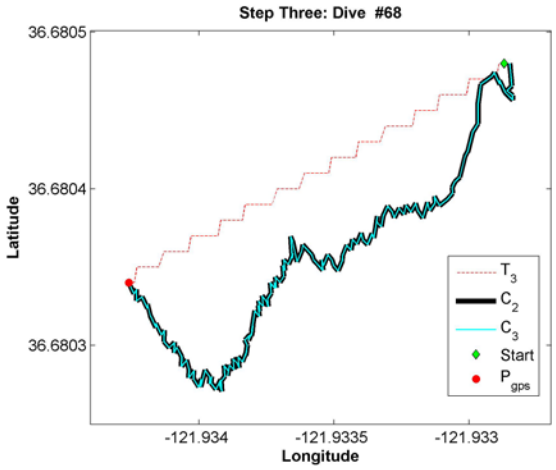
Step Three: Dive #68
36.6805
36.6804
36.6803
Latitude
-121.934
-121.9335
-121.933
Longitude
T3
C2
C3
Start
Pgps

E. STEP FOUR: COMPARISON THREE CORRECTED TRAJECTORIES

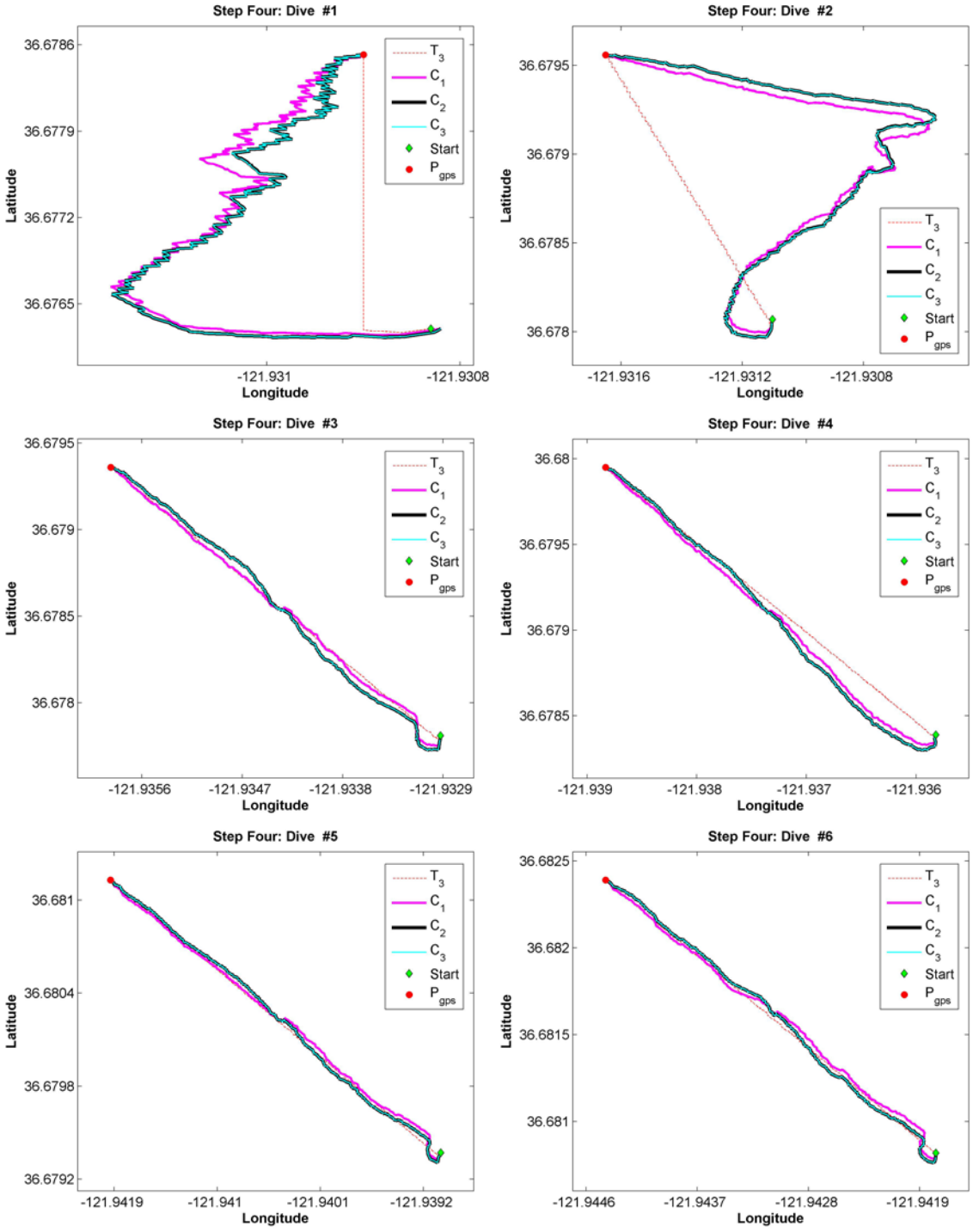

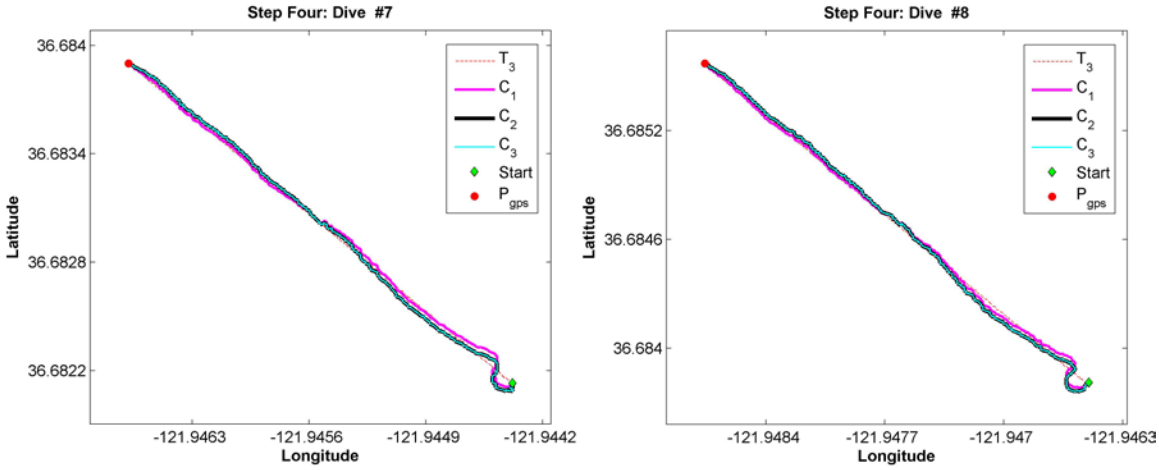
Step Four: Dive #7
Latitude
Longitude
36.684
36.6834
36.6828
36.6822
-121.9463
-121.9456
-121.9449
-121.9442
T3
C1
C2
C3
Start
Pgps

Step Four: Dive #8
Latitude
Longitude
36.6852
36.6846
36.684
-121.9484
-121.9477
-121.947
-121.9463
T3
C1
C2
C3
Start
Pgps

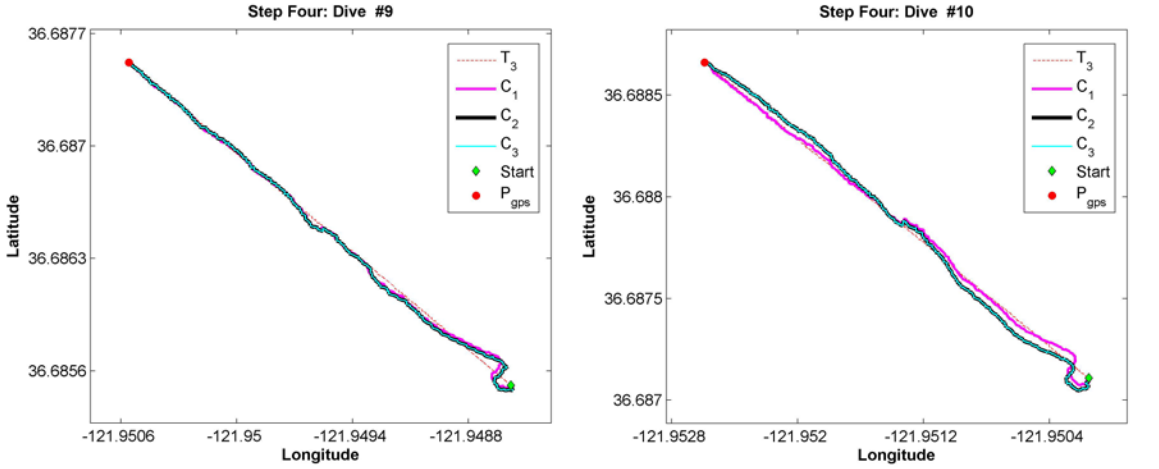
Step Four: Dive #9
Latitude
Longitude
36.6877
36.687
36.6863
36.6856
-121.9506
-121.95
-121.9494
-121.9488
T3
C1
C2
C3
Start
Pgps

Step Four: Dive #10
Latitude
Longitude
36.6885
36.688
36.6875
36.687
-121.9528
-121.952
-121.9512
-121.9504
T3
C1
C2
C3
Start
Pgps

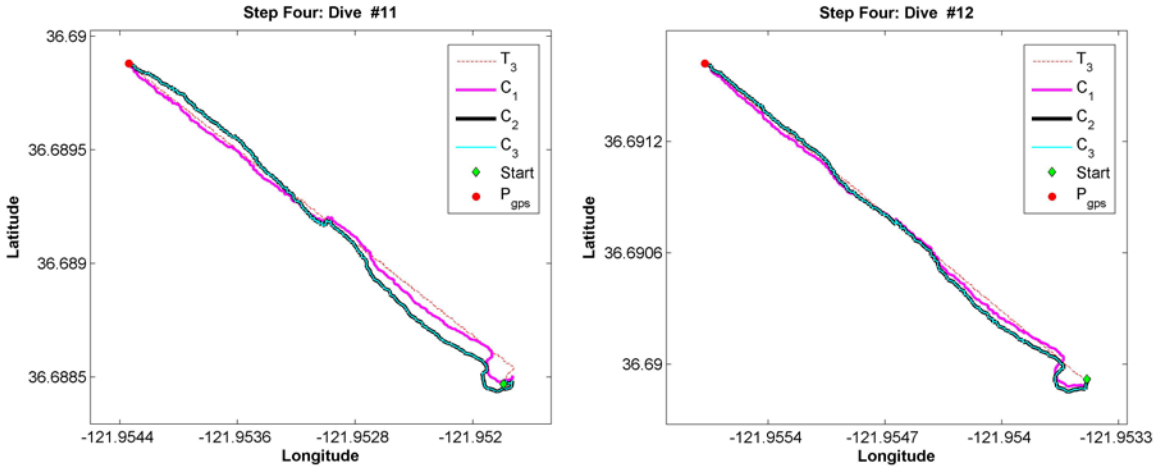
Step Four: Dive #11
Latitude
Longitude
36.69
36.6895
36.689
36.6885
-121.9544
-121.9536
-121.9528
-121.952
T3
C1
C2
C3
Start
Pgps

Step Four: Dive #12
Latitude
Longitude
36.6912
36.6906
36.69
-121.9554
-121.9547
-121.954
-121.9533
T3
C1
C2
C3
Start
Pgps

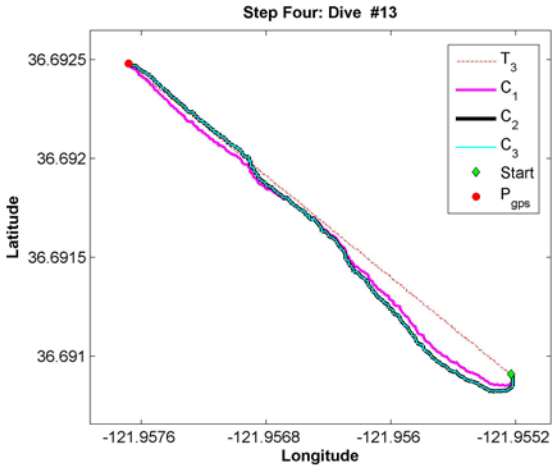
Step Four: Dive #13
Latitude
Longitude
36.6925
36.692
36.6915
36.691
-121.9576
-121.9568
-121.956
-121.9552
T3
C1
C2
C3
Start
Pgps

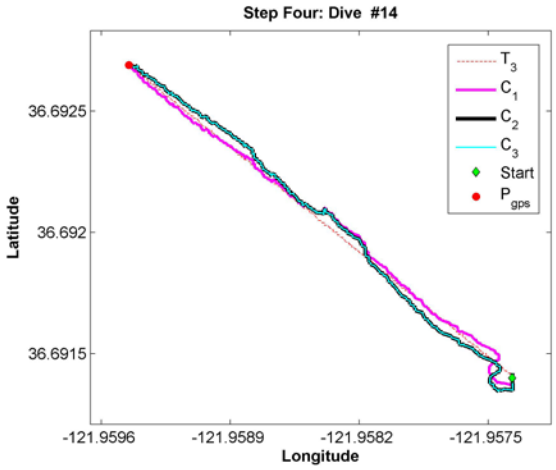
Step Four: Dive #14
Latitude
Longitude
36.6925
36.692
36.6915
-121.9596
-121.9589
-121.9582
-121.9575
T3
C1
C2
C3
Start
Pgps

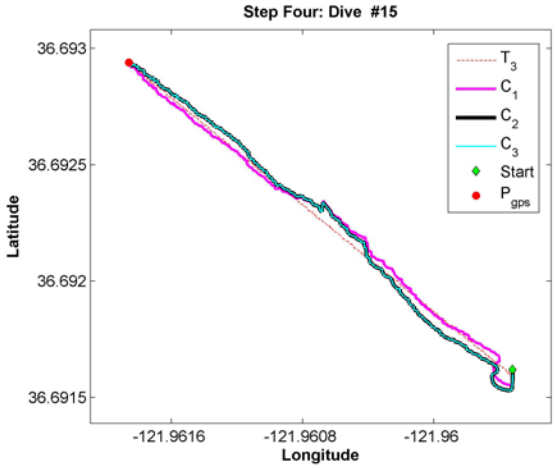
Step Four: Dive #15
Latitude
Longitude
36.693
36.6925
36.692
36.6915
-121.9616
-121.9608
-121.96
T3
C1
C2
C3
Start
Pgps

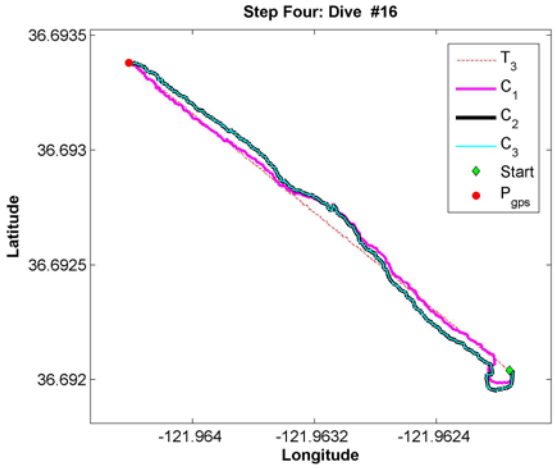
Step Four: Dive #16
Latitude
Longitude
36.6935
36.693
36.6925
36.692
-121.964
-121.9632
-121.9624
T3
C1
C2
C3
Start
Pgps

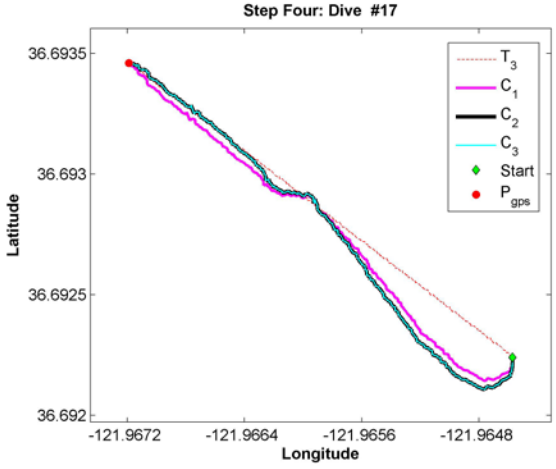
Step Four: Dive #17
Latitude
Longitude
36.6935
36.693
36.6925
36.692
-121.9672
-121.9664
-121.9656
-121.9648
T3
C1
C2
C3
Start
Pgps

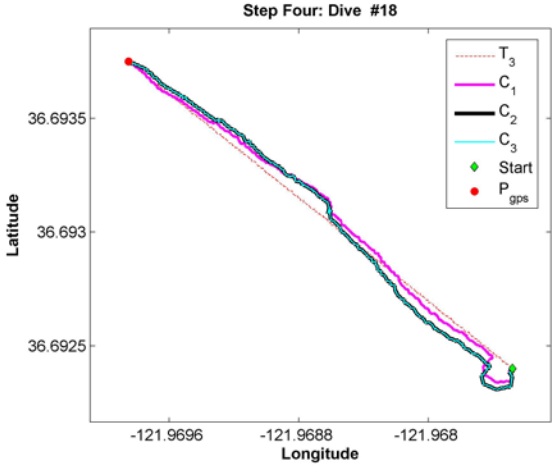
Step Four: Dive #18
Latitude
Longitude
36.6935
36.693
36.6925
-121.9696
-121.9688
-121.968
T3
C1
C2
C3
Start
Pgps

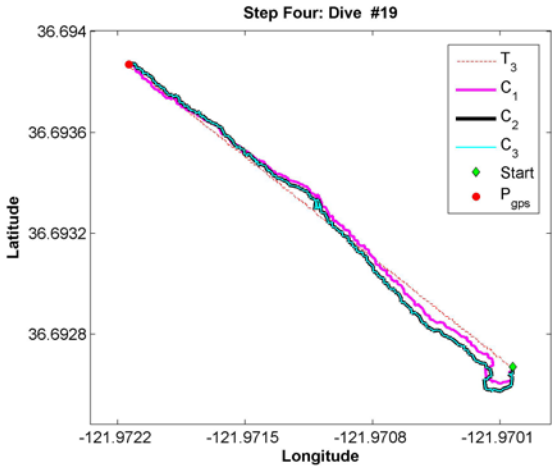
Step Four: Dive #19
36.694
36.6936
36.6932
36.6928
Latitude
-121.9722
-121.9715
-121.9708
-121.9701
Longitude
T3
C1
C2
C3
Start
Pgps

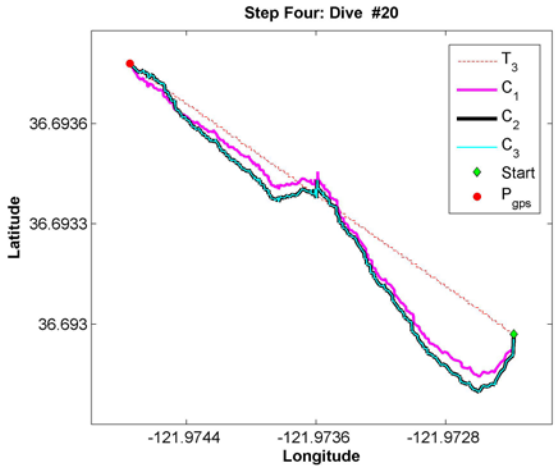
Step Four: Dive #20
36.6936
36.6933
36.693
Latitude
-121.9744
-121.9736
-121.9728
Longitude
T3
C1
C2
C3
Start
Pgps

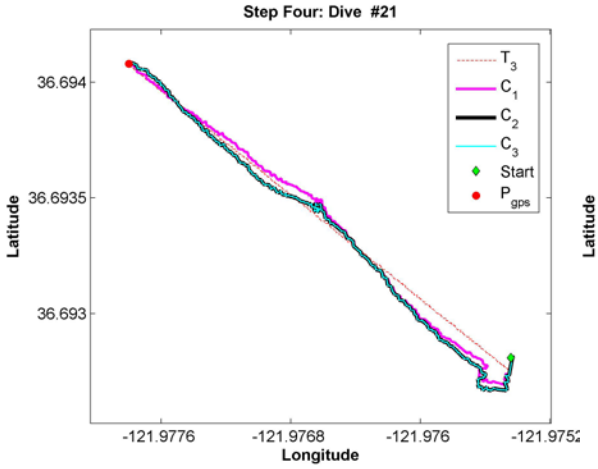
Step Four: Dive #21
36.694
36.6935
36.693
Latitude
-121.9776
-121.9768
-121.976
Longitude
T3
C1
C2
C3
Start
Pgps

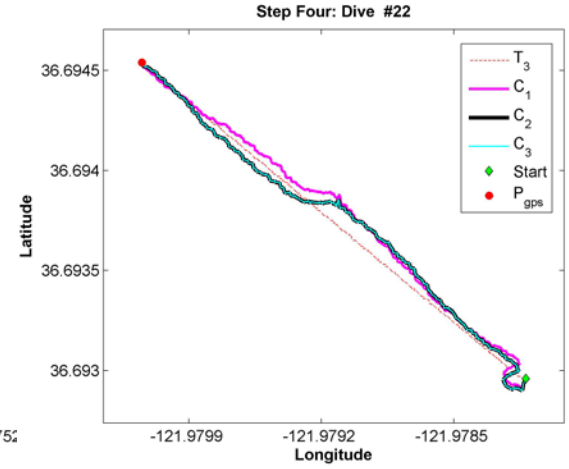
Step Four: Dive #22
36.6945
36.694
36.6935
36.693
Latitude
-121.9799
-121.9792
-121.9785
Longitude
T3
C1
C2
C3
Start
Pgps

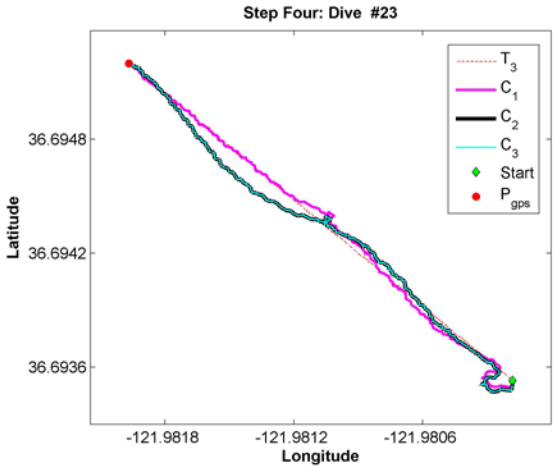
Step Four: Dive #23
36.6948
36.6942
36.6936
Latitude
-121.9818
-121.9812
-121.9806
Longitude
T3
C1
C2
C3
Start
Pgps

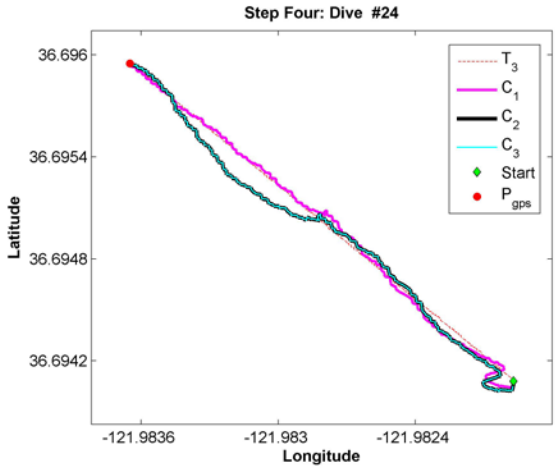
Step Four: Dive #24
36.696
36.6954
36.6948
36.6942
Latitude
-121.9836
-121.983
-121.9824
Longitude
T3
C1
C2
C3
Start
Pgps

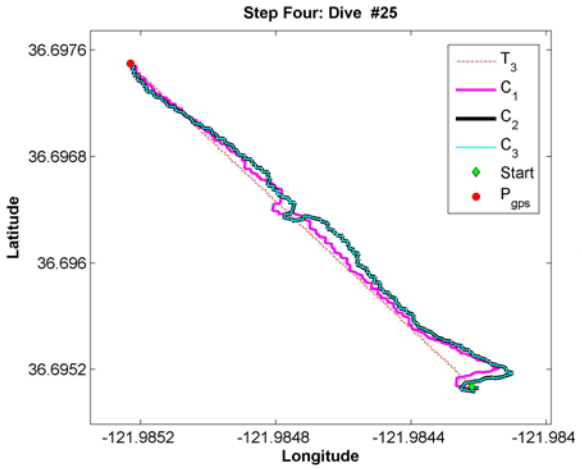
Step Four: Dive #25
36.6976
36.6968
36.696
36.6952
Latitude
-121.9852
-121.9848
-121.9844
-121.984
Longitude
T3
C1
C2
C3
Start
Pgps

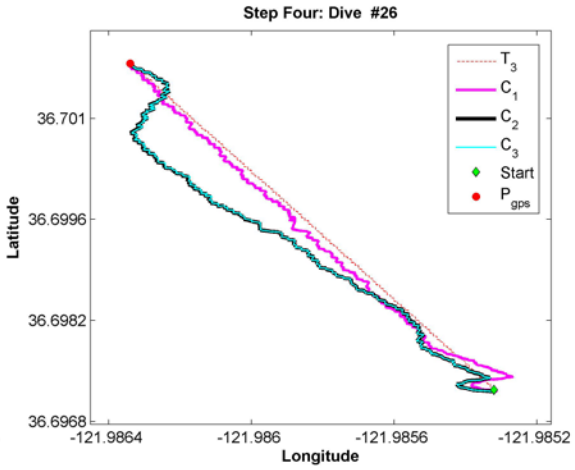
Step Four: Dive #26
36.701
36.6996
36.6982
36.6968
Latitude
-121.9864
-121.986
-121.9856
-121.9852
Longitude
T3
C1
C2
C3
Start
Pgps

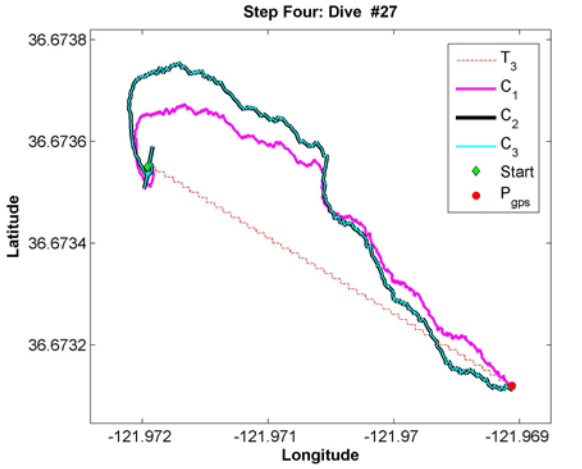
Step Four: Dive #27
36.6738
36.6736
36.6734
36.6732
Latitude
-121.972
-121.971
-121.97
-121.969
Longitude
T3
C1
C2
C3
Start
Pgps

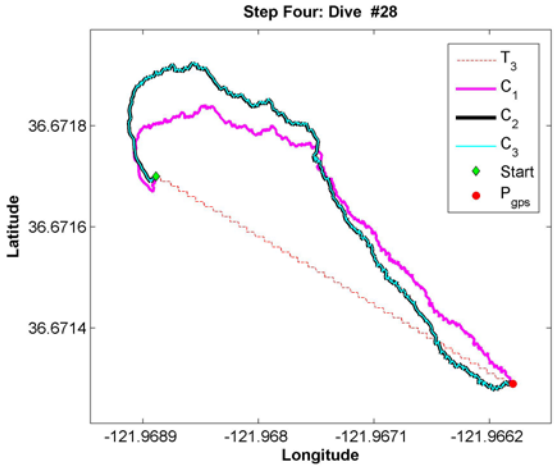
Step Four: Dive #28
36.6718
36.6716
36.6714
Latitude
-121.9689
-121.968
-121.9671
-121.9662
Longitude
T3
C1
C2
C3
Start
Pgps

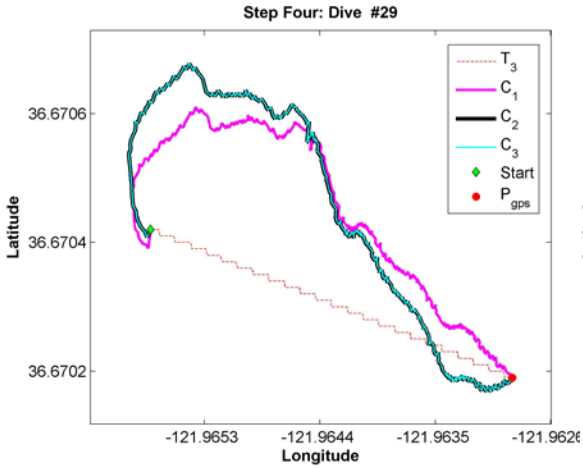
Step Four: Dive #29
36.6706
36.6704
36.6702
Latitude
-121.9653
-121.9644
-121.9635
Longitude
T3
C1
C2
C3
Start
Pgps

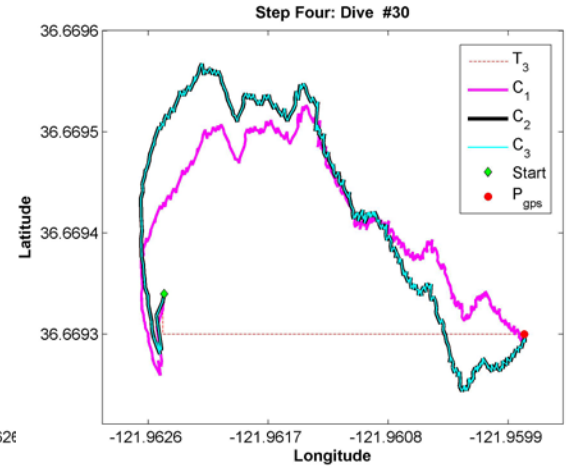
Step Four: Dive #30
36.6696
36.6695
36.6694
36.6693
Latitude
-121.9626
-121.9617
-121.9608
-121.9599
Longitude
T3
C1
C2
C3
Start
Pgps

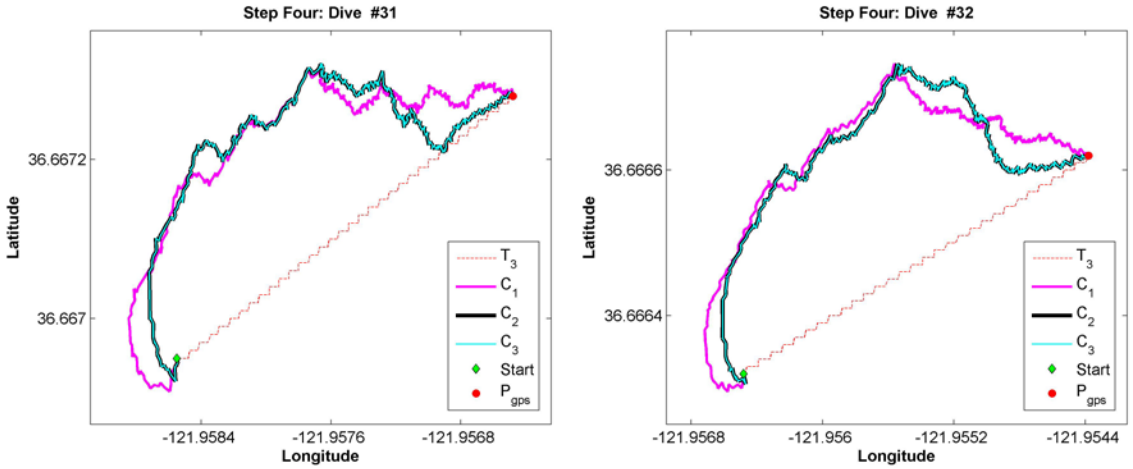
Step Four: Dive #31
Latitude
36.6672
36.667
-121.9584
-121.9576
-121.9568
Longitude
T3
C1
C2
C3
Start
Pgps

Step Four: Dive #32
Latitude
36.6666
36.6664
-121.9568
-121.956
-121.9552
-121.9544
Longitude
T3
C1
C2
C3
Start
Pgps

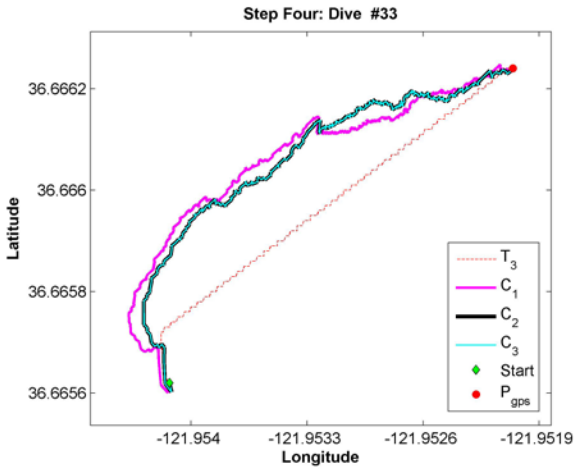
Step Four: Dive #33
Latitude
36.6662
36.666
36.6658
36.6656
-121.954
-121.9533
-121.9526
-121.9519
Longitude
T3
C1
C2
C3
Start
Pgps

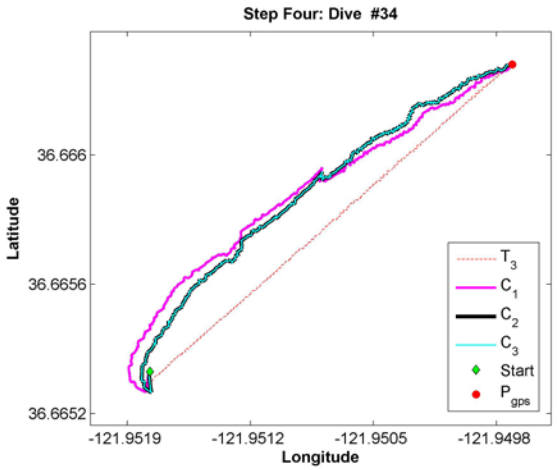
Step Four: Dive #34
Latitude
36.666
36.6656
36.6652
-121.9519
-121.9512
-121.9505
-121.9498
Longitude
T3
C1
C2
C3
Start
Pgps

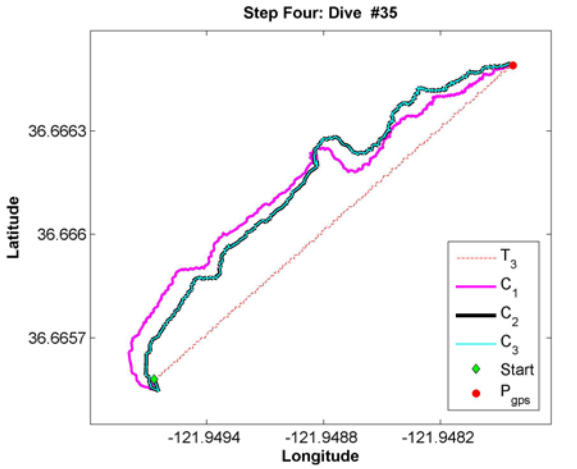
Step Four: Dive #35
Latitude
36.6663
36.666
36.6657
-121.9494
-121.9488
-121.9482
Longitude
T3
C1
C2
C3
Start
Pgps

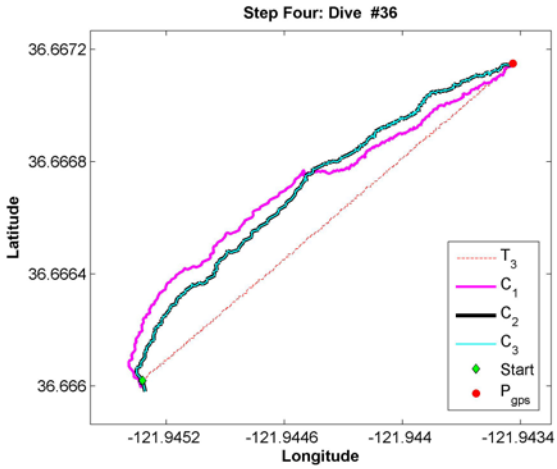
Step Four: Dive #36
Latitude
36.6672
36.6668
36.6664
36.666
-121.9452
-121.9446
-121.944
-121.9434
Longitude
T3
C1
C2
C3
Start
Pgps

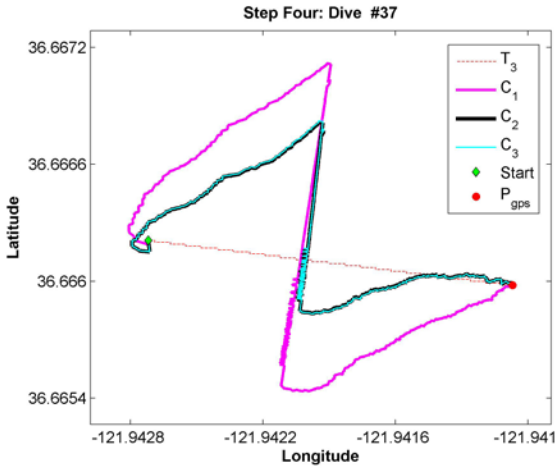
Step Four: Dive #37
36.6672
36.6666
36.666
36.6654
Latitude
-121.9428
-121.9422
-121.9416
-121.941
Longitude
T3
C1
C2
C3
Start
Pgps

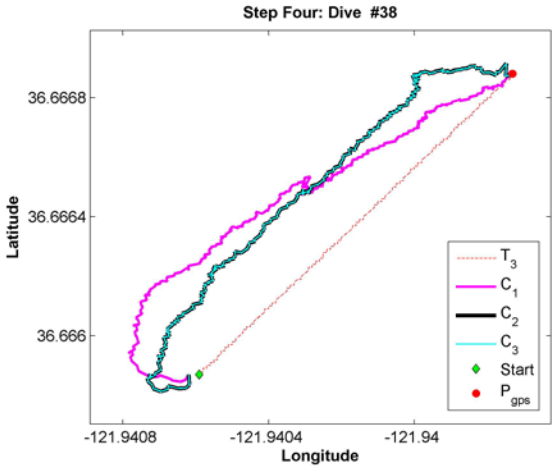
Step Four: Dive #38
36.6668
36.6664
36.666
Latitude
-121.9408
-121.9404
-121.94
Longitude
T3
C1
C2
C3
Start
Pgps

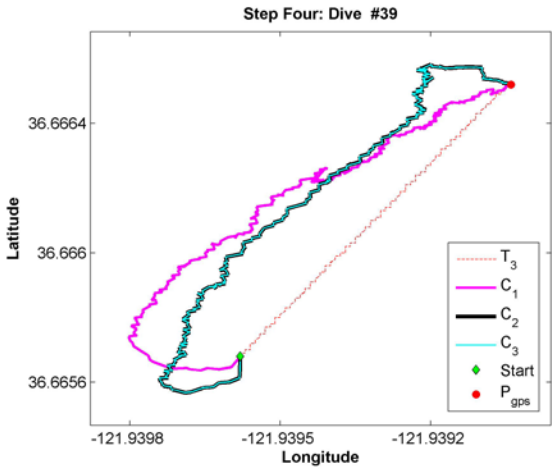
Step Four: Dive #39
36.6664
36.666
36.6656
Latitude
-121.9398
-121.9395
-121.9392
Longitude
T3
C1
C2
C3
Start
Pgps

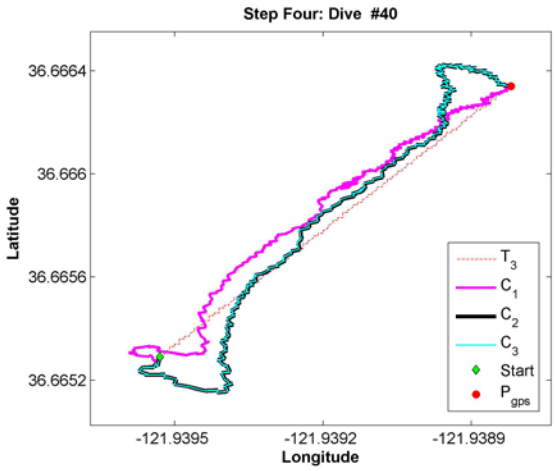
Step Four: Dive #40
36.6664
36.666
36.6656
36.6652
Latitude
-121.9395
-121.9392
-121.9389
Longitude
T3
C1
C2
C3
Start
Pgps

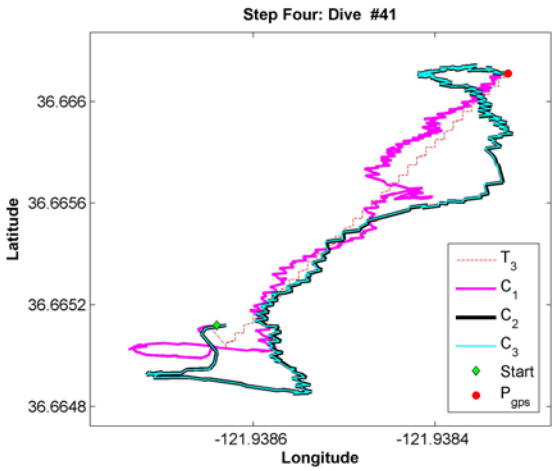
Step Four: Dive #41
36.666
36.6656
36.6652
36.6648
Latitude
-121.9386
-121.9384
Longitude
T3
C1
C2
C3
Start
Pgps

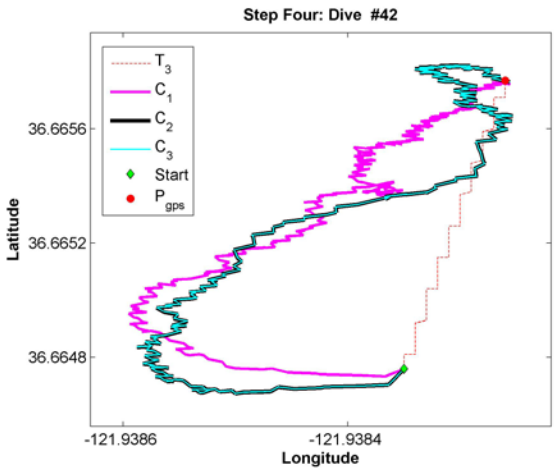
Step Four: Dive #42
36.6656
36.6652
36.6648
Latitude
-121.9386
-121.9384
Longitude
T3
C1
C2
C3
Start
Pgps

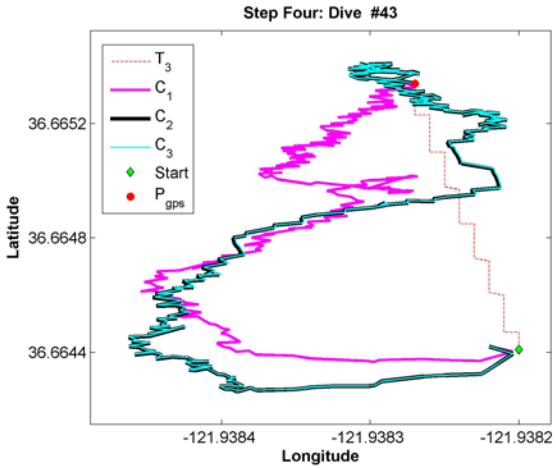
Step Four: Dive #43
T3
C1
C2
C3
Start
Pgps
36.6652
36.6648
36.6644
Latitude
-121.9384
-121.9383
-121.9382
Longitude

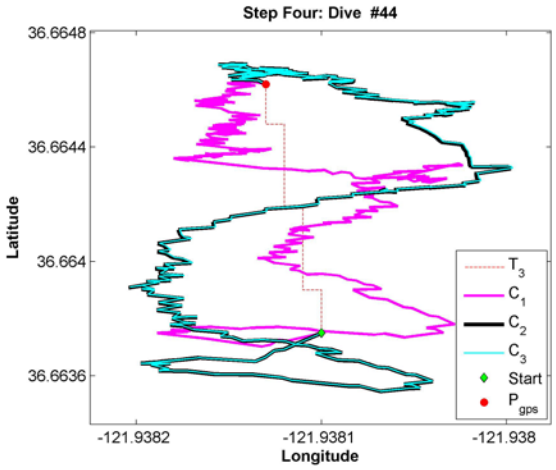
Step Four: Dive #44
36.6648
36.6644
36.664
36.6636
Latitude
-121.9382
-121.9381
-121.938
Longitude
T3
C1
C2
C3
Start
Pgps

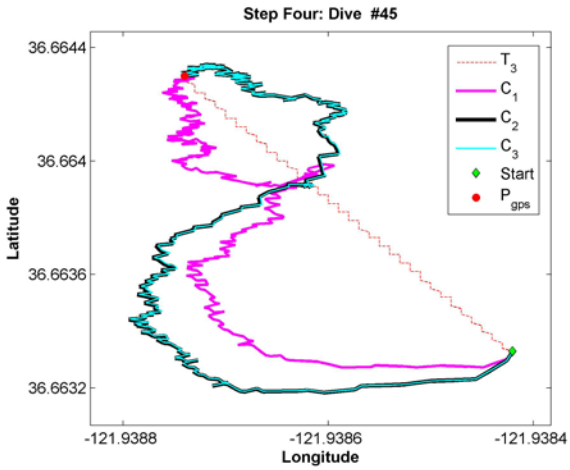
Step Four: Dive #45
36.6644
36.664
36.6636
36.6632
Latitude
-121.9388
-121.9386
-121.9384
Longitude
T3
C1
C2
C3
Start
Pgps

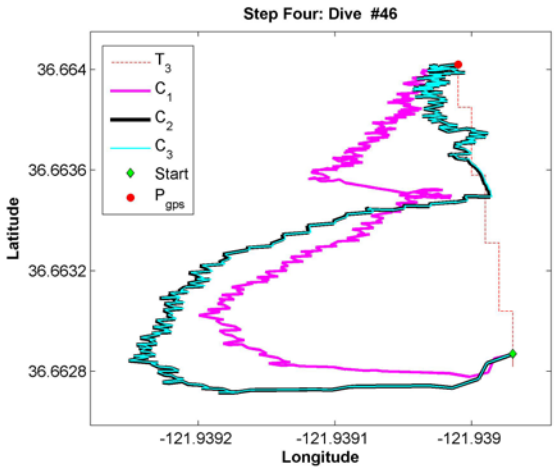
Step Four: Dive #46
36.664
36.6636
36.6632
36.6628
Latitude
-121.9392
-121.9391
-121.939
Longitude
T3
C1
C2
C3
Start
Pgps

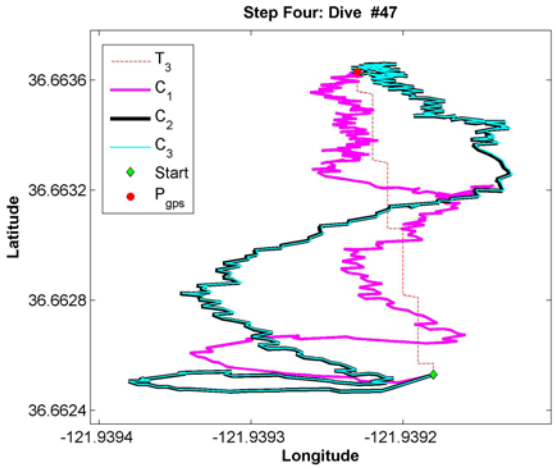
Step Four: Dive #47
36.6636
36.6632
36.6628
36.6624
Latitude
-121.9394
-121.9393
-121.9392
Longitude
T3
C1
C2
C3
Start
Pgps

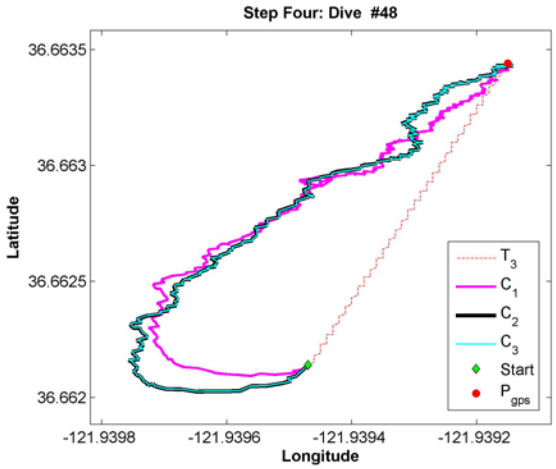
Step Four: Dive #48
36.6635
36.663
36.6625
36.662
Latitude
-121.9398
-121.9396
-121.9394
-121.9392
Longitude
T3
C1
C2
C3
Start
Pgps

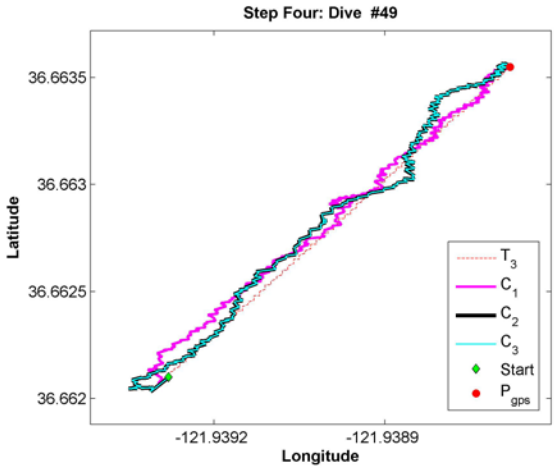
Step Four: Dive #49
Latitude
Longitude
36.6635
36.663
36.6625
36.662
-121.9392
-121.9389
T3
C1
C2
C3
Start
Pgps

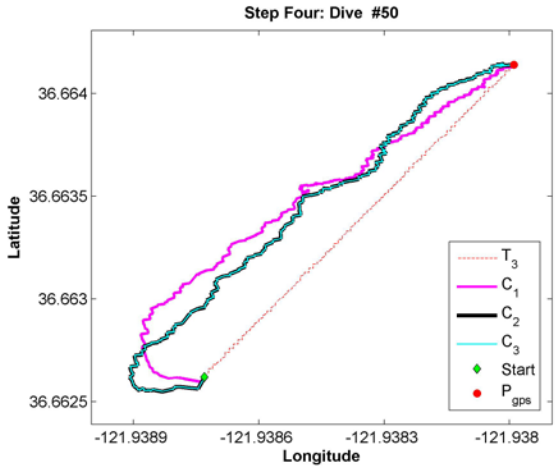
Step Four: Dive #50
Latitude
Longitude
36.664
36.6635
36.663
36.6625
-121.9389
-121.9386
-121.9383
-121.938
T3
C1
C2
C3
Start
Pgps

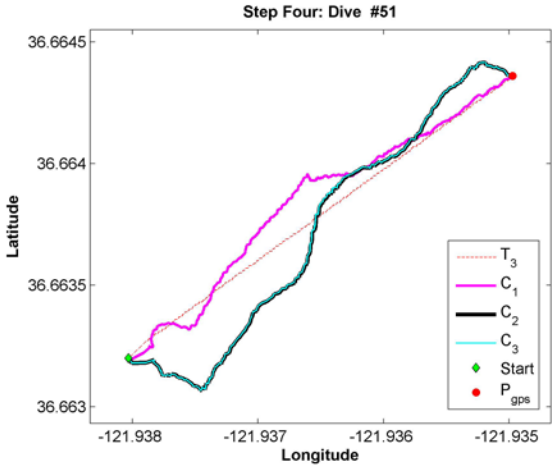
Step Four: Dive #51
Latitude
Longitude
36.6645
36.664
36.6635
36.663
-121.938
-121.937
-121.936
-121.935
T3
C1
C2
C3
Start
Pgps

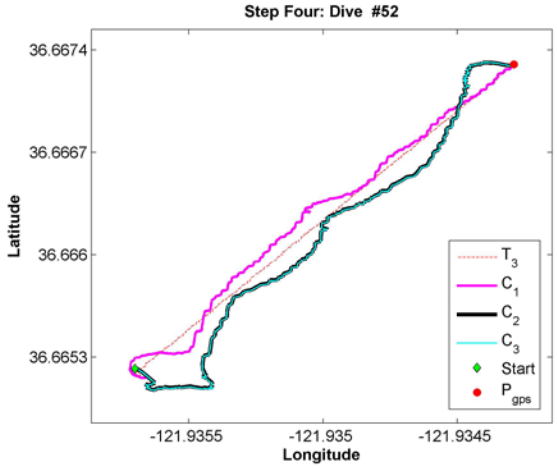
Step Four: Dive #52
Latitude
Longitude
36.6674
36.6667
36.666
36.6653
-121.9355
-121.935
-121.9345
T3
C1
C2
C3
Start
Pgps

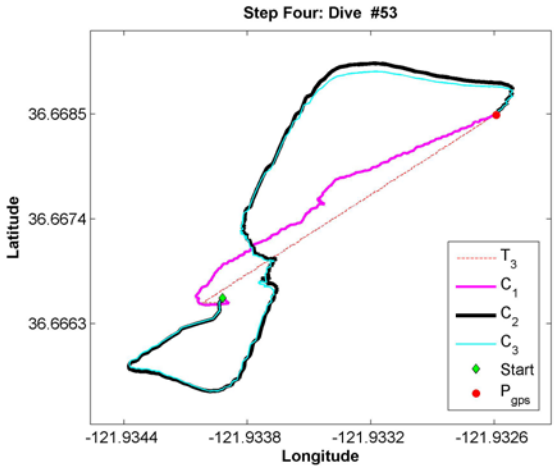
Step Four: Dive #53
Latitude
Longitude
36.6685
36.6674
36.6663
-121.9344
-121.9338
-121.9332
-121.9326
T3
C1
C2
C3
Start
Pgps

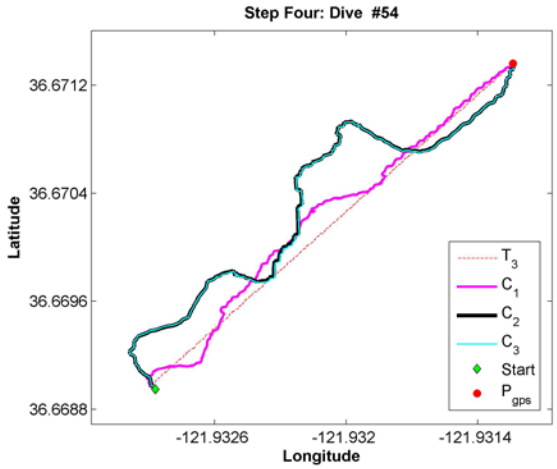
Step Four: Dive #54
Latitude
Longitude
36.6712
36.6704
36.6696
36.6688
-121.9326
-121.932
-121.9314
T3
C1
C2
C3
Start
Pgps

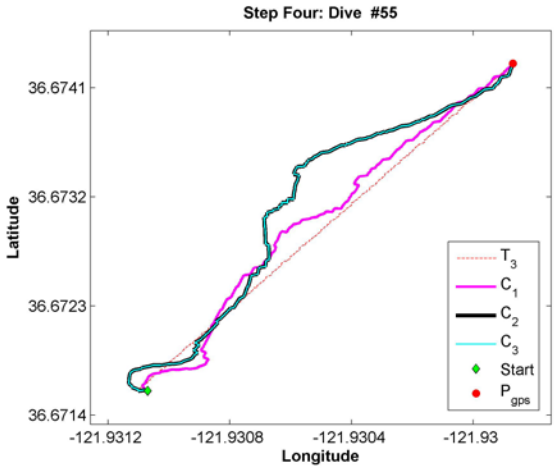
Step Four: Dive #55
Latitude
Longitude
36.6741
36.6732
36.6723
36.6714
-121.9312
-121.9308
-121.9304
-121.93
T3
C1
C2
C3
Start
Pgps

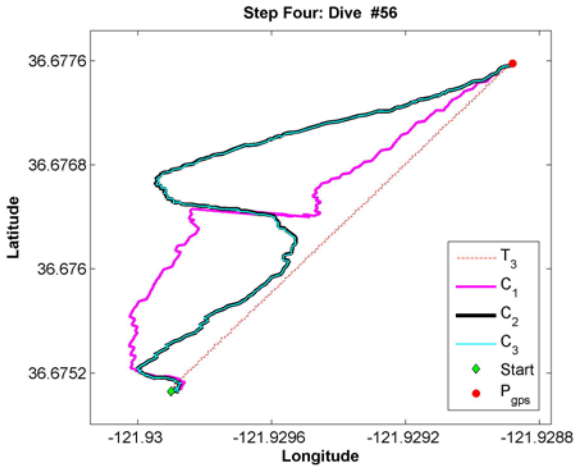
Step Four: Dive #56
Latitude
Longitude
36.6776
36.6768
36.676
36.6752
-121.93
-121.9296
-121.9292
-121.9288
T3
C1
C2
C3
Start
Pgps

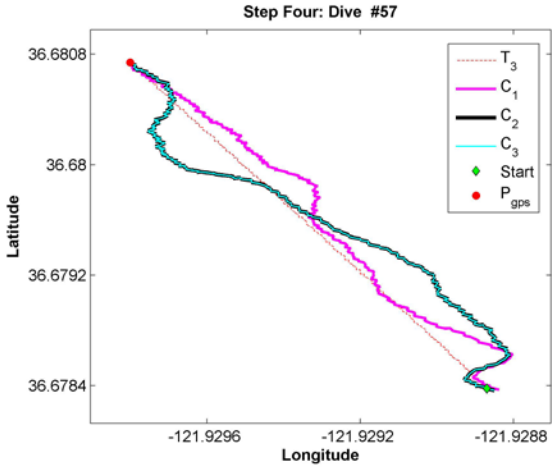
Step Four: Dive #57
Latitude
Longitude
36.6808
36.68
36.6792
36.6784
-121.9296
-121.9292
-121.9288
T3
C1
C2
C3
Start
Pgps

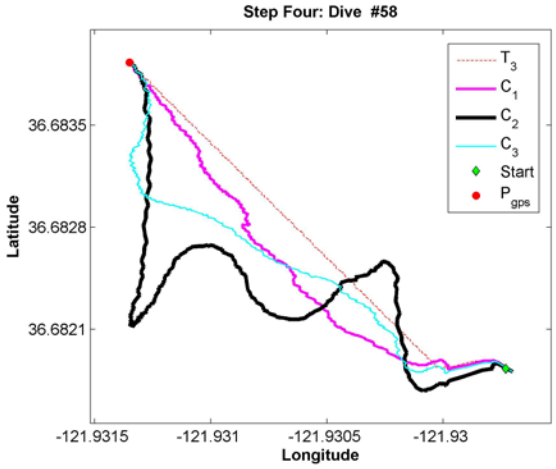
Step Four: Dive #58
Latitude
Longitude
36.6835
36.6828
36.6821
-121.9315
-121.931
-121.9305
-121.93
T3
C1
C2
C3
Start
Pgps

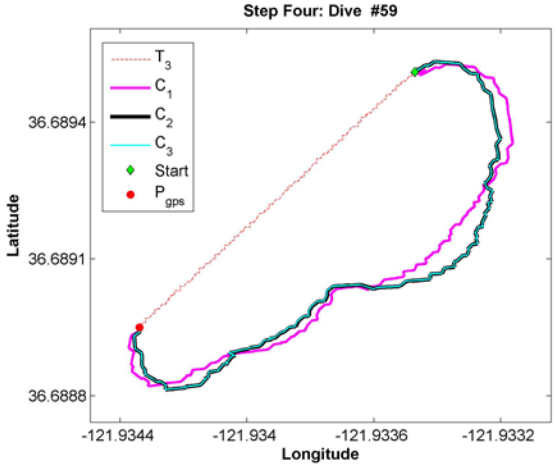
Step Four: Dive #59
Latitude
Longitude
36.6894
36.6891
36.6888
-121.9344
-121.934
-121.9336
-121.9332
T3
C1
C2
C3
Start
Pgps

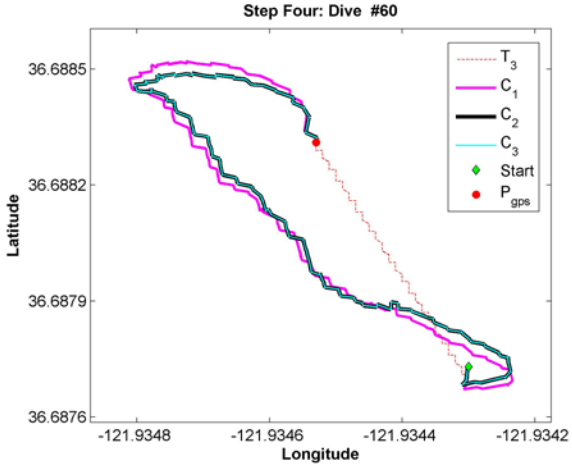
Step Four: Dive #60
Latitude
Longitude
36.6885
36.6882
36.6879
36.6876
-121.9348
-121.9346
-121.9344
-121.9342
T3
C1
C2
C3
Start
Pgps

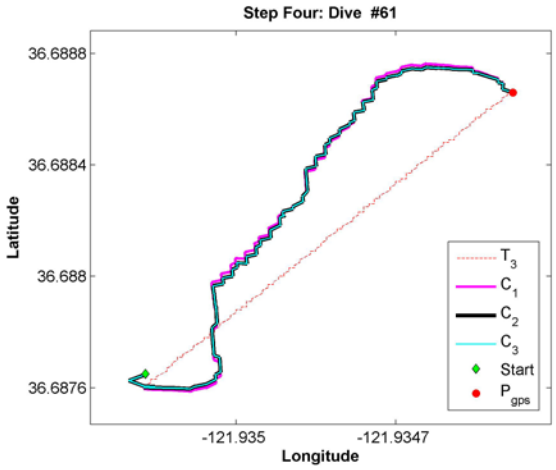
Step Four: Dive #61
36.6888
36.6884
36.688
36.6876
Latitude
-121.935
-121.9347
Longitude
T3
C1
C2
C3
Start
Pgps

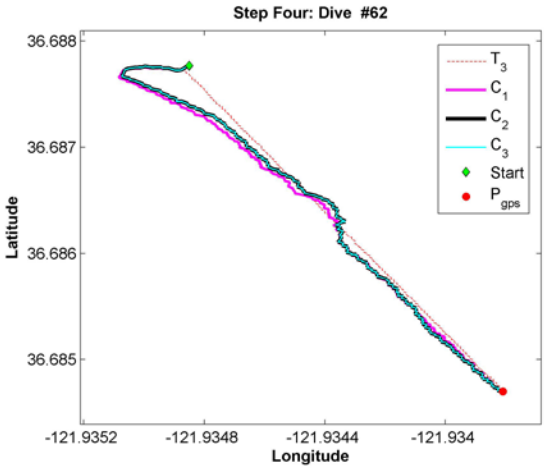
Step Four: Dive #62
36.688
36.687
36.686
36.685
Latitude
-121.9352
-121.9348
-121.9344
-121.934
Longitude
T3
C1
C2
C3
Start
Pgps

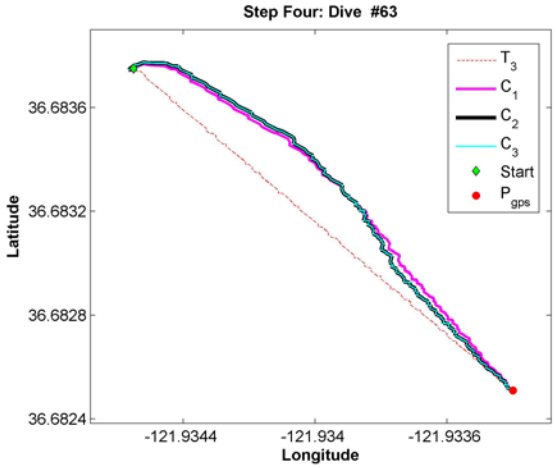
Step Four: Dive #63
36.6836
36.6832
36.6828
36.6824
Latitude
-121.9344
-121.934
-121.9336
Longitude
T3
C1
C2
C3
Start
Pgps

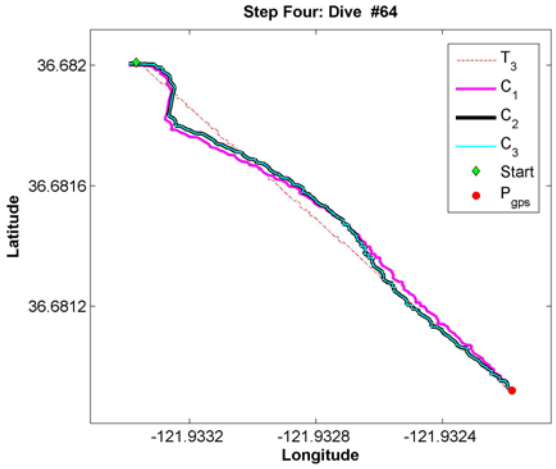
Step Four: Dive #64
36.682
36.6816
36.6812
Latitude
-121.9332
-121.9328
-121.9324
Longitude
T3
C1
C2
C3
Start
Pgps

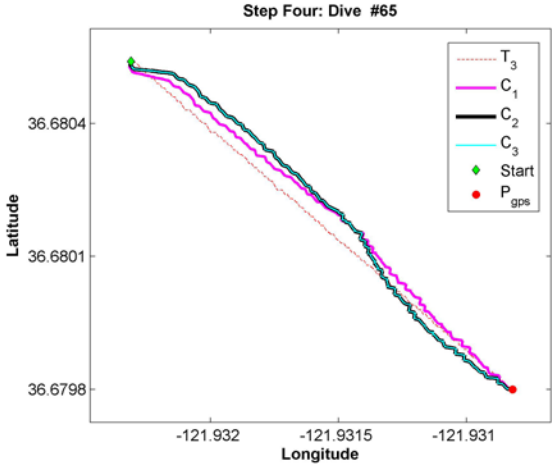
Step Four: Dive #65
36.6804
36.6801
36.6798
Latitude
-121.932
-121.9315
-121.931
Longitude
T3
C1
C2
C3
Start
Pgps

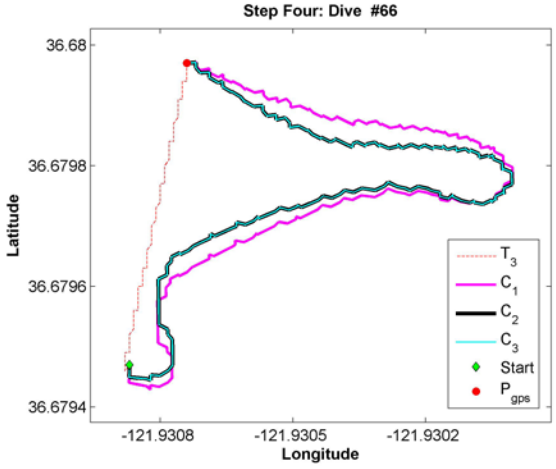
Step Four: Dive #66
36.68
36.6798
36.6796
36.6794
Latitude
-121.9308
-121.9305
-121.9302
Longitude
T3
C1
C2
C3
Start
Pgps

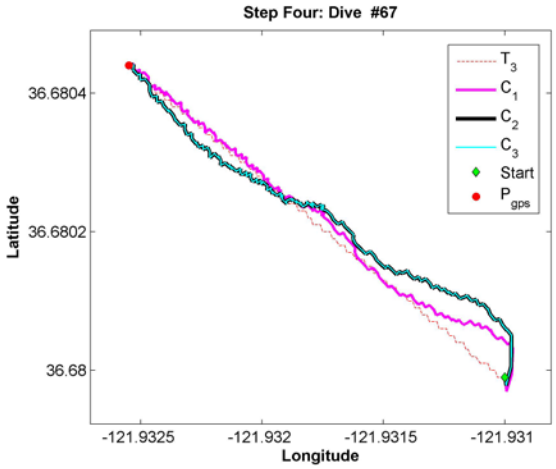
Step Four: Dive #67
T3
C1
C2
C3
Start
Pgps
36.6804
36.6802
36.68
Latitude
-121.9325
-121.932
-121.9315
-121.931
Longitude

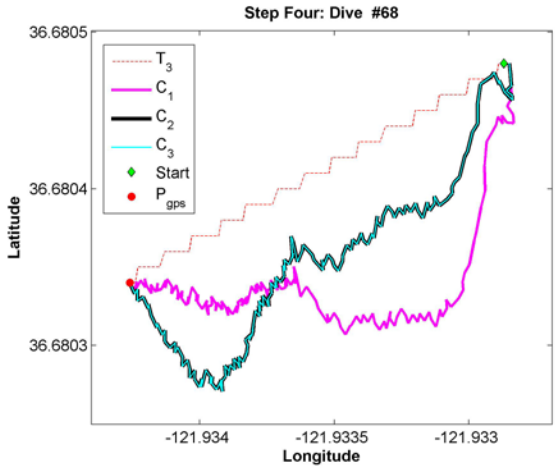
Step Four: Dive #68
T3
C1
C2
C3
Start
Pgps
36.6805
36.6804
36.6803
Latitude
-121.934
-121.9335
-121.933
Longitude

APPENDIX B: COINCIDENCE OF DR AND DR_{NCOM} TRAJECTORY WITH THE DEPTH-DEPENDENT CORRECTION METHOD

In this appendix, we prove the results coincidence of DR (T_1) and DR_{NCOM} (T_2) trajectory with the depth-dependent correction method (see Figure 27 and Figure 28, respectively). It helps us save some effort and process efficiently for improving our method in this study. We form a hypothesis that both corrected trajectories with the depth-dependent correction method have a same result. By proving this hypothesis, the only trajectory that needs to be corrected would be the T_1 to develop our method.

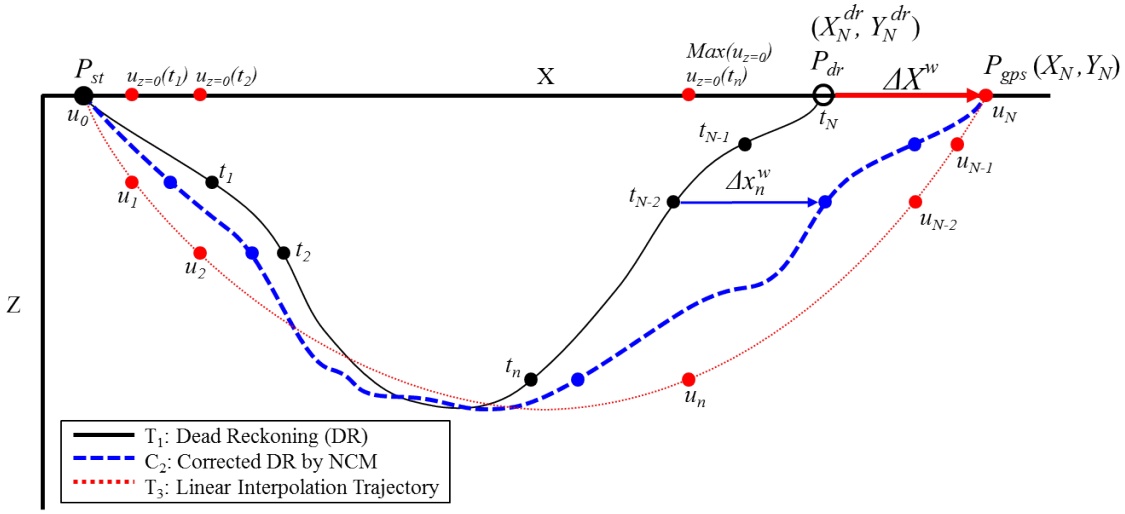

Figure 27. Lateral View of the Eastward Component of the T_1 with the Depth-dependent Correction Method.

Let there be N steps from start to end of each trajectory. Then, the final position of T_1 and T_3 can be expressed as P_{dr} (X_N^{dr}, Y_N^{dr}) and P_{gps} (X_N, Y_N), and the distance error between P_{dr} and P_{gps} also can be presented as $\Delta X^w = X_N - X_N^{dr}$, $\Delta Y^w = Y_N - Y_N^{dr}$. Now, let us correct the T_1 on the *x*-direction by applying the depth-dependent correction method as shown in Chapter III.

The corrected water displacement (Δx_n^w) at each time (t_n) can be expressed as shown in Equation (34) by applying the Equation (27) and Equation (32) in Chapter III.

$$\Delta x_n^w = \Delta X^w \frac{\sum_{i=1}^{n} f_i^z f_i^t \Delta t_i}{\sum_{i=1}^{N} f_i^z f_i^t \Delta t_i}, \text{where } f_i^z = \frac{u_i^{ncom}(z_i, t_i)}{u_i^{ncom}(0, t_i)}, \quad f_n^t = \frac{u_i^{ncom}(0, t_i)}{u_{\max}},$$
$$\text{and } u_{\max} = \max\left[u_i^{ncom}(0, t_i)\right], i = 1, 2, \cdots, N \tag{34}$$

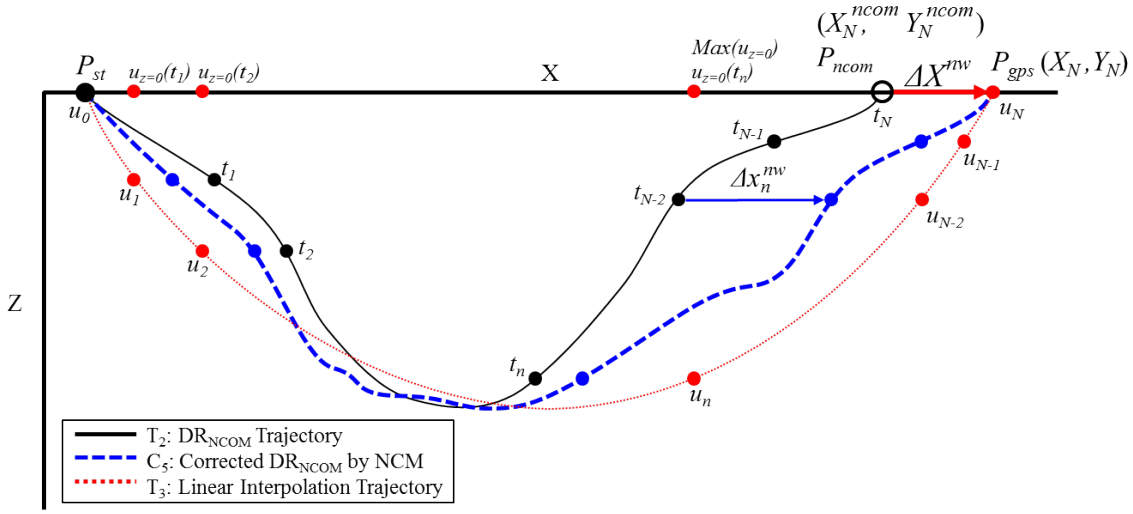

Figure 28. Lateral View of the Eastward Component of the T_2 with the Depth-dependent Correction Method.

At this time, we correct the T_2 on the *x*-direction by applying the depth-dependent correction method. Let the final position of T_2 be P_{ncom} (X_N^{ncom}, Y_N^{ncom}), and the distance error between P_{ncom} and P_{gps} also be $\Delta X^{nw} = X_N - X_N^{ncom}$, $\Delta Y^{nw} = Y_N - Y_N^{ncom}$. Moreover, with the relationship of position between T_1 and T_2, the position of T_2 at each time (t_n) can be expressed as follows.

$$X_n^{ncom} = X_n^{dr} + \sum_{i=1}^{n} u_i^{ncom}(z_i, t_i)\Delta t_i$$
$$Y_n^{ncom} = Y_n^{dr} + \sum_{i=1}^{n} v_i^{ncom}(z_i, t_i)\Delta t_i \tag{35}$$

Then, Equation (35) can be presented as shown in Equation (36).

$$\begin{aligned} X_n^{ncom} &= X_n^{dr} + \sum_{i=1}^{n} u_i^{ncom}(z_i, t_i)\Delta t_i = X_n^{dr} + u_{\max} \sum_{i=1}^{n} \frac{u_i^{ncom}(z_i, t_i)}{u_i^{ncom}(0, t_i)} \frac{u_i^{ncom}(0, t_i)}{u_{\max}} \Delta t_i \\ &= X_n^{dr} + u_{\max} \sum_{i=1}^{n} f_i^z f_i^t \Delta t_i, \text{ where } u_{\max} = \max\left[u_i^{ncom}(0, t_i)\right], i = 1, 2, \cdots, N \end{aligned} \tag{36}$$

In addition, the final position can be presented as shown in Equation (37).

$$X_N^{ncom} = X_N^{dr} + u_{\max} \sum_{i=1}^{N} f_i^z f_i^t \Delta t_i \tag{37}$$

Consequently, the total corrected water displacement will be

$$\Delta X^{nw} = X_N - X_N^{ncom} = \Delta X^w - u_{\max} \sum_{i=1}^{N} f_i^z f_i^t \Delta t_i \tag{38}$$

The corrected water displacement (Δx_n^{nw}) at each time (t_n) can be expressed similar to the Equation (34) by substituting Equation (38) into Equation (34) as shown in Equation (39).

$$\begin{aligned} \Delta x_n^{nw} &= \Delta X^{nw} \frac{\sum_{i=1}^{n} f_i^z f_i^t \Delta t_i}{\sum_{i=1}^{N} f_i^z f_i^t \Delta t_i} = (\Delta X^w - u_{\max} \sum_{i=1}^{N} f_i^z f_i^t \Delta t_i) \frac{\sum_{i=1}^{n} f_i^z f_i^t \Delta t_i}{\sum_{i=1}^{N} f_i^z f_i^t \Delta t_i} \\ &= \left(\Delta X^w \frac{\sum_{i=1}^{n} f_i^z f_i^t \Delta t_i}{\sum_{i=1}^{N} f_i^z f_i^t \Delta t_i} \right) - u_{\max} \sum_{i=1}^{n} f_i^z f_i^t \Delta t_i \\ &= \Delta x_n^w - u_{\max} \sum_{i=1}^{n} f_i^z f_i^t \Delta t_i \end{aligned} \tag{39}$$

Finally, the corrected position of C_2 and C_5 ($\tilde{X}_n^{cdr}, \tilde{X}_n^{cncom}$) at each time is the same, and it can be expressed as shown in Equation (40).

$$\begin{aligned} \tilde{X}_n^{cdr} &= X_n^{dr} + \Delta x_n^w \\ \tilde{X}_n^{cncom} &= X_n^{ncom} + \Delta x_n^{nw} = \left(X_n^{dr} + u_{\max} \sum_{i=1}^{n} f_i^z f_i^t \Delta t_i \right) + \left(\Delta x_n^w - u_{\max} \sum_{i=1}^{n} f_i^z f_i^t \Delta t_i \right) \\ &= X_n^{dr} + \Delta x_n^w = \tilde{X}_n^{cdr} \end{aligned} \tag{40}$$

THIS PAGE INTENTIONALLY LEFT BLANK

APPENDIX C: ITERATION METHOD FOR ESTIMATING AN OPTIMAL UNDERWATER TRAJECTORY OF GLIDER

This appendix describes the iteration method to estimate an optimal trajectory by applying the depth-dependent correction method with C_2. C_2 is the corrected trajectory using the depth-dependent correction method with DR trajectory. In this study, the real underwater trajectory of glider is unknown, thus an optimal trajectory development is needed to determine which corrected trajectory is more precise by comparing the two. The iteration method is described mathematically as follows.

Let $\mathbf{R}(t)$ be the glider's position vector with the function of time, $\mathbf{U}_g(\mathbf{R},t)$ be the glider's velocity vector relative to the ocean currents with the function of the glider's position and time, and $\mathbf{U}_{ncom}(\mathbf{R},t)$ be the water velocity vector with the function of the glider's position and time.

Generally, the glider's position at time t_n can be expressed as shown in Equation (41).

$$\mathbf{R}(t_n) = \mathbf{R}(t_0) + \int_{t_0}^{t_n} \mathbf{U}(\mathbf{R},t)dt = \mathbf{R}(t_0) + \int_{t_0}^{t_n} \mathbf{U}_g(\mathbf{R},t)dt + \int_{t_0}^{t_n} \mathbf{U}_w(\mathbf{R},t)dt \tag{41}$$

In this study, the glider's DR position does not consider the water velocity, so its DR position would be

$$\mathbf{R}_{dr}(t_n) = \mathbf{R}(t_0) + \int_{t_0}^{t_n} \mathbf{U}_g(\mathbf{R},t)dt \tag{42}$$

Then, the final position of glider at time t_N can be presented as shown in Equation (43) by substituting Equation (42) into Equation (41).

$$\mathbf{R}(t_N) = \mathbf{R}_{dr}(t_N) + \int_{t_0}^{t_N} \mathbf{U}_{ncom}(\mathbf{R},t)dt \tag{43}$$

The C_2 is corrected from the T_1 by applying the depth-dependent correction method against the distance difference between P_{dr} and P_{gps} (ΔX^w, see Figure 4). Now, we develop the *x*-direction component of the C_2. Let the glider's *x*-direction component of final position vector at time t_N be $\mathrm{X}_{gps}(t_N)$.

Then, it can be expressed as follows.

$$\mathrm{X}_{gps}(t_N) = \mathrm{X}_{dr}(t_N) + \int_{t_0}^{t_N} u_{ncom}(\mathbf{R}, t)dt$$

where

$X_{dr}(t_N)$: x-direction component of DR position vector

$u_{ncom}(\mathbf{R}, t)$: Eastward component of the Regional NCOM velocity vectors (44)

Then, the distance difference between P_{ncom} and P_{gps} (ΔX^{nw}) would be

$$\Delta X^{w} = X_{gps}(t_N) - X_{dr}(t_N) = \int_{t_0}^{t_N} u_{ncom}(\mathbf{R}, t)dt \tag{45}$$

To correct ΔX^{w}, Equation (46) is obtained by applying Equation (29) and Equation (30).

$$\Delta X^{w} = C\sum_{i=1}^{N} f_i^{z} f_i^{t} \Delta t_i$$

$$C = \frac{\Delta X^{w}}{\sum_{i=1}^{N} f_i^{z} f_i^{t} \Delta t_i}, \text{ C: Correction Coefficient} \tag{46}$$

In addition, the distance difference between T_2 and T_3 (Δx_n^{w}) at each time (t_n) would be

$$\Delta x_n^{w} = C\sum_{i=1}^{n} f_i^{z} f_i^{t} \Delta t_i = \Delta X^{w} \frac{\sum_{i=1}^{n} f_i^{z} f_i^{t} \Delta t_i}{\sum_{i=1}^{N} f_i^{z} f_i^{t} \Delta t_i} \tag{47}$$

After substituting Equation (47) into Equation (40) in Appendix B, the eastward component of glider's corrected position vector $\tilde{X}^{cdr}(t_n)$ at time t_n would be

$$\tilde{X}^{cdr}(t_n) = X_{dr}(t_n) + \Delta X^{w} \frac{\sum_{i=1}^{n} f_i^{z} f_i^{t} \Delta t_i}{\sum_{i=1}^{N} f_i^{z} f_i^{t} \Delta t_i} \tag{48}$$

However, since the variables in Equation (48), f_i^{z}, and f_i^{t} depend on the glider's position and time, the equation is non-linear. Thus, it is difficult to get an exact solution. Therefore, we use the iteration method to reach close to the exact solution.

Let the glider's eastward component of position vector after iteration at time (t_n) be $X^{m+1}(t_n)$, then

$$X^{m+1}(t_n) = X_{dr}(t_n) + \Delta X^w \frac{\sum_{i=1}^{n} f_i^z(m) f_i^t(m) \Delta t_i}{\sum_{i=1}^{N} f_i^z(m) f_i^t(m) \Delta t_i}, \; m = 1, 2, \ldots, M-1, M \tag{49}$$

where $f_i^z(m)$, $f_i^t(m)$: Factors on X^m, Y^m

To determine how many times iteration will be done, we need to set a criterion. We set the relative error of 10–^{5} for this study. Let the reference and iterated trajectory be T_m and T_{m+1}, the sum of distance difference between two trajectories be D_m, and the total length of the reference trajectory be L_m at each step. Then the relative error (E_{rel}) at each step can be calculated by dividing D_m by L_m. Equation (50) presents this procedure mathematically.

$$E_{rel} = D_m / L_m, \; m = 1, 2, \cdots, M-1, M$$

$$D_m = \sum_{n=1}^{N} (X_n^{m+1} - X_n^m)$$

where (50)

$X^{m+1}(t_n)$: The eastward position of glider on the iterated trajectory at time t_n

$X^m(t_n)$: The eastward position of glider on the reference trajectory at time t_n

If E_{rel} is less than 10–^{5}, the iteration is allowed to be terminated.

THIS PAGE INTENTIONALLY LEFT BLANK

LIST OF REFERENCES

Barron, C. N., R. C. Rhodes, L. F. Smedstad, C. D. Rowley, P. J. Martin, and A. B. Kara, 2003: Global ocean nowcasts and forecasts with the Navy Coastal Ocean Model (NCOM). *2003 NRL Review*, Naval Research Laboratory, 175–178.

Barron, C. N., A. B. Kara, H. E. Hurlburt, C. Rowley, and L. F. Smedstad, 2004: Sea surface height predictions from the global Navy Coastal Ocean Model (NCOM) during 1998–2001. *J. Atmos. Oceanic Technol.,* 21, 1876–1894, doi:10.1175/JTECH-1680.1.

Bender, A., D. M. Steinberg, A. L. Friedman, S. B. Williams, 2008: Analysis of an autonomous underwater glider. *Proc. The Australasian Conf. on Robotics and Automation, Canberra,* Australia, The Australian Robotics and Automation Association, 36–45. [Available online at http://www.researchgate.net/publication/230642957_Analysis_of_an_autonomous_underwater_glider/file/d912f50c80a9b28bf7.pdf.]

Clegg, D., and M. Peterson, 2003: User operational evaluation system of unmanned underwater vehicles for very shallow water mine countermeasures. *Proc. OCEANS 2003,* San Diego, California, IEEE, 1417–1423. doi:10.1109/OCEANS.2003.178069.

David, C., M. Peterson, 2003: User operational evaluation system of unmanned underwater vehicles for very shallow water mine countermeasures. *Proc. OCEANS 2003,* San Diego, California, 1417–1423. doi:10.1109/OCEANS.2003.178069.

Davis, R. E., C. C. Eriksen, C. P. Jones, 2002: Autonomous buoyancy-driven underwater gliders. *The Technology and Applications of Autonomous Underwater Vehicles*, G. Griffiths, Ed., CRC Press, 37–58.

DOD (Department of Defense), 2013: *Command and Control for Joint Maritime Operations (Joint Publication 3-32).* U.S. Government Printing Office, Washington, DC, 106 pp.

DON (Department of the Navy), 2004: *The Navy Unmanned Undersea Vehicle (UUV) Master Plan.* Washington, DC.

DON (Department of the Navy), 2007: *Navy Maritime Domain Awareness Concept.* Washington, DC.

Eriksen, C. C., T. J. Osse, R. D. Light, T. Wen, T. W. Lehman, P. L. Sabin, J. W. Ballard, A. M. Chiodi, 2001: Seaglider: A long-range autonomous underwater vehicle for oceanographic research. *IEEE J. Oceanic Eng.*, 26 (4), 424–436, doi:10.1109/48.972073.

Fossen, T. I., 1994: *Guidance and Control of Ocean Vehicles.* John Wiley and Sons, 480 pp.

Government of the Republic of Korea, 2011: *On the Attack against ROK Ship Cheonan White Paper* (in Korean). Government of the Republic of Korea, 309 pp.

Graver, J. G., R. Bachmayer, N. E. Leonard, and D. M. Fratantoni, 2003: Underwater glider model parameter identification. *Proc. 13th International Symposium on Unmanned Untethered Submersible Technology (UUST).* [Available online at http://www.princeton.edu/~naomi/uust03GBLFp.pdf.]

Graver, J. G., 2005: Underwater gliders: Dynamics, control and design. Ph.D. dissertation, Princeton University, 273 pp.

Kara, A. B., C. N. Barron, P. J. Martin, L. F. Smedstad, and R. C. Rhodes, 2006: Validation of interannual simulations from the 1/8 degree global Navy Coastal Ocean Model (NCOM). *Ocean Modell.*, 11, 376–398, doi:10.1016/j.ocemod.2005.01.003.

Martin, P. J., G. Peffion, K. J. Yip, 1998: A comparison of several coastal ocean models. NRL Report NRL/FR/7322–97-9672, 99 pp. [Available online at http://www.dtic.mil/dtic/tr/fulltext/u2/a360771.pdf.]

Martin, P. J., and Coauthors, 2009: User's manual for the Navy Coastal Ocean Model (NCOM) Version 4.0. NRL Report NRL/FR/7320–09-9151, 73 pp. [Available online at http://www.dtic.mil/dtic/tr/fulltext/u2/a508063.pdf.]

Merckelbach, L. M., R. D. Briggs, D. A. Smeed, and G. Griffiths, 2008: Current measurements from autonomous underwater gliders. *CMTC 2008, IEEE/OES 9th Working Conf. on Current Measurement Technology,* Charleston, South Carolina, CMTC/IEEE/OES, 61–67, doi:10.1109/CCM.2008.4480845.

Metzger, E. J., and Coauthors, 2014: U.S. Navy operational global ocean and Arctic ice prediction systems. *Oceanography*, 27 (3), 32–43, doi:10.5670/oceanog.2014.66.

MND (Ministry of National Defense, Republic of Korea), 2010: *Joint Investigation Report: On the Attack against ROK Ship Cheonan.* Ministry of National Defense, Republic of Korea, 313 pp.

MND (Ministry of National Defense, Republic of Korea), 2013: *2012 Defense White Paper*. Ministry of National Defense, Republic of Korea, 415 pp.

Ngodock, H. and M. Carrier, 2014: A 4DVAR System for the Navy Coastal Ocean Model. Part I: System description and assimilation of synthetic observations in Monterey Bay. *Mon. Wea. Rev.*, 142, 2085–2107, doi:10.1175/MWR-D-13-00221.1.

NOAA (National Oceanic and Atmospheric Administration), cited 2014: Navy Hybrid Coordinate Ocean Model. [Available online at http://ecowatch.ncddc.noaa.gov/global-hycom.]

NRL (Naval Research Laboratory), cited 2014: Real-time 1/12˚ Global HYCOM Nowcast/Forecast system information. [Available online at http://www7320.nrlssc.navy.mil/GLBhycom1-12/prologue.html.]

OPC (Ocean Prediction Center), cited 2014: Ocean Model Current Areas. [Available online at http://www.opc.ncep.noaa.gov/newNCOM/NCOM_currents.shtml.]

Paull, L., S. Saeedi, M. Seto, H. Li, 2014: AUV navigation and localization: A review. *IEEE J. Oceanic Eng.*, 39 (1), 131–149, doi:10.1109/JOE.2013.2278891.

Rajendra, A. L., and T.C. Jannett, 2007: Comparison of glider routing algorithms for data acquisition in undersea sensor networks. *Proc. SoutheastCon, 2007,* Richmond, Virginia, IEEE, 533–538. doi:10.1109/SECON.2007.342959.

Rhodes, R. C., and Coauthors, 2002: Navy real-time global modeling systems. *Oceanogr.*, 15 (1), 29–43, doi:10.5670/oceanog.2002.34.

Rudnick, D. L., R. E. Davis, C. C. Eriksen, D. M. Fratanoni, M. J. Perry, 2004: Underwater gliders for ocean research. *Marine Technology Society Journal*, 38 (2), 73–84, doi:10.4031/002533204787522703.

Schofield, O., and Coauthors, 2007: Slocum gliders: Robust and ready. *J. Field Robotics,* 24 (6), 473–485, doi:10.1002/rob.20200.

Sherman, J., R. E. Davis, W. B. Owens, J. Valdes, 2001: The autonomous underwater glider “Spray.” *IEEE J. Oceanic Eng.*, 26 (4), 437–446, doi:10.1109/48.972076.

Singh, P. K., 2014: Design of a robotic bio-sampler and localization improvement for underwater autonomous gliders. M.S. thesis, Dept. of Electrical and Computer Engineering, Rutgers, The State University of New Jersey, 88 pp.

Smith, R. N., A. Pereira, Y. Chao, P. P. Li, D. A. Caron, B. H. Jones, G. S. Sukhatme, 2010a: Autonomous underwater vehicle trajectory design coupled with predictive ocean models: A step study. *2010 IEEE International Conf. on Robotics and Autonomation,* Anchorage, Alaska, IEEE Xplore, 4770–4777, doi:10.1109/ROBOT.2010.5509240.

Smith, R. N., J. Kelly, Y. Chao, B. H. Jones, G. S. Sukhatme, 2010b: Towards the improvement of autonomous glider navigational accuracy through the use of regional ocean models. *Proc. ASME 2010 29th International Conf. on Ocean, Offshore and Arctic Engineering,* 4, Shanghai, China, Ocean, Offshore and Arctic Engineering Division, 597–606. [Available online at http://proceedings.asmedigitalcollection.asme.org/proceeding.aspx?articleid=1617686.]

Smith, R. N., J. Kelly, and G. S. Sukhatme, 2012: Towards improving mission execution for autonomous gliders with an ocean model and Kalman filter. *2012 IEEE International Conf. on Robotics and Autonomation,* Saint Paul, Minnesota, IEEE, 4870–4877, doi:10.1109/ICRA.2012.6224609.

Somers, W., 2011: Doppler-based localization for mobile autonomous underwater vehicles. M.S. thesis, Dept. of Electrical and Computer Engineering, Rutgers, The State University of New Jersey, 66 pp.

Teledyne Webb Research, cited 2014: Slocum G2 glider product catalog 2013. [Available online at http://www.webbresearch.com/pdf/G2_Product_Catalog.pdf.]

Uffelen, L. J, and Coauthors, 2013: Estimating uncertainty in subsurface glider position using transmissions from fixed acoustic tomography sources. *The Journal of Acoustical Society of America,* 134 (4), 3260–3271, doi:10.1121/1.4818841.

Wang, P., P. K. Singh, J. Yi, 2013: Dynamic model-aided localization of underwater autonomous gliders. *2013 IEEE International Conf. on Robotics and Autonomation,* Karlsruhe, Germany, IEEE Xplore, 5565–5570, doi:10.1109/ICRA.2013.6631376.

Webb, D. C., P. J. Simonetti, C. P. Jones, 2001: SLOCUM: An underwater glider propelled by environmental energy. *IEEE J. Oceanic Eng.*, 26 (4), 447–452, doi:10.1109/48.972077.

Woithe, H. C., D. Boehm, U. Kremer, 2011: Improving Slocum glider dead reckoning using a Doppler Velocity Log. *OCEANS 2011,* Waikoloa, Hawaii, IEEE, 1–5.

INITIAL DISTRIBUTION LIST

1. Defense Technical Information Center
   Ft. Belvoir, Virginia

2. Dudley Knox Library
   Naval Postgraduate School
   Monterey, California